aueng.
620.5
458
MAY 21 1935
B9f

U. S. DEPARTMENT OF COMMERCE

BUREAU OF STANDARDS JOURNAL OF RESEARCH

Vol. 7 AUGUST, 1931 No. 2

CONTENTS

RP. No.	TITLE AND AUTHOR	Page
339.	A new apparatus for preparing Ra B+C sources. L. F. Curtiss	215
340.	The photographic emulsion: After-ripening. Burt H. Carroll and Donald Hubbard	219
341.	A simultaneous radiotelephone and visual range beacon for the airways. F. G. Kear and G. H. Winterrnute	261
342.	Design of standards of inductance, and the proposed use of models in the design of air-core and iron-core reactors. H. B. Brooks	289
343.	The heat of formation of water and the heats of combustion of methane and carbon monoxide. A correction. Frederick D. Rossini	329
344.	Elastic problem of a wire-wound cylinder. Chester Snow	331
345.	The restoration of solarized ultra-violet transmitting glasses by heat treatment. A. Q. Tool and R. Stair	357
346.	The determination of oxygen and nitrogen in irons and steels by the vacuum-fusion method. H. C. Vacher and Louis Jordan	375
347.	Some electrical properties of foreign and domestic micas, and the effect of elevated temperatures on micas. A. B. Lewis, E. L. Hall, and Frank Caldwell	403

BUREAU OF STANDARDS JOURNAL OF RESEARCH

CONTENTS OF RECENT NUMBERS

February, 1931 (Vol. 6, No. 2)

RP275. Regularities in the second spectrum of Xenon. C. J. Humphreys, T. L. deBruin, and W. F. Meggers. Price 5 cents.

RP276. The resistance of chromium-plated gages to wear. Harry K. Hirschman. Price 10 cents.

RP277. Compressive tests of jointed H-section steel columns. James H. Edwards, H. L. Whittemore, and A. H. Stang. Price 15 cents.

RP278. Critical study of the bursting strength test for paper. F. T. Carson and F. V. Worthington. Price 10 cents.

March, 1931 (Vol. 6, No. 3)

RP279. A method for the standardization of permeameters at high magnetizing forces. R. L. Sanford. Price 5 cents.

RP280. Determination of the toluene content of a mid-continent petroleum. Johannes H. Bruun, R. T. Leslie, and Sylvester T. Schicktanz. Price 5 cents.

RP281. The mechanism of the atomization of liquids. R. A. Castleman, jr. Price 5 cents.

RP282. Separation of normal octane from petroleum by distillation and crystallization. R. T. Leslie and Sylvester T. Schicktanz. Price 10 cents.

RP283. Further measurements of propeller fan characteristics. Paul S. Ballif and H. L. Dryden. Price 10 cents.

RP284. A precision cryostat with automatic temperature regulation. R. B. Scott and F. G. Brickwedde. Price 5 cents.

RP285. The paper-making properties of phormium tenax (New Zealand flax). Merle B. Shaw, George W. Bicking, and Martin J. O'Leary. Price 10 cents.

RP286. A method for the separation and gravimetric determination of osmium. Raleigh Gilchrist. Price 10 cents.

RP287. Application of the fluorating process to fructose. D. H. Brauns and Harriet L. Frush. Price 5 cents.

RP288. Moisture expansion of glazes and other ceramic finishes. H. G. Schurecht and G. R. Pole. Price 5 cents.

RP289. Extension of the standard visibility function to intervals of 1 millimicron by third-difference osculatory interpolation. Deane B. Judd. Price 5 cents.

RP290. Durability and strength of bond between mortar and brick. L. A. Palmer and J. V. Hall, jr. Price 10 cents.

RP291. Heat transfer through building walls. M. S. Van Dusen and J. L. Finck. Price 15 cents.

April, 1931 (Vol. 6, No. 4)

RP292. Variations caused in heating curves of glass by heat treatment. A. Q. Tool and C. G. Eichlin. Price 10 cents.

RP293. On the vibration of U bars. G. H. Keulegan. Price 10 cents.

RP294. Laundry "winter damage." John B. Wilkie. Price 10 cents.

RP295. The determination of the alpha cellulose content and copper number of paper. John O. Burton and Royal H. Rasch.

RP296. The structure of the arc spectrum of zirconium. C. C. Kiess and Harriet K. Kiess. Price 15 cents.

RP297. Radiation from metals bombarded by low-speed electrons. F. L. Mohler and C. Boeckner.

RP298. Pipe-line currents and soil resistivity as indicators of local corrosive soil areas. E. R. Shepard.

RP299. Two new crystalline difructose anhydrides from hydrolyzed inulin. Richard F. Jackson and Emma McDonald. Price 5 cents.

RP300. Measurement of fiber diameters by the diffraction method. H. J. McNicholas and H. J. Curtis. Price 10 cents.

RP301. Wind pressure on a model of a mill building. Hugh L. Dryden and George C. Hill. Price 10 cents.

RP302. Stabilization of boric acid buffers by aeration. Edna H. Fawcett and S. F. Acree. Price 5 cents.

Research papers are available as separates for purchase from the Superintendent of Documents United States Government Printing Office, Washington, D. C.

U. S. DEPARTMENT OF COMMERCE
R. P. LAMONT, Secretary
BUREAU OF STANDARDS
GEORGE K. BURGESS, Director

BUREAU OF STANDARDS JOURNAL OF RESEARCH

August, 1931
Vol. 7, No. 2

UNITED STATES
GOVERNMENT PRINTING OFFICE
WASHINGTON : 1931

For sale by the Superintendent of Documents, Washington, D. C. - - Price $2.75 Per Year on Subscription

For a partial list of previous research papers appearing in BUREAU OF STANDARDS JOURNAL OF RESEARCH, see pages 2 and 3 of the cover.

RP339

A NEW APPARATUS FOR PREPARING Ra B+C SOURCES

By L. F. Curtiss

ABSTRACT

A simple glass apparatus is described which may be used to serve the purpose of an "emanation pipette" but which eliminates two objectionable features present in the usual forms of this apparatus. Mercury does not come in contact with rubber tubing, since no rubber tubing is used. A further improvement is accomplished by avoiding the necessity for passing mercury through stopcocks.

The preparation of radium B+C sources is usually done by some form of emanation pipette, such as is shown in Figure 1. This consists of a 2-way stopcock with a large glass barrel, *B*, below into which mercury can be forced by a reservoir, *R*, attached to the lower end by rubber tubing, *T*. It is operated first as a pump to exhaust the portion sealed on at *A* where the source is to be prepared. The purified emanation is introduced through *C* into *B* and, by reversing the stopcock, it is forced into *A*. This form of apparatus has two very serious defects which render it unsatisfactory for continuous operation. The rubber tubing soon introduces impurities into the mercury and causes an accumulation of "dirt" on the inside of the barrel which interferes with the efficiency of the device. A more serious trouble arises from the fact that mercury must be forced through the bores of the stopcock at certain stages of the operation of the apparatus. Even with the greatest care in greasing the stopcock, the mercury gradually becomes contaminated with the grease which, under the action of the radon, becomes hard enough to choke the bore of the capillary, especially if the usual rubber greases are used. A description is given below of a device which eliminates both of these difficulties, thereby making the preparation of active deposits from radon a much simpler and less tedious operation. It also possesses the advantage that practically no radon is lost in the preparation of a source by being trapped by dirt which has accumulated in the apparatus. This is very important where it is desired to prepare a number of sources from the same radon.

The essential details of the apparatus, which is entirely of glass, are shown to scale in Figure 2. It consists of two principal parts, one in which the source is actually prepared, and an auxiliary part which is an ordinary Toepler pump arranged to be operated by compressed air. The various parts and their functions can best be described by outlining the method of using the apparatus when preparing a source.

The steel reservoir, *R*, is filled with mercury covering the open end of the capillary at *D*. To prepare the apparatus for use, the stopcock, S_1, is closed and S_2 is opened and the apparatus exhausted by forcing mercury, contained in the bulb *B*, repeatedly into the barrel of the Toepler pump, *T*. The check valve, *G*, has a ground seat which

prevents mercury rising above *G*. The method of using compressed air for operating a Toepler pump has already been described elsewhere.[1] It has been used for several years in the radium laboratory at the National Bureau of Standards, and has proven very satisfactory. Apparently there is no danger of breaking glass parts with pressures required for this purpose, since this laboratory has had no trouble of this kind. As can

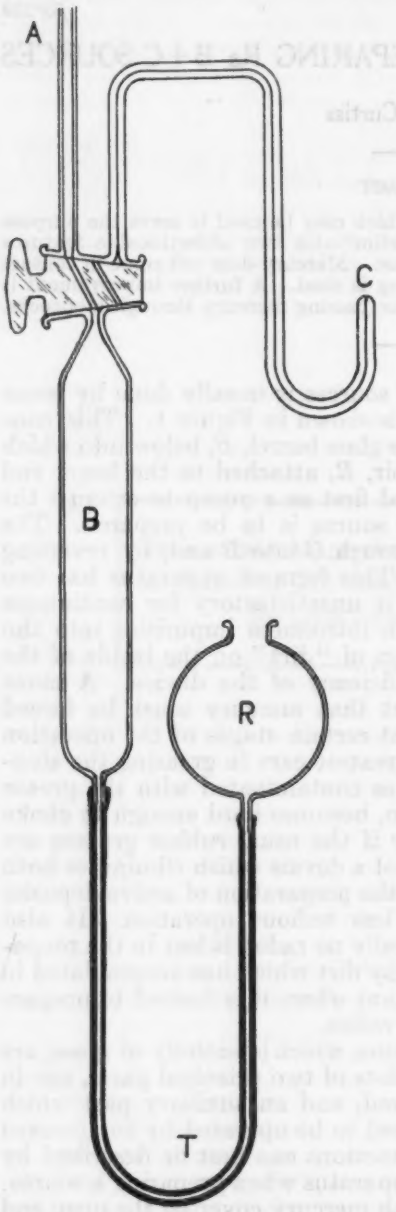

FIGURE 1.—*Old type emanation pipette*

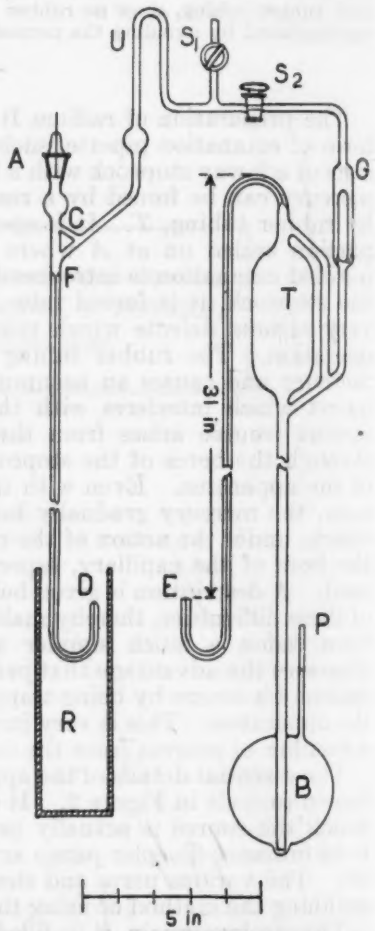

FIGURE 2.—*All-glass apparatus for preparing Ra B+C sources*

be seen it effectually eliminates the contact of mercury with rubber and makes a rapid operation of the pump possible and safe.

[1] L. F. Curtiss, J. Opt. Soc. Am. & Rev. Sci. Inst., **17**, p. 77; 1928.

The mercury reservoir, R, is attached to a counterpoise, not shown, which enables the position of the reservoir to be adjusted and consequently the level of the mercury column in the capillary above it. The next step in the operation is to adjust the level of the mercury in the capillary until it is at some point slightly below F. Then with the purified emanation at hand, stored in the usual way in an inverted test tube over mercury, the level of the mercury is raised by suddenly shifting the reservoir, R, upward about 2 inches. As the mercury rises to fill the branch tube at C, the radon, which is always of small volume, is introduced at D in the same way one would introduce it into an emanation pipette, simply slipping the inverted tube over the end of D. The radon will now rise quickly in the capillary and escape above the mercury column into the space below the stopper at A. Since the mercury level is by this time above the branch tube at C, any bubbles of radon which may rise up the side tube are caught by C and returned to the main volume. The mercury level is now adjusted to give a small volume of gas below the stopper which carries the metal button for receiving the active deposit. The usual voltage connections are made to the wire through the stopper, and by means of the mercury in the reservoir R.

When the exposure has been completed the radon is recovered in the following way. The reservoir R is lowered until the mercury column is again below the side tube at F. This allows the radon to expand into the evacuated tubes leading to the Toepler pump. An inverted test tube filled with mercury is placed over E, which is provided with a mercury reservoir similar to R, and the Toepler pump is operated until all radon has been pumped over into the test tube. Then, in order to remove the stopper, A, and to recover the source, air is admitted by the stopcock, S_1, while S_2 is closed. If desired both stopcocks may be eliminated, since S_2 only permits air to be admitted to the exposing tube without entering the Toepler pump so that the pump is a little easier to start when next used. The function of S_1 can be equally well performed, though less conveniently by a side tube drawn down to smaller diameter so that it may be cracked off to admit air.

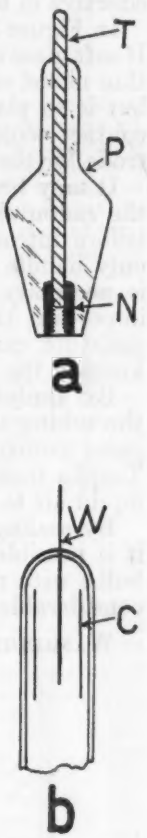

FIGURE 3.—*Pyrex stopper*

(*a*) Details of pyrex stopper; (*b*) arrangement for preparing active deposit on wire.

The two small bulbs shown in the glass tubing are important. The one in the vertical column prevents radon being trapped under a short column of mercury when rising into A. In the same way the bulb below U prevents a bubble of radon from carrying mercury up over the tube U which is purposely made high enough so that a solid column of mercury can not rise over it for any possible position of the reservoir, R.

The apparatus may be constructed either of soft glass or pyrex. For activating metal buttons a pyrex stopper, which, of course, can be ground into apparatus made of soft glass, is shown in Figure 3 (*a*). Since the tungsten wire, T, can not be threaded, a nickel bushing,

N, is held by a drive fit to the lower end which is tapped for a small screw. This combination is sealed into the pyrex as shown, the tungsten making a vacuum-tight seal to the glass. Metal buttons of various shapes, provided with a short threaded boss, may then be screwed into the nickel socket so that they are tight against the lower surface of the stopper, which should be ground flat. There are then no pockets in which radon can accumulate where it would not be effective in forming a deposit on the surface of the metal button.

In Figure 3 (*b*) is shown the usual method of preparing wire sources. If soft glass is used, the wire, *W*, is of platinum and is surrounded by a thin nickel or steel cylinder, *C*, which is not in contact with the wire, but is so placed that the mercury column can be raised to come in contact with it. Thus the nickel cylinder forms the positive electrode for the voltage used in preparing the active deposit.

It may be well to call attention to the fact that for best operation the radon should be freed as well as possible from the other gases before introducing it into the apparatus, since this apparatus can only handle small volumes of gas. A fairly high "purity" of radon is necessary in any case to get strong sources. It is even more important that the radon be carefully dried, since the presence of moisture causes the mercury to adhere to the glass and prevents keeping the glass and mercury surfaces clean.

By applying liquid air to a piece of cotton wool, wrapped about the tubing at *U*, it is possible to condense the radon and remove any gases noncondensable at liquid air temperatures by means of the Toepler pump. Then the radon may be pumped out by allowing the liquid air to evaporate.

By sealing on small diameter tubing at *A* in place of the stopper, it is possible to modify the apparatus so that it may be used to fill bulbs with radon, provided the reservoir, *R*, is designed to permit a considerable movement of the level of the mercury column.

WASHINGTON, May 1, 1931.

THE PHOTOGRAPHIC EMULSION: AFTER-RIPENING

By Burt H. Carroll and Donald Hubbard

ABSTRACT

After-ripening is defined as the increase in sensitivity of photographic emulsions after washing. Following a discussion of the process, and review of the literature, the experimental methods of the National Bureau of Standards photographic emulsion laboratory are described in detail. After-ripening by digestion was studied with respect to eight of the more important variables. The amount of after-ripening which is practicable is dependent on the extent to which sensitivity nuclei have been formed during ripening before washing. The influence of temperatures and of bromide, chloride, and hydrogen ion concentrations, is according to predictions on the basis of chemical reactions forming sensitivity nuclei. The effect of gelatin-silver halide ratio can be explained by its influence on rate of development. Variations between different samples or makes of gelatin are illustrated. The progress of after-ripening with inert gelatin plus known sensitizing materials is very similar to that under the usual conditions, but there are important quantitative differences. The increase in practicable after-ripening with increasing percentage of silver iodide is illustrated. After-ripening during storage of finished plates was found to be similar to that by digestion, but frequently more efficient. Changes in bromide ion concentration during digestion, and in nonhalide silver during digestion or storage, are further proof of reaction during after-ripening, but it is evident that most of the nonhalide silver is photographically inert.

CONTENTS

	Page
I. Introduction	219
II. Experimental methods	222
1. Sensitometry	222
2. Apparatus and procedure used in emulsion making	224
3. Analytical methods	227
III. Effect of certain variables on after-ripening by digestion	228
1. Ripening	228
2. Temperature	230
3. Bromide ion concentration	232
4. Comparison of bromide and chloride	237
5. Hydrogen ion concentration	239
6. Gelatin	241
(*a*) Gelatin-silver halide ratio	241
(*b*) Make or batch of gelatin	243
7. Known nuclear sensitizers	247
8. Percentage of iodide in the silver halide	251
IV. Storage ripening	252
V. Analytical evidence on the mechanism of after-ripening	255
VI. Summary	258
VII. Acknowledgment	258
VIII. Bibliography	258

I. INTRODUCTION

This paper is to be considered as a survey of its limited field rather than a completed investigation. Publication of the material here presented is dictated not only by the considerable length of the article but because the existence of this very important process is apparently

unknown to otherwise well-informed writers on photography. Recent literature has included specific if qualitative references (1), (2), (3), (4), (5) [1] to the fact that the sensitivity of an emulsion may be enormously increased by digestion *after washing*, but the general impression of the emulsion-making process is based on early literature (6) which cautions against such treatment.

We are unable to say how far our experiments correspond to commercial practice,[2] but some of the resulting emulsions are quite similar to very fast commercial products. We are also uncertain how much of the material presented may be common knowledge among emulsion makers, but it has never been published in quantitative form and it seem particularly unlikely that any information on this subject is to be expected from commercial sources.

The term "ripening" has been used to include any digestion or storage after mixing the emulsion, used to increase sensitivity. It is generally understood now, however, to mean digestion in the presence of excess soluble bromide, with or without the addition of ammonia. In the presence of these solvents for silver halide, there is a continuous increase in average size of the silver halide grains, with complicated changes in the size distribution. We will use "ripening" in this sense. "After-ripening" will be understood to mean changes in sensitivity after the silver halide solvents have been removed by washing; it is therefore associated with no appreciable change in grain size. After-ripening is normally carried on by digestion of the melted emulsion after washing; we shall use the term digestion to imply heat treatment of the washed emulsion, as distinct from the ripening by heat before washing. Marked after-ripening may also occur on storage of finished plates, especially if ripening and digestion have been limited; we shall refer to this as "storage ripening."

The impression which is given by the early literature is that the sensitivity of an emulsion is controlled almost entirely by the ripening and this is true of many of the older formulas.

Present procedure is apparently different; several authoritative statements to this effect have been published, for example, the following by Sheppard (Bogue, Colloidal Behavior II, p. 763):

> These relatively coarse-grained negative emulsions are not produced from fine-grained emulsions by ripening, but the grain size is determined by the conditions of initial precipitation. High concentration of the reactants ($AgNO_3$ and KBr), low concentration of gelatin, high temperature of mixing, and retarded addition permit the process of recrystallization to take place at once, with the formation of definite, coarse-grained suspensions.

Our own experience is in excellent agreement with this, but it may be amplified to advantage at one point. If the silver solution is added to the bromide, the first grains are formed in the presence of a high concentration of the latter. Now the solubility of silver bromide in a solution of potassium bromide increases very rapidly with increasing potassium bromide concentration [3] and the rate of ripening (or at least the rate of change in grain size) obviously will increase with the solubility (7) so that there is very rapid ripening during the mixing. If the addition of the silver solution is retarded, using either a

[1] Numbers in parentheses here and elsewhere in the text refer to the bibliography at the end of the paper.
[2] Lüppo-Cramer (reference 1) states that, contrary to a common impression, he has found no significant difference between large and small batches of emulsion made by the same formula, provided that all variables, such as the rate of mixing, were actually kept constant.
[3] Approximately as the fifth power, Hellwig. Z. Anorg. Chem., **25**, p. 183; 1900.

slow continuous stream, or "double emulsification" (8), (9), the ripening of the silver halide first formed may be carried to its practical limit by the time the mixing is completed, and little or no more ripening in the usual sense is desirable.[4] Ripening is followed by washing the emulsion, removing the silver halide solvents, such as soluble bromide and ammonia, so that the grain size and distribution is fixed after washing. It is a common impression [5] that sensitivity is also practically fixed. The emulsions described in the early literature were generally low in iodide and ripened for a long time with ammonia. Emulsions of this type can not be after-ripened to any considerable extent. With other formulas capable of producing emulsions resembling modern commercial products, the sensitivity just after washing may not be more than 5 per cent of the final value which is reached by digestion at temperatures of 35° to 65° C. Our experience is that it is impossible to make a satisfactory fast emulsion of the neutral ("boiled") type without after-ripening, and that it is at least very difficult to do without it in ammonia-ripened emulsions.

In case the emulsion is coated without digestion, there will, in general, be an increase in sensitivity, on keeping the plates, which equals or exceeds the increase which could be produced by digestion This was frequently observed in the early days of dry plates; Eder (11) cited several conflicting observations on this point, and gave the weight of his opinion to the erroneous conclusion of Gaedicke that there was no increase in sensitivity on storage if no trace of ammonia remained in the emulsion. We have already commented briefly on this subject (7).

The number of variables in a photographic emulsion is such that a complete series of independent changes in each one is quite impracticable. We believe that we here present enough data to indicate the sign and order of magnitude of the effect which several of these variables have upon after-ripening, although the exact course of the process with a given formula must obviously always remain a matter for careful determination in each individual case.

The nature of the processes occurring during after-ripening will be discussed at more length in connection with the evidence offered in this paper. As already mentioned, the change in grain size is negligible, since the solubility of the silver halide is practically the same as in pure water. After-ripening is primarily the period of formation of sensitivity nuclei. Thiocarbamides and related sulphur compounds have formed insoluble molecular compounds (12) with the silver halide during the mixing and ripening, but in the absence of ammonia, there is little rearrangement of these to form silver sulphide until the bromide ion concentration has been reduced by washing. Reduction of silver bromide to metallic silver also leaves soluble bromides as a product of the reaction and, therefore, must be much more rapid after washing; to date, there is neither positive proof or dis-

[4] We have already (7) mentioned the marked increase in speed and decrease in contrast produced by slow mixing of a neutral emulsion. Lüppo-Cramer (1) has recently given further illustrations of this, with characteristic curves. Conditions in an ammonia process emulsion are much more complicated because of the competing formation of two kinds of complex ions $(Ag(NH_3)_2)^+$ and $(AgBr_x)^-$, but the wider range in grain sensitivity is still observed, with similar changes in the characteristic curve. Wall (10) has also discussed some of the consequences if the method of mixing the emulsion is varied, for example by addition of the silver and bromide solutions simultaneously to the gelatin; but we doubt if the evidence supports his view that a "slow form" of silver bromide is formed in the presence of a high concentration of soluble bromide.

[5] For example, Neblette, "Principles and Practice of Photography" p. 162, 1926, says that after washing "The emulsion may be regarded as complete."

proof that this reaction is a source of sensitivity nuclei, but the writers agree with Lüppo-Cramer that it is very probably an important part of after-ripening.

II. EXPERIMENTAL METHODS

1. SENSITOMETRY

The usual methods of this bureau were employed—nonintermittent time scale exposure at an intensity of 1 meter-candle, brush development in unbromided pyrogallol at 20° for 3, 6, and 12 minutes, and measurement of density in diffuse illumination by a Martens photometer, the density of the fog strip being automatically subtracted. The illumination was the quality of mean noon sunlight; the more recent tests were obtained with a lamp of color temperature 2,360° and the Davis-Gibson filter tentatively adopted at the International Congress; the previous source was a lamp operated at a color temperature of 2,810° K. and a Corning "Daylite" glass filter giving photographically equivalent quality. The emulsions were machine coated on 5 by 7 inch (or in a few cases 4½ by 6½ inch) plates; three test strips 1⅛ by 5 inches cut from the center of the plate and backed with black shellac. The coating was somewhat heavier than commercial practice; this minimizes the photographic effect of irregularities incident to coating small experimental batches, but it obviously increases the fog density. Because of the very rapid storage ripening in the undigested emulsions, the tests were always made soon after coating (in 12 to 40 hours after drying was complete, unless stated to the contrary). Excepting in Table 1, the term "speed" in all our tables refers to the National Bureau of Standards speed number, $10/i$. The inertia (i) is expressed in candle-meter-seconds. Subscripts, or subheadings under γ and fog, indicate the time of development in minutes; six minutes is approximately the normal time for this developer.[6]

Sensitometry of experimental emulsions unfortunately is especially subject to difficulties in assigning numerical values to the data, as almost invariably some members of a series of emulsions fail to have characteristic curves with satisfactory straight line sections. Our conclusions are in all cases based on comparison of the complete characteristic curves, but by giving both speed and γ in the tables, a reasonably adequate idea of the changes in effective sensitivity has been presented.

A complete set of data illustrating change of sensitivity during after-ripening is given in Table 1 and Figures 1, 2, and 3. We are indebted to Messrs. Raymond Davis and G. K. Neeland for exposures of emulsion 4–68 with sector wheels giving steps on the log E scale of 0.15 and 0.20, as our wheel is of the conventional H and D pattern (nine steps, each twice the preceding one). The characteristic curves for 6 and 12 minute development are plotted in Figures 1 and 2; Figure 3 and Table 1 give the numerical constants assigned to these curves, including speed numbers both by the B. S. system

[6] The order of sensitivity of the experimental emulsions may be judged by comparison with commercial emulsions tested under the same conditions. A moderate speed negative emulsion, Eastman roll film, has a B. S. speed of 220, γ = 0.88; two very fast emulsions, the Hammer Press plate (emulsion 4063), and Eastman Hyper Press plate (emulsion 3082) have speed 660, γ = 1.05 for the former, and speed 1250, γ = 0.86 for the latter.

and by that proposed by Jones and Russell (13). In the latter system, the speed is taken as proportional to the reciprocal of the exposure (E_m) corresponding to the minimum useful gradient, which is taken as G=0.20. For purposes of comparison the maximum value of each of the curves in Figure 3 has been made equal to 1.00.

As in most of the other cases of after-ripening, the curves of 4–68 at various digestion times differ not only in speed but in contrast and shape. The variation in sensitivity can not be adequately expressed by any single constant, but the speed number based on minimum useful gradient is evidently the best approximation to such an expression. Speed numbers in both systems are found to be dependent on time of development, falling in line with the results

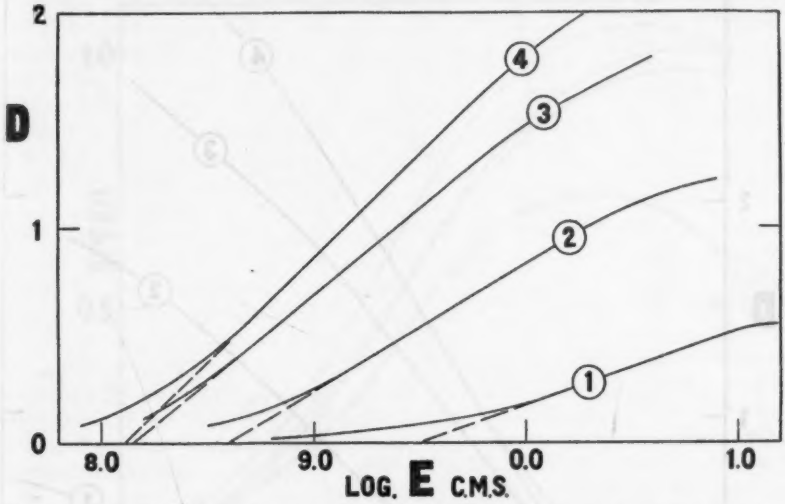

FIGURE 1.—*Characteristic curves, 6-minute development of emulsion 4–68 at four stages of after-ripening*

Digestion at 55°, pH 7 [Br⁻] 5 × 10^{-4} *N*. Curve 1, minimum digestion; curve 2, 1.0 hour; curve 3, 2.0 hours; curve 4, 3.0 hours

obtained by Davis and Neeland (14) with commercial emulsions. The reader is referred to their paper for a more complete intercomparison of the systems. The speed numbers given in this paper are an average value for the three times of development.

TABLE 1.—*Comparison of methods of expressing sensitivity of emulsion 4–68 at different stages of after-ripening*

Time of digestion (in minutes at 55°)	6-minute development				12-minute development			
	B. S. speed number $10/i$	γ	Jones and Russell speed number $10/E_m$	Fog	B. S. speed number $10/i$	γ	Jones and Russell speed number $10/E_m$	Fog
5	31.6	0.35	22.4	0.03	45	0.40	38.9	0.10
60	275	.57	455	.03	182	.92	435	.13
120	710	.81	1,200	.06	505	1.25	1,230	.18
180	735	.99	1,380	.09	435	1.71	1,445	.24

2. APPARATUS AND PROCEDURE USED IN EMULSION MAKING

The emulsions were mixed in batches using 30 to 60 g of silver nitrate (0.176 to 0.35 mol), the final volume being 0.7 to 1.5 liters. These were subdivided into batches of 0.044 mol (equivalent to 7.5 g $AgNO_3$) for comparison of differences in times of digestion or other variables. In all cases, the silver solution was added in a continuous stream to the mixture of bromide, iodide, and gelatin; the rate was varied over a considerable range by the use of separatory funnels fitted with capillary stems of different bores. The mixing vessel was a 1.5 liter Pyrex beaker, with a mechanical stirrer running 200 to

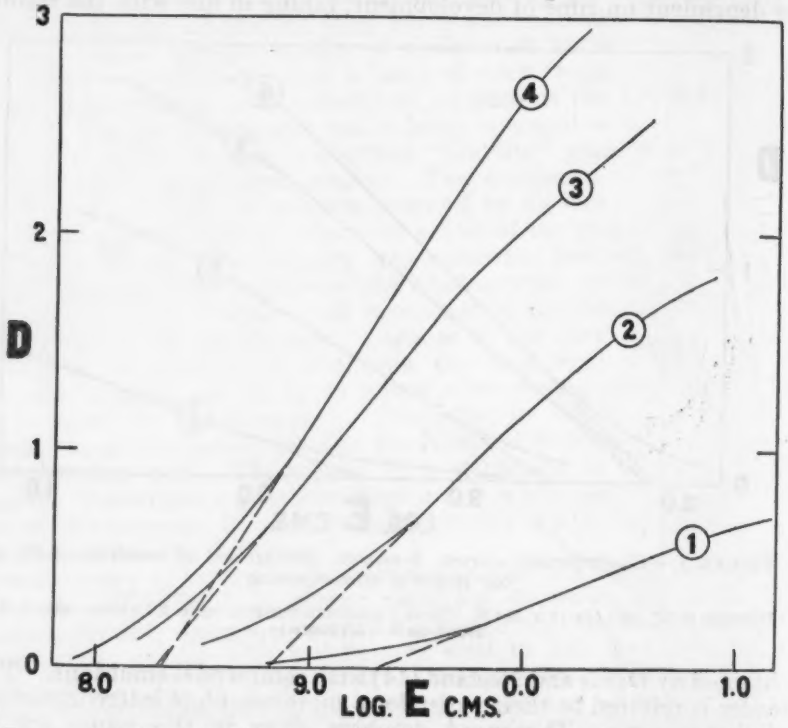

FIGURE 2.—*Characteristic curves, 12-minute development, of same emulsion as in Figure 1*

300 r. p. m. Using a silver shaft running in a glass bearing in the glass cover plate over the beaker, neither the liquid emulsion nor the condensate from it could come into contact with any material except glass or silver. Silver in contact with liquid emulsion was found to blacken quite rapidly in use, apparently from formation of silver sulphide (see Lüppo-Cramer (15)), so the actual stirrer was made of glass.

Both ordinary and centrifugal washing were used. For the ordinary method, the emulsions were rapidly chilled by pouring into a layer 1 to 2 cm thick in a clean enamelled tray floated on water at 5° to 8° C.; unless otherwise stated, they were left overnight at 5° to 8° C. before shredding and washing. Our shredding press forces the

set jelly through a sieve built up from sharpened metal strips set on edge, cutting it into clean "noodles" 5 to 6 mm square in cross section; there is very little formation of fine material, and consequently good circulation of water through the mass of "noodles." Using these relatively large but clean-cut noodles, we find that washing is more rapid than when the emulsion is, for example, shredded through netting into "noodles" which have more tendency to pack into a tight mass. The shredded emulsions were placed in silver-plated cans with 20-mesh screens of pure nickel at the bottom; these rested in slightly larger crocks, and the water, at the rate of at least 0.5 liter per minute, passed down through the emulsion and out over the edge of the crocks. Washington city water was used without treatment

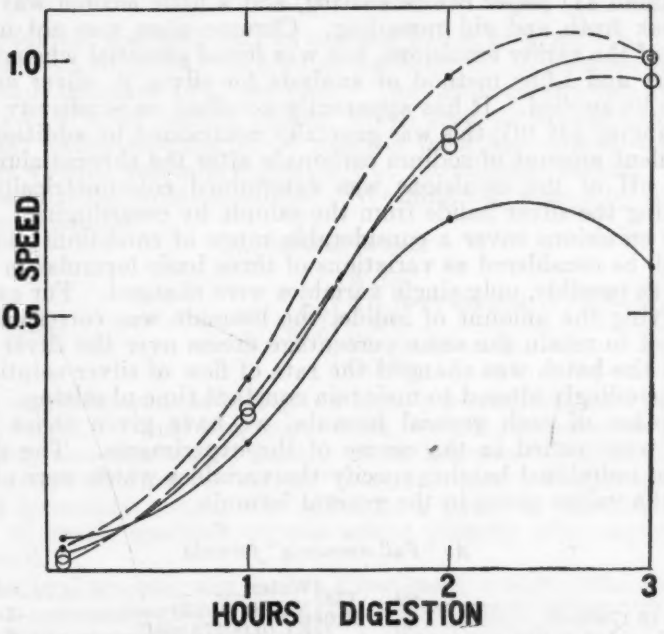

FIGURE 3.—*Speed numbers of emulsion 4–68 at four stages of after-ripening by National Bureau of Standards (.) and Jones and Russell (o) systems, plotted against time of digestion*

The maximum in each system has been made equal to 1. Dashed lines 6-minute development; solid lines, 12-minute development.

other than filtering and cooling; the normal temperature was 7° to 8° C., average hardness of the water, calculated as $CaCO_3$, 80 mg per liter. The washing was very thorough, lasting 6 to 8 hours, with frequent hand stirring of the emulsion; for experimental purposes at least it is much more satisfactory to wash completely and add soluble bromides as desired, rather than to attempt to leave a definite amount. In the absence of ammonia in the emulsion, the pH after washing was 7 ± 0.5; if it was made with ammoniacal silver oxide, the pH might be as high as 8.5.

Our methods of centrifugal washing have already been described (7) (16); briefly, at the end of the desired ripening time, the silver halide is separated from the liquid emulsion, using a 5-inch imperforate

bowl at 3,000 r. p. m. The silver halide collects on the walls of the bowl in an adherent layer carrying considerable adsorbed gelatin, but is readily reemulsified by covering with 1.5 per cent gelatin solution and rubbing gently. This "wash suspension" is again centrifuged, and the silver halide suspended in the more concentrated gelatin (about 60 g per liter) used for coating; two separations reduce the bromide ion concentration to a value comparable with that after ordinary washing.

The emulsion was always stirred continuously during mixing and ripening. This was not always practicable during digestion, but stirring was in every case frequent enough to prevent appreciable sedimentation. All emulsions were filtered through very open (Whatman 41) paper before coating, and a little alcohol was added to break froth and aid spreading. Chrome alum was not used on many of the earlier emulsions, but was found essential whenever the Weigert and Lühr method of analysis for silver + silver sulphide was to be applied. It has apparently no effect on sensitivity except by changing pH (9); this was generally neutralized by addition of an equivalent amount of sodium carbonate after the chrome alum solution. pH of the emulsions was determined colorimetrically after removing the silver halide from the sample by centrifuging.

The emulsions cover a considerable range of conditions, but they may all be considered as variations of three basic formulas in which, as far as possible, only single variables were changed. For example, in varying the amount of iodide, the bromide was correspondingly changed to retain the same percentage excess over the silver; if the size of the batch was changed the rate of flow of silver solution was correspondingly altered to maintain constant time of mixing. In the description of each general formula, we have given those factors which were varied in the course of the experiments. The descriptions of individual batches specify the variables which were changed from the values given in the general formula.

A. "Full ammonia" formula

Water	ml	125	Water	ml	225
$AgNO_3$ (0.176 mol)	g	30.0	NH_4Br (0.220 mol)	g	21.5
NH_4OH, concd. (0.353 mol) to redissolve			KI (0.00175 mol)	g	0.29
			Gelatin	g	12.5

The excess of soluble bromide was maintained at 25 per cent as given. The iodide as given corresponds to the formation of 1.0 mol per cent of AgI, assuming complete precipitation of the iodide, but iodide also was varied from 0 to 5 per cent. The solution of ammoniacal silver oxide, at about 35°, was run into the halide-gelatin solution, held at 45.0° ± 0.5° in 2½ to 4 minutes; ripening was continued at 45° C.

In case centrifugal washing was used, nothing further was added to the emulsion before centrifuging. The quantity given was centrifuged in four batches; it was suspended again in 400 ml of 1.5 per cent gelatin, and might be stored over night at 5°, at this point. After centrifuging again, the emulsion was usually suspended in a total of 700 ml of water and 50 g gelatin; it was digested in this suspension. Where the effect of ripening time was under study, the four batches were taken out at intervals during ripening and kept separate thereafter. The necessary time for centrifuging four

batches was 20 to 25 minutes, so that there was always at least this much difference in the ripening time of the first and fourth.

For ordinary washing, 37.5 g of "secondary" gelatin, previously swelled for 20 minutes in cold distilled water, was added at the conclusion of ripening, and the emulsion rapidly chilled as soon as it was dissolved. It will be noted that the total amount of gelatin in the final suspension is the same in all cases, except in the emulsions where the gelatin-silver halide ratio was the variable under study.

B. "Full ammonia" formula

Water	ml	250	Water	ml	500
$AgNO_3$ (0.353 mol)	g	60.0	NH_4Br (0.409 mol)	g	40.0
NH_4OH, concd. (0.71 mol) to redissolve			KI (0.0035 mol)	g	0.58
			Gelatin	g	30.0

This fomula was used only in one size batch, 60 g $AgNO_3$. Iodide was sufficient to give 1.0 to 5.0 mol per cent AgI, the excess bromide being kept constant at 17 per cent. The halide-gelatin solution was kept at 45.0° ± 0.5° during mixing, which took 4½ to 7 minutes, and ripening. After ripening to 25 minutes from the start of the mix, 70 g of swelled secondary gelatin was introduced, taking 7 to 10 minutes, and the emulsion chilled. Washing was always by the conventional method.

C. Neutral formula

Water	ml	450	Water	ml	350
$AgNO_3$ (0.353 mol)	g	60.0	NH_4Br (0.429 mol) or equivalent KBr	g	42.0
			KI (0.0139 mol)	g	2.30
			Gelatin	g	20.0

The excess bromide is here given as 25 per cent, but 12.5 per cent was also used. Iodide was varied from 1 to 4.0 mol per cent. Time of mixing was also varied from 9 to 30 minutes. The usual temperature was 65°, but 55° and 52° were also used. Eighty grams of swelled secondary gelatin was added to a batch of the above size; unless otherwise specified, it was added directly after mixing was completed.

Centrifugal washing was used in a few cases; except in the specified cases, no secondary gelatin was added before centrifuging. The process was the same as in formula A.

3. ANALYTICAL METHODS

Bromide ion concentration in the emulsions was determined by the silver-silver bromide electrode at 30.0° C.: the apparatus is to be described in a future paper on some of the photographic effects of bromide ion concentration in the emulsion. It was not available for some of the earlier experiments.

The silver-silver bromide electrode is described in the literature as quite imperfectly reproducible, which is correct as compared to standard reference electrodes, but by using well-annealed silver wires, carefully cleaned whenever they showed signs of sluggishness, results were reproducible to ± 1 millivolt or better. This is fortunately negligible in determining any of the photographic effects of bromide ion concentration. Determinations in the emulsions are obviously favored by the enormous surface of the silver halide present, which maintains equilibrium.

III. EFFECT OF CERTAIN VARIABLES ON AFTER-RIPENING BY DIGESTION

1. RIPENING

Because of the limited capacity of our centrifuge, the data in Table 2 were necessarily obtained by making a series of emulsions, each subdivided into batches of different ripening time; digestion time was increased from the practicable minimum for all four batches of 8–101, to a maximum of 145 minutes for 8–99. The average grain

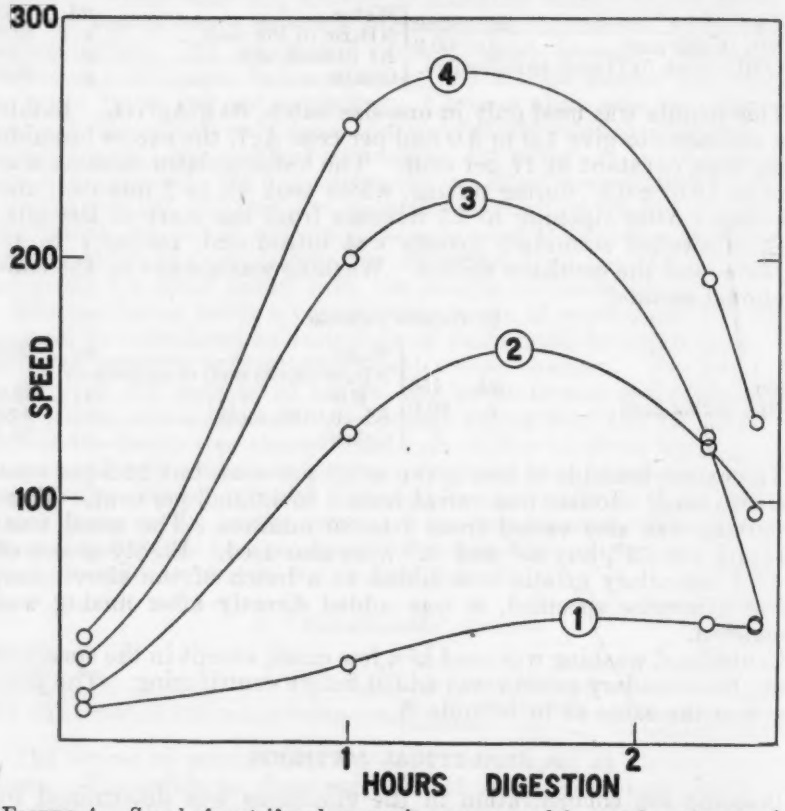

FIGURE 4.—*Speed of centrifuged ammonia-process emulsions at four times each of ripening and digestion*

Ripening time for emulsions in curve 1, approximately 5 minutes; curve 2, 0.5 hour; curve 3, 1.0 hour; curve 4, 2.0 hours

size increased normally with time of ripening: average projective areas for 8–100 were (1) 0.26 μ^2, (2) 0.39 μ^2, (3) 0.52 μ^2, (4) 1.00 μ^2. In view of the similarity of the other conditions, the differences in maximum speeds reached at optimum digestion times may reasonably be ascribed almost entirely to the change in grain size; a quantitative relation would be very difficult to obtain on these emulsions because of the heavy fog correction. In Figure 4, speed, for given ripening time, is plotted against digestion time; the data are seen to fall into a family of curves, with marked maxima. The optimum time of

digestion decreases as the time of ripening increases; as these emulsions were ripened in 0.9 N NH_3, there must have been relatively rapid formation of sensitivity nuclei during ripening, in spite of the presence of 0.11 N NH_4Br. The time of digestion to attain the optimum formation of nuclei is therefore reduced. It will be noted that the optimum digestion time is the same for one hour and two hours ripening and that the fog in the latter case is actually less; this has been previously observed. (See Table 1 reference 7.)

TABLE 2.—*Effect of previous ripening on after-ripening during digestion*

[Formula A, 1 per cent AgI centrifugal washing; Winterthur (8565) gelatin in mix digestion in untreated Winterthur (8565) gelatin]

Emulsion No.	Ripening time	Time of digestion	Speed	γ			Fog		
				3	6	12	3	6	12
	Minutes	*Minutes at 45°*							
8-101-1	6	<10	13	1.05	1.46	1.60	0.05	0.08	0.11
2	35	<10	19	.50	1.15	1.40	.19	.26	.31
3	63	<10	34	.40	.67	.77	.21	.32	.36
4	121	<10	43	.34	.50	.60	.27	52	.09
8-102-1	7	60	33	1.45	2.15	3.00	.10	.11	.15
2	33	60	128	.70	1.30	1.75	.22	.29	.39
3	63	60	200	.55	1.00		.27	.37	
4	119	60	255	.45	.80	1.15	.27	.45	.57
8-100-1	7	135	50	.95	1.45	2.03	.90	.13	.37
2	30	135	127	.70	1.05	1.55	.17	.26	.60
3	62	135	123	.70	1.03	1.37	.24	.46	.85
4	135	135	192	.57	.87	1.33	.28	.41	.82
8-99-1	12	145	49	1.30	2.14	2.77	.06	.10	.25
2	35	145	96	1.04	1.53	1.95	.14	.27	.56
2	62	145	50	.70	1.20	1.47	.27	.56	1.01
4	120	145	133	.55	.87	1.23	.21	.49	.82

TABLE 3.—*Effect of previous ripening on after-ripening during digestion*

[Neutral (C) emulsions; 1 per cent AgI; normal washing; Winterthur and Nelson No. 1 gelatin; digested at 45°]

Temperature of mix	Time of mix	Excess NH_4Br	Bromide ion concentration during digestion	Time of digestion	Speed	γ			Fog			Emulsion No.	Average grain size (projective area in μ^2)
						3	6	12	3	6	12		
	Minutes	*Per cent*		*Minutes at 45°*									
65°	36	25	$1.6 \times 10^{-4} N$	10	160	0.23	0.33	0.42	0.01	0.03	0.11	4-63-1	1.05
				60	245	.40	.63	1.01	.02	.05	.19	2	
				120	440	.46	.75	1.30	.06	.09	.25	3	
				180	505	.65	.80	1.45	.06	.11	.29	4	
55°	31½	25	$1.4 \times 10^{-4} N$	10	80	.25	.36	.48	.00	.02	.05	4-62-1	.53
				80	175	.63	1.09	1.56	.04	.06	.11	2	
				160	265	.81	1.25	1.83	.05	.07	.15	3	
				240	290	.80	1.35	1.89	.08	.11	.20	4	
52°	25½	12.5	$1.8 \times 10^{-4} N$	[1] 10	34	.36	.55	.66	.02	.04	.08	4-64-1	.34
				60	120	.84	1.22	1.75	.07	.10	.18	3	
				130	205	.92	1.14	1.88	.06	.17	.30	5	
				240	215	1.00	1.55	2.23	.16	.22	.39	7	

[1] Bromide ion concentration $7.6 \times 10^{-4} N$.

The data on neutral emulsions with the same percentage silver iodide, show the expected differences in maximum speed corresponding to changes in grain size.

The time required for digestion to maximum speed was about 220 minutes for emulsion 4–62, 195 minutes for 4–64, and 180 minutes for 4–63. It was thus reduced by increase in temperature of ripening, and by decrease in excess of soluble bromide; both of these changes obviously favor the formation of nuclei during ripening. In all three cases, it is considerably greater than is required for ammonia emulsions ripened to the same average grain size.

2. TEMPERATURE

The chemical reactions involved in after-ripening may be expected to have a temperature coefficient of two or more for every 10°. The correlation between these reactions and the photographic properties is unknown, but a similar temperature coefficient for after-ripening is a reasonable prediction. Tables 4, 5, 6, 10, and 11 show that it is verified under a variety of conditions. The rate of photographic change with time can not be satisfactorily expressed by any formula which we have tried, so we can obtain only a rough estimate. The time required to reach maximum sensitivity at 45° is about three times as great as at 55°; taking the initial slope of the speed, time of digestion curve, the coefficient is about 4.

TABLE 4.—*Effect of digestion temperature on after-ripening*

[Neutral (C) emulsion 4–58; 4 per cent AgI; Winterthur and Nelson No. 1 gelatin; normal washing; [Br⁻] $2.5\times10^{-4}N$ at start of digestion; coating pH 7.2]

Digestion temperature	Time of digestion	Speed	γ			Fog		
			3	6	12	3	6	12
	Minutes							
45.0°	10	82	0.21	0.32	0.52	0.02	0.03	0.09
	60	137	.39	.67	.86	.02	.05	.14
	128	290	.47	.64	1.20	.05	.05	.11
	240	355	.62	.87	1.37	.06	.10	.17
	360	310	.58	.82	1.24	.21	.33	.51
54.2°	40	330	.60	.92	1.36	.03	.06	.17
	80	475	.56	.90	1.39	.09	.12	.18
	120	495	.55	.84	1.39	.10	.14	.22

TABLE 5.—*Effect of digestion temperature on after-ripening*

[Neutral (C) emulsion 4–65; 1 per cent AgI; Winterthur and Nelson No. 1 gelatin; normal washing; [Br⁻] $9\times10^{-4}N$, coating pH 7.0]

Digestion temperature	Time of digestion	Speed	γ			Fog		
			3	6	12	3	6	12
	Minutes							
45°	10	32	0.32	0.42	0.63	0.00	0.02	0.05
	75	55	.47	.70	1.16	.01	.02	.05
	135	81	.64	.81	1.43	.03	.05	.10
	240	140	.78	1.21	1.90	.05	.08	.14
	360	140	1.92	1.42	2.40	.22	.26	.45
55°	30	102	.52	.80	1.47	.02	.04	.13
	60	180	.73	1.20	2.03	.05	.07	.21
	90	195	1.02	1.44	2.10	.06	.08	.23

TABLE 6.—*Effect of digestion temperature on after-ripening*

["Full ammonia (B)" emulsion, No. 1-160; 5 per cent AgI; Nelson No. 1 gelatin; initial [Br⁻] during digestion $9\times10^{-4}N$, coating pH 6.9]

Digestion temperature	Time of digestion	Speed	γ			Fog		
			3	6	12	3	6	12
	Minutes							
45°	10	81	0.30	0.33	0.37	0.00	0.03	0.09
	60	127	.84	1.16	1.60	.02	.06	.15
	120	230	.91	1.43	2.25	.04	.09	.19
	240	240	1.04	1.56	2.43	.06	.09	.21
	360	205	1.10	1.75	2.46	.08	.15	.27
54.5°	45	210	1.07	1.79	2.52	.05	.09	.19
	90	220	.91	1.42	2.37	.18	.27	.36
	135	143	1.10	1.75	2.45	.31	.48	.69

Neutral emulsions with 1 per cent AgI were digested at 45° and 55° in two narrow ranges of bromide ion concentration: Curves of speed against time are given in Figure 5 from data in Tables 5, 10, and 11. It will be noted that in the presence of added soluble bromide ([Br⁻] around 1×10^{-3} *N*), the temperature coefficient is greater than in the emulsion as washed ([Br⁻] around 1.8×10^{-5} *N*).

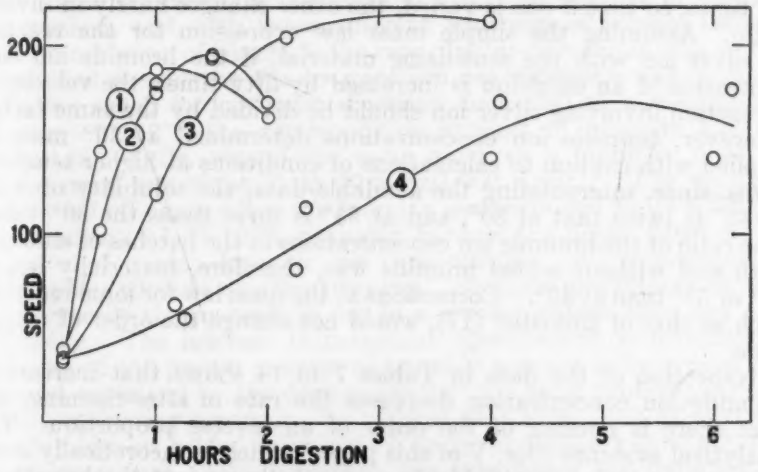

FIGURE 5.—*After-ripening of neutral emulsions, 1 per cent AgI, under varying conditions of digestion*

Curve 1, 55°, as washed; curve 2, 55°, with 5 KBr per 1,000 AgBr; curve 3, 45°, as washed; curve 4, 45°, with 5 KBr per 1,000 AgBr

The maximum sensitivity reached at 45° and at 55° C. is not widely different in any case. In spite of statements in the literature (3), (2), that low temperature and long time are generally desirable, 55° is very definitely better than 45° for the neutral emulsions with 4 per cent AgI. (Table 4.) In the neutral emulsions with 1 per cent AgI, the order depends on the bromide ion concentration during digestion. The ammonia process emulsion with 5 per cent AgI is slightly better at 45°. One feature of the long digestion at 45° is noteworthy—the sudden increase in fog after four hours (Tables 4, 5, and 10); this is not associated with sedimentation, since the emulsions were stirred continuously during this period.

3. BROMIDE ION CONCENTRATION

Any reaction forming silver or silver sulphide from silver bromide is practically sure to liberate bromide ions, the only other alternative being the formation of an un-ionized addition product. It is therefore obvious that after-ripening will be retarded by increasing bromide ion concentration,[7] if it is actually a matter of the formation of silver or silver sulphide nuclei. The extent of the retardation may be expected to throw some light on the mechanism of the reaction, although interpretation of the photographic data is again handicapped because we do not know the relation between the extent of the reaction and the resulting changes in photographic sensitivity. Sheppard and his associates have shown that the formation of silver sulphide during after-ripening takes place by rearrangement of the adsorbed complex of silver bromide and sensitizer, and we believe that the evidence indicates that, if reduction to metallic silver plays a part in after-ripening, it takes place by a similar mechanism. It is at least quite improbable that sensitivity nuclei are produced by the reduction or other reaction of the silver halide in solution in the emulsion. It may safely be assumed that in the emulsion, with the enormous available surface of the silver bromide grains, the product of silver and bromide ion concentrations is practically constant [8] at all times, so that if one is varied, the other changes nearly in inverse ratio. Assuming the simple mass law expression for the reaction of silver ion with the sensitizing material, if the bromide ion concentration of an emulsion is increased by fifty times, the velocity of a reaction involving silver ion should be divided by the same factor. However, bromide ion concentrations determined at 30° must be applied with caution to calculations of conditions at higher temperatures, since, interpolating the available data, the solubility of AgBr at 45° is twice that at 30°, and at 55° is three times the 30° value. The ratio of the bromide ion concentrations in the batches of emulsion with and without added bromide was, therefore, materially less at 45° or 55° than at 30°. Corrections to the mass law for ionic reactions such as that of Bronsted (17), would not change the order of magnitude.

Inspection of the data in Tables 7 to 14 shows that increase in bromide ion concentration decreases the rate of after-ripening, but that there is nothing of the order of an inverse proportion. The analytical evidence (Sec. V of this paper) which is theoretically much better than the photographic, is as decidedly against the hypothesis of an ionic reaction.

The curve of speed against time of digestion has a distinct S shape. This might be interpreted as an autocatalytic reaction; there is some justification for this, in that the formation of the new phase (Ag or Ag_2S) might catalyze the further breakdown of the silver bromide-sensitizer addition product. It is more likely that it represents the varying rate of change in photographic sensitivity with a relatively constant rate of reaction; if we assume that fog is caused by the formation of oversize sensitivity nuclei (18), the enormous increase

[7] The concentrations used during ripening and digestion were of different orders of magnitude; the maximum amount present during digestion probably tends to decrease the solubility of silver bromide by mass action, rather than to raise it by complex ion formation as do the high concentrations used in ripening.

[8] The solubility product of silver bromide is not affected by the gelatin (Winther, Trans. Faraday Soc., **19**, p. 280; 1923); it must be slightly affected by the proportion of silver iodide, but our statement is correct for the results of adding soluble bromide to a given emulsion.

in fog, which can occur if after-ripening is continued too long, indicates that only a small proportion of the sensitizer has been used when the sensitivity reaches its maximum. On this basis, the relatively flat maximum found in most cases is readily explained by a balance between the grains still increasing in sensitivity and those lost by increase in fog or reduced in sensitivity by competition between nuclei (20). This reasoning must be used with caution, as the growth of fog has some of the characteristics of a secondary reaction. (See discussion (18).) This in turn may be explained by the very probable assumption that the hydrolysis of the gelatin during ripening or digestion continually liberates active sensitizing or fogging materials from less labile compounds. The curves of speed against time of digestion could not be fitted by any simple equation with sufficient accuracy so that the constants would be useful as a measure of change in sensitivity. One of the most obvious extensions of this investigation will be a more accurate and complete determination of the progress of after-ripening under known conditions, such as inert gelatin plus a sensitizer.

Tables 7 to 14 are designed to show the effect of bromide concentration during digestion, with a wide variety of emulsions. The most complete set of data on a single type are given in Table 9 and Figure 6. These represent the digestion of a high-speed type of emulsion as washed, and with three different additions of soluble bromide. On examination of Figure 6, the rate of after-ripening is seen to have decreased steadily as the bromide ion concentration was increased, but the speed for optimum digestion time rose to a maximum at $[Br^-]=9.6\times10^{-4}$; the corresponding amount of bromide added, 5 KBr/1,000 AgBr, was of the same order as is found in most fast commercial emulsions (3 to 10 KBr/1,000 AgBr).[9] The maximum speed fell off again when the bromide was increased to 20 KBr/1,000 AgBr ($[Br^-]=4.7\times10^{-3}$), probably because the direct effect on sensitivity of a high bromide ion concentration (19) counteracts the favorable influence on after-ripening. Bromide present during digestion retards the increase in fog to a greater extent than the after-ripening. The increase in maximum speed which is permitted by the use of the proper amount of bromide appears to be greater than can be explained by the decrease in fog; the same problem comes up when increasing amounts of a nuclear sensitizer, such as allyl thiocarbamide, are added to emulsions under presumably constant digestion conditions (20). Sheppard has introduced the hypothesis of competition between nuclei on the same grain to explain the existence of an optimum concentration of sensitizer. This may equally well be applied to the existence of an optimum time of digestion, and less plausibly, to the increase in maximum speed obtained by adding bromide before digestion. In this last case the reduced rate of reaction might favor the continued growth of a single nucleus as against the further formation of new ones. Many of our emulsions (Sec. IV of this paper) have reached higher sensitivity by storage ripening than by digestion; here we have a slow process in which the formation of a new phase might be strongly inhibited, so that again the

[9] Our analyses, which agree with those published by the Eastman laboratories at various times, show that soluble bromide is either added after washing, or else the washing is stopped short of completion. Wall, Photographic Emulsions, p. 154, refers to the addition of bromide as "an heirloom from the early days when a clean-working emulsion was practically an exception," but present quantities are, instead, considerably larger than those recommended by Eder.

growth of a nucleus already started would be favored against the beginning of a new one.

The after-ripening of all the types of emulsion is qualitatively very similar. We may make the rough generalizaton that a given amount of soluble bromide (5 KBr/1,000 AgBr) retards after-ripening most in those cases where it is the most rapid at a given temperature; the ammonia-process emulsions furnish the examples of this, prob-

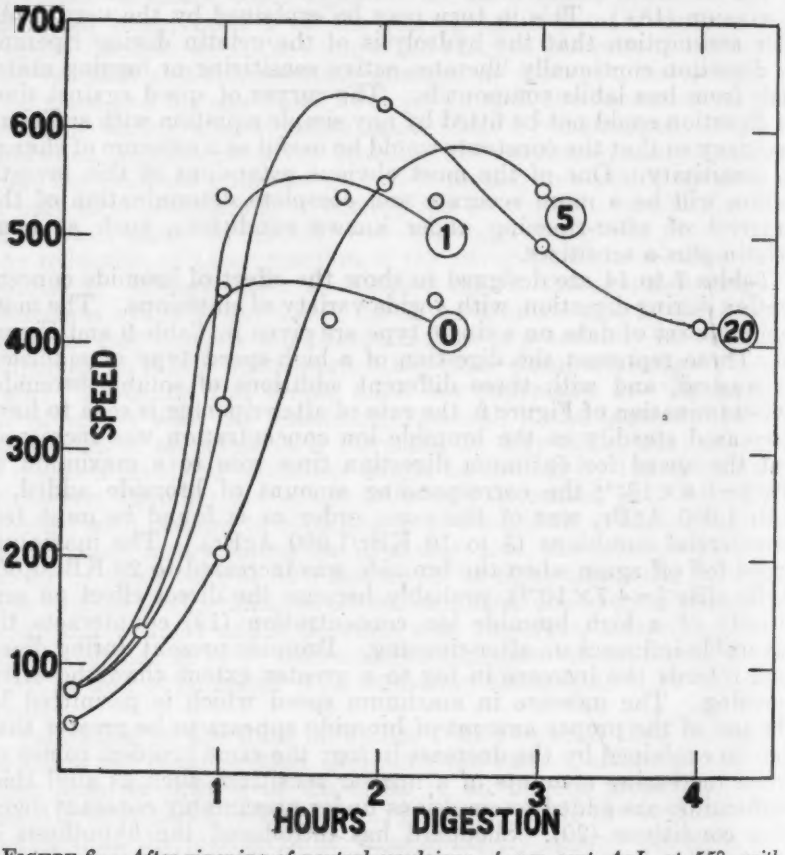

FIGURE 6.—*After-ripening of neutral emulsions, 4 per cent AgI, at 55°, with varying concentrations of soluble bromide*

Numbers of curves indicate the amount of bromide added, in terms of mols KBr per 1,000 mols AgBr

ably because of their higher pH. We have already observed the greater effect on emulsion 4–64 (Table 10) which was digested at 45°, as compared to the otherwise identical 4–66, digested at 55° (Table 11). Much more complete data will be necessary for mathematical analysis of any of the cases.

Increase in fog during after-ripening was less than we had expected. Table 12 gives an unusually favorable case in which there was actually a decrease. In general, the fog increases suddenly after a certain time, but this is usually past that required for the maximum sensi-

tivity: after-ripening is more likely to be limited by decrease in speed than by increase in fog. The addition of soluble bromide considerably increases the margin of safety in time between the points of maximum sensitivity and of rapid increase in fog, and reduces the rate of increase of fog during the useful period of digestion. We have already noted (p. 231) that the cases in which the sudden deterioration began before the maximum sensitivity was reached were on prolonged digestion at 45°.

TABLE 7.—*Effect of bromide ion concentration during digestionon after-ripening*

[Emulsion 4-53; neutral "C" formula; 4 per cent AgI, 25 per cent excess NH_4Br; mixed at 65°; Winterthur gelatin; digested at 55°; coating pH 5.9]

Bromide ion concentration at beginning of digestion	Time of digestion	Speed	γ			Fog		
			3	6	12	3	6	12
	Minutes							
6.4×10^{-4} *N* (as washed)	5	42	0.31	0.48	0.63	0.02	0.05	0.09
	30	92	.58	.92	1.21	.02	.04	.13
	60	200	.63	1.01	1.25	.03	.07	.13
	100	350	.64	1.03	1.23	.05	.11	.17
5.1×10^{-4} *N* $\left(\frac{5\ KBr}{1{,}000\ AgBr}\right)$	5	17	.27	.35	.40	.02	.04	.09
	30	31	.37	.57	.73	.02	.04	.09
	68	100	.43	.67	.96	.03	.06	.09
	135	270	.54	.86	1.08	.04	.07	.11

TABLE 8.—*Effect of bromide ion concentration during digestion on after-ripening*

[Emulsion 4-59; 4 per cent AgI; 25 per cent excess NH_4Br; Winterthur gelatin; neutral mixed at 65° followed by ammonia ripening at 45°; coating pH 6.8. Digested at 55°]

Bromide ion concentration at beginning of digestion	Time of digestion	Speed	γ			Fog		
			3	6	12	3	6	12
	Minutes at 55°							
1.2×10^{-3} *N* (as washed)	5	70	0.34	0.50	0.66	0.03	0.04	0.13
	45	300	.63	1.07	1.49	.04	.10	.21
	90	390	.66	.94	1.24	.09	.11	.16
	135	340	.59	-------	1.45	.20	-------	.31
3.3×10^{-4} *N* $\left(\frac{2.5\ KBr}{1{,}000\ AgBr}\right)$	45	182	.49	.85	1.15	.04	.08	.17
	95	400	.60	1.03	1.47	.06	.11	.24
	140	420	.53	.80	1.26	.15	.19	-------
	190	[1] 315	.65	1.01	1.51	.19	.24	.34

[1] No decrease in effective sensitivity.

TABLE 9.—*Effect, on after-ripening, of bromide ion concentration during digestion*

[Emulsions 4-61 and 4-68; neutral (*C*), 4 per cent AgI, 25 per cent excess NH_4Br, Winterthur and Nelson No. 1 gelatin; mixed at 65° in 26–7 minutes]

Soluble bromide added after washing	Bromide ion concentration at beginning of digestion	Time of digestion	Speed	γ			Fog			Emulsion No.
				3	6	12	3	6	12	
		Minutes at 55°								
None	$1.5\times10^{-3}N$	60	450	0.81	1.04	1.50	0.09	0.14	0.26	4-61-2
		100	425	.65	1.06	1.60	.19	.34	.54	4
		140	440	.64	.96	1.50	.22	.43	.67	6
1 KBr / 1,000 AgBr	$1.5\times10^{-4}N$	30	132	.51	.83	1.24	.02	.04	.14	4-68-1
		60	535	.54	1.23	1.45	.06	.10	.20	2
		105	535	.57	.99	1.56	.10	.18	.29	3
		140	535	.66	1.06	1.65	.10	.18	.31	4
5 KBr / 1,000 AgBr	$9.6\times10^{-4}N$	5	76	.16	.20	.32	.03	.08	.13	4-61-1
		60	345	.46	.76	1.24	.05	.08	.14	3
		120	625	.64	.90	1.53	.08	.13	.18	5
		180	495	.66	.90	1.43	.16	.29	.37	7
		240	420	.66	1.12	1.68	.13	.24	.40	8
20 KBr / 1,000 AgBr	$4.7\times10^{-3}N$	5	45	.21	.25	.47	.00	.02	.05	4-68-5
		60	205	.35	.53	.80	.01	.03	.06	6
		120	550	.42	.73	1.20	.04	.05	.11	7
		180	545	.50	.90	1.54	.06	.09	.16	8

TABLE 10.—*Effect of bromide ion concentration during digestion, on after-ripening*

[Neutral (C) emulsion No. 4-64; 1 per cent AgI, Winterthur and Nelson No. 1 gelatin; digested at 45°]

Bromide ion concentration during digestion	Time of digestion	Speed	γ			Fog		
			3	6	12	3	6	12
	Minutes at 46°							
$7.6\times10^{-4}N\left(\frac{5\text{ KBr}}{1{,}000\text{ AgBr}}\right)$	10	34	0.36	0.55	0.66	0.02	0.04	0.08
	70	62	.46	.77	1.13	.02	.04	.09
	140	114	.64	.94	1.20	.04	.07	.13
	245	165	.66	1.04	1.76	.07	.09	.16
	370	175	.71	1.13	2.11	.27	.46	.67
$1.8\times10^{-3}N$ (as washed)	60	121	.84	1.22	1.75	.07	.10	.18
	130	205	.92	1.14	1.88	.06	.17	.30
	240	215	1.00	1.55	2.23	.16	.22	.39

TABLE 11.—*Effect of bromide ion concentration during digestion, on after-ripening*

[Emulsion 4-66, neutral (C) formula, 1 per cent AgI; Winterthur and Nelson No. 1 gelatin; digested at 55°]

Bromide ion concentration at beginning of digestion	Time of digestion	Speed	γ			Fog		
			3	6	12	3	6	12
	Minutes at 55°							
$1.5\times10^{-3}N$ (as washed)	30	150	1.12	1.83	2.35	0.09	0.13	0.22
	60	190	1.23	1.55	2.38	.15	.24	.37
	90	180	1.01	1.41	2.12	.13	.20	.36
	120	160	.83	1.60	1.91	.11	.21	.48
$1.2\times10^{-3}N\left(\frac{5\text{ KBr}}{1{,}000\text{ AgBr}}\right)$	5	39	.26	.33	.48	.00	.00	.03
	60	175	.65	1.18	1.85	.03	.08	.18
	90	195	.80	1.26	2.23	.08	.11	.26
	120	170	1.02	1.63	1.88	.10	.14	.34

TABLE 12.—*Effect on after-ripening of bromide ion concentration during digestion*

[Emulsion 1-159; "B" formula, 5 per cent AgI, Nelson No. 1 gelatin. Digested at 45°, pH 8.3; coating pH 6.1]

Bromide ion concentration at beginning of digestion	Time of digestion,	Speed	γ			Fog		
			3	6	12	3	6	12
	Minutes at 45°							
$3.3\times10^{-4}N$ (No bromide added after washing)	<10	59	0.41	0.63	0.95	0.01	0.06	0.19
	53	110	.65	1.37	2.27	.01	.07	.28
	110	200	.79	1.37	2.04	.01	.07	.16
	180	200	.85	1.56	2.32	.02	.06	.15
$5.8\times10^{-4}N$ (5 KBr per 1,000 AgBr added after washing)	<10	22	.25	.37	.44	.07	.09	.21
	60	28	.40	.81	1.00	.01	.06	.19
	120	49	.54	.93	1.16	.02	.07	.12
	205	92	.66	1.15	1.60	.01	.06	.09

TABLE 13.—*Effect on after-ripening of bromide ion concentration during digestion*

[Emulsion 1-161; "B" formula, 5 per cent AgI, Winterthur gelatin. Digested at 45°, pH 8.0]

Bromide ion concentration at beginning of digestion	Time of digestion,	Speed	γ			Fog		
			3	6	12	3	6	12
	Minutes at 45°							
$1.8\times10^{-4}N$ (No bromide added after washing)	60	165	0.66	1.28	1.95	0.02	0.08	0.21
	130	320	.73	1.34	1.94	.04	.12	.27
	185	360	.82	1.47	2.14	.07	.12	.29
$8.6\times10^{-4}N$ (5 KBr per 1,000 AgBr added after washing)	<10	66	.22	.51	.61	.00	.03	.14
	90	115	.55	.89	1.12	.01	.04	.15
	180	240	.63	1.03	1.60	.02	.04	.14
	270	340	.71	1.15	1.68	.03	.04	.18
	360	400	.74	1.29	1.77	.11	.13	.24

TABLE 14.—*Effect on after-ripening of bromide ion concentration during digestion*

[Emulsion 1-162; "B" formula, 1 per cent AgI, Winterthur gelatin. Digested at 45°, pH 8.3]

Bromide ion concentration at beginning of digestion	Time of digestion,	Speed	γ			Fog		
			3	6	12	3	6	12
	Minutes at 45°							
$1.75\times10^{-4}N$ (No bromide added after washing)	60	87	0.95	1.70	2.13	0.01	0.07	0.19
	120	105	1.10	2.04	2.72	.04	.09	.27
	180	108	1.16	1.94	2.72	.06	.13	.33
$8.6\times10^{-4}N$ (5 KBr per 1,000 AgBr added after washing)	<10	46	.88	1.23	1.59	.00	.02	.10
	60	60	1.00	1.36	1.63	.01	.02	.10
	125	75	.95	1.44	1.78	.00	.02	.09
	210	88	1.01	1.51	2.02	.01	.04	.16
	300	107	1.02	1.65	2.23	.00	.06	.19

4. COMPARISON OF BROMIDE AND CHLORIDE IONS

The effect of bromide and chloride ions on after-ripening would be expected to be qualitatively similar; a considerable quantitative difference is introduced because the solubility of silver chloride (in mols per liter) is sixteen times that of the bromide, and the effect of chloride on silver ion concentration is correspondingly smaller. We should hardly have taken up this point if commercial emulsions had not been found (by electrometric titration of extracts) to contain as much as 38 mols of soluble chloride per 1,000 of silver halide. This

amount can be introduced into the emulsion by adding gelatin after washing, since some brands, especially those of European manufacture, were found to contain as much as 3.0×10^{-4} mol of soluble halide per gram of gelatin. We have never found it necessary to use this procedure, but it is recommended in many emulsion formulas; the reason, when any is given, is to make the emulsion set more readily.

TABLE 15.—*Comparison of effects of bromide and chloride ions on after-ripening during digestion.*

[Neutral ("C") emulsions, Winterthur gelatin, normal washing]

Mol per cent AgI in emulsion	Soluble halide added after washing, in mols per 1,000 mols AgBr	Time of digestion, hours at 45°	Speed	γ			Fog		
				3	6	12	3	6	12
0.0	0	<0.2	44	0.47	0.78	0.87	0.09	0.18	0.28
	0	2.5	64	.58	.83	1.03	.10	.15	.28
	1 KBr	2.5	69	.70	1.12	1.30	.08	.23	.39
	50 NaCl	2.5	68	.50	.77	.90	.10	.20	.36
0.0	0	<.2	40	.48	.80	1.07	.08	.17	.33
	0	2.5	56	.68	1.00	1.21	.10	.19	.40
	1 KBr	2.5	61	.63	1.10	1.42	.08	.18	.36
	50 NaCl	2.5	39	.64	.93	1.14	.09	.18	.40
1.0	0	<.2	49	.46	.69	.92	.03	.04	.14
	0	2.5	82	.69	1.10	1.58	.05	.12	.25
	1 KBr	2.5	69	.67	.96	1.34	.02	.08	.18
	50 NaCl	2.5	84	.60	.86	1.30	.04	.09	.27
2.25	0	2.5	55	.61	.88	1.25	.03	.11	.20
	1 KBr	2.5	34	.44	.59	.80	.02	.05	.14
	25NaCl	2.5	47	.44	.64	.90	.03	.08	.21
2.25	0	<.2	57	.37	.54	.65	.05	.12	.21
	0	2.5	70	.53	.74	1.12	.08	.14	.27
	1 KBr	2.5	63	.47	.67	1.03	.08	.13	.27
	50 NaCl	2.5	70	.37	.56	.80	.07	.14	.27

TABLE 16.—*Comparison of effects of bromide and chloride ions on after-ripening by digestion*

["A" emulsions, Winterthur gelatin, normal washing]

Ripening temperature	Mol per cent AgI in emulsion	Soluble halide added after washing, mols per 1,000 mols AgBr	Time of digestion, hours at 45°	Speed	γ			Fog		
					3	6	12	3	6	12
40°	0.0	0	2.5	119	1.43	2.02	2.70	0.05	0.08	0.17
		1 KBr	2.5	39	1.35	1.90	2.35	.02	.07	.08
		25 NaCl	2.5	86	1.40	1.90	2.50	.02	.06	.11
	1.0	0	<.2	63	1.45	2.04	2.57	.05	.07	.13
		0	2.5	134	1.80	2.58	3.20	.05	.13	.21
		1 KBr	2.5	87	1.46	2.10	2.70	.02	.07	.10
		25 NaCl	2.5	150	1.55	2.10	2.90	.03	.11	.16
	2.25	0	<.2	27	1.70	2.30	2.60	.02	.08	.19
		0	2.7	58	2.25	3.30	4.60	.05	.10	.29
		1 KBr	2.7	34	2.00	2.60	2.80	.02	.07	.17
		25 NaCl	2.7	63	1.70	2.42	3.04	.03	.09	.25
45°	0.0	0	<.2	63	1.06	1.60	2.38	.06	.10	.24
		0	2.5	125	1.30	1.93	2.40	.06	.12	.30
		1 KBr	2.5	92	1.27	1.83	2.63	.05	.12	.29
		50 NaCl	2.5	141	1.23	1.63	2.32	.04	.11	.27
	1.0	0	<.2	61	.95	1.35	1.85	.03	.09	.25
		0	2.5	146	1.21	1.84	2.70	.06	.09	.34
		1 KBr	2.5	124	1.10	1.65	2.30	.04	.09	.28
		50 NaCl	2.5	167	1.12	1.45	2.15	.03	.11	.30
	2.25	0	<.2	44	1.22	1.90	2.30	.05	.10	.18
		0	2.5	77	1.58	2.24	2.95	.05	.13	.27
		1 KBr	2.5	55	1.55	2.40	3.00	.04	.08	.24
		50 NaCl	2.5	79	-------	1.90	2.64	-------	.10	.27

The experiments recorded in Tables 15 and 16 were made earlier than those in Tables 1, 2, and 3; the silver electrode apparatus was not yet in use, and the emulsions were all digested for 2½ hours at 45°.[9] This was near the optimum time for digestion, without added halide, of all the emulsions on which this point had been determined. It was possibly too much for the pure bromide emulsions, and very probably too little for those with 2.25 per cent AgI, so the results are considerably confused by the varying positions of this single time on the curve; they illustrate more than anything else, the danger of this procedure. The obvious difference between chloride and bromide is the depressing action of the former on the contrast. Higher densities were selectively depressed, with the result that the speed number was frequently highest in the batch digested with chloride.[10] It is impossible from these data to give an accurate estimate of the amount of chloride necessary to produce an effect equivalent to one part of bromide, but the ratio must be of the order of 50 to 1.

5. HYDROGEN ION CONCENTRATION

The reversible effect of hydrogen ion concentration on sensitivity was discovered by Rawling and Glassett (4) in an investigation of after-ripening. Rawling also mentions (9) the existence of an irreversible effect. We have measured changes in sensitivity in connection with the equilibrium between hydrogen ion, silver ion, and gelatin (to be published later), but have done relatively little with the important relation between hydrogen ion concentration and the rate of after-ripening.

The data in Table 17 make it possible to compare the after-ripening, during a single time of digestion, in two portions of the same emulsion at different hydrogen ion concentrations. Since figures are given for unripened and ripened portions at each value of pH, it is possible to eliminate the direct effect of hydrogen ion concentration on sensitivity; the work of Rawling (9) has shown that the ratio of sensitivity at two values of pH is unaffected by sensitization with thiocarbamide, and may, therefore, be expected to be independent of the degree of after-ripening. Comparing the ratios of the digested and undigested portions of both 1–148 and 1–149, it is evident that there was much less after-ripening at the lower pH. In emulsion 1–148, the speed of the undigested portion of pH 6 was 0.89 times that of the undigested portion of pH 8; the corresponding ratio for the portions digested without bromide is 0.56. In emulsion 1–149 the corresponding ratios are 0.85 undigested and 0.65 digested. In both emulsions γ was nearly independent of pH, so that the sensitivity ratio may be measured by the speed alone.

[9] Data on the undigested emulsions are given for comparison in most cases.

[10] The data on pure bromide emulsions, Table 15, show a higher speed for the batches digested with bromide than those digested as washed; this is almost certainly because the latter were past the optimum.

TABLE 17.—*Variation in both hydrogen and bromide ion concentrations during digestion*

[Emulsions made by "A" formula Winterthur gelatin]

Emulsion No.	Soluble bromide added after washing, mols per 1,000 mols AgBr	pH	Time of digestion	Speed	γ			Fog		
					3	6	12	3	6	12
			Hours at 45°							
1–148, pure AgBr	0	8.1	<0.2	62	0.90	1.57	2.10	0.05	0.09	0.18
	0	8.1	2.3	126	1.12	1.74	2.26	.09	.13	.24
	2	8.1	2.3	70	1.00	1.70	2.10	.05	.09	.14
	0	6.0	<.2	55	.95	1.37	1.98	.06	.09	.21
	0	6.0	2.3	65	1.06	1.67	2.24	.05	.15	.25
	2	6.0	2.3	54	.88	1.50	2.02	.06	.09	.17
1–149 2.25 mol per cent AgI	0	8.2	<.2	33	1.55	1.80	2.40	.06	.12	.33
	0	8.2	2.5	45	2.15	3.05	4.40	.07	.14	.49
	2	8.2	2.5	37	1.86	2.60	3.70	.05	.14	.40
	0	6.5	<.2	28	1.67	2.26	3.00	.05	.12	.37
	0	6.5	2.5	29	1.90	2.78	4.28	.05	.17	.55
	2	6.5	2.5	13	1.90	2.64	3.90	.05	.14	.49

The emulsions listed in Table 18 were not tested without digestion, so that the reversible pH effect can not be eliminated; the object of this series was to compare the effect of a given addition of soluble bromide at two hydrogen ion concentrations. The result of changing pH before digestion is seen to be highly dependent on the gelatin, as already observed by Rawling for the reversible effect. The decrease in sensitivity with decreasing pH was greatest in emulsion 4–41. Emulsions 1–151 and 4–43, made with the same gelatin by different formulas, showed about the same effect, in agreement with the observations of Rawling; the magnitude is less than in 4–41. In emulsion 4–42, the normal effect of pH showed only on addition of bromide; when the emulsion was digested as washed, the very heavy fog at the higher pH indicates excessive after-ripening with consequent loss of speed, which obscures the normal effect. In this connection, it may be pointed out that, while our data agree with those of Rawling that the fog is practically independent of changes in pH just before coating, it is frequently dependent on pH during digestion.

In Tables 17 and 18 there are six cases in which a given amount of soluble bromide was added to two portions of the same emulsion, adjusted to different hydrogen ion concentrations. With the exception of emulsion 1–148, the bromide retarded after-ripening to a greater extent at the lower pH. The comparison was made only at a single time of digestion, and is less satisfactory than the complete curve of after-ripening against time, but it seems sufficient. This result may be stated in another way, that the effect of hydrogen ion concentration on after-ripening is greater at a lower bromide ion concentration. In this form, it may be predicted from the data on bromide ion concentration given in Table 18. On increasing the hydrogen ion concentration of an emulsion, there is a decrease in bromide ion concentration, because silver ions previously in combination with the gelatin are released. This decreasein bromide ion concentration acts in opposition to the increase in hydrogen ion concentration, since it accelerates after-

ripening. In thoroughly washed emulsions, with very low bromide ion concentrations, the proportional change in concentration is much larger than in those to which soluble bromide has been added after washing; the observed effect of changing pH is therefore less.

TABLE 18.—*Variation in both hydrogen and bromide ion concentrations during digestion*

[All batches digested two and one-half hours at 45°. Emulsion 1–151 made by formula "A"; emulsions 4–41, 42, 43 made by that given by Rawling, reference 9, with increased time and temperature for the addition of the neutral silver nitrate solution]

Emulsion No.	Mol per cent AgI	Gelatin	Soluble bromide added after washing, mols per 1,000 mols AgBr	pH	Bromide ion concentration N	Speed	γ			Fog		
							3	6	12	3	6	12
1–151	1.0	UCOP 3029	0.0	7.0	5.4×10^{-4}	97	1.16	1.77	2.54	0.04	0.08	0.25
			1.0	7.0	4.3×10^{-4}	75	1.08	1.50	2.20	.02	.07	.16
			0.0	5.7	1.0×10^{-4}	83	1.04	1.53	2.70	.01	.11	.22
			1.0	5.7	3.1×10^{-5}	58	.97	1.55	2.08	.00	.08	.21
4–41	4.0	Winterthur	0.0	7.7	7.4×10^{-4}	405	.67	1.04	1.48	.28	.50	.74
			2.4	7.7	2.5×10^{-4}	360	.77	1.35	1.86	.08	.13	.24
			0.0	5.5	7×10^{-7}	135	.75	1.25	1.98	.10	.22	.37
			2.4	5.5	2.3×10^{-4}	88	.67	1.25	1.98	.02	.08	.18
4–42	4.0	UCOP R–1333	0.0	7.8	8.5×10^{-4}	330	.71	1.07	1.50	.41	.76	1.37
			2.4	7.8	2.8×10^{-4}	290	.78	1.20	1.77	.24	.50	1.02
			0.0	5.9	1.1×10^{-4}	485	.63	1.15	1.80	.08	.24	.44
			2.4	5.9	2.4×10^{-4}	220	.83	1.40	2.10	.05	.20	.26
4–43	4.0	UCOP 3029	0.0	7	8.5×10^{-4}	160	1.00	1.55	2.25	.07	.11	.21
			1.0	7.5	8.2×10^{-3}	130	1.03	1.52	2.18	.04	.08	.18
			0.0	5.7	1.3×10^{-4}	123	.91	1.51	2.40	.02	.09	.22
			1.0	5.7	5.6×10^{-5}	87	.96	1.52	2.44	.02	.08	.20

6. GELATIN

(a) GELATIN-SILVER HALIDE RATIO

The addition of gelatin to the emulsion after washing frequently results in a decrease in sensitivity. In a few cases only this can be explained by decreased after-ripening as the result of adding chloride with the gelatin. The effect of gelatin-silver halide ratio per se was determined by the use of the centrifuge process, portions of the silver halide from a single batch of emulsion being suspended and digested in varying amounts of gelatin. Table 19 gives the results with two concentrations each of three gelatins of varying activity, the entire experiment being repeated with a change in the gelatin used for emulsification. Table 20 gives data on a single emulsion, with four different concentrations of the same gelatin used for after-ripening. It is evident that the speed is practically unaffected, but there is an appreciable decrease in contrast with increasing gelatin concentration. In Table 20 the values of c and u for the underexposure region (22) show that the effect is essentially the same here. It may readily be explained by a decrease in the rate of development in the thicker film.

Tables 21 and 22 show the results of adding gelatin to washed emulsions at the start of after-ripening. The depression in contrast was produced in all cases. In the ammonia-process emulsions, the addition of untreated gelatin also produced a distinct decrease in speed, and usually an appreciable increase in fog. If the gelatin had

been thoroughly washed, or treated with ammonia and washed, before adding it to the emulsion, neither speed nor fog was affected and only the decrease in contrast was observed. The chloride in the untreated Winterthur gelatin amounted to 13 mols per 1,000 of silver bromide, which would be hardly appreciable. The pH of the ammonia-process emulsions was appreciably decreased, since the untreated Winterthur gelatin has a pH of 5.2, the Nelson No. 1, 7.0. This again is not sufficient to account for the results, although the sum of the chloride and pH effects would be appreciable. It is probable that in the ammonia-process emulsions, which were further sensitized (in the sense of formation of nuclei) before digestion, the addition of the untreated gelatin increased the amount of available sensitizers past the optimum.

TABLE 19.—*Effect of gelatin-silver halide ratio on sensitivity*

["Full ammonia" (A) emulsions, 1 per cent AgI, washed by centrifuge and suspended in 3 different gelatins at 2 concentrations. All batches digested at two and one-half hours at 45°]

Gelatin used for mix and ripening	Gelatin used for digestion and coating	Gelatin-silver halide ratio	Speed	γ			Fog		
				3	6	12	3	6	12
Winterthur (8763) untreated emulsion 8–156.	Winterthur (8763) untreated	1.51:1	34	1.26	2.00	2.80	0.08	0.17	0.38
		2.31:1	32	1.17	1.97	2.20	.07	.11	.25
	Winterthur (8763) washed	1.51:1	12.6	------	1.41	1.78	.08	.11	.14
		2.31:1	15.4	.84	1.26	1.46	.06	.14	.20
	Drescher (6136) digested with NH_3 and washed	1.51:1	14.9	1.50	1.82	2.30	.08	.12	.18
		2.31:1	13.8	1.05	1.54	1.85	.08	.13	.19
Winterthur (8763) washed emulsion 8–155.	Winterthur (8763) untreated	1.51:1	78	1.01	1.53	2.10	.14	.24	.55
		2.31:1	72	.81	1.31	1.80	.08	.27	.55
	Winterthur (8763) washed	1.51:1	11.6	1.00	1.33	1.45	.08	.11	.18
		2.31:1	11.4	.95	1.23	1.55	.05	.14	.21
	Drescher (6136) digested with NH_3 and washed	1.51:1	15.0	1.20	1.63	2.00	.07	.11	.21
		2.31:1	13.9	1.02	1.42	1.75	.06	.14	.22

TABLE 20.—*Effect of gelatin-silver halide ratio on sensitivity*

[Centrifuge-washed (A) emulsion, 1 per cent AgI, suspended in washed Winterthur gelatin at varying gelatin-silver halide ratios, and digested two and one-half hours at 45°]

Ratio gelatin: Silver halide	Speed	γ			Fog			c	u
		3	6	12	3	6	12		
1.07:1	9.5	1.27	1.65	2.10	0.11	0.14	0.20	0.02	0.38
1.51:1 (normal)	9.	1.10	1.36	1.68	.06	.10	.18	.01	.30
2.14:1	9.	1.04	1.40	1.60	.06	.12	.19	.03	.30
3.01:1	9.	.85	1.06	1.58	.06	.11	.18	.01	.28

TABLE 21.—*Effect on after-ripening of gelatin added after washing*

[Gelatin was added to portions of the emulsion on remelting after washing, raising the gelatin-silver halide ratio from the usual 1.51:1 to 2.31:1]

Emulsion	Time of digestion	Gelatin added after washing	Speed	γ			Fog			pH
				3	6	12	3	6	12	
	Hours at 45°									
1-139, "A" formula 1 per cent AgI.	0.2	None	30	1.54	2.10	2.42	0.01	0.08	0.18	8.0
	2.5	do	66	1.98	2.80	3.60	.04	.10	.28	8.0
	2.5	Winterthur (8763) untreated.	50	1.36	2.05	2.75	.07	.16	.44	7.5
	2.5	Winterthur (8763) digested with NH_3 and washed.	63	------	2.27	3.00	------	.13	.25	8.0
4-28, "C" formula 12 per cent excess KBr 2¼ g AgI.	2.5	None	58	1.07	1.43	2.05	.12	.18	.42	7.0
	2.5	Winterthur (8763) washed in sheets.	61	.74	1.13	1.65	.08	.17	.34	7.0
	2.5	Winterthur (8763) washed in shreds.	69	.75	1.14	1.62	.08	.15	.34	7.0
	2.5	Winterthur (8763) digested with NH_3 and washed.	67	.78	1.17	1.67	.08	.18	.40	7.0
1-140, "A" formula 5 per cent AgI.	.2	None	41	.53	.68	.77	.03	.12	.24	8.0
	2.5	do	140	1.27	1.76	2.05	.05	.12	.28	8.0
	2.5	Winterthur (8763) untreated.	102	1.06	1.60	2.34	.04	.14	.33	7.5
	2.5	Winterthur (8763) digested with NH_3 and washed.	145	.87	1.27	1.60	.03	.14	.30	8.0

TABLE 22.—*Effect on after-ripening of gelatin added after washing*

Emulsion	Gelatin added after washing	Time of digestion	Speed	γ			Fog		
				3	6	12	3	6	12
		Minutes at 45°							
4-11, 5 per cent AgI 12 per cent excess NH_4Br Winterthur gelatin "C" formula.	None	10	20	1.00	1.30	1.70	0.05	0.08	0.13
		75	92	1.15	1.85	2.07	.05	.14	.22
		130	150	1.08	1.70	2.60	.04	.15	.37
		195	155	1.07	1.65	2.50	.07	.17	.38
	60 per cent more	60	94	.86	1.37	1.57	.05	.12	.17
		120	165	1.00	1.60	1.70	.04	.14	.26
		180	205	.90	1.40	1.97	.05	.15	.39
1-118, 1 per cent AgI Nelson No. 1 gelatin "B" formula.	None	10	62	.85	1.30	1.72	.06	.12	.27
		75	195	.92	1.38	1.90	.06	.19	.42
		135	255	.87	1.55	2.08	.09	.20	.56
		210	240	.96	1.44	1.87	.10	.32	.70
	60 per cent more	60	75	.80	1.30	1.75	.09	.22	.50
		125	108	.71	1.10	1.61	.13	.35	.77
		200	105	.63	1.10	1.50	.18	.41	.91

(b) MAKE OR BATCH OF GELATIN

The results of the entire process of emulsion making are notoriously dependent on the gelatin which is used, and after-ripening is affected as much as any other step. We shall not attempt in this paper anything more than recognition of this fact, with a few illustrations of the results of substituting different gelatins in a given formula.

Table 23 compares results for the "C" formula, with 4.0 mol per cent AgI and 25–7 minutes mixing time. With suitable gelatin, such as the Winterthur-Nelson combination, this will give an emulsion which would be rated commercially as very fast. We have included results with a sample of deashed gelatin. The deashing

process can cause considerable deactivation, as first reported by C. R. Smith (21), but the connection between removal of ash and of sensitizing materials is apparently accidental; thorough washing with water alone will reduce the activity of most gelatins to a considerable extent. It will be noted that the maximum sensitivity in this case is reached in an hour, followed by relatively slow deterioration. The treatment of the gelatin used in emulsion 46–69, consisting of one-half hour digestion with normal ammonia at 45°, followed by washing for a day, is by no means a complete deactivation, but it approaches it about as nearly as any other which we have tried; it is particularly successful in reducing fog. It will be noted that the contrast of the emulsion is always low. The indications are that the more labile sensitizing materials have been removed, but that there is a reserve of less reactive substances which come into play only on long-continued ripening. Analysis by the method of Sheppard and Hudson (26) indicated that one-third to one-half of the labile sulphur had been removed. As this method uses digestion with concentrated ammoniacal AgCl as a test of lability, it includes sulphur compounds not labile under the conditions of emulsion making.

When two samples of gelatin are compared as to their value for photographic emulsions, the relative rating may be altered or even reversed by a change in the emulsion formula. This condition is to be expected on the very probable assumption that all gelatins contain a mixture of sensitizing materials of varying reactivity. The results of using a gelatin in a neutral formula with the pH never greater than 7 can not be expected to be the same as those from a "full ammonia" formula in which ripening is carried on at a pH of 11, with free ammonia present in a concentration of nearly half normal. Again, it is probable that the optimum ratio of silver or silver sulphide (as nuclei) to silver halide varies with the proportion of silver iodide, and with the conditions under which it is formed. With this in mind, it is not surprising that, for example, the relative behavior of Winterthur and Nelson No. 1 gelatins differs for all three classes of emulsions represented in Tables 23, 24, and 25.

The use of centrifugal washing, which we have found quite useful in some classes of experimental work, creates conditions during after-ripening which can not be made exactly the same as those after conventional washing. This may be illustrated by considering the case of a known sensitizer, allyl thiocarbamide. It is water soluble, and hence can be removed from gelatin by thorough washing. If present in a neutral emulsion during ripening, it forms the water-insoluble complex with silver bromide, which will go through either type of washing process practically unchanged, breaking down to silver sulphide during the after-ripening. If, therefore, untreated gelatin is used both for the original emulsification and for the final suspension of the silver halide, there will be present during after-ripening all the allyl thiocarbamide from both portions of gelatin. The use of washed gelatin for either mixing or digestion approaches, but hardly duplicates, the conditions of conventional washing. Table 26 shows the progress of after-ripening in emulsions of the "C" type, 4 per cent AgI with centrifugal washing; the mixing time was somewhat less than that of the emulsions in Table 23, giving less speed and more contrast. An active gelatin was used for the original mix (emulsification). In one case it was centrifuged without addition of the secondary

gelatin and suspended in untreated active gelatins; in the other the full quota of secondary gelatin was added, but the final suspension was in ammonia-treated gelatin. The maximum sensitivity was practically the same in both cases. After-ripening was more rapid in the first case. This is somewhat unexpected, as in the second case the silver halide might have carried with it sufficient sensitizer-silver halide complex without further contribution from the coating gelatin. Tables 27 and 28 illustrate the results of various combinations of active and deactivated gelatins used for mix and ripening, and for after-ripening and coating. In these ammonia emulsions, ripening in an active gelatin may produce the optimum effect, so that further use of active gelatin is a liability (emulsion 8–153); or else there may still be the normal difference between coating gelatins (emulsions 8–103 and 106). The ammonia treatment did not produce a uniform product, but the three treated gelatins are more nearly the same than in their untreated states.

TABLE 23.—*Comparison of after-ripening in emulsions made with different gelatins*

[Neutral emulsions, 4.0 mol per cent AgI; digested at 55° without addition of soluble bromide]

Gelatin	Time of digestion	Speed	γ			Fog			Emulsion No.
			3	6	12	3	6	12	
	Minutes at 55°								
Winterthur (9262) [1]	[2] 5	17.3	0.27	0.35	0.40	0.02	0.04	0.09	4-53-1
	30	92	.58	.92	1.21	.02	.04	.13	4
	60	200	.63	1.01	1.25	.03	.07	.13	6
	100	350	.64	1.03	1.23	.05	.11	.17	7
Winterthur (9262) (60 per cent) and Nelson No. 1 (40 per cent) [3] [4]	5	83	.21	.32	.52	.02	.03	.09	4-58-1
	40	330	.60	.92	1.36	.03	.06	.17	2
	80	475	.56	.90	1.39	.09	.12	.18	4
	120	495	.55	.84	1.39	.10	.14	.22	5
Deashed gelatin from limed calfskin stock, treated by Northrop and Kunitz method	[2] 5	8.9	.43	.54	.65	.00	.03	.12	4-67-1
	60	205	.76	1.43	2.22	.03	.10	.28	3
	120	160	.70	1.31	1.97	.16	.31	.46	5
	180	125	.81	1.27	1.83	.26	.51	.69	7
UCOP (3029) digested with NH_3 and washed	15	95	.15	.26	.29	.02	.03	.11	4-69-1
	50	152	.16	.29	.34	.01	.01	.08	3
	90	150	.26	.44	.58	.01	.04	.08	5
	185	310	.50	.71	1.06	.07	.10	.20	7

[1] Coating pH 5.9.
[2] Figures for undigested portions are for those melted with addition of KBr.
[3] Digested at 54°.
[4] Coating pH 7.2.

TABLE 24.—*Comparison of after-ripening in emulsions made with different gelatins*

["Full ammonia" (B), 5.0 mol per cent AgI; digested at 45° without addition of soluble bromide]

Gelatin	Time of digestion	Speed	γ			Fog			Emulsion No.
			3	6	12	3	6	12	
	Minutes at 45°								
Winterthur (9262)	5	66	0.22	0.51	0.61	0.00	0.03	0.14	1-161-1
	60	165	.66	1.28	1.95	.02	.08	.21	2
	130	320	.73	1.34	1.94	.04	.12	.27	4
	185	360	.82	1.47	2.14	.07	.12	.29	6
Nelson No. 1	10	82	.30	.33	.37	.00	.03	.09	1-160-1
	60	127	.84	1.16	1.60	.02	.06	.15	3
	120	230	.91	1.43	2.25	.04	.09	.19	5
	240	240	1.04	1.56	2.43	.06	.09	.21	7
	360	205	1.10	1.75	2.46	.08	.15	.27	8

TABLE 25.—*Comparison of after-ripening in emulsions made with different gelatins*

["Full ammonia" (B), 1 per cent AgI; digested at 45° without addition of soluble bromide]

Gelatin	Time of digestion	Speed	γ			Fog			Emulsion No.
			3	6	12	3	6	12	
	Minutes at 45°								
Winterthur (9202)	5	46	0.88	1.23	1.59	0.00	0.02	0.10	[1]1-162-1
	60	87	.95	1.70	2.13	.01	.07	.19	3
	120	106	1.10	2.04	2.72	.04	.09	.27	5
	180	108	1.16	1.94	2.72	.06	.13	.33	6
Nelson No. 1	10	62	.85	1.30	1.72	.06	.12	.27	1-115-1
	70	195	.92	1.38	1.90	.06	.19	.42	3
	130	255	.87	1.55	2.08	.09	.20	.56	5
	205	240	.96	1.44	1.87	.10	.32	.70	7

[1] [Br] $9.8\times10^{-4}N$; digestion of 3, 5, and 6 at [Br⁻] $1.8\times10^{-4}N$.

TABLE 26.—*After-ripening of neutral emulsions with centrifugal washing*

[4 per cent AgI; mixing time, 18½ minutes. Coating pH 6.6. Winterthur (9262) gelatin in original mix]

Secondary gelatin	Coating gelatin	pH during digestion	[Br⁻] during digestion	Time of digestion	Speed	γ			Fog		
						3	6	12	3	6	12
				Hours at 55°							
None	⅜ Winterthur (9262) ⅜ Nelson No. 1.	6.2	$1.7\times10^{-4}N$	0.5	115	0.56	0.83	1.38	0.03	0.26	0.39
				1.0	175	.67	1.19	1.63	.20	.27	.45
				1.5	122	.80	1.15	1.99	.23	.34	.57
				2.0	110	.78	1.23	1.87	.26	.37	.59
Equal parts Winterthur (9262) and Nelson No. 1.	NH_2- treated UCOP(3029)	7.3	$1.0\times10^{-4}N$	0.5	80	.30	.53	.77	.19	.28	.40
				1.0	150	.45	.74	1.13	.20	.28	.40
				1.5	180	.58	1.00	1.48	.19	.31	.40
				2.0	165	.59	1.03	1.53	.30	.51	.70

TABLE 27.—*Comparison of after-ripening in emulsions washed in centrifuge and suspended in different gelatins*

[Formula "A," 1.0 mol per cent AgI, digested at 45°]

Gelatin used for digestion and coating	Time of digestion,	Speed	γ			Fog			Emulsion No.
			3	6	12	3	6	12	
	Minutes at 45°								
Winterthur (8565) untreated	<10	24	1.17	1.78	2.06	0.11	0.14	0.23	8-103-1
	60	94	.97	1.77	2.37	.13	.19	.27	2
	120	126	1.05	1.65	2.25	.14	.24	.41	3
	180	109	1.04	1.62	2.30	.15	.27	.58	4
Winterthur (8565), previously digested with ammonia and washed	<10	18	1.23	1.80	2.15	.15	.18	.22	8-106-1
	60	17	1.43	2.10	2.58	.13	.17	.22	2
	120	22	1.50	2.25	2.70	.16	.18	.24	3
	180	35	1.55	2.10	2.50	.15	.20	.28	4

TABLE 28.—*Comparison of after-ripening in untreated and ammonia-deactivated gelatins*

[Emulsions made by "A" formula, 1.0 mol per cent AgI; washed by centrifuge and suspended for digestion and coating in different gelatins. All batches digested 2.5 hours at 45°]

Gelatin used for mix and ripening	Gelatin used for digestion and coating	Speed	γ			Fog		
			3	6	12	3	6	12
Winterthur (8763) untreated. Emulsion 8-153.	Winterthur (8763) untreated	50	1.10	1.89	2.57	0.06	0.15	0.35
	Winterthur (8763) digested with NH_3 and washed.	55	1.08	2.70	3.30	.05	.10	.18
	Drescher (6136) digested with NH_3 and washed.	55	1.55	2.50	3.30	.05	.10	.18
	American Glue Co. "A" digested with NH_3 and washed.	34	1.90	2.75	3.10	.05	.09	.18
American Glue Co. "A" digested with NH_3 and washed. Emulsion 8-154.	Winterthur (8763) untreated	31	1.71	2.90	3.41	.08	.14	.27
	Winterthur (8763) digested with NH_3 and washed.	15	1.63	2.35	2.53	.05	.10	.18
	Drescher (6136) digested with NH_3 and washed.	12.5	1.95	2.48	2.95	.07	.13	.18
	American Glue Co. "A" digested with NH_3 and washed.	12.6	1.87	2.32	2.63	.07	.11	.21

7. KNOWN NUCLEAR SENSITIZERS

It seemed instructive to make the comparison between after-ripening in emulsions made with active gelatin, and those made with deactivated gelatin plus definite amounts of sensitizing materials known to function by formation of silver sulphide nuclei. As already mentioned, it has so far been impossible to secure a completely deactivated gelatin, but there were available materials of activity very low compared to that of proper amounts of sensitizers. It should, perhaps, be pointed out that our experiments are not considered to represent the optimum results which can be obtained with allyl thiocarbamide or sodium thiosulphate; no attempt was made to do more than approximate the results obtained with active gelatin.

Neutral emulsions with 4 per cent AgI, on which the most after-ripening data were already available, were chosen for the comparison. In order to secure as nearly as possible the same conditions as with the natural sensitizers in gelatin, allyl thiocarbamide was introduced into the emulsions by swelling the secondary gelatin with a solution of it. Sodium thiosulphate had to be introduced after washing; a dilute solution was poured over the "noodles" before remelting. The allyl thiocarbamide can be introduced before washing, since it forms an insoluble addition compound with silver bromide (12), even in the presence of soluble bromide. Sodium thiosulphate must undergo a metathesis with silver bromide, liberating soluble bromide, before there is formed the silver thiosulphate which breaks down to silver sulphide. If introduced into the unwashed emulsion at a high bromide ion concentration, thiosulphate will, therefore, be lost on washing; this was verified by experiment. The metathesis equilibrium is probably far over toward silver bromide, and therefore quite sensitive to bromide ion concentration. The decomposition of silver thiosulphate liberates no bromide, and should be relatively independent of this variable as compared to the decomposition of the silver bromide-thiocarbamide complex. Both decompositions liberate acid, and should be retarded by increasing hydrogen ion concentration. Sheppard has stated that the formation of silver sulphide from thiocarbamides occurs at a "sufficiently alkaline reaction." Silver thiosulphate might decompose more rapidly in alkaline solution, but

all thiosulphates are unstable in acid solution, so that there is probably no pH at which it is stable.

The emulsions listed in Table 29 were made with a commercial sample of gelatin which, as shown by the control, was gratifyingly inert if the emulsion was made without addition of ammonia or other alkali. The data on addition of allyl thiocarbamide to an emulsion made with this gelatin are given to illustrate the marked effect of pH on the sensitization; on digestion at pH 6.3 the after-ripening was practically the same as in the control. The thiocarbamide was still there, since bathing in ammonia hypersensitized the finished plates,

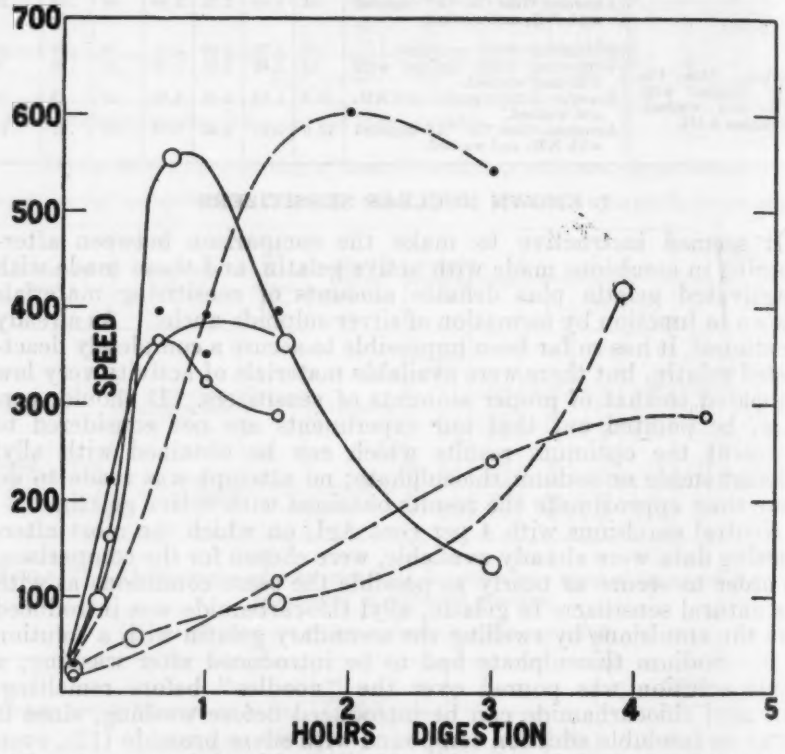

FIGURE 7.—*After-ripening of neutral emulsions 4 per cent AgI, mixed with inert gelatin*

Solid curves indicate digestion, at 55°, as washed; dashed lines, digestion at 55° with 5 KBr per 1,000 AgBr●, sensitized with active secondary gelatin; o, O sensitized with allyl thiocarbamide sufficient to convert 1.6×10^{-3} and 2.4×10^{-4}, respectively, of silver bromide to silver sulphide.

but not those coated with the control emulsion. It is obvious that conditions of this nature may cause erroneous conclusions as to the value of sensitizing materials if the investigator has not given the attention to details which is necessary in photographic research. The emulsions listed in Tables 30 and 31 were made with different batches of ammonia-deactivated gelatin. At the higher values of pH in these emulsions, the gelatin was more active, especially on very long digestion.

After-ripening after addition of allyl thiocarbamide closely resembles that in active gelatin, as would be predicted from the natural occurrence of this sensitizer in gelatin. The qualitative similarity of the curves in Figure 7 is striking, and in view of the way in which

photographic sensitivity varies with small changes in conditions, the quantitative agreement is also good. It is strong proof that the processes occurring are of the same character in both cases. There is, however, an important difference which is evident on inspection of Tables 29, 30, and 31, and the curves. The presence of soluble bromide (5 KBr/1,000 AgBr) during digestion retards after-ripening with allyl thiocarbamide much more than with active gelatin. The difference is so marked that it seems a strong indication of the presence of other sensitizers in gelatin, although it can hardly be used as evidence of their character. The difference in the effect of bromide

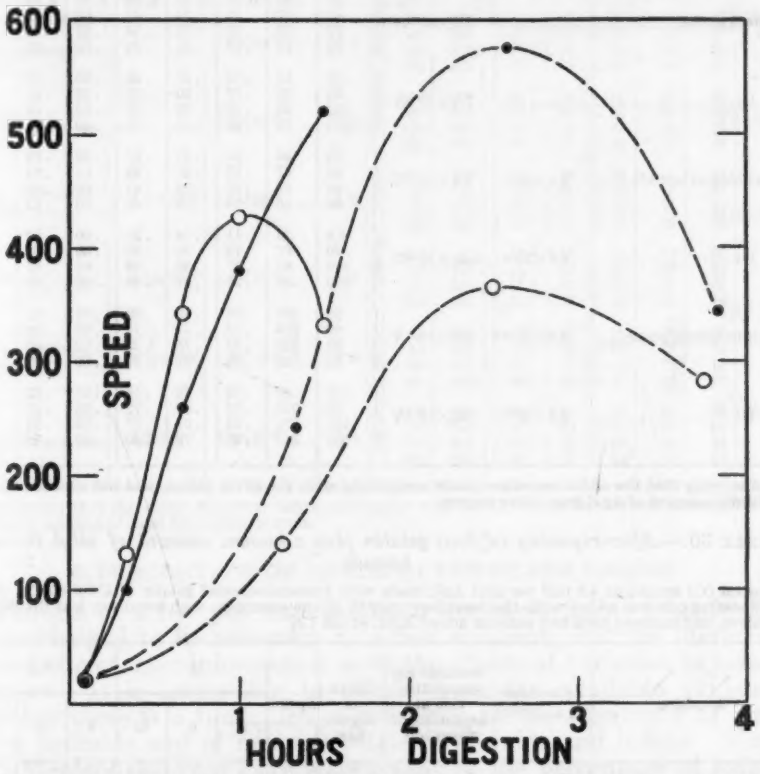

FIGURE 8.—*After-ripening of neutral emulsions, 4 per cent AgI, made with inert gelatin and sensitized with sodium thiosulphate*

Solid lines indicate digestion as washed; dashed lines, digestion with 5 KBr per 1,000 AgBr. Digested at 55°; ●, pH 6.3; O, pH 7.9.

appears in another way. With active gelatin, the maximum speed was higher at increased bromide ion concentration (figs. 3 and 5), but with either of the sensitizers the maximum was higher when the emulsion was digested without addition of bromide.

The data for sodium thiosulphate are presented in Tables 29 and 31 and Figure 8. They are very similar to those for active gelatin and allyl thiocarbamide. The decrease in rate of after-ripening produced by adding bromide is intermediate between the other two; it is greater at pH 7.9 than at pH 6.3. At pH 6.3, the after-ripening with thiosulphate has the peculiarity that the growth of fog is almost unaffected by the bromide.

TABLE 29.—*After-ripening in inert gelatin plus known amounts of sensitizers*

[Neutral (C) emulsions, 4.0 mol per cent AgI, made with commercial inert gelatin (UCOP 2939-1). The allyl thiocarbamide was added with the secondary gelatin; sodium thiosulphate was added after washing. pH during digestion, 6.3]

Sensitizer	Ag as Ag_2S / Ag as AgBr[1]	Bromide ion concentration at beginning of digestion	Time of digestion	Speed	γ			Fog		
					3	6	12	3	6	12
			Minutes at 55°							
None (control)		$1.1\times10^{-4}N$	20	30	0.15	0.23	0.36	0.00	0.02	0.08
			40	31	.15	.25	.45	.02	.03	.09
			60	30	.19	.31	.50	.01	.03	.10
			90	39	.17	.31	.52	.00	.02	.09
Do		$7.9\times10^{-4}N$	<5	15	.13	.16	.23	.00	.01	.04
			90	29	.17	.30	.40	.02	.02	.09
			180	46	.19	.36	.53	.00	.02	.11
			270	78	.23	.46	.70	.00	.05	.21
Allyl thiocarbamide	2.4×10^{-5}	$4.8\times10^{-5}N$	20	46	.14	.24	.37	.02	.02	.08
			40	47	.15	.27	.38	.01	.02	.08
			60	57	.17	.29	.41	.00	.02	.09
			90	55	.18	.33	.46	.00	.02	.09
Do	2.4×10^{-5}	$1.03\times10^{-3}N$	<5	25	.11	.14	.20	.00	.02	.04
			90	61	.13	.20	.30	.00	.02	.05
			180	83	.17	.30	.39	.01	.03	.08
			270	99	.21	.37	.48	.00	.03	.12
Sodium thiosulphate	2.3×10^{-5}	$2.9\times10^{-4}N$	20	100	.20	.42	.60	.02	.05	.11
			40	260	.38	.57	1.14	.02	.06	.24
			60	365	.38	.75	1.22	.02	.06	.25
			90	520	.46	.82	1.35	.02	.09	.34
Do	2.3×10^{-5}	$1.02\times10^{-3}N$	<5	19	.12	.13	.18	.01	.02	.08
			80	240	.22	.43	.72	.03	.08	.29
			155	575	.39	.61	.07	.04	.24	.73
			230	345	.41	.72	1.20	.06	.39	.96

[1] Assuming that the added sensitizer reacts completely with the silver halide, and not considering the unknown amount of Ag_2S from other sources.

TABLE 30.—*After-ripening in inert gelatin plus a known amount of allyl thiocarbamide*

[Neutral (C) emulsions 4.0 mol per cent AgI, made with ammonia-treated gelatin (UCOP 3029). Allyl thiocarbamide was added with the secondary gelatin of one emulsion; each emulsion was divided in halves, and digested with and without added KBr, at pH 7.5]

Sensitizer	Ag as Ag_2S / Ag as AgBr[1]	Bromide ion concentration at beginning of digestion	Time of digestion	Speed	γ			Fog		
					3	6	12	3	6	12
			Minutes at 55°							
None (control)	0	$2.2\times10^{-5}N$	15	95	0.15	0.26	0.29	0.02	0.03	0.11
			50	152	.16	.29	.34	.01	.01	.06
			90	150	.26	.44	.58	.01	.04	.08
			185	310	.50	.71	1.06	.07	.10	.26
Do	0	$1.4\times10^{-3}N$	<5	40	.12	.16	.20	.00	.02	.07
			30	58	.13	.18	.19	.00	.02	.07
			90	81	.17	.27	.34	.00	.03	.07
			225	240	.44	.73	1.03	.04	.06	.13
Allyl thiocarbamide	2.4×10^{-5}	$1.8\times10^{-4}N$	15	95	.33	.41	.61	.02	.03	.16
			45	555	.76	1.17	1.64	.03	.05	.23
			93	360	.69	1.35	1.95	.19	.34	.62
			180	134	.80	1.19	1.60	.55	.94	1.54
Do	2.4×10^{-5}	$1.15\times10^{-3}N$	<5	21.7	.20	.22	.26	.00	.02	.11
			30	57	.22	.22	.23	.00	.04	.12
			90	95	.25	.33	.37	.00	.03	.08
			225	420	.54	.86	1.34	.04	.07	.14

[1] Assuming that the added sensitizer reacts completely with the silver halide, and not considering the unknown amount of Ag_2S from other sources.

TABLE 31.—*After-ripening with allyl thiocarbamide, sodium thiosulphate, and naturally occurring sensitizers of gelatin*

[Neutral (C) emulsions, 4.0 mol per cent AgI, made with ammonia-treated gelatin (American Glue Co. "A"); secondary gelatin, the same where known sensitizers were used]

Sensitizer	$\frac{Ag\ as\ Ag_2S}{Ag\ as\ AgBr}$[1]	Bromide ion concentration at beginning of digestion	pH	Time of digestion	Speed	γ			Fog		
						3	6	12	3	6	12
				Minutes at 55°							
Active secondary gelatin (Winterthur and Nelson)		1.7×10^{-5}	6.8	20	220	0.54	1.07	1.16	0.11	0.15	0.21
				40	400	.67	1.13	1.57	.11	.17	.27
				60	350	.77	1.10	1.80	.19	.28	.36
				90	400	.70	1.33	1.93	.18	.27	.37
Do		8.6×10^{-4}	6.8	<5	36	.26	.34	.41	.00	.03	.08
				60	395	.61	.97	1.34	.06	.10	.14
				120	605	.64	1.06	1.63	.12	.18	.27
				180	540	.66	1.01	1.63	.17	.19	.31
Allyl thiocarbamide	1.6×10^{-3}	1.1×10^{-3}	7.9	20	162	.60	.93	1.95	.14	.20	.34
				40	365	.90	1.36	2.35	.13	.23	.41
				60	320	.87	1.36	2.30	.18	.31	.44
				90	290	1.08	1.53	2.10	.30	.50	.81
Do	1.6×10^{-3}	8.1×10^{-4}	7.9	<5	17	.41	.63	.79	.02	.06	.15
				90	117	.55	.70	.94	.02	.10	.16
				180	240	.57	.90	1.31	.05	.07	.21
				270	285	.74	1.13	1.62	.08	.13	.27
Sodium thiosulphate	2.3×10^{-3}	1.0×10^{-3}	7.9	20	132	.72	1.06	1.69	.05	.10	.23
				40	345	.88	1.30	2.05	.09	.13	.29
				60	430	.87	1.26	1.98	.11	.18	.34
				90	330	.89	1.38	2.17	.19	.30	.44
Do	2.3×10^{-3}	9.2×10^{-4}	7.9	<5	24	.34	.36	.42	.03	.09	.17
				75	140	.74	.95	1.48	.04	.09	.20
				150	365	.87	1.28	1.98	.10	.16	.29
				225	285	.96	1.38	2.35	.15	.23	.41

[1] Assuming that the added sensitizer reacts completely with the silver halide, and not considering the unknown amount of Ag_2S from other sources.

8. PERCENTAGE OF IODIDE IN THE SILVER HALIDE

The use of a few per cent iodide in the silver halide is generally acknowledged to be necessary to a fast emulsion, but the literature gives little specific information as to the effects of variation in iodide content. It is impossible to decide from the available evidence whether there is a fundamental difference in the sensitivity of pure silver bromide and of mixed crystals of bromide and iodide. Huse and Meulendyke (23) have shown that as the percentage of iodide is increased the spectral absorption extends to longer wave lengths; it is very probable that the total energy absorbed from incident white light is also increased, but their data do not shown whether the increase in absorption would cause an appreciable increase in sensitivity. Trivelli (24) suggested that the introduction of silver iodide into the silver bromide crystal lattice should cause a distortion of the latter; Wilsey (25), by X-ray crystal analysis, found that the spacing of the lattice was definitely increased, which might set up strains resulting in greater photochemical sensitivity. Our experiments are entirely too limited for generalization on this subject, but in the neutral emulsions compared in Table 32, we have an example of the type of data which we hope at some time to secure in sufficient quantity to be conclusive. By reducing the temperature of mixing and the excess

of ammonium bromide, the emulsions with 1 per cent silver iodide were made to have the same average grain size as those with 4 per cent; the distribution of grain size was similar, although not identical. Both were digested to optimum sensitivity under similar conditions, the time being shorter for the emulsion with less iodide. The difference in maximum speeds under these conditions appears to indicate an inherent difference in the sensitivity of the two mixtures of halides. The ammonia-process emulsions can not be compared at equal grain sizes, since the ripening was the same for both proportions of iodide,[11] but the evidence appears to be qualitatively the same.

Table 32 has been arranged to shown the most definite connection between iodide content and after-ripening, which is that the practicable increase in sensitivity by after-ripening increases with increasing iodide. As would be expected, there is a considerable dependence on the gelatin and the emulsion formula. The emulsions with higher iodide content are notable for very low contrast before after-ripening; if the speeds before and after digestion were expressed by threshold value or by the system of Jones and Russell (13) instead of the H. & D. system, the ratio would be greatly increased.

Inspection of Tables 9, 11, 13, and 14 shows that the rate of after-ripening under comparable conditions decreases with increasing percentage iodide, but the difference is not large.

TABLE 32.—*Comparison of after-ripening in emulsions with 1.0 and 4.0 or 5.0 mol per cent silver iodide*

Formula and No.	Mol per cent AgI	Average grain size	Gelatin	Digestion	Speed	γ			Fog		
						3	6	12	3	6	12
		μ^3									
C, 4-68	4.0	0.36	Winterthur-Nelson	Minimum	76	0.16	0.20	0.32	0.03	0.08	0.13
				Optimum	625	.64	.90	1.53	.08	.13	.18
C, 4-65	1.0	.34	do	Minimum	39	.26	.33	.48	.00	.00	.03
				Optimum	195	.80	1.26	2.29	.08	.11	.26
B, 1-161	5.0	.34	Winterthur	Minimum	66	.22	.51	.61	.00	.03	.14
				Optimum	360	.82	1.47	2.14	.07	.12	.29
B, 1-162	1.0	.37	do	Minimum	46	.88	1.23	1.59	.00	.02	.10
				Optimum	108	1.16	1.94	2.72	.06	.13	.33
B, 1-160	5.0	.33	Nelson	Minimum	81	.30	.33	.37	.00	.03	.09
				Optimum	240	1.04	1.56	2.43	.05	.09	.21
B, 1-118	1.0	.44	do	Minimum	62	.85	1.30	1.72	.06	.12	.27
				Optimum	255	.87	1.55	2.08	.09	.20	.56

IV. STORAGE RIPENING

As already stated, after-ripening goes on slowly during storage of dried plates coated with undigested emulsions. Tables 33 to 38 give the data on storage ripening of several types of emulsions coated after varying amounts of ripening and digestion. To keep the tables from being too unwieldy, γ and fog are given only for 6-minute devel-

[11] It must be known to anyone with experience in emulsion making that, with the same ripening conditions, the grain size decreases with increasing proportion of iodide, but we have found only one explicit statement to this effect in the literature. Lüppo-Cramer (1) points out that pure bromide neutral emulsions have a grain very much larger than those with 1 per cent iodide, made under the same conditions. In addition to the data in Table 32, the grain size of emulsion 4-63, 1 per cent AgI, Table 3 may be compared with that of emulsion 4-68, 4 per cent AgI, Table 32 mixed at the same temperature with the same excess bromide.

opment; the speed number is also taken from that curve only instead of from the mean of the three. Random errors of coating and development are, therefore, more conspicuous than in the other tables. Considerably more data have been obtained than are given here.

Inspection of the tables shows that in every case the after-ripening on storage was at least equal to that on digestion; in general, it was somewhat greater. As would be expected, when the emulsion was digested to a maximum sensitivity, there was no after-ripening on storage; there was also the unexpected consequence that deterioration by fog in 1-year storage was generally less than in the undigested portions. Storage ripening in the neutral and ammonia-process emulsions was of the same order of magnitude, proving that it can not be ascribed to traces of free ammonia. (See p. 221 and reference 11.)

TABLE 33.—*Storage ripening of emulsion 4–11*

["C" formula, 5.0 per cent AgI, 15 per cent excess KBr, Winterthur gelatin. All data for six minutes development]

	Time of digestion	Directly after coating			After 1 month storage			After 3 months, storage			After 12 months, storage		
		Speed	γ	Fog	Speed	γ	Fog	Speed	γ	Fog	Speed	γ	Fog
	Minutes at 45°												
Digested as washed	<10	20	1.30	0.08	105	1.45	0.09	220	1.60	0.11	125	2.05	0.47
	75	83	1.85	.14	110	1.65	.06	180	1.63	.12	160	1.93	.33
	130	160	1.70	.15	125	1.85	.09	140	1.85	.12	175	1.75	.32
	195	165	1.65	.17	165	1.80	.09	180	1.90	.13	180	1.90	.24
Dry gelatin added after washing, 60 per cent of original amount	60	87	1.37	.12	175	1.23	.09	230	1.35	.10	115	1.55	.31
	120	140	1.60	.14	190	1.42	.09	145	1.53	.12	130	1.58	.25
	180	195	1.40	.15	175	1.50	.11	110	1.68	.15	125	1.50	.24

TABLE 34.—*Storage ripening of emulsion 4–14*

["C" formula, 1.0 per cent AgI, 16 per cent excess KBr, Winterthur gelatin. Digested as washed. All data are for six minutes development]

Time of digestion (minutes at 45°)	Directly after coating			After 1 month storage			After 3½ months, storage			After 13 months, storage		
	Speed	γ	Fog	Speed	γ	Fog	Speed	γ	Fog	Speed	γ	Fog
<10	45	1.00	0.05	180	1.45	0.07	315	1.77	0.17	210	1.78	0.55
65	63	1.50	.06	138	1.43	.09	230	1.58	.12	210	1.60	.34
125	100	1.78	.11	150	1.65	.08	210	1.77	.13	220	1.55	.30
180	125	1.80	.14	165	1.65	.09	220	1.87	.16	230	1.50	.29

TABLE 35.—*Storage ripening of emulsion 6–46*

["C" formula, 5 per cent AgI, 16 per cent excess KBr, 14 minutes' mixing time. Washed by centrifuge and suspended in untreated Winterthur gelatin. All data are for six minutes' development]

Time of digestion (minutes at 45°)	Directly after coating			After 1 month storage			After 4 months' storage			After 13 months' storage		
	Speed	γ	Fog	Speed	γ	Fog	Speed	γ	Fog	Speed	γ	Fog
10±5	7.3	1.01	0.19	48	1.34	0.19	91	1.58	0.34	50	1.72	0.49
60±5	38	1.41	.23	69	1.42	.24	------	------	------	60	1.83	.49
120±5	71	1.70	.27	87	1.60	.23	100	1.57	.35	72	1.75	.40
180±5	78	1.80	.30	87	1.75	.28	66	1.90	.35	66	1.77	.48

TABLE 36.—*Storage ripening of emulsion 6–48*

["C" formula, 1 per cent AgI, 16 per cent excess KBr, 14 minutes' mixing time. Washed by centrifuge and suspended in untreated Winterthur gelatin. All data are for six minutes' development]

Time of digestion (minutes at 45°)	Directly after coating			After 1 month storage			After 3 months' storage			After 12½ months' storage		
	Speed	γ	Fog	Speed	γ	Fog	Speed	γ	Fog	Speed	γ	Fog
10±5	33	0.98	0.28	120	1.30	0.30	138	1.78	0.38	138	1.65	0.71
60	43	1.35	.28	105	1.32	.28	150	1.56	.37	160	1.72	.60
120	120	1.54	.29	115	1.60	.33	145	1.65	.40	145	1.58	.56
180	115	1.75	.36	132	1.74	.39	138	1.70	.49	132	1.65	.55

TABLE 37.—*Storage ripening of emulsion 1–118*

["B" formula, 1 per cent AgI, Nelson No. 1 gelatin. All data are for 6 minutes development]

	Time of digestion	Directly after coating			After 25 days' storage			After 3 months' storage			After 13 months' storage		
		Speed	γ	Fog	Speed	γ	Fog	Speed	γ	Fog	Speed	γ	Fog
	Minutes at 45°												
Digested as washed	<10	62	1.30	0.12	160	1.18	0.10	260	1.80	0.13	330	1.65	0.44
	75	200	1.38	.19	250	1.65	.14	240	1.92	.20	300	1.65	.31
	135	245	1.55	.20	330	1.60	.17	280	1.81	.28	180	1.70	.52
	210	240	1.44	.32	275	1.70	.24	215	1.93	.26	220	1.55	.46
Dry gelatin added after washing, 60 per cent of original amount	60	76	1.30	.22	126	1.37	.18	230	1.48	.22	210	1.13	.65
	135	100	1.10	.35	140	1.30	.29	175	1.44	.41	220	.97	.63
	200	102	1.10	.41	140	1.26	.35	105	1.53	.48	120	1.16	.68

TABLE 38.—*Storage ripening of emulsions made by formula "A"*

[1 per cent AgI, and washed by centrifuge. All data are for 6 minutes development]

Emulsion No. and gelatin	Time of digestion	Time of ripening	Directly after coating			After 1 month storage			After 3 months' storage [1]			After 13 months' storage [2]		
			Speed	γ	Fog	Speed	γ	Fog	Speed	γ	Fog	Speed	γ	Fog
	Minutes at 45°	*Minutes at 45°*												
8–101, Winterthur, untreated	[3] 10	6	12	1.46	0.08	36	2.30	0.05	66	2.30	0.14	72	2.14	0.34
		35	16	1.15	.26	47	1.50	.21	145	1.60	.29	132	1.60	.35
		63	34	.67	.32	138	.90	.28	350	1.08	.28	265	1.12	.48
		120	43	.50	.52	182	.67	.48	480	1.76	.52	350	1.15	.58
8–100, Winterthur, untreated	135	5	51	1.45	.13	43	1.70	.15	48	1.55	.12	30	1.70	.28
		30	135	1.05	.26	100	1.32	.24	110	1.31	.31	72	1.15	.42
		62	118	1.03	.46	175	1.10	.39	125	1.10	.49	200	.90	.64
		135	200	.87	.41	200	1.00	.46	210	.95	.45	240	.95	.55
8–108, Winterthur, digested with NH_3 and washed	145	7	20	1.63	.11	25	1.85	.13	43	1.60	.15	95	1.55	.14
		29	31	.97	.22	45	1.00	.24	79	1.10	.25	190	1.05	.23
		59	39	.53	.30	39	.68	.31	180	.65	.28	315	.77	.30
		120	50	.34	.33	91	.38	.41	290	.58	.41	550	.68	.38

[1] 4 months' storage of 8–108. [2] 12 months' storage of 8–108. [3] Approximately.

After-ripening by storage and by digestion are equally dependent on the gelatin. The ammonia-treated gelatins have a peculiarity which was indicated in Table 27 and is more evident in Table 38, emulsion 8–108; there may be little after-ripening over a considerable time of digestion or storage, followed ultimately by a great rise

of sensitivity. In emulsion 4–69, the after-ripening in the last 90 minutes of digestion was greater than in the first 90; in emulsion 8–108, storage for a year produced clean plates of unusually high speed numbers, although the contrast was still below normal. The obvious interpretation of this is that the more labile sensitizing materials were removed by the ammonia treatment but that a considerable amount of slowly reacting sensitizers was left.

The very important question of the effect of soluble bromide on storage ripening and deterioration by fog will be taken up in a later communication, as plates now in storage are expected to furnish data which should be included.

The processes occurring in storage ripening would be expected to be essentially the same as in after-ripening by digestion. The amounts of silver plus silver sulphide, as found by the Weigert and Lühr method (Pt. V of this paper), support this expectation. The only explanation which we can offer for the greater effectiveness of storage ripening has already been given on page 233, that in the slow process of storage ripening there is relatively little tendency toward the formation of new nuclei. It is therefore a process of growth of small numbers of nuclei per grain, leading to the most efficient utilization of the silver and silver sulphide formed, and also leading to rapid increase in fog when the nuclei increase past the optimum size. If the emulsion has previously been digested to maximum speed, this may have resulted in greater numbers of nuclei than if it had been subject only to storage ripening, with the further possibility that a higher proportion of the silver sulphide (or silver) particles have been formed by reaction with dissolved silver halide. These last may be independent of silver halide grains and, therefore, inert both as to sensitivity and fog. The supply of sensitizers has been partly exhausted, so that storage ripening in this case proceeds with a lowered rate of formation of silver and silver sulphide, distributed among a larger number of nuclei, some of which are ineffective; increase of any of the nuclei to the size causing fog is therefore retarded.

V. ANALYTICAL EVIDENCE ON THE MECHANISM OF AFTER-RIPENING

Digestion of silver bromide with gelatin may be expected to result in some reduction to metal. The analysis of the emulsion gelatins used in this investigation, by the method of Sheppard and Hudson (26), gives results of the order of 2×10^{-5} g. labile sulphur per gram of gelatin, at least part of which may react under the conditions of after-ripening. The total fraction of silver bromide converted to other (nonhalide) forms will, however, be very small. The available evidence on the photolysis of silver bromide indicated that the silver of the latent image corresponding to ordinary exposures was less than could be detected by any analytical method. As it was assumed that the ripening nuclei must be a much smaller quantity, it was not until Weigert and Lühr (27) extended their investigations of photolysis from "print-out" to "developing-out" emulsions that there was any attempt to determine the "ripening silver" by chemical analysis. In a forthcoming paper we will describe experiments with the Weigert and Lühr method in full detail; in the discussion of the connection

between after-ripening and nonhalide ("ripening") silver, the analytical results may be taken roughly at their face value.

Reduction or other reaction of the silver bromide during digestion could also be detected by an increase in the bromide ion concentration, when it was sufficiently low.

A number of typical results are given in Table 39. It will be noted that the rate of increase at a given temperature is greater for the emulsions with the lower proportions of iodide. It is less in the emulsion made with the deashed gelatin than the corresponding one with normal gelatin. Both these differences would be predicted, since increase in proportion of iodide makes reduction more difficult, and the deashing process probably removes reducing materials. The amount of silver bromide reacting can not be calculated from the change in bromide ion concentration, since there is not only the change in free silver and bromide ions, but a larger one in silver ion combined with the gelatin, and probably another of similar magnitude in bromide ion absorbed to the silver bromide. The errors in determination of these are too large to make the computation of any value.

Table 40 gives the results, both of digestion and of storage ripening, on the nonhalide silver, and photographic properties, of two emulsions. The increase produced by either digestion or storage ripening is much larger than the variations in the silver determinations; the values for each of the latter are given separately to indicate the reproducibility. It is evident that the increase in silver is more rapid at lower bromide ion concentrations, which is according to prediction, although, at 45°, increase in the bromide ion concentration by a factor of 40 divides the rate by 4 only, and at 55° by less than this. The rate of increase at 55°, without added bromide, is between two and three times as great as under the corresponding conditions at 45°, which is the normal value for a chemical reaction. The increase in nonhalide silver on storage was of the same order as that on digestion to a corresponding speed, and the effect of soluble bromide was very similar. On storage of 4–64–1 and 6, the increase in nonhalide silver, expressed in parts per 100,000, was 3.5 and 2.7; in 4–64–7, with no added bromide, the increase was 7.4. In emulsion 4–66, the corresponding values are 9.1 and 9.5 with added bromide, 18.2 without it. The difference between the two emulsions is unexplained. The data for digestion of emulsion 4–59, Table 41, are quite similar to those for 4–64 and 4–66.

TABLE 39.—*Change in bromide ion concentration of emulsions during digestion*

[Photographic data on these emulsions will be found in Tables 9, 10, 11, 12, 14, and 23]

Emulsion No.	Gelatin	Mol per cent AgI	pH	Time of digestion	Temperature of digestion	Bromide ion concentration at beginning of digestion, normality	Bromide ion concentration at end of digestion, normality
				Hours	°C.		
4–47	Winterthur	0.0	6.6	1.0	54	1.43×10^{-3}	1.92×10^{-3}
4–64	Winterthur-Nelson No. 1	1.0	6.9	4.0	45	1.8×10^{-5}	2.5×10^{-4}
4–66	do	1.0	7.0	2.0	55	1.5×10^{-3}	3.8×10^{-3}
1–162	Winterthur	1.0	8.3	3.0	45	1.75×10^{-4}	2.25×10^{-4}
4–61	Winterthur-Nelson No. 1	4.0	6.9	2.3	55	1.5×10^{-4}	2.7×10^{-4}
4–67	Deashed, from limed stock	4.0	7.1	3.0	55	1.42×10^{-3}	2.20×10^{-3}
1–159	Nelson No. 1	5.0	8.3	3.0	45	3.3×10^{-4}	5.8×10^{-4}

TABLE 40.—*Effect of digestion and storage on photographic properties and nonhalide silver (determined by the modified Weigert and Lühr method)*

[Emulsions made by "C" formula, 1 per cent AgI, 12.5 per cent excess NH_4Br, Winterthur and Nelson gelatin; mixed in 26 minutes at 52°]

Emulsion No.	Bromide ion concentration during digestion N	Time of digestion (minutes) and temperature	Directly after coating				Three months after coating			
			Ratio $\frac{Ag \times 10^5}{AgBr}$	Speed	γ 6	Fog 6	Ratio $\frac{Ag \times 10^5}{AgBr}$	Speed	γ 6	Fog 6
4-64-1	7.6×10^{-4}	<10	6.0, 5.6	34	0.55	0.04	9.3	125	1.03	0.04
4-64-6	7.6×10^{-4}	245, 45°	8.6, 7.3	170	1.04	.09	10.7	190	1.37	.12
4-64-7	1.8×10^{-3}	240, 45°	15.9, 15.3	215	1.55	.22	22.0	210	1.52	.34
4-66-5	1.2×10^{-3}	<10	4.4, 10.0 4.5, 4.2	39	.33	.00	13.5	134	.84	.03
4-66-8	1.2×10^{-3}	120, 55°	12.5, 12.4	170	1.63	.14	22.0	130	1.53	.37
4-66-4	3.8×10^{-3}	120, 55°	14.8, 15.1	162	1.60	.21	33.2	150	1.57	.32

TABLE 41.—*Change in nonhalide silver on digestion*

[See Tables 8 and 12 for photographic data on these emulsions]

Emulsion No.	Digestion time	Bromide ion concentration, normality	Nonhalide silver by Weigert and Lühr method $Ag/AgBr \times 10^5$	Digestion temperature	pH
	Minutes				
1-159-2	<10	3.3×10^{-4}	36.8, 28	45°	8.3
4	53		17.6, 11.9		
6	110		16.9, 12.7		
7	180		13.2, 10.1		
4-59-1	<5	1.2×10^{-4}	8.1, 9.8	55°	7.5
7	135		14.3, 12.2		
8	190	3.3×10^{-4}	11.7, 11.6		

In the case of emulsion 1–159 we have an anomalous behavior which was also observed on a smaller scale in the early stages of digestion of other emulsions. More nonhalide silver was found in the undigested portion than in the others; except for the undigested portion, the differences are within the limits of error of analysis. We have no reason to suspect random errors of analysis in these cases. It is possible that conditions favor a considerable systematic error. However, it is significant that the portion of this same emulsion which was digested with added bromide decreased in fog during digestion, so that an actual decrease in the nonhalide silver appears to be a possibility.

Granting that the nonhalide silver is real and that its changes are in most cases to be predicted from the chemistry of the system, the correlation with photographic properties is hardly close enough to be useful. The quantity of nonhalide silver found by the Weigert and Lühr method is invariably too large to be ascribed only to sensitivity nuclei. Reference to Tables 29 to 31 shows the large photographic effects of 2 parts of nonhalide silver per 100,000, when introduced by use of efficient sensitizers. The minimum value by analysis in the insensitive and very clean 4–66–5 was 4 parts per 100,000, and it generally rose to 10 to 15 parts on digestion to maximum sensitivity. In the opinion of the writers, only a small part of this nonhalide silver functions as sensitivity nuclei; the rest is dispersed

through the gelatin, but not adsorbed to silver halide grains. The initial amounts in undigested emulsions may have been formed during ripening, but an equally plausible explanation is given by the presence of traces of colloidal silver in silver nitrate, unless exceptional precautions have been taken to prevent it. The increase in nonhalide silver during digestion must, to a large extent, represent reaction of "silver gelatinate" and free silver ions with reducing materials or labile sulphur, leading to a free particle of silver or silver sulphide, in contrast to the adsorbed sensitivity nuclei formed by rearrangement of a compound already adsorbed to the surface of a grain.

VI. SUMMARY

1. This paper is a survey of the changes taking place in a photographic emulsion after it has been washed, and of the effects of eight independent variables or groups of variables.

2. In studying the independent variables of the process, experiments have been repeated using emulsions of varying iodide content, with and without ammonia, and with different samples of gelatin.

3. The dependence of after-ripening by digestion on temperature, bromide ion concentration and hydrogen ion concentration indicates that it is the result of a chemical reaction or reactions of the silver halide. Chemical analysis shows an increase in nonhalide silver roughly parallel to the photographic changes but in quantity too large to be explained as sensitivity nuclei only.

4. Experiments on after-ripening in inert gelatin plus known sensitizing materials (allyl thiocarbamide, sodium thiosulphate) gave results qualitatively very similar to those in active gelatin, although the characteristics of active gelatin can not be explained by allyl thiocarbamide alone.

5. If digestion after washing is omitted, there is a slow after-ripening on storage, with effects generally similar to those of digestion.

VII. ACKNOWLEDGMENT

C. F. Kretchman has assisted in the coating and testing of most of the experimental emulsions recorded in this paper.

VIII. BIBLIOGRAPHY

1. Lüppo-Cramer, Grundlagen der photographischen Negativverfahren. Also chapter on emulsion formulas in Wentzel (reference 2), pp. 157–176, and Zeit. f. wiss. Phot., **28**, p. 350; 1930.
2. Wentzel, Die Fabrikation der photographischen Platten usw., pp. 134–137.
3. Kieser, Z. Angew., Chem., **41**, p. 1292; 1928.
4. Rawling and Glassett, Phot. J., **66**, p. 495; 1926.
5. Thorne-Baker, Brit. J. Phot., p. 349; 1925.
6. For example, Eder, Ausführliches Handbuch der Photographie, 5th ed., III, p. 393; 1903.
7. Carroll and Hubbard, J. Phys. Chem., **31**, p. 906; 1927.
8. Renwick, Sease, and Baldsiefen, Phot. J., **66**, p. 163; 1926.
9. Rawling, Phot. J., **69**, p. 83; 1929.
10. Wall, Photographic Emulsions, pp. 45–47.
11. Eder, Handbuch III, pp. 55, 444, 5th ed.; 1903.
12. Sheppard and Hudson, J. Am. Chem. Soc., **49**, p. 1814; 1927.
13. Jones and Russell, Proc. 7th Int. Cong. Phot., pp. 130–143.
14. Davis and Neeland, This Journal.

15. Lüppo-Cramer, Grundlagen, p. 65, footnote.
16. Carroll and Hubbard, This Journal, **1**, p. 565; 1928.
17. Brönsted and Livingston, J. Am. Chem. Soc., **49**, p. 435; 1927.
18. Trivelli, Wightman, and Sheppard, Phot., J., **65**, p. 134; 1925.
19. Sheppard and Wightman, Phot. J., **69**, p. 134; 1929.
20. Sheppard, Phot. J., **66**, p. 393; 1926.
21. C. R. Smith, J. Am. Leather Chemists Assoc.; October, 1922.
22. Renwick, Phot. J., **53**, p. 127; 1913.
23. Huse and Meulendyke, Phot. J., **66**, p. 306; 1926.
24. Trivelli, Rec. Trav. Chim., **42**, p. 714; 1923.
25. Wilsey, J. Frank. Inst., **200**, p. 739; 1925.
26. Sheppard and Hudson, Ind. Eng. Chem., Analytical Ed., **2**, p. 73; 1930.
27. Weigert and Lühr, Naturwissenschaften, **15**, p. 788; 1927.

WASHINGTON, April 1, 1931.

A SIMULTANEOUS RADIOTELEPHONE AND VISUAL RANGE BEACON FOR THE AIRWAYS

By F. G. Kear and G. H. Wintermute

ABSTRACT

Increased use of the airway radio services by transport operators has resulted in a demand for continuous range-beacon service. At the same time the weather broadcast information has increased in importance and the interruptions to the beacon service have become more frequent. To eliminate difficulties arising from this conflict a transmitting system has been developed which provides simultaneous transmission of visual range-beacon and radiotelephone signals.

This system is designed to employ existing equipment so far as possible. By combining two transmitting sets into one the cost of buildings and antenna equipment is reduced. Continuous check on the operation of both systems can be obtained with less personnel than required at present.

The transmitting set consists of a 2-kw. radiotelephone transmitter operating into a nondirective antenna system and an additional set of amplifier branches supplying power through a goniometer into two loop antennas. The two antenna systems are symmetrically disposed with respect to each other, and coupling effects are balanced out to prevent distortion of the space pattern. The phase of the currents in the different antenna systems is controlled by a phase shift unit and means for checking the adjustment of this phase relationship continuously is provided.

The equipment on the airplane to receive this service is changed only by the addition of a small filter unit which keeps the low-frequency reed voltages from reaching the head telephones and the voice frequencies from the reed indicator.

Numerous flight tests on the system have shown it to provide very satisfactory service under adverse interference conditions.

The distance range is the same as that provided by the present visual range-beacon service.

CONTENTS

	Page
I. Introduction	262
II. Preliminary work	263
III. The transmitting problem	265
1. Factors influencing the design	265
2. The experimental transmitter	268
(*a*) Master oscillator	269
(*b*) Phase shifting unit	269
(*c*) Radiophone and carrier amplifier	272
(*d*) Speech amplifiers	272
(*e*) Beacon amplifiers	272
(*f*) Antenna system	273
3. Tests on completed unit	273
(*a*) Phase shift unit	273
(*b*) Speech amplifier and phone unit	275
(*c*) Beacon amplifier branches	276
(*d*) Antenna system	278
IV. The reception problem	280
1. Filter units	283

Page
V. Further work 285
1. Course bending 285
2. Application of system to 12-course radio range beacon 285
3. Possible modifications in design 286
(*a*) Carrier suppression 286
(*b*) Course stability 286
VI. Flight tests 287
VII. Acknowledgments 287

I. INTRODUCTION

In order to facilitate traffic over the airways of the United States, the Department of Commerce provides two types of radio aids to navigation. The first to be employed was the broadcast of weather information at regular intervals and later the radio range beacon marked out a radio path for the airplane to follow.

For some time the weather information was broadcast on a different frequency than the range-beacon service, but this required constant tuning of the receiving set on the part of the pilot. At the request of the operating companies the weather broadcast from a given field was transmitted on the same frequency as the range-beacon service from that field. In order to do this the length of the broadcast was reduced to a minimum and the range beacon shut down during this period. The cessation of the range-beacon signals informed the pilot that the weather information was due and the voice broadcast aided in identifying the station from which he was receiving guidance. This latter point is of great importance where several range-beacon stations are located close together. Such identifying means as are now employed on the aural beacon service, for instance, a characteristic code letter transmitted at regular intervals, would not be readily applicable to the visual beacon transmitter. Because of this the voice broadcast is relied upon to a great extent for identification.

This second scheme operated fairly well until pilots began to depend upon the range-beacon signals to locate their landing field. If the signals ceased when near the field, it frequently meant missing the field entirely and a loss of time in reorientation. Furthermore, when a great number of airways converge at a field, the time taken up by the weather broadcast is a considerable percentage of the entire time, and in such installations some new scheme was imperative. As itinerant fliers begin to equip their airplanes with radio, the problem becomes even more important. The intermediate frequency phone station is the one which will handle messages from and to such itinerant pilots. If this traffic reaches any considerable size, the time during which the range-beacon service is available would be very short indeed.

In order to provide these services satisfactorily, the research division, Aeronautics Branch, of the Department of Commerce, commenced a research program for the development of a transmitting set which would furnish visual range-beacon signals and speech modulation simultaneously without interruption of either service.

Such a system has been developed at the experimental flying field of the National Bureau of Standards, and is described in this paper. It supplies the pilot with continuous signals of the visual range-

beacon type, and allows voice communication with the pilot at any time with no interruption to the range service.

This is accomplished with no changes in the installation in the airplane except the addition of a small filter unit to separate the speech frequencies from the reed frequencies. No new method of operation is required and no extra strain is imposed upon the pilot.

This system presents additional advantages over the present method of transmission. By combining the two transmitters into one unit, the total amount of equipment required is greatly reduced. The same building is employed for both services, and much of the rotating machinery is used simultaneously on both portions of the transmitter. Since a radio operator is constantly on duty at the phone station, the combined system insures a constant monitoring of the beacon operation which at the present time can only be done with additional personnel. Many similar advantages are readily apparent and, consequently, from an economic viewpoint, the combined transmission is very desirable.

II. PRELIMINARY WORK

During the preliminary development of the 12-course visual range beacon in January, 1929, the idea of a simultaneous radiophone and range-beacon transmitter first appeared. When the three amplifier branches of this type of radio range are excited with the radio-frequency in time phase, the resultant carrier is suppressed by the goniometer and loop antenna system. The reason for this is readily apparent. Considering only the carrier current in each goniometer stator, these produce three figures-of-eight separated in space by 120°. If the carrier currents are in time phase, the resultant field will be the sum of three equal vectors with 120° space phase. The resultant of three such vectors is zero at any point in space. The side bands, being of different frequencies, will not combine but will appear as true figures-of-eight at 120° space phase, giving the conventional space pattern. In order to utilize this signal, it is necessary to resupply the carrier, and it was proposed to erect a suitable open antenna symmetrically located with respect to the loop antennas and radiate carrier from this. It was suggested at this time that the carrier might well be modulated with voice for identification purposes and general communication with the pilots.

However, as work on the 12-course system progressed it was found a simpler matter to use a 120° time-phase displacement in the beacon amplifiers to avoid suppression of the carrier. The need for a simultaneous transmission was not apparent at this time, so no further work was done along this line.[1]

In the fall of 1929 the necessity for providing continuous range-beacon service became apparent, and preliminary experiments were conducted to determine the feasibility of a simultaneous transmitting system. In order to secure some test data, with as little change in existing apparatus as possible, the 12-course experimental beacon was employed for this work.

The modulated amplifiers of this beacon were redesigned to receive a direct voltage on their plates in place of the alternating voltage

[1] H. Diamond and F. G. Kear, A 12-Course Radio Range for Guiding Aircraft With Tuned Reed Visual Indication, B. S. Jour. Research, 4; March, 1930.

previously supplied from the modulation frequency alternators. Each amplifier was provided with a Heising choke and the alternating voltage applied across this choke. This voltage was so proportioned as to give a 50 per cent modulation of the radio-frequency instead of the previous 100 per cent.

The master oscillator of this beacon employed two 50-watt tubes in parallel. A modulating amplifier consisting of four 50-watt tubes in parallel was applied to this oscillator and the grids of these tubes excited from a 3-stage speech amplifier. This combination modulated the carrier to a maximum of about 40 per cent.

This voice-modulated carrier was fed to each amplifier branch where it was further modulated by the reed frequencies and then radiated through the loop antenna system. The reed frequency side bands still maintained their figure-of-eight pattern while the voice side bands were radiated circularly in the same manner as the carrier.

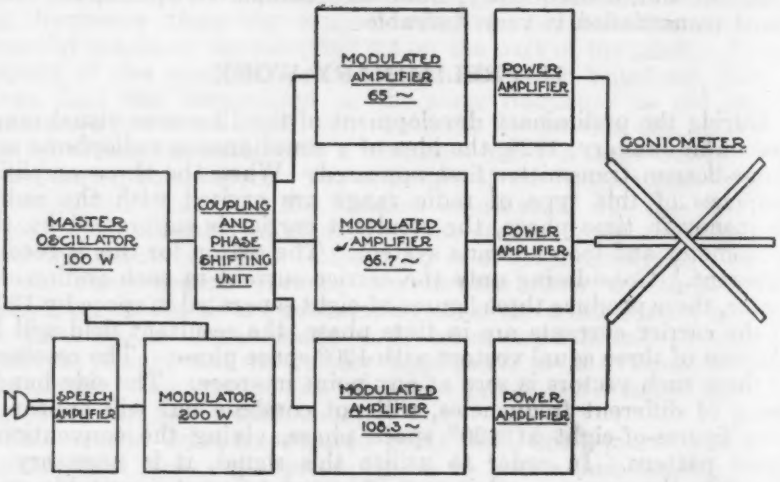

FIGURE 1.—*Schematic circuit arrangement of 12-course radio range beacon with radiotelephone modulation*

Figure 1 shows the schematic circuit while Figure 2 shows details of the modulation units and intermediate amplifiers.

It is obvious that such a modulation system would produce a great number of extraneous frequencies as a result of cross modulation; however, it afforded a simple way of getting a rapid check on the possibilities of the project.

In the latter part of 1929 field tests were made on this system. The reed indicator operated with very little irregularity and the voice quality was much better than would have been expected.

Having found this scheme to be practicable, work was begun upon a transmitter which would reduce the number of extraneous audio-frequencies and thereby improve the operation.

Two methods of attack were conceived at this time. The first required applying the voice modulation to the modulated amplifiers in series with the reed frequency modulation already present. By properly proportioning the relative voltages, any desired modulation ratio could be obtained. This would reduce the number of unwanted

frequencies to those introduced by the class C power amplifiers and it was felt that they would not be of serious magnitude.

The second method was that of a separate radio-frequency amplifier stage which received the voice modulation. This was to be of the balanced-amplifier type and so connected as to suppress the carrier and supply only the voice side bands to an open antenna system symmetrically disposed within the loop antenna structure. This last means would eliminate all the cross modulation frequencies and, in addition, would provide a simple control of the modulation ratio.

It was evident that any system in which the major portion of the power was radiated by the loop antennas must be a highly inefficient solution and would require too great a loss of power to be practical as a final product. Therefore, instead of trying out these last two methods experimentally, it was decided that the tests already made had shown the idea to be practical, and, a transmitter should be

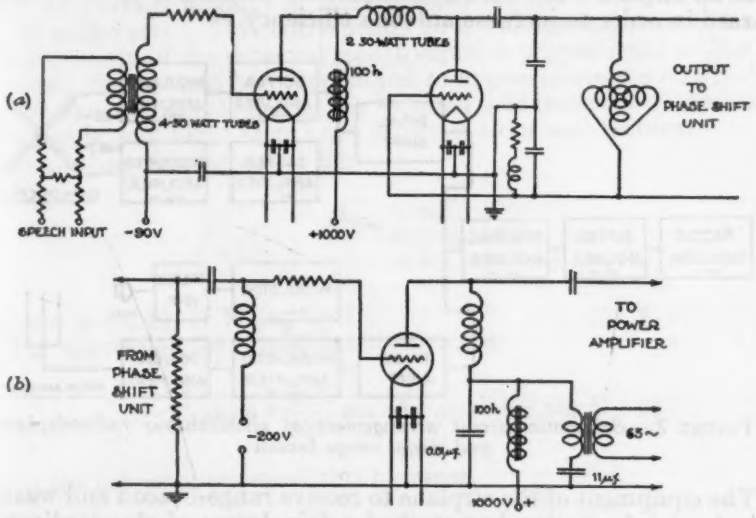

FIGURE 2.—*Electrical circuit details of 12-course radio range beacon with radiotelephone modulation*

developed of a design which could be employed along the airways. In a conference with members of the Bell Telephone Laboratories, a schematic circuit arrangement of a suitable transmitter was developed. This is illustrated in Figure 3. This circuit arrangement formed the basis of an investigation which has resulted in the development of a suitable transmitting system. This system has proven eminently satisfactory and provides simultaneous transmission of voice and radio-range signals with a minimum of expenditure and alteration to existing stations. It is with this transmitter that the paper is most concerned.

III. THE TRANSMITTING PROBLEM

1. FACTORS INFLUENCING THE DESIGN

In the design of the new transmitting system, it was not possible to start from purely theoretical considerations and so develop what would be, in the light of present radio technique, an ideal unit. Cer-

tain limiting factors entered and circumscribed the sphere of development.

The first consideration was that of power rating. The present range beacons and phone transmitters have demonstrated that they provide adequate service on the airways; hence any new unit must provide, as a minimum requirement, the same received-signal voltages at a given point as the existing equipment.

The ratio of speech side band to range beacon side band is fairly well fixed. The present reed course indicator requires approximately 6 milliwatts of power or about 0 db absolute level. (This zero level of 6 milliwatts is commonly used in telephony and radio broadcasting). In order to insure intelligible speech in the airplane, the phones must have available 60 milliwatts or +10 db. This ratio must be attained in the field strength pattern at any point in space.

The antenna system was restricted in size on account of its location near an airport. It would be undesirable to increase the obstruction hazard in order to increase antenna efficiency.

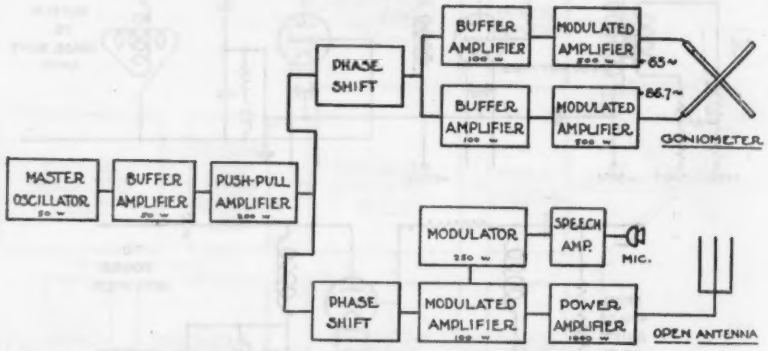

FIGURE 3.—*Schematic circuit arrangement of simultaneous radiotelephone and visual range beacon*

The equipment of the airplane to receive range-beacon and weather broadcast information has reached a fair degree of standardization. Any system of communication requiring much additional apparatus or considerable change in present equipment would meet with great opposition from the operating companies. The ideal solution would be one requiring no change in existing installations.

The civil airways at the present time are rather comprehensively covered with a network of radiophone and range-beacon installations. This equipment represents a considerable investment, and to adopt a design which would render all existing stations obsolescent would be economically poor. The new system must employ a maximum amount of existing equipment in its design.

Finally, much of the apparatus employed will be operated by remote control. This necessitates a design of great inherent stability and freedom from variations due to changing weather conditions. These requirements are all met in the present design. The result is a unit which is well suited to the present needs of the airways.

The foundation for the preliminary design was the 2-kw radiophone transmitter which has been used on the airways for several years and has proven very satisfactory. When used with the type of antenna

structure for which it was designed, this transmitter will produce a field intensity of 6,500 μv/m at a distance of 10 miles over average terrain. This is modulated to a peak of approximately 60 per cent by the voice frequency.

Assuming square law detection in the aircraft radio receiver, the detected voltage is proportional to the product of the percentage modulation and the square of the carrier field intensity.

$$i_d \propto mE^2$$

from which

$$i_d \propto 0.6 \quad (6{,}500)^2$$
$$\propto 25{,}000{,}000 \text{ approximately}$$

As mentioned before, the reed indicator requires 0 db level or 6 milliwatts for an "on-course" indication, and the head telephones with an average amount of noise present require a level of +10 db, or 60 milliwatts. This corresponds to a voltage ratio of 3.16 to 1. Consequently, if the detected speech signal is proportional to 25×10^6, the reed signal must be proportional to approximately 8×10^6. This factor was used in calculating the required field intensity of the beacon side bands, and flight tests have shown it to be satisfactory.

Employing this factor we find

$$i_{d_{reed}} \propto mE_o^2$$
$$\propto m(6{,}500)^2$$
$$\propto 8 \times 10^6$$

whence $m = 0.19$, or 19 per cent.

The expression for a modulated carrier is

$$E = E_o \sin \theta + \frac{mE_o}{2} \sin (\theta - \varphi) + \frac{mE_o}{2} \sin (\theta + \varphi)$$

With the carrier suppressed this becomes

$$E_1 = \frac{mE_o}{2} \sin (\theta - \varphi) + \frac{mE_o}{2} \sin (\theta + \varphi)$$

If the field intensity is measured by the usual method this will be

$$E_{eff} = \sqrt{\left(\frac{mE_o}{2}\right)^2 + \left(\frac{mE_o}{2}\right)^2}$$

$$E_{eff} = \frac{mE_o}{\sqrt{2}}$$

Substituting the known values for m and E_o

$$E_{eff} = \frac{0.19 \times 6{,}500}{\sqrt{2}}$$

$$E_{eff} = 874 \ \mu v/m$$

Using loop antennas with the dimensions of those at the College Park experimental station, this field intensity is obtained with an antenna current of slightly less than 8 amperes. The loop antenna resistance being 8 ohms, the antenna power is approximately 500 watts.

The beacon amplifier branches must, therefore, be capable of delivering 500 watts of side-band power to the loop antennas to secure the proper ratio of speech to beacon field intensity with the same useful range as the present airway equipment.

It is worthy of note at this point that if the computations were made on the basis of the field intensities of the present range-beacon stations, the power required would be much less. For example, the 4-course visual radio range beacon has a carrier field intensity of 734 μv/m at 10 miles. The detected voltage assuming 100 per cent modulation would then be proportional to $(734)^2$ or 540,000. This value, being only one-sixteenth of that used in the foregoing, would mean much lower power in both beacon and phone amplifiers.

However, while this low figure is satisfactory for use with visual range-beacon signals alone, when speech is supplied on the same channel, the increased sensitivity required in the radio receiver results in a very unfavorable static to signal ratio, and the useful distance range is greatly reduced. Because of this the power calculations were made upon the basis of the radiophone transmitter performance instead of the range-beacon transmitter data.

The transmitting system requirements, from a consideration of the foregoing factors, may be, therefore, summed up as follows:

Carrier and speech supply to consist of a 2 kw phone transmitter modulated 60 per cent peak and operating into an open antenna 75 feet high with four flat top sections 80 feet long bisecting the angles of the loop antennas.

Range beacon supply to comprise two balanced amplifier branches supplied with carrier from the 2 kw unit. Modulation to be accomplished by the use of alternating current from special low-frequency alternators and the carrier to be suppressed by some suitable arrangement. The amplifier branches to operate through a conventional goniometer into two loop antennas. The antenna height to be 75 feet and the base of the loop antennas 300 feet long. Each amplifier to have sufficient capacity to deliver 500 watts of side band power to the loop antennas.

It was felt that this system would provide adequate transmission for the needs of the airways. The next problem was to construct a unit from available material and secure actual operating data.

2. THE EXPERIMENTAL TRANSMITTER

Since no equipment of the type employed on the airways was available for use in the experimental transmitter, an entirely new unit was constructed. This unit differs considerably in arrangement from the conventional type, but, all the limiting factors being considered, the relative performance is very similar.

In order to attain flexibility, the transmitter was built upon the individual unit plan. These units are as follows:

(*a*) A master oscillator which supplies push-pull radio-frequency power to the amplifiers. This is designed so that variations in load do not affect the frequency or balance of the push-pull amplifiers.

FIGURE 4.—*General view of the experimental transmitting set at College Park.*

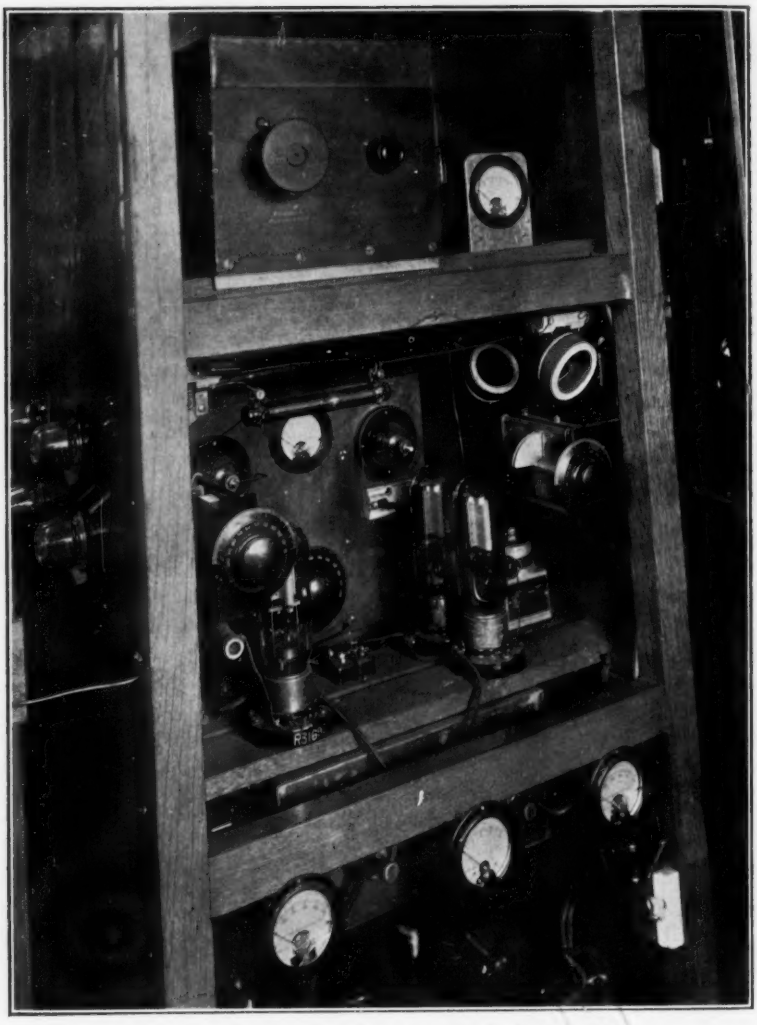

FIGURE 5.—*Front view of master oscillator unit*

(*b*) A phase-shifting unit to control the phase of the radio-frequency applied to the separate amplifiers.

(*c*) A radiophone and carrier amplifier branch which supplies carrier-frequency power to a nondirectional vertical antenna, with provision for modulating the carrier with the voice frequencies.

(*d*) A speech amplifier which modulates the carrier to a maximum of 60 per cent, with a flat response from 300 to 6,000 cycles, but which does not pass the low voice frequencies in the region of the reed modulation frequencies.

(*e*) Two beacon amplifier branches, which receive the radio-frequency from the master oscillator, modulate it with desired reed frequencies and then, having suppressed the carrier, deliver the side bands to the goniometer.

(*f*) An antenna system providing directional transmission from the beacon amplifiers and nondirectional transmission from the carrier and speech amplifier.

These units were constructed, tested individually, and then modified to correct such deficiencies as were found in the tests.

Figure 4 shows the installation at the College Park field station.

A description of the units as finally employed follows:

(a) MASTER OSCILLATOR

The master oscillator employs a 50-watt tube with the Colpitts oscillating circuit. The frequency is adjustable by means of a variable inductor over the present aircraft beacon range of 235 to 350 kilocycles. A peizo-controlled unit has been designed to replace this in a permanent installation. This ouptut, in turn, excites another 50-watt amplifier through a high resistance feed to prevent reaction due to change of load. The amplifier tube, through a coupling transformer, supplies a tuned circuit, the extremities of which are connected to the grids of a second amplifier, consisting of two sets of two 50-watt tubes in push-pull. These are cosss-neutralized. From the plates of these tubes is obtained the push-pull radio-frequency output. This unit is complete within itself and is thoroughly shielded. It is illustrated in Figure 5.

(b) PHASE-SHIFTING UNIT

In any system of carrier suppression where both side bands are radiated it becomes necessary to resupply the carrier in the proper phase in order to prevent distortion. This may readily be demonstrated as follows:

The conventional expression for a modulated radio-frequency signal is

$$E \sin \theta \ (1+m \cos \phi)$$

where

$$\theta = 2\pi f_c \, t$$

$$\phi = 2\pi \, f_m \, t$$

f_c being the carrier frequency, f_m being the modulating signal frequency, and m is the percentage of modulation.

This may be rewritten

$$E\left(\sin \theta + \frac{m}{2} \sin \ (\theta+\phi) + \frac{m}{2} \sin \ (\theta-\phi)\right)$$

the first term of this expression being the carrier and the last two the side bands.

In carrier-suppressed transmission the equation reduces to

$$E\left(\frac{m}{2}\sin(\theta+\phi)+\frac{m}{2}\sin(\theta-\phi)\right)$$

Assume the carrier to be resupplied at a slightly different angle α

The transmitted wave now is

$$e_t = E\left[\sin(\theta+\alpha)+\frac{m}{2}\sin(\theta+\phi)+\frac{m}{2}\sin(\theta-\phi)\right]$$

Assuming square law detection

$$i_d = Ae_t^2$$

The components of the detected signal become

$$AE^2\Big[\sin^2(\theta+\alpha)+\frac{m^2}{4}\sin^2(\theta+\varphi)+\frac{m^2}{4}\sin^2(\theta-\varphi) + m\sin(\theta+\alpha)\sin(\theta+\varphi)+m\sin(\theta+\alpha)\sin(\theta-\varphi) + \frac{m^2}{2}\sin(\theta+\varphi)\sin(\theta-\varphi)\Big]$$

The first three terms are radio-frequencies and can be neglected. Expanding the fourth term:

$$m\sin(\theta+\alpha)\sin(\theta+\varphi)=\frac{m}{2}\cos(\theta+\alpha-\theta-\varphi)-\frac{m}{2}\cos(\theta+\alpha+\theta+\varphi)$$
$$=\frac{m}{2}\cos(\alpha-\varphi)-\frac{m}{2}\cos(2\theta+\alpha+\varphi)$$

Likewise expanding the fifth term:

$$m\sin(\theta-\alpha)\sin(\theta-\varphi)=\frac{m}{2}\cos(\theta+\alpha-\theta+\varphi)-\frac{m}{2}\cos(\theta+\alpha+\theta-\varphi)$$
$$=\frac{m}{2}\cos(\alpha+\varphi)-\frac{m}{2}\cos(2\theta+\alpha-\varphi)$$

Expanding the last term:

$$\frac{m^2}{2}\sin(\theta+\varphi)\sin(\theta-\varphi)=\frac{m^2}{4}\cos(\theta+\varphi-\theta+\varphi)+\frac{m^2}{4}\cos(\theta+\varphi+\theta-\varphi)$$
$$=\frac{m^2}{4}\cos 2\varphi+\frac{m^2}{4}\cos 2\theta$$

Considering only the audio-frequency terms of the detected signal, we find

$$i_d=AE^2\left[\frac{m}{2}\cos(\alpha-\varphi)+\frac{m}{2}\cos(\alpha+\varphi)+\frac{m^2}{4}\cos 2\varphi\right]$$

or

$$i_d=AE^2\left[m\cos\varphi\cos\alpha+\frac{m^2}{4}\cos 2\varphi\right]$$

Now if $\alpha = 90°$, the first term of the above expression will disappear, leaving only the double frequency term. If $\alpha = 0°$, the equation reduces to

$$i_d = AE^2\left[m \cos \varphi + \frac{m^2}{4} \cos 2\varphi\right]$$

which is the usual equation for a detected signal. Consequently, if the carrier is suppressed at the transmitter and then resupplied, it must have its original phase or the detected signal components will tend to cancel each other, leaving a double-frequency term. The degree of this cancellation will increase with an increase of phase difference.

In the 4 and 12 course radio range beacons it was necessary to provide a phase shift in each amplifier to prevent carrier combination.[2] In the carrier-suppressed beacon this is no longer necessary. Since no carrier is radiated it can not combine to distort the space pattern. Hence, both beacon amplifiers are supplied in phase and the resultant pattern is the conventional crossed figures-of-eight.

The loop antenna introduces a phase shift of another sort. The received voltage at a given point in space is the vector sum of two voltages. One is induced by the one side of the loop antenna and one by the other. The currents in the two sides of a single loop antenna are 180° out of phase when considered with respect to a distant receiving antenna and the vector sum of the induced voltages is in quadrature with these currents regardless of the point of reception.[3]

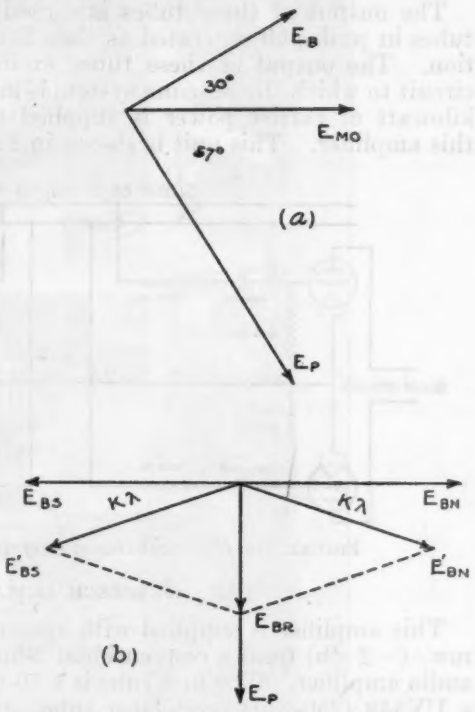

FIGURE 6.—*Vector diagram showing phase relations in combined transmission*

(a), phase relations within the transmitting set: E_b, voltage across beacon amplifiers; E_{mo}, voltage across master oscillator; E_p, voltage across carrier amplifiers.

(b), phase relations at point of reception: E_{bn}, voltage across north end of loop antenna; E_{bs}, voltage across south end of loop antenna; E'_{bs}, voltage across north end retarded $k\lambda$; E'_{bs}, voltage across south end advanced $k\lambda$; E_{nr}, resultant voltage induced by loop antenna; E_p, voltage due to open antenna; $K\lambda$, inherent phase shift of loop antennas.

Since the carrier must be resupplied in the same phase as the beacon side bands, a phase shift must be introduced at the transmitting end. The phase relations existing in the transmitter are illustrated in Figure 6. The first diagram shows the phase relations within the transmitter while the second shows those existing at the receiving point.

[2] H. Diamond, applying the Visual Double Modulation Beacon to the Airways, B. S. Jour. Research, (RP148); February, 1930; Proc. I. R. E., 17, p. 253; December, 1929.
[3] J. H. Morecroft, Principles of Radio Communication, p. 709 et seq.

The 90° phase shift is accomplished in the same way as was heretofore used in the 4-course beacon. The circuit diagram (fig. 7) is self-explanatory.

(c) RADIOPHONE AND CARRIER AMPLIFIER

This amplifier receives its excitation from the master oscillator upon the grids of two 50-watt tubes in push-pull. These are operated as class C amplifiers and their grids are shunted by a relatively low resistance to insure good regulation. These tubes are the modulated amplifiers and the Heising choke is incorporated into their plate circuit.

The output of these tubes is directly coupled to two 1-kilowatt tubes in push-pull, operated as class B amplifiers to minimize distortion. The output of these tubes excites a high capacitance tuned circuit to which the antenna system is inductively coupled. One-half kilowatt of carrier power is supplied to the antenna system from this amplifier. This unit is shown in Figures 8 and 9.

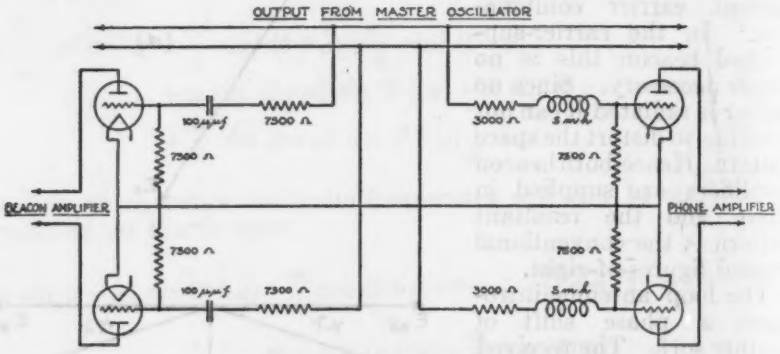

FIGURE 7.—*Electrical circuit diagram of phase-shifting unit*

(d) SPEECH AMPLIFIER

This amplifier is supplied with speech frequency at a level of 3.75 mw. (−2 db) from a conventional 2-button microphone and 3-stage audio amplifier. The first tube is a 50-watt tube which is coupled to a UV849 (250-watt modulator tube) through a filter section which rejects frequencies below 250 cycles. At an input level of 3.75 mw. the modulation is 60 per cent peak on the modulated amplifiers. The speech input equipment is shown in Figure 10.

(e) BEACON AMPLIFIERS

The beacon amplifiers are in duplicate throughout to supply power to the two stators of the goniometer. In each amplifier branch, radio-frequency from the master oscillator is supplied to the grids of two 50-watt screen grid tubes in push-pull. These tubes act only as buffer amplifiers to prevent reaction of the low reed frequencies on the speech and carrier amplifier.

These tubes are direct coupled to two ¼-kilowatt tubes operated as class C amplifiers. The plates of these latter are fed in push-pull from transformers operated at the reed frequency. The output is taken off in parallel to the goniometer, thereby suppressing the carrier but radiating the side bands.

FIGURE 8.—*Radiophone and carrier amplifier unit (side view)*

UNIV. OF MICH.

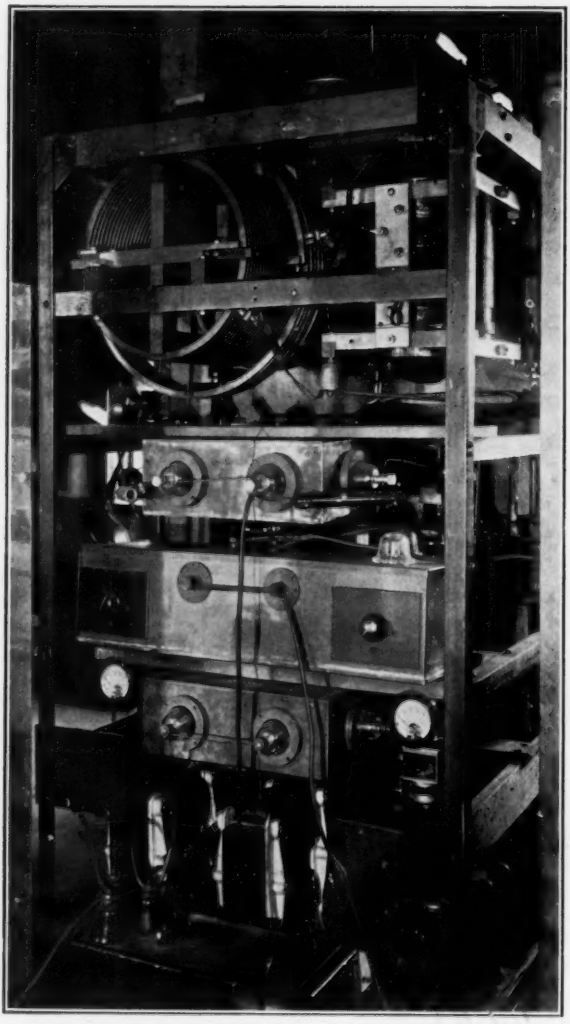

FIGURE 9.—*Radiophone and carrier amplifier unit (rear view)*

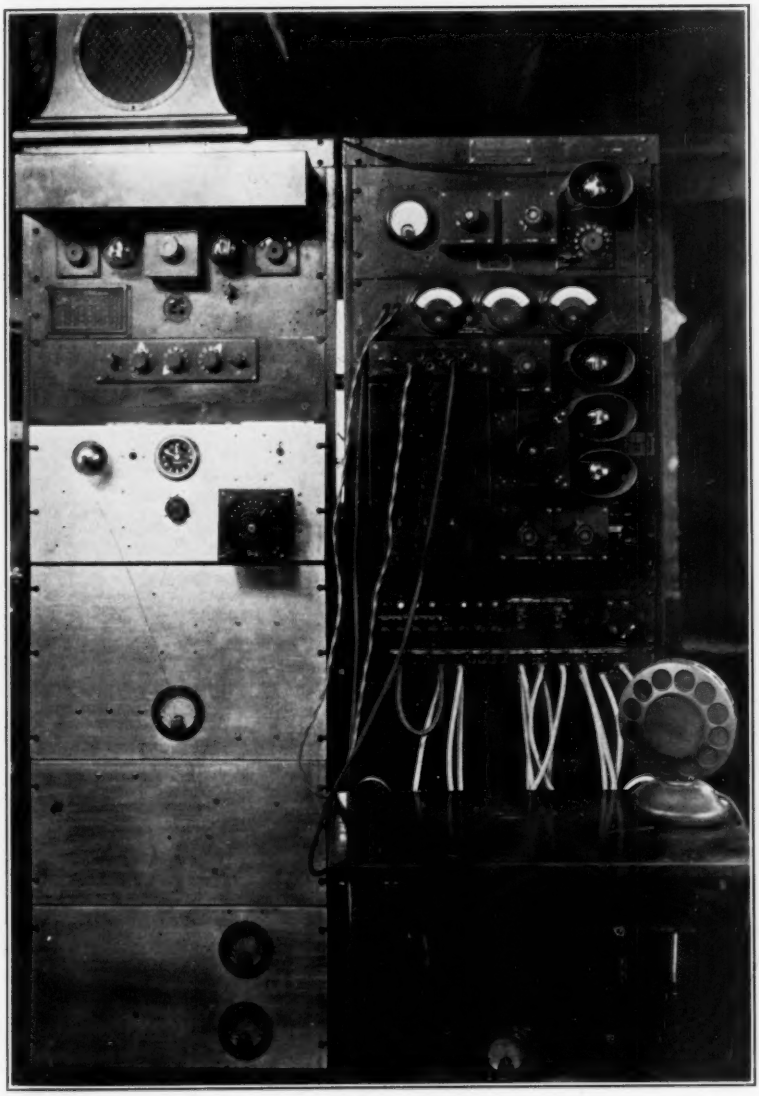

FIGURE 10.—*Speech input equipment*

UNIV. OF MICH.

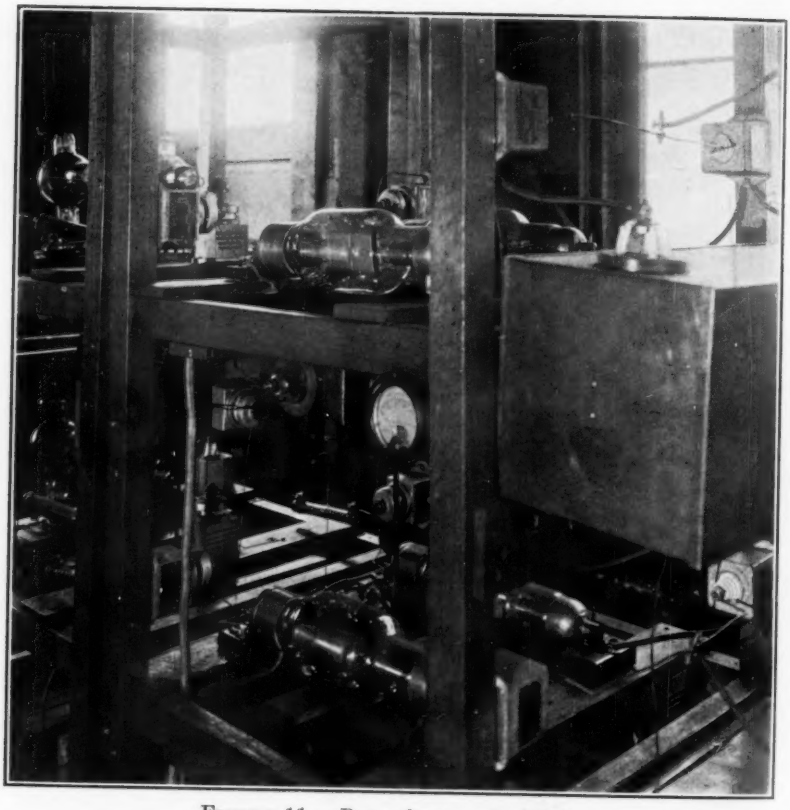

FIGURE 11.—*Range-beacon amplifiers*

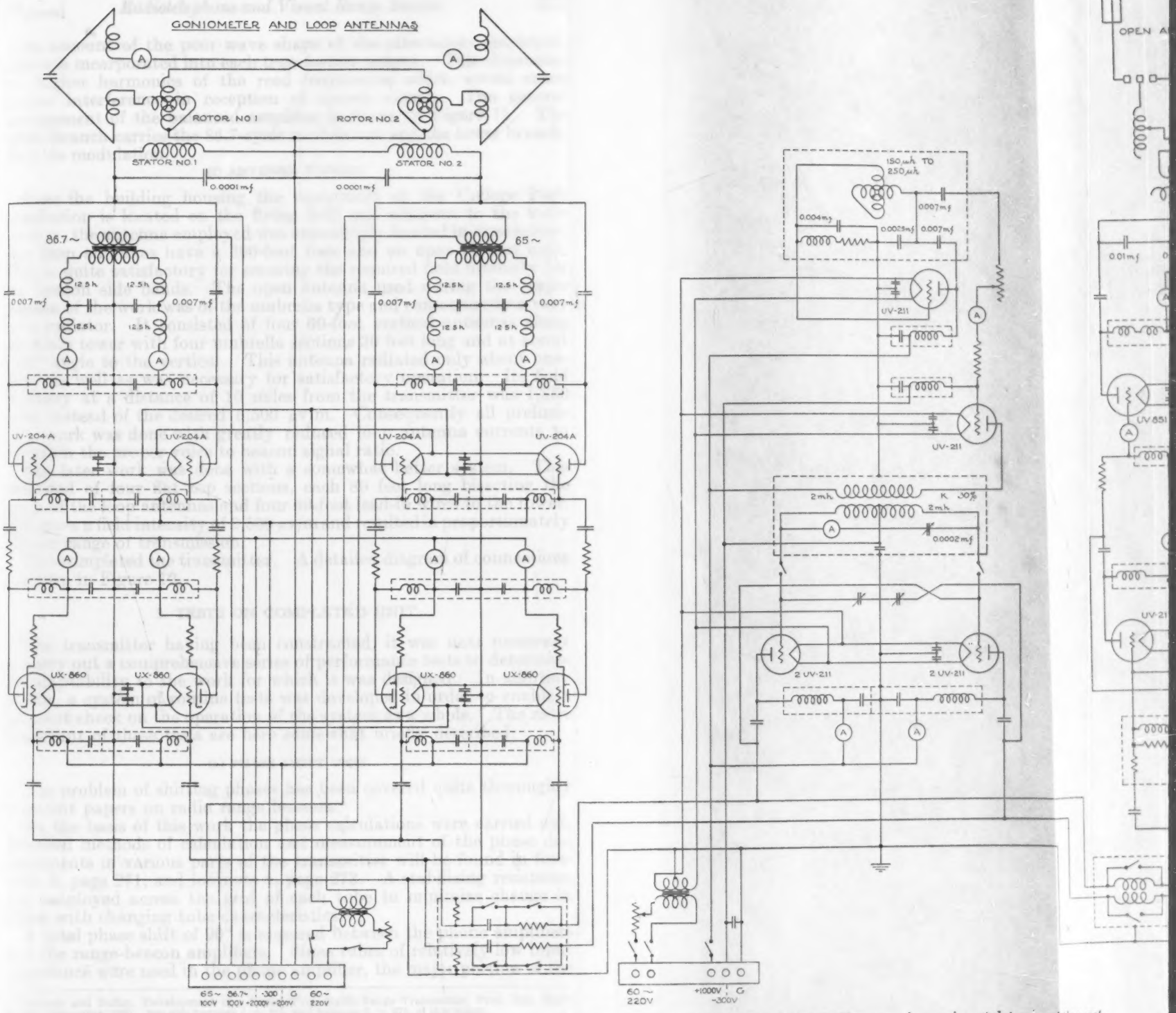

FIGURE 12.—*Detailed electrical circuit diagram of experimental transmitting set*

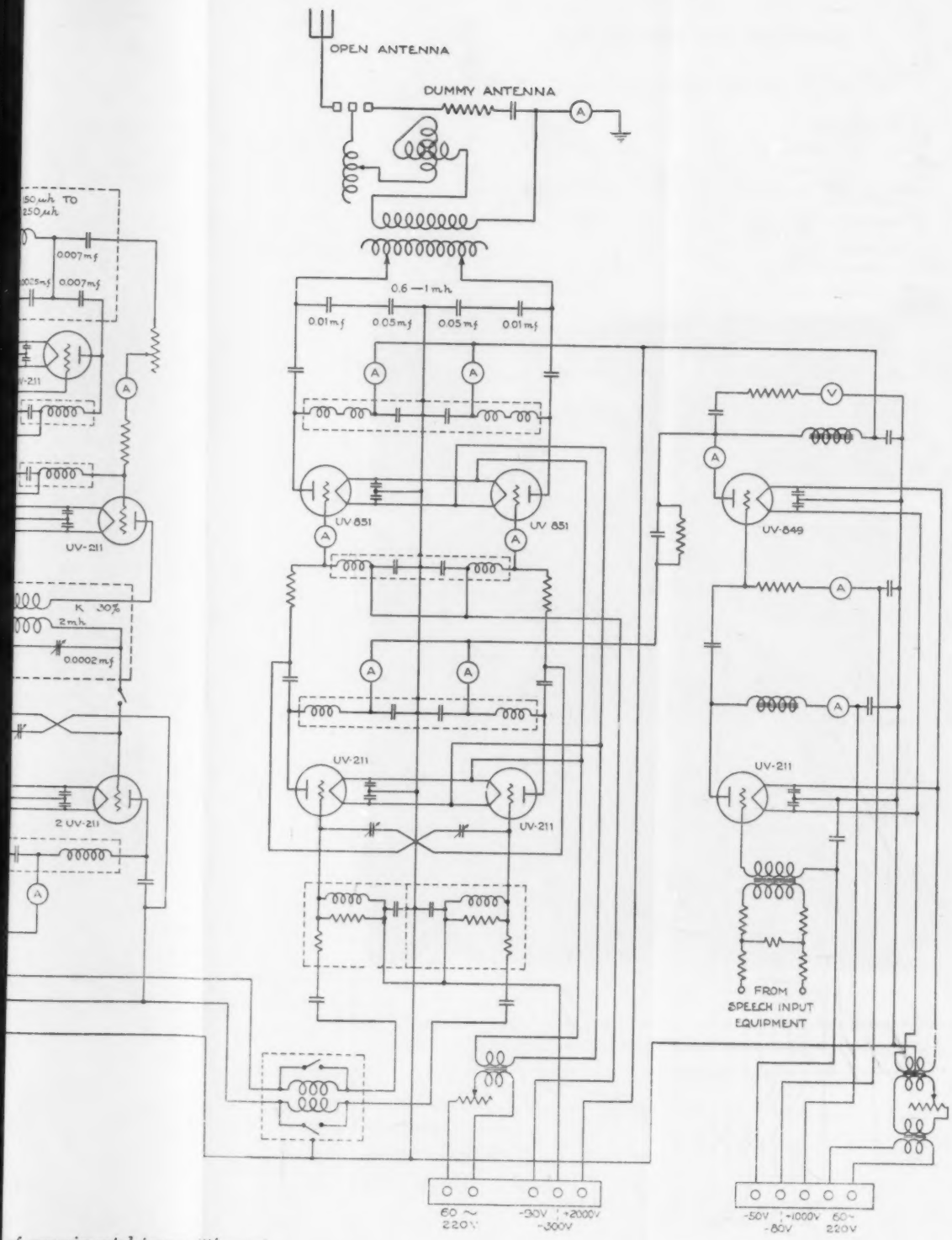

of experimental transmitting set

64825—31. (Face p. 272.)

On account of the poor wave shape of the alternators employed, a filter is incorporated into each transformer output. This eliminates the higher harmonics of the reed frequencies which would cause serious interference in reception of speech signals. The general arrangement of the balanced amplifier is shown in Figure 11. The upper branch carries the 86.7-cycle modulation and the lower branch, 65-cycle modulation.

(f) ANTENNA SYSTEM

Since the building housing the equipment at the College Park installation is located on the flying field and adjacent to the main runway, the antenna employed was exceedingly limited in dimensions. The loop antennas have a 300-foot base and an apex 70 feet high. This is quite satisfactory for securing the required field intensity for the beacon side bands. The open antenna used during the major portion of the work was of the umbrella type and consequently a very poor radiator. It consisted of four 60-foot vertical antennas along the main tower with four umbrella sections 30 feet long and at about a 40° angle to the vertical. This antenna radiated only about one-third as well as was necessary for satisfactory operation. Its field intensity at a distance of 10 miles from the transmitter was 1,850 μv/m instead of the desired 6,500 μv/m. Consequently all preliminary work was done with greatly reduced loop antenna currents to maintain the proper voice to beacon signal ratio.

The later work was done with a somewhat better system. This consisted of four flat top sections, each 80 feet long bisecting the angle of the loop antennas and four 60-foot lead-in wires to the tower. This gave a field intensity of 2,500 μv/m and resulted in proportionately greater range of transmission.

This completed the transmitter. A detailed diagram of connections is shown in Figure 12.

3. TESTS ON COMPLETED UNIT

The transmitter having been constructed, it was next necessary to carry out a comprehensive series of performance tests to determine its adaptability to the work for which it was designed. In addition to this, a system of routine tests was developed in order to enable a frequent check on the operation of the system as a whole. The more important of these tests are here somewhat briefly described.

(a) PHASE SHIFT UNIT

The problem of shifting phases has been covered quite thoroughly in recent papers on radio range beacons.[4]

On the basis of this work the phase calculations were carried out. Detailed methods of calculation and measurement of the phase displacements in various parts of the transmitter will be found in footnote 2, page 271, and footnote 4, page 273. A stabilizing resistance was employed across the grid of each tube to minimize change in phase with changing tube characteristics.

A total phase shift of 90° is required between the phone amplifiers and the range-beacon amplifiers. Since tubes of relatively low input impedance were used in the phone amplifier, the major portion of the

[4] Jackson and Bailey, Development of a Visual Type Radio-Range Transmitter, Proc. Inst. Radio Engrs.; December, 1930. See also footnote 1, p. 263, and footnote 2, p. 271, of this paper.

phase shift (approximately 60°) was introduced into this circuit network. The remaining 30° shift was placed in the circuit network to the screen grid buffer amplifiers.

Previous work on phase adjustments had shown the input impedance of a UV–211 tube acting as a class C amplifier to be approximately 5,000 ohms. Likewise two UX–860 tubes in parallel have an input impedance of 10,000 ohms. Neglecting tube capacity, the equivalent circuit of the phone branch would be that of Figure 13 (*a*) and that of the range-beacon branches Figure 13 (*b*). In the phone branch the total resistance equals 6,000 ohms. The inductive reactance, X_2, equals 9,100 ohms at 290 kc. The resultant phase angle (θ_1) is therefore 56°. Similarly, the beacon branches have an equivalent resistance of 9,280 ohms. The capacitative reactance, X_c, equals 5,500 ohms. The phase angle (θ_2) is therefore equal to 30°. Consequently, the total phase shift is 87°, or approximately 90°. Since the resultant detected signal varies proportionately to the sine of θ, variations of a few degrees either way make no apparent difference in signal strength.

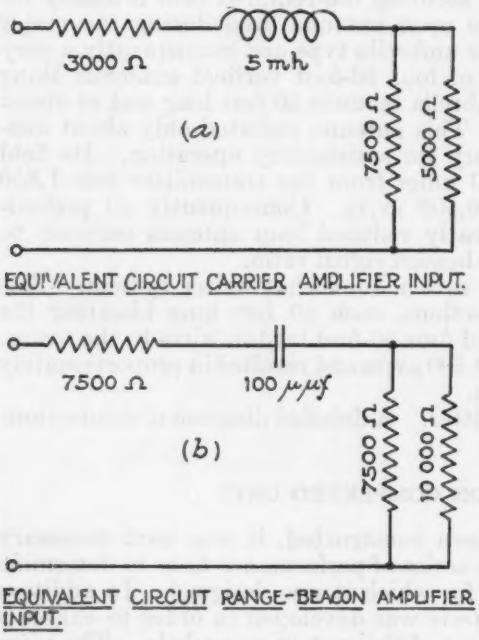

FIGURE 13.—*Equivalent circuits*

(*a*) Carrier amplifier input; (*b*) range-beacon amplifier input.

Methods of checking these phase adjustments by measurements have been referred to previously. However, it was found more convenient to utilize a method which has not heretofore been described. Since the detected signal strength is a function of the phase relationship, the first measurements were made by observing the reed indicator deflections for various phase angles. This provided a rough check and was very valuable in securing a rough adjustment to somewhere near the desired value. However, the fact already mentioned, namely, that the variation is proportional to the sine of θ, made a close adjustment impossible by this means.

In order to secure a sharper indication, the output of the receiving set was connected to an oscillograph. As the phase changes from the optimum value, the second harmonic term begins to predominate and when the phase is 90° from the correct value, the double frequency alone will appear, as has been shown previously. Using the oscillograph in this manner, it was possible to check the previous data very closely. However, the presence of a second harmonic voltage, even at optimum conditions, made this check but little better than the use of reeds. It was noticed during these measurements that the

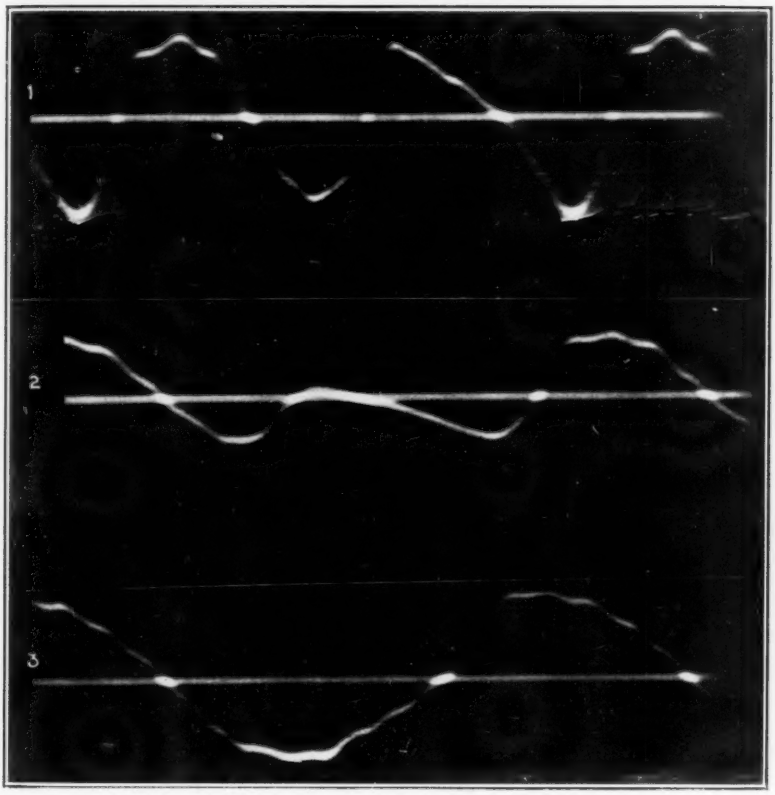

FIGURE 14.—*Oscillographs showing means of checking phase relations*

1, Carrier approximately 5° from correct phase. Successive peaks have almost same amplitude; *2*, carrier 30° from correct phase. Note decided drop in center peak; *3*, carrier 90° from correct phase. Center peak completely reversed.

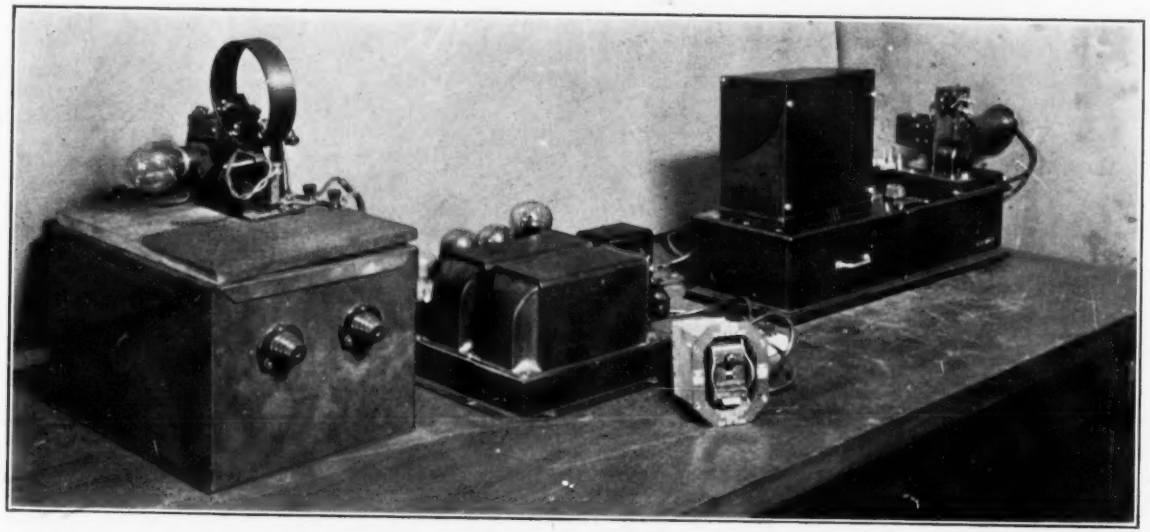

FIGURE 15.—*Equipment used to check phase relations*

position of poorest phase relationship was quite critical. When the phase was exactly 90°, the double frequency would be very sharply defined, but a slight shift would cause an immediate drop in the alternate voltage peaks.

It was decided to utilize this phenomenon, so a thermionic rectifier was closely coupled to the loop antenna system and to the open antenna system. Since the pick-up from the loop antenna was now purely inductive, the inherent phase shift introduced by radiation from the loop antenna already mentioned did not occur. Consequently, when the phases were so adjusted as to give maximum detected signal in a distant receiver, they were giving the minimum or double-frequency signal in the output of the local rectifier. This output was amplified and observed on an oscillograph. The indication of optimum conditions was now exceedingly sharp. This is shown in Figure 14. Three different phase adjustments are shown. The ratio of carrier to side band was very high for the conditions under which these oscillograms were taken, and the detector was considerably overloaded with carrier in order to give a reasonable vibrator deflection. However, this is not important, since the phase is not determined by the wave shape, but merely by the height of successive voltage peaks.

The equipment used to obtain these checks is illustrated in Figure 15. A detector tube shown on the left in the photograph is coupled loosely to the two antenna systems by the coil shown immediately above it. This tube is operated as a Fleming valve, and its output is amplified by means of the 2-stage power amplifier to a magnitude sufficient to operate the oscillograph. It is necessary to locate the pick-up coil with some care in order that the ratio of carrier and beacon side bands shall be satisfactory.

In beacon installations along the airways, it would not be economically possible to install an oscillograph at each station for a continuous phase check. In such cases, after the adjustment is once made for optimum relationship, a reed indicator may be substituted for the oscillograph. The reed indicator is unaffected by the double frequency and so long as the indicator does not vibrate, the phase is well within the desired limits.

(b) SPEECH AMPLIFIER AND PHONE UNIT

With the exception of a series of fidelity graphs, no special tests were made on the speech equipment. Figure 16 shows a series of fidelity measurements at different points in the system. These tests were all made by means of a variable frequency oscillator whose input to the speech equipment was held constant at 3.75 mw (−2 db), while the frequency was varied from 100 to 6,000 cycles.

Graph *A* shows the speech input equipment characteristic as determined by measurement of the voltage across the Heising choke. The action of the filter section in attenuating the low frequencies in the neighborhood of the reed frequencies is quite marked. On the other hand, the reproduction of the higher frequencies in the intelligibility range is very good indeed.

Graph *B* shows the received signal under the same conditions, employing a standard aircraft receiver. The high frequencies are now attenuated to a considerable degree. This is intentional in

the design of the receiver with the idea of reducing atmospheric noises. The intelligibility of speech is dependent to a great degree upon the fidelity of reproduction in this range, and the result is a considerable sacrifice of intelligibility in order to obtain some reduction of noise.

Graph *C* shows the received signal corrected for the poor audio-frequency characteristic of the radio receiver. The performance indicated in this graph should be the minimum requirement for aircraft receiving sets.

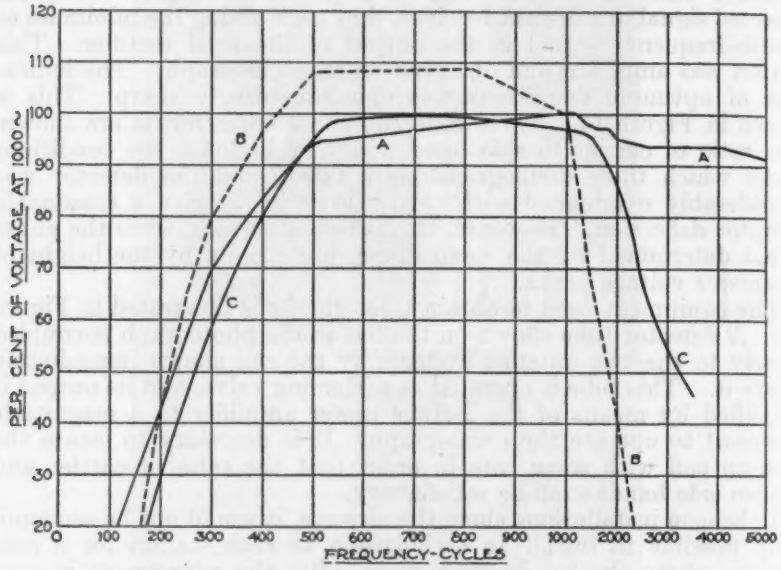

FIGURE 16.—*Fidelity characteristics of speech equipment*

a, characteristic of speech amplifier system; *b*, over-all received characteristic; and *c*, over-all characteristic corrected for audio-amplifier.

(c) BEACON AMPLIFIER BRANCHES

There are three major requirements for successful operation of the beacon amplifier branches. These are (1) equality of phase shift in the two branches, (2) total suppression of carrier in each branch, and (3) fidelity of reproduction of the modulation frequencies. In addition to these, the usual requirements of stability, efficiency, and freedom from parasitic oscillations must be met.

In carrier-suppressed beacon transmission it is essential that the phase of each set of side bands radiated from the loop antennas be identical. Any difference of phase introduced herein would result in a difference of phase between the resupplied carrier and one or the other sets of side bands. This would cause a change of course with variations in the phase of the carrier. Slight variations in carrier phase, due to detuning, are inevitable. Care must, therefore, be taken to prevent appreciable phase displacement between the two sets of beacon side bands. Consequently, it is necessary to insure that the amplifier branches and goniometer circuits produce the same phase shift, regardless of the goniometer position.

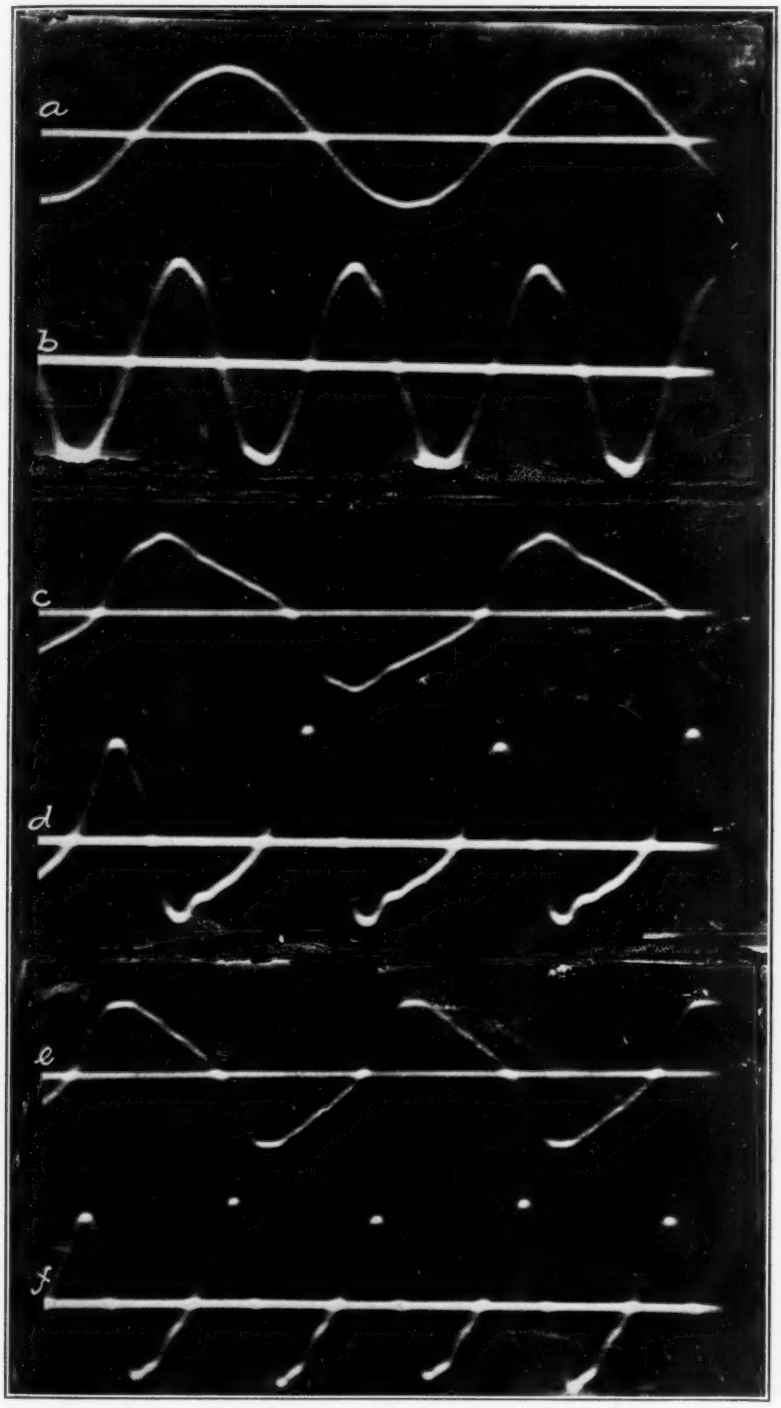

FIGURE 17.—*Oscillograms showing operation of range-beacon amplifiers*

a, 60 cycles from mains applied to beacon amplifier; *b*, received signal side bands only; *c*, 65 cycle alternator rated load unity p. f.; *d*, received signal side bands only; *e*, 86.7 cycle alternator rated load unity p. f.; *f*, received signal side bands only.

These phase relations are best checked by means of pick-up coils, coupled to the loop antennas and connected to a thermogalvanometer. The procedure is as follows:

With one amplifier branch excited, the goniometer is adjusted to supply current to both loop antenna systems. The coupling coils are then moved until the voltages induced by each loop antenna, as indicated by the galvanometer, are identical. The pick-up coils are then connected in series with the galvanometer, first aiding and then opposing. If the loop antenna currents are in phase, the currents in the two pick-up coils will also be in phase and in one case the current will double, while with the coils opposing no current will flow. This test may be repeated for several goniometer positions and indicates merely the proper operation of the goniometer system.

Both amplifier branches are now excited and modulated with the same reed frequency. The goniometer is set on either 0° or 90°. This directs all of the output of one amplifier into one loop antenna and all of the other into the second loop antenna. Having equalized the pick up in each coil, the currents are again measured aiding and opposing. If the reading of the meter is alternately double that due to one coil and zero, it may safely be assumed that the phase of the two amplifier branches is identical. This satisfies the first requirement. In making this test, it is necessary that the same modulation frequency be used. Since the carrier does not appear in the loop antenna, only the side-band frequencies can be compared, and these must be the same for a phase measurement to be made.

In checking the percentage of carrier suppression, an oscillograph was connected to the output of a receiving set located some distance from the transmitter and the beacon amplifiers excited one at a time with the open-type antenna disconnected. When suppression was most nearly complete, the detected signal was a pure second harmonic of the reed frequency. Any unbalance would cause alternate voltage peaks to assume different amplitudes, and when no suppression occurred, the fundamental frequency alone appeared. This test showed the amplifiers to give very good performance under wide variations of load.

The third test, that of fidelity of reproduction of modulation frequency, was also made with the oscillograph. The results of this test are shown in Figure 17. These oscillograms were taken with carrier suppressed; consequently the received signal is the second harmonic of the reed modulation frequency. Graphs *a* and *b* show the result of applying the 60-cycle line voltage to the transformers modulating the amplifier. This gives a resultant signal which has an excellent wave shape. Graphs *c* and *d* show the voltage of the 65-cycle alternator under normal load with the resultant badly distorted received signal. Graphs *e* and *f* show the 86.7-cycle alternator under the same conditions with its resultant signal.

From these oscillograms it is safe to assume that the amplifiers will produce a good wave form if supplied with a voltage of equally good wave form. A poor alternator, however, will cause audio-frequency harmonics in the transmitted signal, thereby producing frequencies which may interfere with the voice transmission. In spite of the irregular wave shape of the alternators employed in these tests, the resultant signal did not contain sufficient harmonics to

noticeably impair the speech quality. It would be very desirable, however, to use alternators with as good a wave form as possible to insure a minimum of interference with the speech reception.

The transformer output in each beacon amplifier is provided with a filter circuit to eliminate frequencies above 200 cycles. However, the major harmonics are the second and third which are below the filter cut-off point. Consequently the filter is of little value. A filter to cut-off at a lower point would require coils whose loss would be excessive. Hence, the best solution is to employ alternators whose wave form is approximately sinusoidal.

Since most of the test work on the transmitter was carried on with the inefficient umbrella type of open antenna, the output of the beacon amplifiers was proportionately reduced in order to maintain the proper voltage ratio of beacon to phone signals. The carrier field intensity of this arrangement was 1,850 μv/m at 10 miles distance from the transmitter. With a phone modulation of 60 per cent peak, the detected signal voltage is proportional to mE^2 or $0.6(1{,}850)^2$, giving a factor of approximately 2.05×10^6, or only 10 per cent of that provided in the final design. To maintain the same ratio of beacon to phone signals E_1 must equal $0.19 \times E_0$, or 350 microvolts. The corresponding field instensity is $\frac{350}{\sqrt{2}}$ or 245 μv/m. This is obtained with a loop antenna current of 2 amperes. With this power output, test flights during the months of January, February, and March showed a reliable distance range for the combined transmission of 100 miles. It is estimated, however, that the equivalent distance range under summer conditions would be reduced to the order of 60 to 75 miles.

(d) ANTENNA SYSTEM

The type of antenna system employed has already been briefly described. A better idea of its construction may be gained by reference to Figure 18.

The field intensities obtained from various transmitting systems are listed in Table 1. The approximate reliable service range of each type of transmission is also included in this tabulation.

TABLE 1.—*Field intensity chart (various transmitting arrangements)*

Type of transmitter	Antenna system	Nominal power rating	Location	Carrier field intensity at 10 miles	Useful distance range
		kw		*μv/m*	*Miles*
Radio phone	T, 125 feet high, 200 feet long.	2	Hadley Field, N. J.	6,500	180
Aural radio range	Loop □, 40 feet high, 250 feet base.	2	do	800	100
Visual radio range	Loop □, 40 feet high, 250 feet base.	2	Detroit, Mich.	800	150
Do	Loop △, 65 feet high, 300 feet base.	2	College Park, Md.	800	150
Simultaneous phone range.	Loop △, 65 feet high, 300 feet base; vertical umbrella, 60 feet high.	¾	do	1,850	75
Do	Loop △, 65 feet high, 300 feet base; vertical, 75 feet high, 180-foot flat top.	¾	do	2,500	100
Do	Loop △, 40 feet high, 300 feet base; vertical, 70 feet high, 160 feet flat.	3	do	[1] 6,000	[1] 180

[1] Estimated value if 2 kw airway radiophone transmitter was employed.

It has been shown by Smith-Rose and others [5] that the Adcock type of antenna provides directional transmission with a marked reduction in night course shift errors over those due to the use of loop antennas.[6] This led to some consideration of this type of antenna for use with the combined phone and beacon. However,

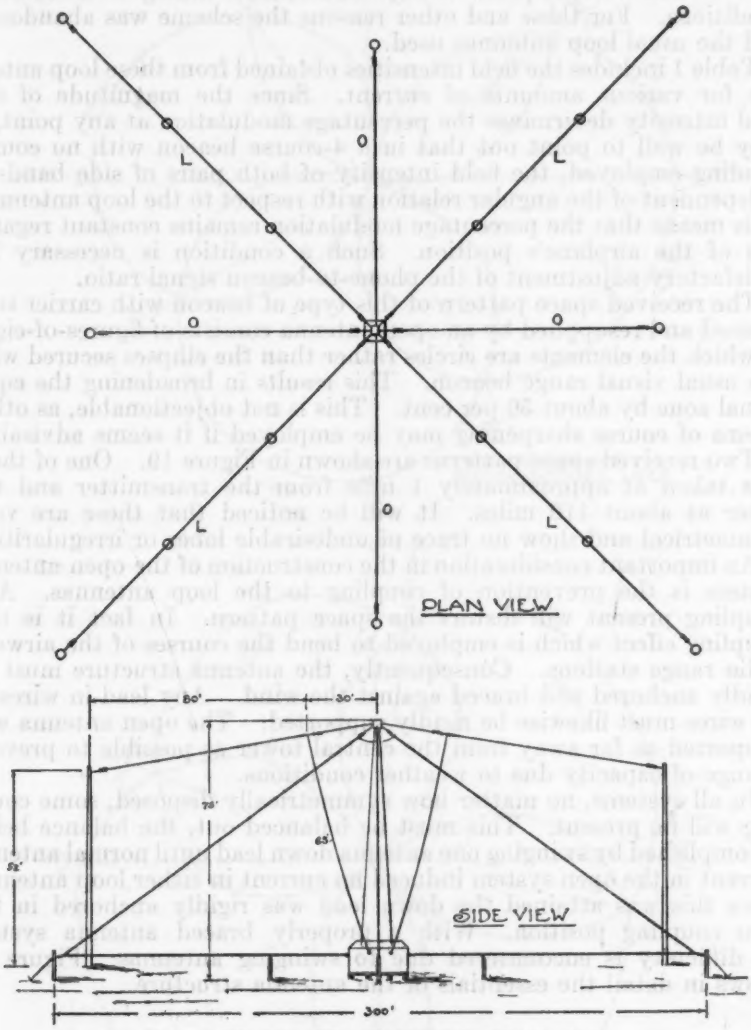

FIGURE 18.—*Antenna system*

several serious difficulties were encountered, and in consequence thereof it was not tested. The first of these was the necessity for very accurate control of frequency. A change of more than 100 cycles in 290 kc. would seriously affect their operation. While such

[5] R. L. Smith-Rose and R. H. Barfield, The Cause and Elimination of Night Errors in Radio Direction finding, J. Inst. Elect. Engrs. (London), 64 pp. 831-843; Aug. 26, 1926.
[6] H. Pratt, Apparent Night Variations With Crossed Coil Radio Beacons, Proc. Inst. Radio Engrs., 16, p. 653; May, 1928.

control can be obtained, the necessity for close tuning of the antenna system introduces disadvantages in operation. A second objection was the high voltage gradient near the ground. The physical size of the antennas being limited, a great deal of loading would be necessary in the base of the down lead. This creates high potentials near the ground and a consequent change of antenna tuning with weather conditions. For these and other reasons the scheme was abandoned and the usual loop antennas used.

Table 1 includes the field intensities obtained from these loop antennas for various amounts of current. Since the magnitude of the field intensity determines the percentage modulation at any point, it may be well to point out that in a 4-course beacon with no course bending employed, the field intensity of both pairs of side bands is independent of the angular relation with respect to the loop antennas. This means that the percentage modulation remains constant regardless of the airplane's position. Such a condition is necessary for satisfactory adjustment of the phone-to-beacon signal ratio.

The received space pattern of this type of beacon with carrier suppressed and resupplied by an open antenna consists of figures-of-eight of which the elements are circles rather than the ellipses secured with the usual visual range beacon. This results in broadening the equisignal zone by about 50 per cent. This is not objectionable, as other means of course sharpening may be employed if it seems advisable.

Two received space patterns are shown in Figure 19. One of these was taken at approximately 1 mile from the transmitter and the other at about 110 miles. It will be noticed that these are very symmetrical and show no trace of undesirable lobes or irregularities.

An important consideration in the construction of the open antenna system is the prevention of coupling to the loop antennas. Any coupling present will distort the space pattern. In fact it is this coupling effect which is employed to bend the courses of the airways radio range stations. Consequently, the antenna structure must be rigidly anchored and braced against the wind. Any lead-in wires or tie wires must likewise be rigidly supported. The open antenna was supported as far away from the central tower as possible to prevent change of capacity due to weather conditions.

In all systems, no matter how symmetrically disposed, some coupling will be present. This must be balanced out, the balance being accomplished by swinging one antenna down lead until normal antenna current in the open system induced no current in either loop antenna. Once this was attained the down lead was rigidly anchored in the zero coupling position. With a properly braced antenna system no difficulty is encountered due to swinging antennas. Figure 18 shows in detail the essentials of the antenna structure.

IV. THE RECEPTION PROBLEM

The problem of receiving the combined signals in the airplane and properly separating them required a different method of attack than that employed in the design of the transmitter. As previously mentioned, receiving set equipment on airplanes has become standardized to a certain degree and every effort was made to provide a transmission system which would require a minimum amount of change in the aircraft equipment. In addition to this, the limitations on receiv-

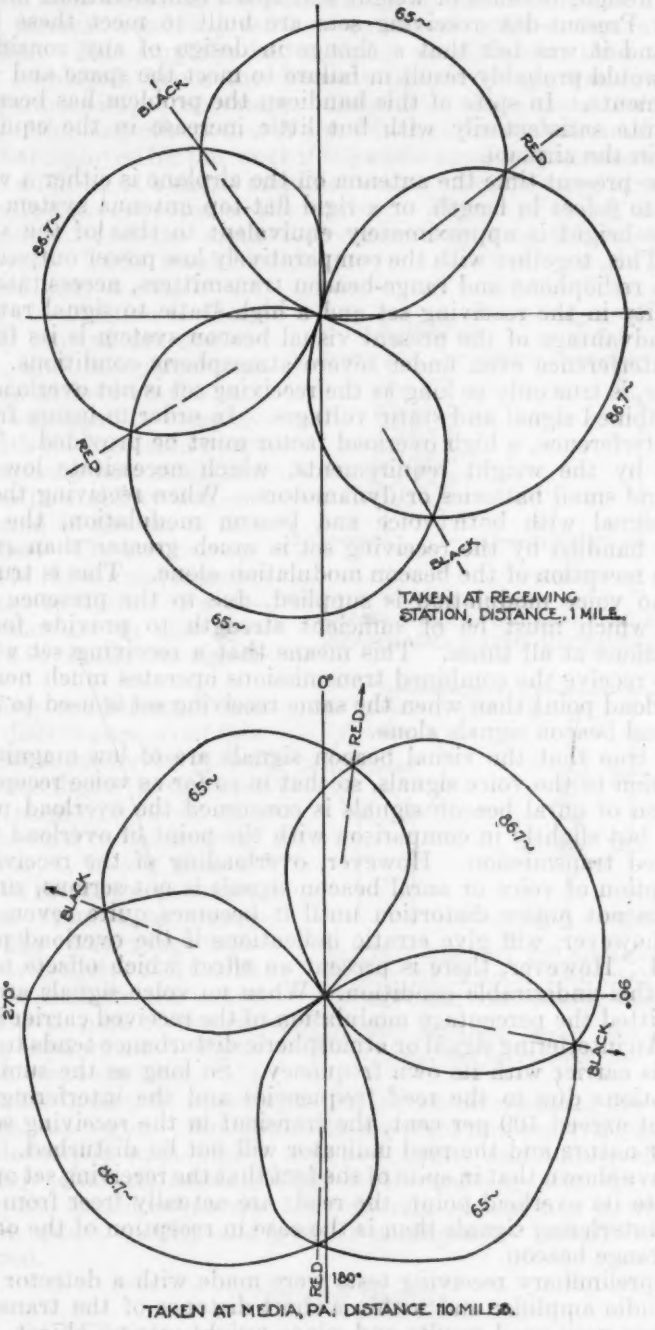

FIGURE 19.—*Polar patterns for combined transmitting set*

ing set design, because of weight and space considerations are quite severe. Present-day receiving sets are built to meet these limitations, and it was felt that a change in design of any considerable extent would probably result in failure to meet the space and weight requirements. In spite of this handicap the problem has been dealt with quite satisfactorily with but little increase in the equipment carried in the airplane.

At the present time the antenna on the airplane is either a vertical pole, 5 to 6 feet in length, or a rigid flat-top antenna system whose effective height is approximately equivalent to that of the vertical pole. This, together with the comparatively low power output of the airways radiophone and range-beacon transmitters, necessitates high sensitivity in the receiving set and a high static to signal ratio. A major advantage of the present visual beacon system is its freedom from interference even under severe atmospheric conditions. This, however, is true only so long as the receiving set is not overloaded by the combined signal and static voltages. In order to insure freedom from interference, a high overload factor must be provided. This is limited by the weight requirements, which necessitate low-power tubes and small batteries or dynamotors. When receiving the combined signal with both voice and beacon modulation, the signal voltage handled by the receiving set is much greater than encountered in reception of the beacon modulation alone. This is true even when no voice modulation is supplied, due to the presence of the carrier which must be of sufficient strength to provide for both modulations at all times. This means that a receiving set which is used to receive the combined transmissions operates much nearer to its overload point than when the same receiving set is used to receive the visual beacon signals alone.

It is true that the visual beacon signals are of low magnitude in proportion to the voice signals, so that in so far as voice reception or reception of aural beacon signals is concerned the overload point is altered but slightly in comparison with the point of overload for the combined transmission. However, overloading of the receiving set in reception of voice or aural beacon signals is not serious, since the ear does not notice distortion until it becomes quite severe. The reeds, however, will give erratic indications if the overload point is reached. However, there is present an effect which offsets to some extent this undesirable condition. When no voice signals are being transmitted the percentage modulation of the received carrier is quite low. An interfering signal or atmospheric disturbance tends to modulate this carrier with its own frequency. So long as the sum of the modulations due to the reed frequencies and the interfering signal does not exceed 100 per cent, the transient in the receiving set is of a minor nature and the reed indicator will not be disturbed. Flight tests have shown that in spite of the fact that the receiving set operates nearer to its overload point, the reeds are actually freer from flutter due to interfering signals than is the case in reception of the ordinary visual range beacon.

The preliminary receiving tests were made with a detector and 2-stage audio amplifier and within a short distance of the transmitter. This gave very good results and, since weight was no object, the set was designed for high overload; consequently, no difficulty was encountered.

When tests were made at a distance from the transmitter a conventional aircraft receiving set was employed with a separate audio amplifier. This amplifier had a higher amplification than that normally employed, hence the detector signal voltage was lower than would otherwise be necessary. Results of these tests were so free from overloading effects that it was felt that the conventional receiver could be employed for this work if the audio amplification was increased by the addition of a single amplifier stage. Accordingly, an amplifier was built and connected to the receiver. Figure 20 shows the circuit arrangement and the method of connecting it to the receiving set employed. This amplifier required only a small "C" battery in addition to those already carried for the receiver, and the percentage increase in load on the batteries was small in comparison with the increased overload capacity now available. No loss in stability was encountered in the use of this amplifier. The receiver operated in the normal manner with the exception of a decided increase in the permissible static to signal ratio.

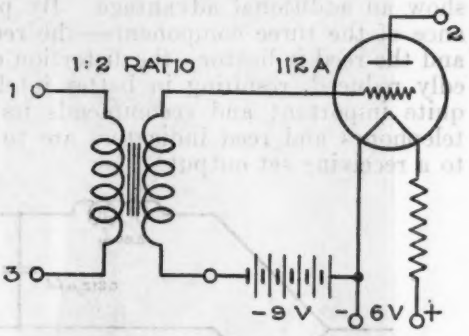

AMPLIFIER UNIT, FOR USE WITH STANDARD RADIO RECEIVER.

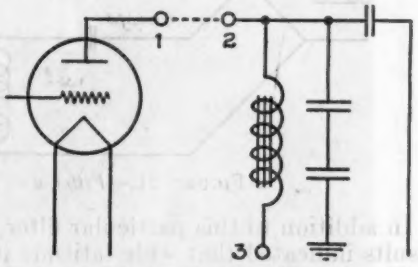

OUTPUT CIRCUIT OF AIRCRAFT RADIO RECEIVER SHOWING MEANS OF CONNECTING AMPLIFIER.

FIGURE 20.—*Electrical circuit arrangement of amplifier for receiving set*

During conditions of low static disturbance, even this amplifier is unnecessary, and numerous flights have been made employing only the conventional radio receiver. However, it is felt that in order to retain the desirable freedom from interference which the visual range beacon provides, it is well worth while to include the extra amplifier as part of the receiving equipment. Tests on this system were all made with an aircraft receiving set which was available at the time the research was begun. Since that time several new receiving sets have been developed with higher overload points and improved audio-frequency characteristics. When such receiving sets are used to receive the combined service the amplifier should not be necessary and the speech quality and general intelligibility should be greatly improved.

1. FILTER UNITS

The output of the receiving set may be directly connected to a reed course indicator and head telephones with no additional apparatus. This will cause a low-frequency hum in the telephones and cer-

tain voice frequencies which are harmonics of the reed frequencies will cause a slight flutter in the indicator. Neither of these effects are serious and they can be neglected. They may be entirely eliminated by the use of a suitable filter circuit which provides the reeds with reed frequencies only and the head telephones with frequencies over 250 cycles only. A filter suitable for use with the receiving set employed is shown in Figure 21. This has a cut-off at 300 cycles and a characteristic impedance of 5,000 ohms. Its use insures steady operation of the reed indicator and silence in the head phones during the period when no voice broadcast is made. Oscillographic studies show an additional advantage. By properly matching the impedance of the three components—the receiving set, the head phones, and the reed indicator—the distortion of the received signal is markedly reduced, resulting in better intelligibility. This advantage is quite important and recommends its employment whenever head telephones and reed indicators are to be connected simultaneously to a receiving set output.

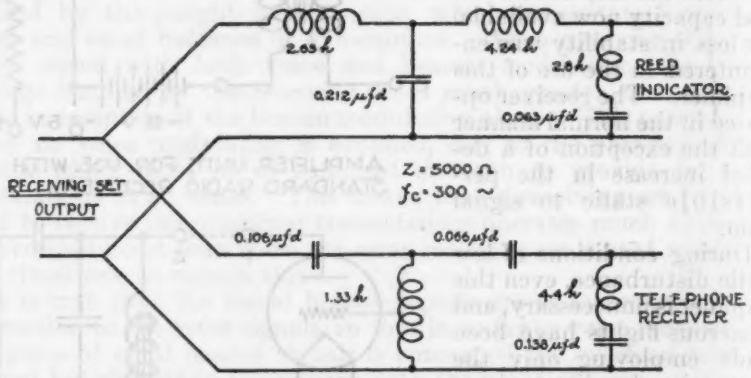

FIGURE 21.—*Filter unit for use on airplane*

In addition to this particular filter, several others were tried. The results indicated that wide latitude in design is permissible.

The use of a filter of this type is also advantageous in that it permits employment of automatic volume control, details of which have recently been published.[7] This type of volume control has a decided advantage over other systems, since it is applicable regardless of whether signals are being received from the visual range beacons or the combined visual beacon and phone transmitter.

The equipment used at the receiving station during these tests is shown in Figure 22. From right to left it shows the aircraft radio receiver, the 1-stage amplifier and the receiving set control box, the output filter unit, the reed indicator, an impedence matching transformer, and the oscillograph used to check the operation of the system. The filter unit and the 1-stage amplifier are shown to better advantage in Figure 23.

While it is assumed that the reed course indicator [8] will be used with this system, any other type of course indicator utilizing low fre-

[7] W. S. Hinman, Automatic Volume Control for Aircraft Receivers, B. S. Jour. Research, **7** (RP330); July, 1931.

[8] F. W. Dunmore, A Tuned Reed Course Indicator for the 4 and 12 Course Radio Range; B. S. Jour. Research, **4** (RP160); April, 1930; also Proc. Inst. Radio Engrs., **18**, pp. 963–982.

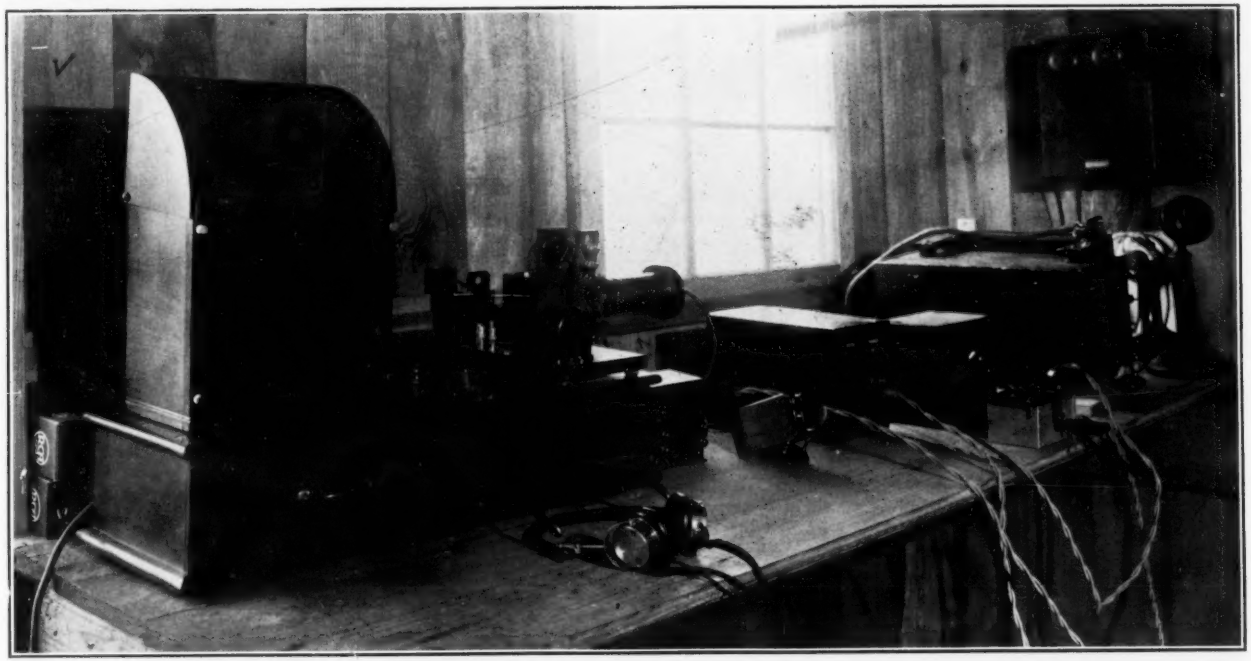

FIGURE 22.—*Receiving station equipment*

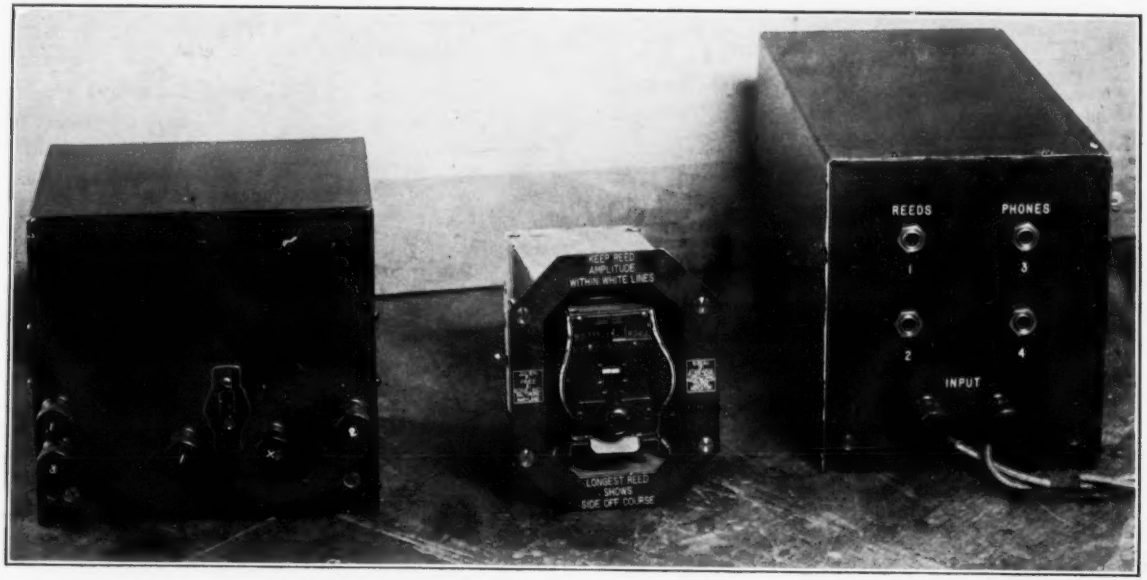

FIGURE 23.—*Filter unit and amplifier*

quency alternating voltage for indication will serve equally well. For example, the reed converter, together with a zero center pointer type instrument,[9] has been successfully employed in various tests with no change in either the transmitting or receiving equipment.

V. FURTHER WORK

1. COURSE BENDING

The courses of the combined system may be adjusted to fit the airways in the same manner employed on the present beacon system.[10]

The open-antenna system necessary for shifting the 90° courses is already in place. It is only necessary to apply a modulation of the proper reed frequency to the carrier supplied to this antenna. Since the phase of the radio-frequency voltages is already the optimum relation for shifting the course, no change is required other than proper control of the percentage modulation. However, the phase of the applied reed frequency voltage must be such that it will add in the correct phase in the radio receiver. This can best be determined by the use of an oscillograph at the receiving point. By observation of the phase of the detected signal with and without modulation of the carrier it is possible to make this adjustment quite accurately. The amount of modulation required on the carrier will be quite low, necessitating the use of small audio-frequency currents. The phase can, therefore, be controlled by chokes and condensers when necessary in the same manner as the radio-frequency phases are adjusted. The low percentage modulation required also insures that the voice frequencies will not be affected by its presence in the speech circuits.

2. APPLICATION OF SIMULTANEOUS TRANSMISSION TO THE 12-COURSE RADIO RANGE BEACON

While all of the recent work on simultaneous transmission has been performed on the 4-course beacon, the same principle may be applied to the 12-course beacon.

It has already been demonstrated that this may be accomplished by supplying the three amplifier branches in time phase, thereby suppressing the carrier. The carrier and voice would then be supplied over an open antenna system. This would probably be unsatisfactory due to goniometer coupling and general unavoidable dissymmetry. The preferred plan would be to utilize three amplifier branches modulated to the reed frequencies and suppressing the carrier within themselves. The three sets of side bands would then be supplied to the loop antennas through a 3-stator goniometer. This method permits of a better check on carrier suppression and also permits course alignment without a reintroduction of carrier due to dissymmetry.

With such a system it probably would be necessary to employ link circuits in the goniometer stators to prevent intercoupling. The action of these circuits has been described in detail in a previous paper.[11] With the exception of the use of these link circuits, it is apparent that no change in design is necessary to employ the 12-course beacon.

---

[9] F. W. Dunmore, A Course Indicator of Pointer Type for the Visual Radio Range Beacon System, B. S. Jour. Research, 7 (RP 336); July, 1931.

[10] See footnote 2, p. 271.

[11] See footnote 1, p. 263.

The overloading of the receiving set would be increased due to the presence of a third unused frequency, but the percentage of this is so small compared with the amount of carrier present that the effect should be negligible.

3. POSSIBLE MODIFICATIONS OF DESIGN

(a) CARRIER SUPPRESSION

Several modified designs can be employed which would give substantially the same results. For example, it is unnecessary to use a complete balanced amplifier system. This was merely a matter of convenience in the installation at College Park. If the more usual single-sided amplifier is used, the carrier may be suppressed in the goniometer or in a tuned circuit within the amplifier. This is accomplished by supplying the grids of the modulated amplifiers in parallel and the alternating plate voltage in push-pull. The radio-frequency output is supplied to the extremities of a tuned circuit (or the goniometer) in push-pull. This method is probably somewhat simpler than that previously described. Either method will produce the same results.

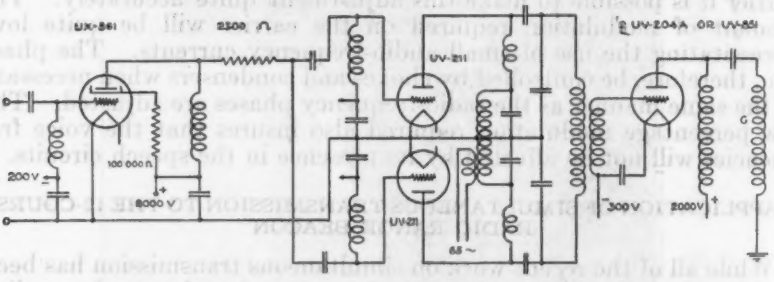

FIGURE 24.—*Modified range-beacon amplifier circuit showing (1) carrier suppression in tuned circuit; (2) elimination of balanced amplifiers; and (3) class C power amplifier for stability*

(b) COURSE STABILITY

The present method of modulation on the last tubes of the beacon amplifiers might profitably be changed in a final design. With this method of modulating, any change in plate voltage will produce a change in the course. In an experimental transmitter this made no difference as the voltage could be kept constant. In a remote-controlled installation, this would probably not be satisfactory unless voltage regulators were provided for the modulation frequency alternators. However, if the modulation and carrier suppression is accomplished in an intermediate stage and the last stage is a class C amplifier, then the courses will be independent of the alternator voltages. Furthermore, the plate voltage on the class C amplifiers being from the same source will vary the same amount on each amplifier branch. A change in this voltage will change the transmitted power but not the course. This is the method employed in the present range beacons to reduce the possibility of a course change.

Figure 24 shows the modified beacon amplifier with modulation on an intermediate stage. It also illustrates the second means of carrier suppression without the use of balanced amplifiers.

The use of class C amplifiers after a modulating stage introduces harmonics which are undesirable. The increased stability of service offered by their use, however, may be sufficiently great to outweigh the effects of harmonic distortion.

VI. FLIGHT TESTS

The proof of a satisfactory design for an airways transmitting system lies in the results of exhaustive flight tests. Such flight tests on the College Park installation have shown the service rendered to be consistently good. The quality of speech is superior to that usually encountered in aircraft reception and the freedom from interference in the reception of the beacon signals is very marked. On several flights over Aberdeen, Md., interfering code signals made the use of head telephones unbearable. At the same time the reeds were entirely free from flutter.

All test flights were made with an early model of commercial aircraft radio receiver. A filter unit was used, but not the extra stage of amplification. This, together with the fact that flights were made along the Atlantic seaboard with excessive marine radio interference, meant that the ratio of signal to noise was very unfavorable. In spite of this, the beacon service was remarkably free from interruption, although frequently the interference completely blanketed the voice signals.

Since these tests proved so satisfactory, it is reasonable to assume that an airplane equipped with an amplifier in addition to the standard receiving set, or with a later type of aircraft radio receiver designed with a higher overload point, can expect to receive a thoroughly satisfactory radio telephone and range beacon service with the type of transmitting set herein described.

VII. ACKNOWLEDGMENTS

The authors wish to acknowledge the assistance rendered by the other members of the research division of the Aeronautics Branch during the progress of this research.

Particular acknowledgement is made to H. Diamond's suggestions in initiating the work on the combined phone and beacon system, and for many subsequent suggestions in regard to circuit arrangements.

The assistance of the engineering staff of the Bell Telephone Laboratories in collaborating in the design of a circuit arrangement which formed the basis of the research is also acknowledged.

The speech input equipment used in the transmitter was furnished by the Chesapeake & Potomac Telephone Co. It was formerly part of the equipment of station WCAP, at one time operated by them in Washington, D. C.

Credit is also due to Justus U. Steele for assistance in field measurement work and flight tests, and to H. M. Horsman for mechanical work in the construction of the various units.

WASHINGTON, May 23, 1931.

DESIGN OF STANDARDS OF INDUCTANCE, AND THE PROPOSED USE OF MODEL REACTORS IN THE DESIGN OF AIR-CORE AND IRON-CORE REACTORS

By H. B. Brooks

ABSTRACT

After a brief discussion of the various uses of reactors and the general characteristics of formulas for the self-inductance of coils, a number of useful general relations concerning the self and mutual inductance of geometrically similar coils are given with illustrative derivations of some of these relations. Three applications of some of these relations are developed in the remainder of the paper. The first is a simple and straightforward procedure for the design of air-core coils to serve as standards of self-inductance and is believed to be the first such design procedure for this specific purpose to be published. The second application proposes that the self and mutual inductance of the large current-limiting reactors used in power systems may be advantageously predetermined, or their computed values checked, by laboratory tests made on small-scale models. The third application proposes to use models for the checking or predetermination of the properties of iron-core air-gap reactors. In developing the theory of this application it is shown that such reactors have their desirable optimum performance—that is, minimum power factor—when the relative length of the air gap is such as to make the copper loss equal to the core loss for the desired maximum magnetic flux density in the core.

CONTENTS

	Page
I. Introduction	290
1. Definitions	290
2. Some of the uses of reactors	291
(*a*) As laboratory standards of inductance	291
(*b*) In electrical instruments	291
(*c*) For compounding synchronous converters	291
(*d*) For paralleling transformers of unlike inherent reactance	291
(*e*) For limiting short-circuit currents	291
3. Objects of this paper	292
4. The criterion, time constant	292
5. General characteristics of formulas for the self-inductance of a coil	292
6. Optimum form of coil	293
7. Improved form of Maxwell-Rosa formula for the self-inductance of a circular coil of rectangular cross section	294
8. Convenient condensed formulas for the self-inductance of coils of optimum form	295
II. General relations concerning self and mutual inductance of geometrically similar coils	296
III. Design of standards of self-inductance	298
1. Range of frequencies covered	298
2. Requirements to be met by standards of self-inductance for laboratory use	299
3. Procedure for the design of self-inductance standards	299
(*a*) General considerations affecting the design	299
(*b*) Desired value of time constant is the starting point	300
(*c*) Design of a coil of 1 millihenry inductance	300
(*d*) Design of a coil of any value of inductance	304
(*e*) Deviation of actual wire from tabular data	305
(*f*) Checking the design values; taking care of variations	305

III. Design of standards of self-inductance—Continued.
3. Procedure for the design of self-inductance standards—Con. Page
(*g*) Time constant and weight of final coil 307
(*h*) Numerical example of design 307
(*i*) Design of a coil of given inductance to fill a given spool 309
(*j*) Design of a coil of given inductance of wire of given diameter 310
(*k*) Data for the plotting of the design curves 310
(*l*) Adjustment of the standard to its nominal value 310
(*m*) Materials for the spool; binding posts 311
(*n*) Temperature coefficient of standards of inductance 312
(*o*) Sets of inductance coils 312
IV. Current-limiting reactors for power systems 313
1. Special requirements 313
(*a*) Ability to withstand heating caused by heavy overloads 314
(*b*) Ability to withstand destructive forces during short circuits 314
(*c*) High flash-over voltage 314
(*d*) Low skin-effect resistance ratio 314
2. Design procedures in use 314
3. Usefulness of models to designers in various fields 315
4. Suggested use of models in the design of current-limiting reactors 316
(*a*) Useful relations 316
(*b*) Checking the self inductance of full-size reactors 316
(*c*) Checking the skin-effect resistance ratio of full-size reactors 317
(*d*) Checking the mutual inductance between full-size reactors 318
(*e*) Checking the electrodynamic forces between full-size reactors 318
(*f*) Electrodynamic torque between reactors 320
V. Iron-core air-gap reactors 320
1. Scope of this discussion 320
2. Reason for the use of an air gap 320
3. Condition for the desirable minimum power factor 321
4. Suggested use of model reactors as a check on present methods of design 322
5. Suggested use of model reactors as an independent basis of design 325
(*a*) Uncertainty as to gap reluctance, stray flux, etc 325
(*b*) Choice of form of core and location of gap 326
(*c*) Choice of core material and maximum flux density 326
(*d*) Experiments to be made with the model 326
(*e*) Working up the results of experiments with the model 327
6. Condition for minimum power factor in each of a series of geometrically similar reactors 327
VI. Acknowledgment 328

I. INTRODUCTION

1. DEFINITIONS

A reactance coil, or for brevity, a reactor, is a device used for the purpose of introducing inductive reactance in an electric circuit, and is usually designed to have a high time constant (ratio of inductance to resistance). This is because the useful property is the inductance,[1]

[1] While the term "inductor" would have the advantage of not necessarily implying operation on alternating current, it and the related word "induction" have been rather overworked in electrotechnics. The term "reactor" has the disadvantages of involving the idea of some definite frequency, and is also ambiguous to the extent that reactance, strictly speaking, may be either inductive or capacitive. This latter aspect is being taken care of, to some extent, by the growing tendency to speak of a device possessing capacitive reactance as a "capacitor"; a term free from the ambiguity of the earlier and illogical term "condenser," and in line with the useful term "resistor."

and, therefore, the reactance at a specified frequency; and the associated resistance is ordinarily either useless or detrimental. One of the major problems in reactor design is therefore to keep the resistance at the lowest value possible with the expenditure of a given amount of material.

For convenience, reactors may be divided into two general classes, namely, air-core reactors and iron-core reactors. The expression "air-core" might be replaced by "ironless." It does not exclude the use of any material for the core or other supporting structure of the reactor which has a permeability of unity and is either a nonconductor or is so arranged that eddy currents will not be set up in it. The term "iron-core reactor" is self-defining.

2. SOME OF THE USES OF REACTORS

(a) AS LABORATORY STANDARDS OF INDUCTANCE

Reactance coils used for this purpose are of two general classes; first, those wound on precisely measured forms in such a way that the inductance can be computed from the dimensions; and second, coils wound in any convenient form and adjusted to definite values of inductance by reference to known standards. The former class will not be considered in this paper. In both classes the coil must be wound on supports of nonmagnetic insulating material.

(b) IN ELECTRICAL INSTRUMENTS

Iron-core reactors of small size are used in frequency meters and some other alternating-current instruments.

(c) FOR COMPOUNDING SYNCHRONOUS CONVERTERS

Larger iron-core reactors are used in the alternating-current circuit supplying a synchronous converter in order to secure compounding.

(d) FOR PARALLELING TRANSFORMERS OF UNLIKE INHERENT REACTANCE

Transformers of like ratio but of unlike characteristics as regards relative resistance and leakage reactance may operate satisfactorily in parallel on light loads but may divide heavier loads so disproportionately as to overload some of the transformers seriously. The addition of suitable amounts of external resistance and reactance to those transformers having relatively small values of these quantities will cause the load to be divided properly.

(e) FOR LIMITING SHORT-CIRCUIT CURRENTS

Probably the most conspicuous use of reactors at the present time is for the purpose of limiting the amount of current which can flow in the generators, busses, and feeders of electric-power systems. Without the protection afforded by current-limiting reactors or some equivalent device [2] it would not be practicable to use generating units of the very large ratings now used because of the extremely destructive forces and heating effects which would be caused by short-circuit currents.

---

[2] Resistors of iron strips have been used experimentally in Germany for this purpose. They are dimensioned to have only a small temperature rise with the working current, but to approach a red heat at maximum short-circuit current. The use of resistors in parallel with reactors has been investigated by Kierstead, Rorden, and Bowley; see Trans. Amr. Inst. Elec. Engrs., **49**, pp. 1161–1178; 1930.

3. OBJECTS OF THIS PAPER

The objects of this paper are to present a number of useful general relations concerning the self and mutual inductance of geometrically similar coils, and to illustrate their usefulness by making three applications of them. The first application relates to coils serving as standards of self-inductance for laboratory purposes. The advantages of the Maxwell-Shawcross-Wells optimum form of coil for this purpose are emphasized, and a convenient and rapid procedure for the design of such coils is given. The second proposed application is the use of small model coils for predetermining the dimensions and performance of large current-limiting reactors as used in power plants. In the third application the use of small-scale iron-core air-gap reactors is proposed for the predetermination of the dimensions and performance of large reactors of this type. In developing the theory of this last application it is brought out that iron-core air-gap reactors have the desirable minimum power factor when the length of the air gap is such that the copper loss equals the core loss.

4. THE CRITERION, TIME CONSTANT

The unavoidable resistance of a reactor is often a disadvantage, and the wire used in its construction should, therefore, be wound to form a coil having the greatest possible ratio of inductance to resistance; that is, the highest possible time constant.[3] The circular form of coil is clearly to be preferred, and a rectangular cross section of winding is obviously the most convenient one. It has been found that from the standpoint of maximum time constant the most suitable rectangle is a square. The remaining question to be determined is the ratio of the side of the square cross section to the mean diameter of the winding.

5. GENERAL CHARACTERISTICS OF FORMULAS FOR THE SELF-INDUCTANCE OF A COIL

Examination of formulas for the calculation of the self-inductance of coils will show that the self-inductance is the product of three characteristic factors which may best be illustrated by an example. Referring to Figure 1 (*a*), which shows a circular coil of rectangular cross section, Maxwell's approximate formula [4] for the self-inductance is,

$$L = 4\pi a N^2 \left(\log_e \frac{8a}{R} - 2 \right) \tag{1}$$

where

L = inductance in abhenries (millimicrohenries),
a = mean radius in centimeters,
N = total number of turns in the coil, and
R = geometric mean distance [5] of the cross section of the winding in centimeters.

---

[3] When it is desired to have an inductance standard which will be nearly astatic as to local magnetic field, a sacrifice in time constant must be made. For example, the coil may be wound on a supporting torus of nonmagnetic material. A lesser degree of astaticism may be secured by the use of two coils in series, held in a fixed relation to each other, the coils having opposite instantaneous polarities as viewed from one side.

[4] Maxwell, Electricity and Magnetism, **2**, sec. 706.

[5] The geometric mean distance of a rectangle of sides b and c may be taken to be equal to $0.2236\,(b+c)$. While the coefficient actually varies between the limits 0.2231 and 0.2237 for rectangles of various relative proportions, the intermediate value 0.2236 gives results more than sufficiently accurate for engineering purposes. See B. S. Bull. **8**, p. 168, 1912; Sci. Paper No. 169.

The quantity in parentheses is the difference of two abstract numbers, and is a constant for all coils of the given form having the same relative values of a, b, and c. The three characteristic factors in the above expression for L are the linear dimension a, the square of the number of turns, and the numerical coefficient whose value depends upon the relative proportions of the coil.

6. OPTIMUM FORM OF COIL

There are an infinite number of possible forms of circular coil of rectangular cross section which may be made from a given length of wire. One extreme is formed by winding the whole length to form a single very large circular turn. This gives the greatest possible value of a, but because the inductance varies as the square of the number of turns the resulting inductance is far below the maximum value possible. The other extreme is the case of a coil in which the

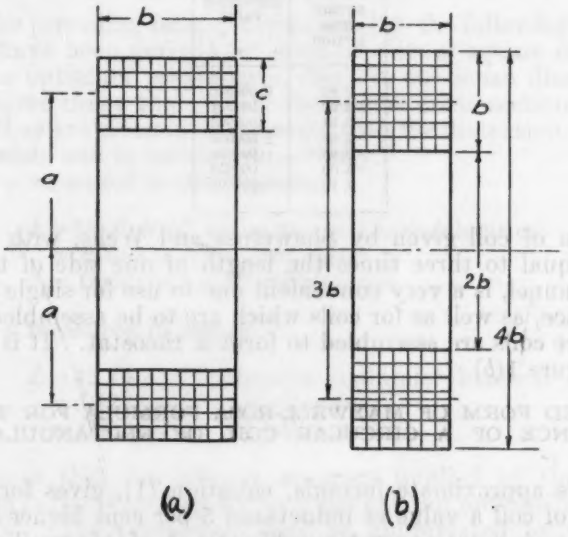

FIGURE 1.—*Cross-sectional diagrams of circular coils of rectangular cross section*

(*a*), general form, without restriction as to relations between the values of a, b, and c; (*b*) optimum form for maximum time constant. Note the simple and easily remembered dimensional relations in the latter, namely, that the side of the square section, the inner diameter, mean diameter, and outside diameter of the coil are as 1:2:3:4.

radius a of the mean turn is equal to one-half the side of the square cross section; that is, there is no hole through the center of the coil. This also gives a value of inductance which is less than that obtainable by an intermediate form.

Maxwell investigated the question of the most advantageous form[6] of coil, but apparently did not carry enough terms of the formula he used to locate the maximum point as well as has been done later. He gave as the optimum form, for a coil of square cross section ($b=c$ in fig. 1(*a*)), one in which the mean diameter, $2a$, equals 3.7

[6] Maxwell, Electricity and Magnetism, 3d ed., **2**, pp. 345-346.

times the side b. It has since been found[7] that the relation $2a=3b$, in other words, mean diameter equal to three times the side of the square cross section, gives a value of L/R slightly greater (0.5 per cent) than is given by Maxwell's proportions.

Although the inductance theoretically has its maximum value when the ratio of the mean diameter to the side of the square cross section is 2.95, the curve is so flat near the maximum that the use of the more convenient value 3 is fully warranted, as will appear from the following table, for which the author is indebted to Dr. Frederick W. Grover:

TABLE 1.—*Inductance of a coil made of a given length of wire as a function of its form*

Ratio of mean diameter to side of square cross section	Inductance in terms of maximum value
2.80	0.999606
2.90	.999971
2.94	.999994
2.95	1.000000
2.96	.999994
3.00	.999953
3.10	.999594

The form of coil given by Shawcross and Wells, with the mean diameter equal to three times the length of one side of the square winding channel, is a very convenient one to use for single standards of inductance, as well as for coils which are to be assembled in a box as resistance coils are assembled to form a rheostat. It is shown to scale in Figure 1(b).

7. IMPROVED FORM OF MAXWELL-ROSA FORMULA FOR THE SELF-INDUCTANCE OF A CIRCULAR COIL OF RECTANGULAR CROSS SECTION

Maxwell's approximate formula, equation (1), gives for the optimum form of coil a value of inductance 5 per cent higher than that given by Rosa's more accurate modification[8] of Maxwell's formula. Since this modified formula, as printed in Scientific Paper No. 169, is in an ambiguous form and involves the use of natural logarithms, and since common (base 10) logarithms are much more convenient to use, the following equivalent formula is given. In it the symbols a, b, and c have the meanings assigned to them in Figure 1(a) and N is the number of turns in the coil. It should be noted that this formula is general as to the relative values of a, b, and c; much simpler formulas will be derived from it for coils of the optimum form.

$$L=4\pi aN^2\left\{\left[2.303\ \log_{10}(35.78\,\frac{a}{b+c})\right]\left[1+0.0094\left(\frac{b+c}{a}\right)\right]-\left[2+0.0031\,(\frac{b+c}{a})^2\right]\right\} \quad (2)$$

[7] Shawcross and Wells, Electrician, **75**, p. 64; 1915. These writers used a formula more accurate than the approximate one used by Maxwell. J. Hak, Elektrotechnik und Maschinenbau, *46*, pp. 249-250; 1928, arrives at practically the same result, namely, that the mean diameter should be 2.95 times the side of the square cross section.

[8] Rosa and Grover, B. S. Bull., **8**, p. 136, equation (86); 1916; Sci. Paper No. 169.

If the linear dimension a in the quantity $4\pi aN^2$ is in centimeters, this formula gives the inductance in abhenries (millimicrohenries). The quantity $a/(b+c)$ and its reciprocal are abstract numbers which depend upon the form of the coil, but not on its size, and do not change when a, b, and c are expressed in other units. Consequently, for any given form of coil, the entire expression following N^2 is a numerical constant.

While the above formula of Rosa is not rigorously exact, it is sufficiently so for engineering purposes. Dr. Frederick W. Grover has kindly computed the inductance of a coil, of the optimum form about to be described, by the accurate formula of Lyle and has found that the above formula (2) gives a result 1 per cent lower than that given by Lyle's formula.

8. CONVENIENT CONDENSED FORMULAS FOR THE SELF-INDUCTANCE OF COILS OF OPTIMUM FORM

From the preceding formula, equation (2), the following convenient formulas have been derived for circular coils of square cross section having the optimum proportions, namely, the mean diameter ($2a$) equal to three times the side of the square cross section. For convenience they are given in two groups, with the dimension a expressed in centimeters and in inches, respectively.

Radius a measured in centimeters:

$$L = 16.83\ a\ N^2 \text{ abhenries (millimicrohenries)} \quad (3)$$
$$= .01683\ a\ N^2 \text{ microhenries} \quad (4)$$
$$= .00001683\ a\ N^2 \text{ millihenries} \quad (5)$$

Radius a measured in inches:

$$L = 42.74\ a\ N^2 \text{ abhenries (millimicrohenries)} \quad (6)$$
$$= .04274\ a\ N^2 \text{ microhenries} \quad (7)$$
$$= .00004274\ a\ N^2 \text{ millihenries} \quad (8)$$

It is obvious that the 4-figure accuracy implied by the numerical coefficients in the preceding six formulas can not ordinarily be realized in a or N^2. The coefficients may be abbreviated by the user as circumstances may justify. These formulas presuppose uniform distribution of the current over the square cross section of the coil. The design curves of Figures 3 and 4 are for the case of round wires with insulation of negligible thickness. Although the inductance in the latter case is slightly larger than would be given by the above uniform-distribution formulas, the correction term for coils of 100 turns or more is negligible for the present purpose. As a matter of theoretical interest, the magnitude of the correction for any given number of turns in the coil may be readily found by comparing the result given by formula (3) with that obtained from the approximate but sufficiently accurate expression

$$L = 16.83\ a\ N^2 \left(1 + \frac{0.116}{N}\right) \text{ abhenries} \quad (3a)$$

which is formula (3) with a correction factor added.

II. GENERAL RELATIONS CONCERNING SELF AND MUTUAL INDUCTANCE OF GEOMETRICALLY SIMILAR COILS

The following general relations apply to geometrically similar coils of any form whatever, located in media of equal and constant permeability. The coils under comparison are assumed to be closely wound of wires of the same resistivity and the same density, and (where so specified) of the same space factor. While the relations are assumed primarily to apply to closely wound coils, for which the diameter of the wire (over the insulation) determines the number of turns per layer and the number of layers, they hold also (with obvious changes in wording) for coils with air spaces between adjacent turns and between adjacent layers, if the specification of geometrical similarity includes the cross sections of the conductors and of the air spaces about the conductors.

(*a*) For coils of the same absolute size the self-inductance is proportional to the square of the number of turns; conversely, the number of turns is proportional to the square root of the self-inductance.

(*b*) For coils of the same absolute size the self-inductance is inversely proportional to the fourth power of the diameter of the wire over the insulation; conversely, the diameter of the wire over the insulation is inversely proportional to the fourth root of the inductance.

(*c*) For coils of a given self-inductance the diameter of the wire over the insulation is proportional to the five-fourths power of a given coil dimension; conversely, each coil dimension is proportional to the four-fifths power of the diameter of the wire over the insulation.

(*d*) For coils of a given self-inductance the number of turns is inversely proportional to the square root of a given coil dimension.

(*e*) For coils of a given self-inductance wound with wires having the same space factor, the diameter of the wire over the insulation is proportional to the five-eighths power of the time constant.

(*f*) For coils of a given self-inductance, wound with wires having the same space factor, each coil dimension is proportional to the square root of the time constant.

(*g*) For coils having the same number of turns the self-inductance is proportional to the first power of a given coil dimension.

(*h*) For coils wound with wire of the same diameter over the insulation, the self-inductance is proportional to the fifth power of a given coil dimension; conversely, each coil dimension is proportional to the one-fifth power of the self-inductance.

(*i*) For coils wound with wires having the same space factor the time-constant L/R is proportional to the square of a given coil dimension.

(*j*) For coils wound with wires having the same space factor the mass of conducting material in the coil is proportional to the three-halves power of the time constant, and the mass of conducting material per unit of time constant is proportional to the first power of a given coil dimension. Large coils thus require more conducting material per unit of time constant than small ones.

(*k*) For coils of a given size, wound with wires having the same space factor, the time constant, the mass of conducting material in the coil, and the mass of conducting material per unit of time constant are independent of the size of the wire and, therefore, of the value of the inductance.

The following relations apply to the mutual inductance of geometrically similar pairs of coils in geometrically similar relative positions, under the same general conditions specified for the cases of self-inductance:

(*l*) For pairs of coils of the same absolute size the mutual inductance is proportional to the product, primary turns times secondary turns, for the respective pairs of coils. Note that the value of the mutual inductance of any pair of coils does not depend on which one is taken as the primary.

(*m*) For pairs of coils of the same absolute size having a constant ratio of diameter (over insulation) of wire in the primary coil to diameter of wire in the secondary coil, the mutual inductance varies inversely as the fourth power of the diameter of the wires in corresponding coils of the two pairs; conversely, the diameter of the wires in corresponding coils is inversely proportional to the fourth root of the mutual inductance.

(*n*) For pairs of coils having the same number of turns in corresponding coils, the mutual inductance is proportional to the first power of a linear coil dimension.

Relations (*l*), (*m*), and (*n*) are merely extensions of relations (*a*), (*b*), and (*g*) for the self-inductance of geometrically similar coils. They indicate the manner in which relation (*c*) and others for the case of self-inductance may be restated for the case of mutual inductance. With suitable additional limitations made necessary by the magnetic properties of iron and similar magnetic materials, general relations may be stated for the self-inductance of iron-core air-gap reactors. Such of these relations as are necessary for the purpose are given later in this paper (p. 322) in discussing the proposed use of small-scale iron-core reactors as a basis for designing full-size reactors. Certain general relations concerning mutual translational forces and mutual torques of geometrically similar pairs of coils are developed in a later section of this paper (p. 318) on current-limiting reactors for power systems.

An obvious practical limitation, which is ignored in stating some of the above relations, is that, in general, for an arbitrarily chosen diameter of wire over the insulation, there will not be an exactly integral number of turns per layer or of layers in the coil. This matter is readily cared for in the design and construction of actual coils. (See p. 305.)

It is obvious that the relations above given do not exhaust the list of possible relations of this kind, but it is believed that they include all of the more important ones of practical applicability.

The process of reasoning by which the preceding general theorems are demonstrated may be illustrated by giving the derivation of relations (*g*), (*i*), and (*j*). Assume two geometrically similar 1-turn coils, *a* and *b*, made of identical conducting material, each dimension of *b* being n times the corresponding dimension of *a*. Let l_a, l_b, s_a, s_b denote the lengths and cross sections of the two conductors, and R_a, R_b, L_a, L_b their resistances and inductances. Then we have

$$\frac{R_b}{R_a}=\frac{\rho n l_a/n^2 s_a}{\rho l_a/s_a}$$

from which

$$R_b=R_a/n$$

The magnetic circuit of coil b has everywhere a cross section n^2 times as great as the corresponding cross section of a, and the length of each flux path in b is n times as great as that of the corresponding flux path in a; hence the reluctance of the magnetic circuit of b is $1/n$ times that of a. Unit current flowing in b will thus set up n times as many linkages as will be caused by unit current in a, which is equivalent to the statement that

$$L_b = nL_a$$

If instead of one turn the conducting material now forms m turns in each coil, both L_a and L_b are multiplied by m^2, but L_b is still n times as great as L_a. This proves relation (g).

Coil b has n times the inductance of coil a and $1/n$ times the resistance of coil a; hence the ratio of their time constants is

$$\frac{\tau_b}{\tau_a} = \frac{nL_a/(R_a/n)}{L_a/R_a}$$

from which

$$\tau_b = n^2\tau_a$$

which proves relation (i).

The mass of conducting material in coil b is n^3 times that in coil a, and the time constant of b is n^2 times that of a; hence the mass of conducting material is proportional to the 3-halves power of the time constant, and the mass of conducting material per unit of time constant is proportional to the first power of a given coil dimension. These results prove relations (j).

While some of the general relations given above are so well known as to be almost axiomatic, others have not been given previously, to the writer's knowledge. Some of these relations have formed the basis on which a simple and sufficiently accurate procedure has been devised for the design of coils to serve as standards of self-inductance. This is believed to be the first straightforward design procedure for this particular purpose, and will now be described.

III. DESIGN OF STANDARDS OF SELF-INDUCTANCE

1. RANGE OF FREQUENCIES COVERED

The form of coil and the design procedure about to be described are intended to be used for frequencies of not more than say several thousand cycles per second. The reason for this limitation is that in addition to inductance and the usually undesirable resistance, inductance coils have capacitance between each element of conductor surface and every other element. The effect of this distributed capacitance is to make the effective inductance of the coil vary with the frequency. For the closely wound coils which are discussed in this section of this paper, capacitance effects are small for frequencies up to a few hundred cycles per second, but may amount to several per cent for frequencies of say 1,000 to 3,000 cycles per second. The magnitude of the effect is greater for inductance standards of the higher values. For example, the inductance of a 1-henry standard changed 3 parts in 1,000 when the frequency was changed from 100 to 1,000 cycles, and 3 per cent for a change from 100 to 3,000 cycles. For a 100-millihenry standard the corresponding changes were about one-tenth of these figures.

These observed results are in good agreement with the approximate formula [9]

$$L' = L\,(1+\omega^2\,CL) \tag{9}$$

in which L' is the measured inductance, L the true inductance, C the capacitance which, in parallel with the coil, would produce the same effect as the actual distributed capacitance, and ω equals 2π times the frequency.

2. REQUIREMENTS TO BE MET BY STANDARDS OF SELF-INDUCTANCE FOR LABORATORY USE

Standards of self-inductance for laboratory purposes are ordinarily used with currents small enough not to cause appreciable heating. The principal limiting performance consideration is usually the time constant L/R. The larger the coil, other things being equal, the larger the time constant; that is, the smaller the undesirable resistance of the coil for a given value of inductance. The most suitable material for the wire is copper. The ideal coil would be wound with square (or rectangular) wire with insulation of zero thickness; such a coil would have a "space factor" of unity. A coil of round wire with insulation of zero thickness, closely wound so that the turns do not imbed,[10] will have a space factor of 0.7854. The nearest approach to the ideal zero-thickness insulation is the so-called enamel insulation, for which the thickness of the insulation ranges from about 1 per cent of the diameter of the bare wire, in the largest sizes, to about 5 per cent in fine sizes.

3. PROCEDURE FOR THE DESIGN OF SELF-INDUCTANCE STANDARDS

(a) GENERAL CONSIDERATIONS AFFECTING THE DESIGN

The design procedure about to be described could have been worked out to apply to coils of any specified form. As given, however, it makes use of formulas (3) to (8), and consequently is limited to circular coils of square cross section having the mean diameter equal to three times the side of the square cross section, as shown in Figure 1 (*b*).

Assuming that the currents to be carried are small, the limiting considerations in projecting the design of an inductance standard or a set of standards will usually be the size, weight, and cost of the coil. The desirable operating quality, which even with the optimum form of coil is to be had only at the expense of size, weight, and cost, is a sufficiently high value of time constant. A convenient unit for this quantity, for the present purpose, is the millisecond.[11] Small coils for use in making up a set of four or more standards of inductance will have a time constant of about 1 millisecond. Larger coils for use as single standards have time constants of 2 to 10 milliseconds. A

---

[9] Rosa and Grover, B. S. Bull. 3, p. 303; 1907.

[10] Solenoids, by Underhill, 2d ed., p. 232.

[11] If a coil having a time constant of 1 millisecond is connected to a noninductive d. c. source of negligible resistance and inductance (a storage cell is a good approximation to this) the current rises along a logarithmic curve and at the end of 0.001 second reaches a value of (1-1/e) times its final steady value; that is, 0.632 times this final value.

The concept of time constant is not limited, however, to that above outlined for the case of growth of current in a coil suddenly connected to a direct-current source. In the case of a coil connected to an a. c. source of frequency f, the time constant may be regarded as the quotient of tan θ (equals $L\omega/R$) by ω, where ω is equal to $2\pi f$. The time constant is thus a constant of the coil which is independent of frequency (leaving out of consideration the change in skin effect with frequency) but which, with the frequency, determines the angle of lag. If the time constant $\tau = L/R$ of the coil is large in comparison with the period T of the a. c. source, the reactance of the coil predominates; if τ is small compared with T, its resistance predominates.

number of such coils are shown in Figure 2, to serve as illustrations of usual practice. Particulars concerning these coils are given in Table 2.

TABLE 2.—*Data on standards of inductance*

Symbol	Inductance	Resistance	Time-constant	Weight	
	Millihenries	*Ohms*	*Milliseconds*	*Kilograms*	*Pounds*
A [1]	1	0.75	1.3	0.124	0.27
B [2]	1	.39	2.6	.69	1.52
C [2]	10	2.88	3.5	.88	1.94
D [2]	100	24.2	4.1	1.17	2.58
E [3]	1,000	97.0	10.3	4.03	8.9
F [3]	100	10.1	9.9	2.65	5.8
G [4]	100	20.8	4.8	3.46	7.6
H [5]	1,000	96.0	10.4	4.73	10.4

[1] Wound on maple spool; one of the set of coils. (Fig. 8.)

[2] Wound on white marble spools; of German manufacture. Spools B and C are of identical dimensions. The low value of time constant of B results from an unsuitable choice of diameter of wire, in consequence of which the desired inductance of 1 millihenry is had when only three-fourths of the winding space is filled. Note the difference in weight of the 2 coils.

[3] Wound on mahogany spool; of French manufacture. The binding posts might well be reduced in size, placed closer together and farther from the axis of the coil.

[4] Wound on impregnated marble spool; of German manufacture. The binding posts are of the smallest practicable dimensions. For its size, weight, and value of inductance, this coil has a low value of time constant because the winding is made of "litzendraht" with the intention of making the coil suitable for higher frequencies. The space factor of litzendraht is low.

[5] Wound on serpentine spool; of German manufacture. Binding posts have the good features of being small, close together, and in the best possible location as regards the magnetic field.

(b) DESIRED VALUE OF TIME CONSTANT IS THE STARTING POINT

The larger the time constant, the larger, heavier, and more expensive will be the inductance standard. The representative coils shown in Figure 2, with the accompanying data in Table 2, will assist in the choice of a feasible preliminary value of time constant. To simplify the work, the curves of Figures 3 and 4 have been prepared, the former in metric units, the latter in English units of coil dimensions and wire diameters. The auxiliary curve (fig. 5) applies to either case, and is merely a method of graphically finding the reciprocal of the fourth power of any number within a given range. Because of the various kinds of wire insulations, for each of which the space factor of a winding varies, in general, with the diameter of the wire, the curves of Figures 3 and 4 are prepared for an ideal case of round wires having insulation of zero thickness, wound closely without embedding of the layers. The first values taken from these curves consequently need subsequent modification to care for the lower space factors of actual insulated wires. The manner of doing this will be indicated. Two design procedures are described, one for use when the desired value of inductance is 1 millihenry, the other for any other value L millihenries. The former case is simpler, and will be taken up first.

(c) DESIGN OF A COIL OF 1 MILLIHENRY INDUCTANCE

The curves of Figure 3 or Figure 4 are entered with the desired value of time constant, and preliminary values b', d', and w' of the length of the side of the square cross section of the coil, the diameter of the wire, and the weight of copper are found. These values apply to the ideal case of insulation of zero thickness.

Reference to a table of data on wires having the desired kind of insulation will usually show that the preliminary value d' lies

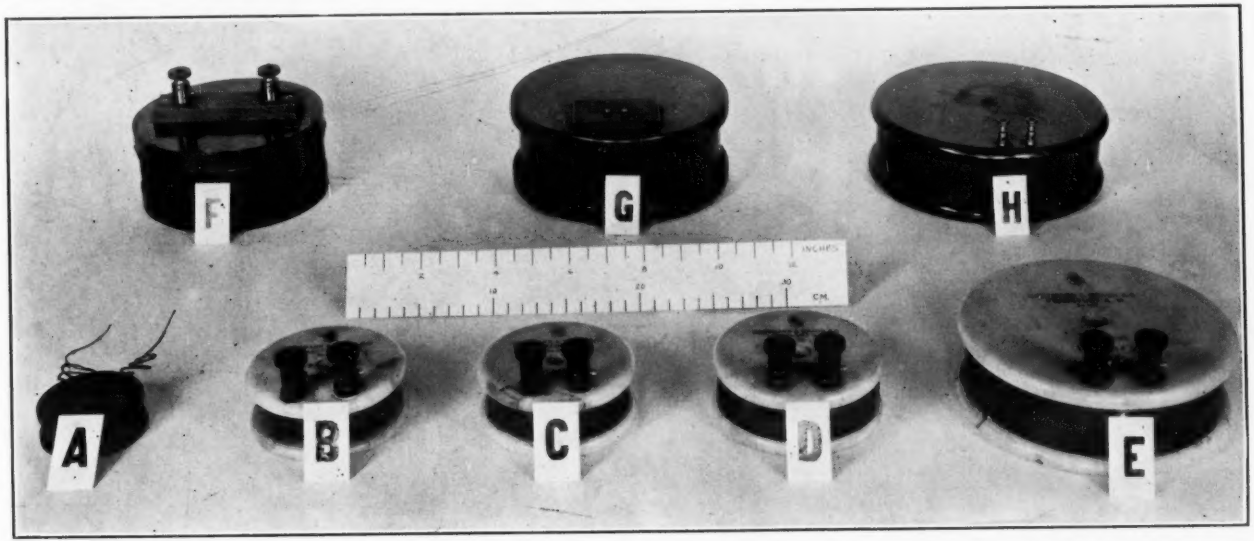

FIGURE 2.—*Standards of self inductance of various sizes, wound on supporting spools of various materials. For particulars see Table 1.*

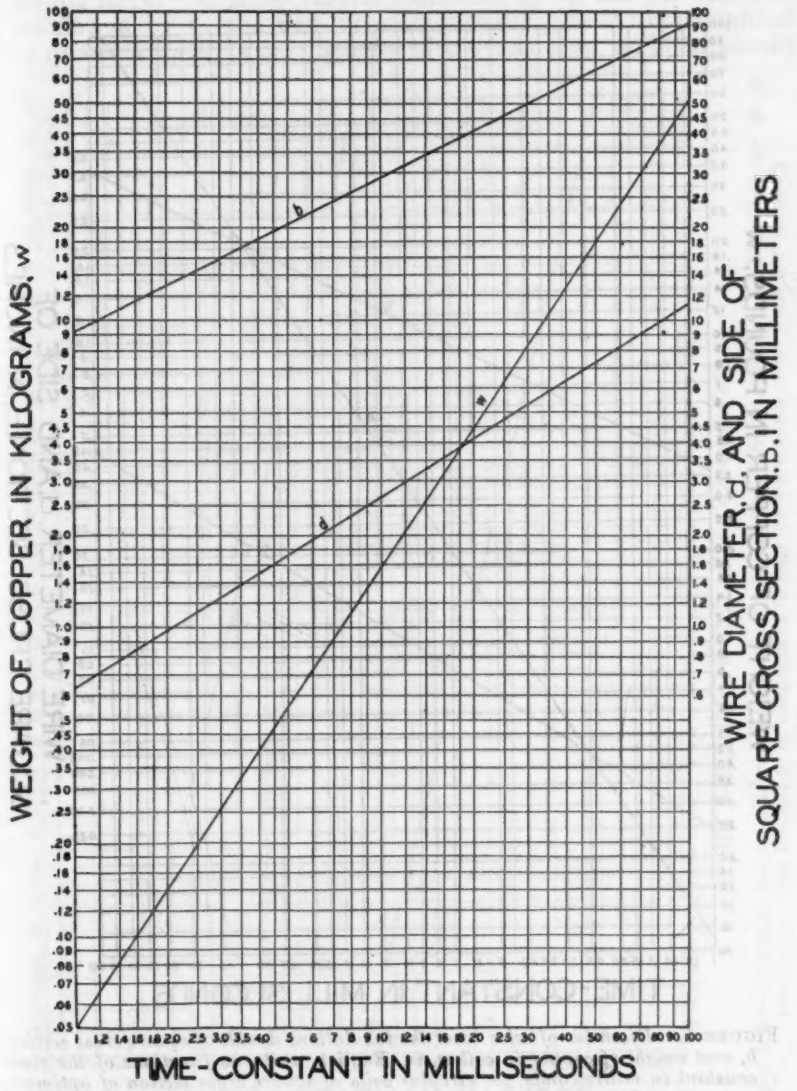
WEIGHT OF COPPER IN KILOGRAMS, w
WIRE DIAMETER, d, AND SIDE OF SQUARE CROSS SECTION, b, IN MILLIMETERS
TIME-CONSTANT IN MILLISECONDS
b
d
w

FIGURE 3.—*Diameter of wire (over the insulation) d, side of square cross section b, and weight of copper in coil w, in metric units, as functions of the time constant in milliseconds, for circular coils of square cross section of optimum proportions (mean diameter of winding equal to three times the side of the square cross section)*

Denoting the time constant in milliseconds by τ, and expressing b and d in millimeters and w in kilograms, the equations of these curves are as follows:

$$b = 9.142\tau^{\frac{1}{4}}$$
$$d = .6336\tau^{\frac{1}{2}}$$
$$w = .05027\tau^{\frac{3}{4}}$$

The value of τ is based on the resistivity of copper of 100 per cent purity at 25° C., and on the assumptions that ideal insulation of zero thickness is used and that there is no embedding of turns.

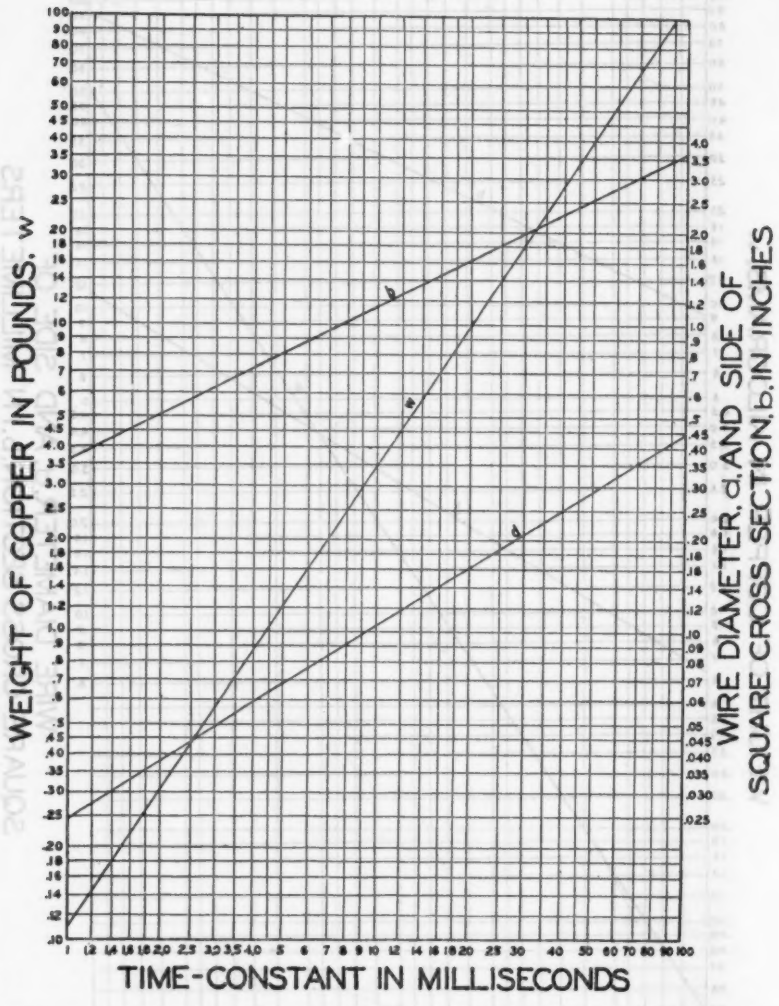
WEIGHT OF COPPER IN POUNDS, w
WIRE DIAMETER, d, AND SIDE OF SQUARE CROSS SECTION, b, IN INCHES
TIME-CONSTANT IN MILLISECONDS
b
w
d

FIGURE 4.—*Diameter of wire (over the insulation) d, side of square cross section b, and weight of copper in coil w, in English units, as functions of the time constant in milliseconds, for circular coils of square cross section of optimum proportions (mean diameter of winding equal to three times the side of the square cross section)*

Denoting the time constant in milliseconds by τ, and expressing b and d in inches and w in pounds, the equations of these curves are as follows:

$$b = 0.3599\tau^{\frac{1}{3}}$$
$$d = .02494\tau^{\frac{1}{3}}$$
$$w = .1108\tau^{\frac{3}{3}}$$

The value of τ is based on the resistivity of copper of 100 per cent purity at 25° C., and on the assumptions that ideal insulation of zero thickness is used and that there is no embedding of turns.

between the diameters (over insulation) of two adjacent gage sizes. Denoting larger [12] of these tabular diameters by d_1, and the thickness of insulation by t_1, the first revision factor $d_1/(d_1-2t_1)$ is computed. (The quantity d_1-2t_1 is the diameter of the bare wire, and can usually

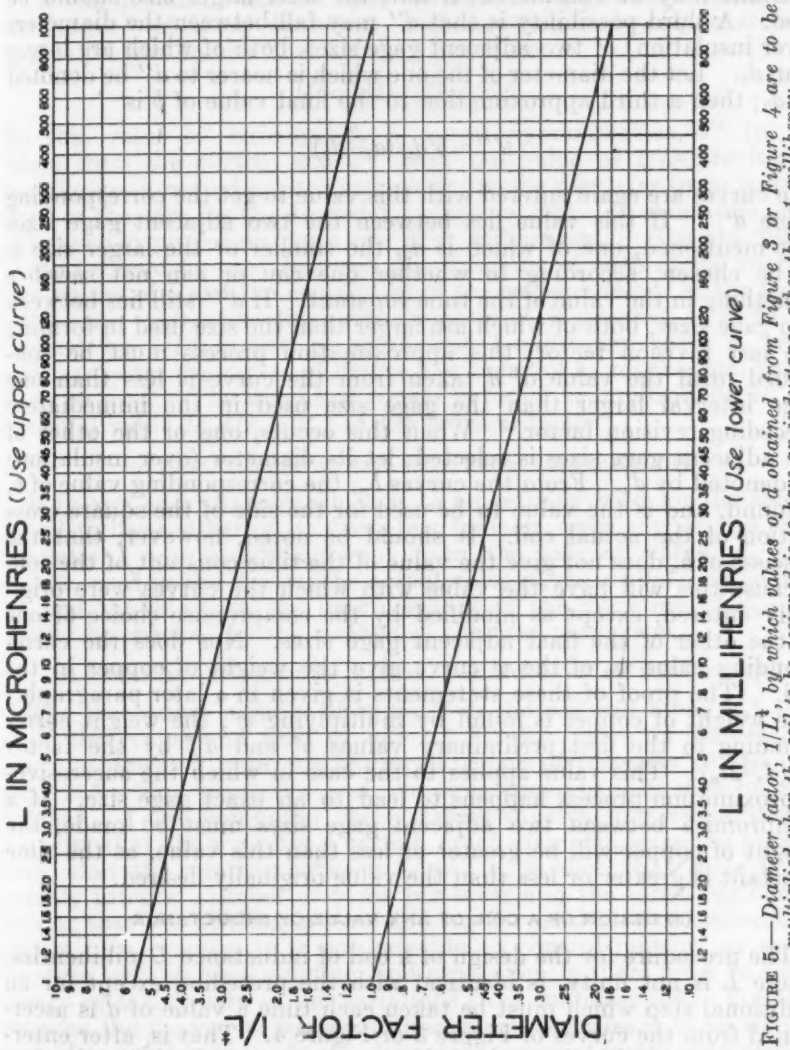

FIGURE 5.—*Diameter factor, $1/L^{\frac{1}{4}}$, by which values of d obtained from Figure 3 or Figure 4 are to be multiplied when the coil to be designed is to have an inductance other than 1 millihenry*

be taken directly from the table). Then a second approximation for b is

$$b''=b'd_1/(d_1-2t_1)$$

Again referring to the curves, and entering with the value of b'', the corresponding value of wire diameter d'' is read off. If this should happen to coincide with d_1, wire of this diameter (over insula-

[12] Even if d' coincides with the diameter (over insulation) of a gage size, the diameter of the next larger gage size should be used as d_1.

tion) should be used; the value of b'' gives the side of the square cross section of the coil, and the mean radius of the coil is $a=1.5\ b''$. If the second approximate value d'' should fall between d_1 and the next larger gage size, d_1 may be chosen if some sacrifice in time constant may be considered; if not, the next larger size should be used. A third possibility is that d'' may fall between the diameters (over insulation) of two adjacent gage sizes, both of which are larger than d_1. Let the diameter of the one which is nearer to d'' be denoted by d_2; then a third approximation to the final value of b is

$$b'''=b'd_2/(d_2-2t_2)$$

The curves are again entered with this value to get the corresponding value d'''. If this value lies between the two adjacent gage sizes just mentioned, one of which is d_2, the smaller or the larger size is to be chosen, according to whether one can or can not sacrifice something in the value of the time constant. If d''' still lies between two gage sizes, both of which are larger than the size used in forming the last revision factor, this approximation process must be continued until the value of d taken from the curve is less than one gage interval larger than the gage size used in the immediately preceding revision factor.[13] When this occurs, one or the other of the adjacent gage sizes is selected; let its diameter (over insulation) be denoted by d_n. From the curves b_n, the corresponding value of b, is found, and is the value to be used for the side of the square cross section of the actual coil. It should be noted, however, that the abscissa of b_n does not give the value of the time constant of the coil, because this will have the value with which the curves were originally entered, except as modified by the compromise choice of one or the other of the final adjacent gage sizes. Nor does the corresponding value w_n of the w curve give the weight of copper in the coil. (The proof of these statements is given in a later paragraph.) The weight of copper is found by multiplying w', the weight corresponding to the first preliminary values b' and d', by the factor $d_n/(d_n-2t_n)$. This value applies to the case in which the successive-approximation process happens to lead to an exact gage size. If a compromise between two adjacent gage sizes must be made, the weight of copper will be greater or less than this value, as the time constant is greater or less than the value originally desired.

(d) DESIGN OF A COIL OF ANY VALUE OF INDUCTANCE

The procedure for the design of a coil of inductance L millihenries, where L is not unity, is identical with the preceding except for an additional step which must be taken each time a value of d is ascertained from the curves of Figure 3 or Figure 4. That is, after entering the curves with the desired time constant and obtaining the first preliminary values d', b', and w', it is necessary to translate d' into the diameter for a coil of L millihenries. This is done by using relation (b), page 296, and to avoid computation the curves of Figure 5

[13] The necessity for this succession of approximations lies in the fact that even for the same kind of insulation the space factor $\frac{\pi}{4}\left[(d-2t)/d\right]^2$ usually varies from one gage size to the next. (This does not always apply to "enamel" insulated wire, for which the space factor is sometimes closely constant over a considerable number of sizes.) For insulations which are wholly or partly fibrous the rate of change of the space factor increases as the diameter decreases, and the number of approximations required in the design of inductance coils increases in consequence.

may be used. Entering with L as abscissa, the value of $1/L^{\frac{1}{2}}$ is obtained and d' is multiplied by it to get the first preliminary (L millihenry) value D' of wire diameter. Like d' in the 1-millihenry case, this value applies for wire of zero-thickness insulation, and, like d', it will ordinarily fall between two adjacent gage sizes. Choosing the larger[14] of these diameters, and denoting it by D_1, a second approximation to the final value of b will be

$$b'' = b' D_1/(D_1 - 2t_1)$$

To this value b'' corresponds a second approximation d'' (to be taken from the curve), and d'' times the value of $1/L^{\frac{1}{2}}$ previously found gives a second approximation D'' to the diameter (over insulation) of the wire for the desired L-millihenry coil. In short, the only difference in procedure, for a coil of L millihenries, is that the value of $1/L^{\frac{1}{2}}$ should be used between the obtaining of each of the successive values of b and the calculation of the revision factor of the form $D/(D-2t)$. After the final wire diameter D_n is selected, it is to be divided by $1/L^{\frac{1}{2}}$ to get an equivalent 1-millihenry value d_n with which to enter the curves of Figure 3 or Figure 4 to get the final value b_n to be used. The weight of copper is found by multiplying w' by the final value $D_n/(D_n - 2t_n)$ of the revision factor.

(e) DEVIATION OF ACTUAL WIRE FROM TABULAR DATA

If in any case the wire which is to be actually used for the coil is found to have either of its diameters (namely, over copper and over insulation) appreciably different from the tabular values d_n and $d_n - 2t_n$ used in the design, the actual value d_n should be used to find b_n, and the effect on the time constant of the variation of $d_n - 2t_n$ should be checked by the method of the next paragraph.

(f) CHECKING THE DESIGN VALUES; TAKING CARE OF VARIATIONS

The theoretical number of turns N in the coil will be b_n^2/d_n^2, and with this value and that of $a(=1.5\ b_n)$ the value of inductance may be checked from the appropriate one of formulas (3) to (8), page 295. The resistance and the time constant may then be calculated. These computed check values involve four assumptions, namely, that the wire has a certain exact diameter, over the insulation; that the relation between b_n and d_n is such that there is an exactly integral number of turns per layer and the same number of layers; that the winding is close and regular, and that no embedding occurs. In practice it is not possible to control matters so as to produce such an ideal winding, and consequently there must be some means of taking care of the variations from the ideal coil. For this purpose the flanges of the spool upon which the wire is to be wound should preferably be made of a diameter somewhat larger than merely enough to accommodate a winding of square cross section. Figure 6 shows the manner of variation of inductance of a coil of fixed axial length of winding when the radial depth of winding is changed from 20 per cent less to 20 per cent more than the depth for a square cross section.

In the case of coils of relatively low inductance, in which there are relatively few turns per layer, the value b_n finally chosen should

[14] Even if D' coincides with a gage diameter, the diameter (over insulation) of the next larger gage size should be taken as D_1.

be increased slightly, if necessary, to accomodate an integral number of turns per layer.

Adjacent sizes of wire, American Wire Gage, differ in diameter by the factor 1.123. By relation (*b*), page 296, two coils of the same dimensions, wound with wires of adjacent gage sizes and of the same space factor, will have inductances in the ratio of $(1.123)^4$ to 1; that is, 1.6 to 1. It is almost always necessary to compromise on

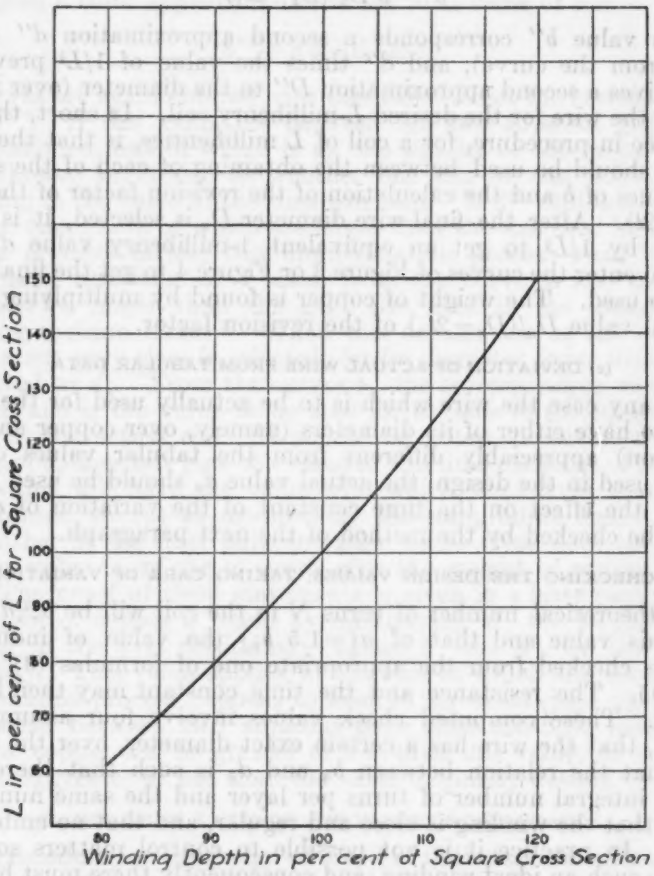

FIGURE 6.—*Manner of variation of the self-inductance of a circular coil, nominally of square cross section of optimum proportions (mean diameter of winding equal to three times the side of the square cross section), as the depth of winding progresses from 20 per cent below to 20 per cent above that which forms a square cross section*

the nearest gage size because of the inconvenience and expense of having special sizes of wire supplied to order. An obvious alternative, however, is to wind the coil partly of one of the two adjacent sizes and then to complete it with the other size.

The space factor of fine wires with any given kind of insulation is, in general, lower than that of coarse wires; consequently, if a set

of inductance coils is to be designed, all to be wound on one uniform size of spool and to have a time constant which in no case shall be less than a prescribed value, the coil of the greatest self-inductance should be designed first and the spool be designed to accommodate it.

(g) TIME CONSTANT AND WEIGHT OF FINAL COIL

The design curves were entered with a desired value of time constant for which the side of the square cross section is b' for wire having zero-thickness insulation. The subsequent steps of the design have led to higher values of b, ending with a final value b_n. The time constant, however, does not increase with b, but retains the value with which the curves were originally entered, except as modified by the compromise choice of one or the other of the gage sizes between which d_n lies. In the following demonstration of this fact it is assumed for simplicity that wire of diameter b_n is available for the coil.

When the preliminary value b' is multiplied by the final revision factor $d_n/(d_n-2t_n)$, which may be called K for brevity, the area of cross section of the coil is increased by the factor K^2. Since d_n has the same abscissa as Kb' the inductance of the coil will still be 1 millihenry because the relation of the curves is such that $d_n=K^{\frac{1}{2}}d'$; see relation (*c*), page 296. The mean radius of the coil and hence the mean length of a turn increases by the factor K; the number of turns becomes lower by the factor $K^2/(K^{\frac{1}{2}})^2=1/K^{\frac{1}{2}}$; consequently the total length of wire in the coil becomes greater by the factor $K^{\frac{1}{2}}$. The diameter of the bare wire becomes greater by the factor $K^{\frac{1}{2}}/K=K^{\frac{1}{2}}$, hence its cross-sectional area becomes greater by the factor $K^{\frac{1}{2}}$, which maintains the original value of resistance in spite of the increased length of wire in the coil. The time constant thus remains at its original value.

The mass of copper becomes greater by the product of the factors of increase of length, $K^{\frac{1}{2}}$, and that of increase of area, $K^{\frac{1}{2}}$; that is, the actual coil of wire diameter (over insulation) d_n and thickness of insulation t_n, while of the same resistance and inductance as the ideal coil of wire diameter d' with zero-thickness insulation, has a mass of copper which is greater than the ideal value w' by the factor $K=d_n/(d_n-2t_n)$.

(h) NUMERICAL EXAMPLE OF DESIGN

A coil of 100 millihenries is to be wound of copper wire insulated with "enamel" and one covering of silk, and is to have a time constant of 3 milliseconds. Required the size of the wire, the dimensions of the coil, and the weight of copper composing it. The curves of Figures 4 and 5 will be used. Entering the curves of Figure 4 with $\tau=3$ milliseconds,

$$b'=0.625 \text{ inch}$$
$$d'=0.0495 \text{ inch}$$
$$w'=0.575 \text{ pound}$$

From Figure 5

$$1/L^{\frac{1}{2}}=0.320$$

whence

$$D'=0.320\times 0.0495$$
$$=0.0158 \text{ inch}$$

From a table for a particular make of this kind of insulated wire the following data are extracted:

Size, American Wire Gage		25	26	27	28
Diameter bare wire	inches	0.0179	0.0159	0.0142	0.0126
Diameter over insulation	do	.0216	.0195	.0176	.0160
Resistance at 25° C. per 1,000 feet	ohms	33.0	41.6	52.5	66.2
Weight per 1,000 feet	pounds	.970	.769	.610	.484

It may be seen that D' nearly coincides with the diameter (over insulation) of No. 28 wire. That of No. 27 is taken as D_1, and the first value of the revision factor is

$$D_1/(D_1-2t_1)=0.0176/0.0142$$
$$=1.239$$

Hence

$$b''=b'D_1/(D_1-2t_1)$$
$$=0.625\times1.239$$
$$=0.775 \text{ inch}$$

Curve d of Figure 4 is entered with this value and d'' is found to be 0.0640 inch. Then

$$D''=0.320\times0.0640$$
$$=0.0205 \text{ inch}$$

This value lies midway between the figures for No. 25 and No. 26. For No. 25,

$$D_2/(D_2-2t_2)=0.0216/0.0179$$
$$=1.207$$
$$b'''=b'D_2/(D_2-2t_2)=0.625\times1.207$$
$$=0.754 \text{ inch}$$

Curve d of Figure 4 is entered with this value, and d''' is found to be 0.0622 inch. Also

$$D'''=0.320\times0.0622$$
$$=0.0199 \text{ inch}$$

This value lies between the same pair of gage sizes as D'', hence the choice of the wire to be used for the coil lies between No. 25 and No. 26. D''' is much closer to No. 26, and the choice of the latter will give a value of time constant which, while below the desired value, will be the closer approximation to it. D_3 is now taken as 0.0195 inch, from which

$$d_3=D_3/(1/L^{\frac{1}{2}})$$
$$=0.0195/0.320$$
$$=0.0610 \text{ inch}$$

Corresponding to this value in Figure 4 is the value $b_3=0.741$ inch, the value to be used for the side of the square cross section. The mean radius of the coil is $a=1.5b=1.5\times0.741$ equals 1.111 inch, and the over-all diameter of the coil is $4b=2.964$ inches.

Check:

$$N=(0.741/0.0195)^2=1{,}444 \text{ turns}$$
$$a=1.111 \text{ inch}$$
$$L=0.00004274aN^2$$
$$=0.00004274\times1.111\times(1{,}444)^2$$
$$=99.1 \text{ millihenries}$$

The length of wire in the coil is

$$2\pi aN = 6.283 \times 1.111 \times 1,444$$
$$= 10,085 \text{ inches}$$
$$= 840 \text{ feet}$$

The resistance at 25° C is

$$R = 0.840 \times 41.6$$
$$= 34.9 \text{ ohms}$$

and the time constant is

$$\tau = L/R$$
$$= 99.1/34.9$$
$$= 2.83 \text{ milliseconds}$$

The weight of copper in the coil is

$$0.840 \times 0.769 = 0.646 \text{ pound}$$

If No. 25 wire had been chosen, the following results would be obtained:

$$d_3 = 0.0216/0.320$$
$$= 0.0675 \text{ inch}$$

From Figure 4, for this value of d_3

$$b_3 = 0.802 \text{ inch}$$

Check:

$$N = (0.802/0.0216)^2 = 1,379 \text{ turns}$$
$$a = 1.5b = 1.5 \times 0.802$$
$$= 1.203 \text{ inch}$$
$$L = 0.00004274 \times 1.203 \times (1,379)^2$$
$$= 97.7 \text{ millihenries}$$

The length of wire in the coil is

$$2\pi aN = 6.283 \times 1.203 \times 1,379$$
$$= 10,420 \text{ inches}$$
$$= 868 \text{ feet}$$

Its resistance at 25° C. is

$$0.868 \times 33.0 = 28.66 \text{ ohms}$$

and its time-constant is

$$\tau = 97.7/28.66$$
$$= 3.41 \text{ milliseconds}$$

The weight of copper in the coil is

$$0.868 \times 0.970 = 0.842 \text{ pound.}$$

(i) DESIGN OF A COIL OF GIVEN INDUCTANCE TO FILL A GIVEN SPOOL

If a spool of the optimum proportions of given size is to be wound to have a given inductance, the curve b is entered with the value of b for this spool. The corresponding value of d gives the diameter of the wire (over the insulation) to be used for an inductance of 1 millihenry. For any other value of L this value of d is to be multiplied by the appropriate value of $1/L^{\frac{1}{4}}$ from Figure 5.

(j) DESIGN OF A COIL OF GIVEN INDUCTANCE, OF WIRE OF GIVEN DIAMETER

In this case, for a coil of 1 millihenry, the curve d is entered with the given diameter of wire (over the insulation) and the corresponding value of b is the side of the square cross section of the coil. For a coil of L millihenries, the given diameter is first to be multiplied by $L^{\frac{1}{4}}$; that is, divided by the value of $1/L^{\frac{1}{4}}$ taken from one of the curves of Figure 5.

(k) DATA FOR THE PLOTTING OF THE DESIGN CURVES

The curves of Figures 3 and 4, plotted on large sheets of logarithmic coordinate paper, will permit more convenient interpolation than is possible with the small-scale figures of this paper. The curves are nominally straight lines having the following equations, in which b, d, and w have the same meanings as in Figures 3 and 4, and τ denotes the time constant in milliseconds:

Metric units; b and d in mm, w in kg:

$$b=9.142\ \tau^{\frac{1}{4}},\ d=0.6336\ \tau^{\frac{1}{4}},\ w=0.05027\ \tau^{\frac{1}{4}} \tag{10}$$

English units; b and d in inches, w in pounds:

$$b=0.3599\ \tau^{\frac{1}{4}},\ d=0.02494\ \tau^{\frac{1}{4}},\ w=0.1108\ \tau^{\frac{1}{4}} \tag{11}$$

The numerical coefficients in these six equations are based on the following data: Density of copper, 8.89; resistance between opposite faces of a centimeter cube of copper at 25° C., 1.757 microhms. (These figures correspond to 100 per cent conductivity, International Annealed Copper Standard.)

Because of slight imperfections in the coordinate paper, it is best to plot more than two points and to draw the curve through the plotted points rather than as a strictly straight line. Each of the curves of Figures 3 and 4 was drawn through computed points for $\tau=1$, 3, 10, 30, and 100 milliseconds. These computed values are as follows:

$\tau=1$	3	10	30	100	milliseconds
$b=9.14$	15.83	28.91	50.1	91.4	millimeters
$=.360$	.623	1.138	1.971	3.599	inches
$d=.634$	1.259	2.672	5.31	11.27	millimeters
$=.0249$	.0496	.1052	.2090	.444	inches
$w=.0503$	.2612	1.590	8.26	50.3	kilograms
$=.111$	.576	3.50	18.21	110.8	pounds

(l) ADJUSTMENT OF THE STANDARD TO ITS NOMINAL VALUE

Since the two binding posts are preferably to be located close together in order to avoid forming a loop when making connections to the standard, one is, in general, restricted to an integral number of turns. In general, therefore, a coil of N turns would have to be left with an error of $1/N$ part [15] of its nominal value. For coils of a large number of turns this degree of precision of adjustment may be sufficient. Where the number of turns and the inductance are small,

[15] The worst case would be where the nominal value required that the number of turns differ from an integral number by one half-turn; since the inductance varies as the square of the number of turns, the effect of a half-turn in N turns is one part in N in inductance. This is an approximate statement only, because the effect of an outside turn is, in general, different from that of a mean turn.

some means for obtaining closer adjustment is necessary. One way of doing this is illustrated in Figure 7. A circular recess is made in the spool, into which opens the small hole, through which the starting end of the wire is passed. After the coil is wound, and adjusted to the nearest whole (outside) turn for which the inductance is either a little low or a little high, the wire near the starting end may be made into a little coil within the recess, in inductive relation to the main coil, and any desired precision of adjustment obtained. This method also provides for subsequent readjustment if necessary. The small coil may be protected from derangement by a suitable cover for the circular recess in which it lies.

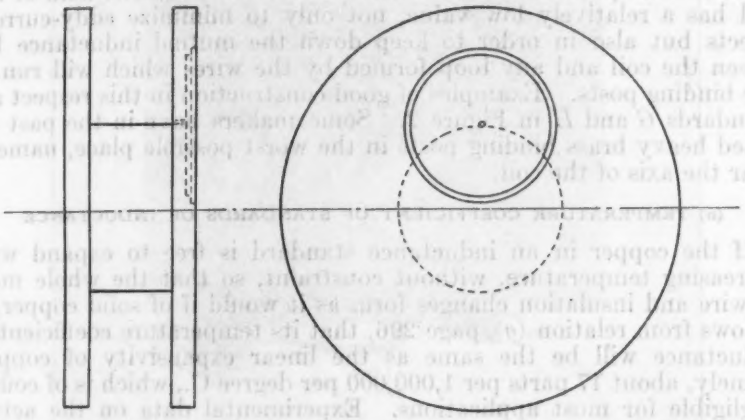

FIGURE 7.—*Form or spool for standard of self-inductance, showing circular recess within which the inner end of the winding may be coiled to effect the final precise adjustment of inductance.*

(m) MATERIALS FOR THE SPOOL; BINDING POSTS

Coils to be used as standards of inductance have been wound on forms or spools of various materials. Mahogany saturated with paraffine has been used to a limited extent. German makers at one time used serpentine, but in the case of certain coils, this was later shown [16] to be slightly magnetic and, therefore, unsuitable. White marble is free from this defect, and its expansivity appears to be close to the desirable value, but it has the undesirable property of irreversible growth [17] when heated above room temperature.

Porcelain 1-piece spools have been used to a limited extent. Porcelain has valuable properties for this purpose. The linear expansivity of various kinds of porcelain has been found [18] to vary from about 3 to 20 parts per million per degree C., a range which includes the value for copper. Porcelain of such composition as to have approximately the expansivity of copper should be very suitable. Porcelain is free from the phenomenon of growth noted in marble.

Phenol condensation products, such as bakelite, condensite, etc., as a rule, have expansivities exceeding that of copper, and they shrink if kept at temperatures above 60° C. The expansivity of mahogany

[16] Rosa and Grover, B. S. Bull. **3**, pp. 337-348; 1907; Reprint No. 15.
[17] Souder and Hidnert, B. S. Bull. **15**, pp. 411-416; 1919-20; Sci. Paper No. 352.
[18] Souder and Hidnert, B. S. Bull. **15**, pp. 391-398; 1919; Sci. Paper No. 352.

across the grain is more than twice that of copper; with the grain, about one-fifth that of copper. All untreated woods are, of course, objectionable because they change form as their moisture content changes. Hard rubber and vulcanized fiber are objectionable because their expansivities are four or five times those of copper, and vulcanized fiber swells and warps when exposed to moist air.

While the size and location of binding posts is usually a matter of mere convenience and appearance in most electrical apparatus, it is not so in the case of standards of inductance. To minimize the effect of eddy currents the binding posts should be made of metal of high resistivity and should be as small as is consistent with other requirements. The posts should be located where the magnetic field of the coil has a relatively low value, not only to minimize eddy-current effects but also in order to keep down the mutual inductance between the coil and any loop formed by the wires which will run to the binding posts. Examples of good construction in this respect are standards *G* and *H* in Figure 2. Some makers have in the past located heavy brass binding posts in the worst possible place, namely, near the axis of the coil.

(n) TEMPERATURE COEFFICIENT OF STANDARDS OF INDUCTANCE

If the copper in an inductance standard is free to expand with increasing temperature, without constraint, so that the whole mass of wire and insulation changes form as it would if of solid copper, it follows from relation (*g*), page 296, that its temperature coefficient of inductance will be the same as the linear expansivity of copper, namely, about 17 parts per 1,000,000 per degree C., which is of course negligible for most applications. Experimental data on the actual temperature coefficient of inductance standards seem to be lacking.

(o) SETS OF INDUCTANCE COILS

When a number of inductance coils are to be assembled in a box, they should be arranged so that the mutual inductance between coils will be very small. Three coils, assembled in a row with their planes mutually perpendicular will have zero mutual inductance between any pair. After the first coil is mounted in position, the second coil can be readily located in the position of zero mutual inductance by passing an alternating current through the first coil, attaching a telephone receiver to the second coil, and securing the latter in a position such that there is no sound in the receiver. Then each of the first two coils can be used as a primary and the third coil can be located in the position which gives silence in the receiver in each case. A fourth coil can be located to have zero mutual inductance with respect to coils 2 and 3 but necessarily has some mutual inductance with coil 1. However, the mutual inductance between two coils decreases very rapidly[19] as their distance apart increases.

Figure 8 shows a set of 8 standards of self-inductance, consisting of 2 rows of 4 coils, each row being mounted in the manner just described. To reduce mutual inductance between the coils of one row and those of the other to a negligible amount, the rows are separated as shown. Eight noninductive copper coils also are provided, each adjusted to have the same resistance as one of the induc-

[19] Approximately, the mutual inductance varies inversely as the cube of the distance between the coils, when this distance is large compared with the diameter of the coils.

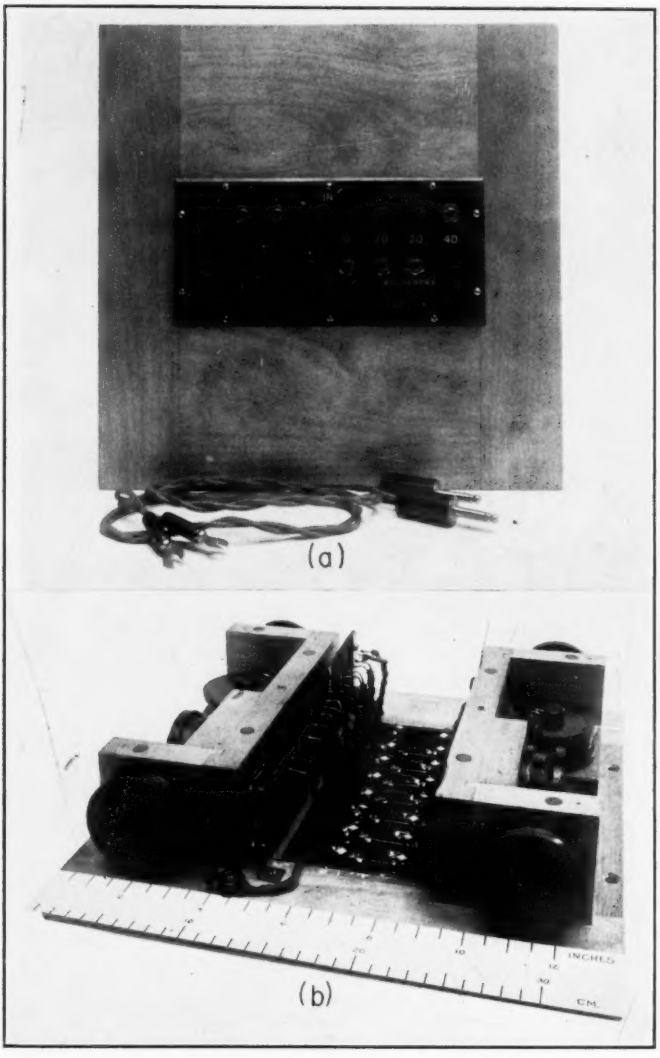

FIGURE 8.—*Set of eight standards of self-inductance*

a, Complete in case; *b*, removed from case. The coils in one row have the values 1, 2, 3, and 4, millihenries; in the other, 10, 20, 30, and 40 millihenries. The coils in each row are located to minimize mutual inductance between coils, and the two rows are spaced far enough apart to make mutual inductance between rows negligibly small. The pair of flexible leads with "traveling plugs" is for use when connection is to be made (for special purposes) to one or several of the individual coils.

tive coils. The plug switchboard makes it possible to cut into circuit any one or more of the inductive coils and to replace those out of circuit by their corresponding noninductive coils. The total resistance between the terminals is thus kept constant, regardless of the value of the inductance. This feature is convenient when the set is used in one arm of an inductance bridge. The switchboard is composed of regular commercial radio parts, namely, 16 "short jacks" and 8 "duplex plugs." Each of these plugs has its two contact parts (tip and sleeve) short-circuited within the handle. A plug inserted in any hole in the upper row (marked "In") inserts the correspondingly numbered inductive coil; in the lower row, the noninductive coil.

In some cases it is desirable to use one or several of the inductive coils of the set without including in the circuit any unnecessary resistance. The flexible leads shown in Figure 8 are for this purpose. One lead is connected to the tip of its plug, the other to the sleeve of its plug. Single coils, either inductive or noninductive, may be picked out with these "traveling plugs." If several coils in series are wanted, the traveling plugs are used in conjunction with one or more of the regular (short-circuited) plugs. Other connections are possible; for example, connections may be made to any coil to be used as a primary coil and to any other to serve as a secondary. This permits the checking of the mutual inductance between the coils to see whether it is sufficiently low (with respect to the sum of their self-inductances) to be negligible.

As compared with an equal number of single standards of inductance, such a set of standards has the advantage that the mutual inductance between each coil and every other one is small and fixed. In using a number of single standards care must always be exercised to keep them far enough apart to make the mutual inductance negligible; and this precaution may easily be neglected by inadvertence. The set of coils has the further advantage of requiring less table space when in use. It has two disadvantages, namely, the greater storage space occupied when the set is not in use, and the fact that the individual coils can not be used in different places on occasion.

Two sets of inductance coils, of much larger dimensions than the ones shown in Figure 8, are used in the current-transformer laboratory of the National Bureau of Standards in the setting up of artificial burdens. With 8 coils ranging from 10 to 500 microhenries, any value of inductance from 10 to 1,100 microhenries can be used. To obtain the highest practicable time constant with a given cost for copper, the coils were wound with square[20] copper wire. The time-constants range from 2.5 milliseconds for the 10-microhenry coil to 17 milliseconds for the 500-microhenry coil.

IV. CURRENT-LIMITING REACTORS FOR POWER SYSTEMS

1. SPECIAL REQUIREMENTS

Inductance coils of large size, known as current-limiting reactors (protective reactors), must meet certain extraordinary requirements which make it impracticable to construct them in the closely wound form described in the preceding section of this paper. In spite of

[20] The side of the square cross section of the wire is 0.162 inch.

the fact that a high time constant is just as desirable in a protective reactor as in an inductance standard for laboratory purposes, and that departure from the optimum form involves an extra cost for copper for a given inductance, the other considerations compel a deviation from the optimum form. These requirements and their effect on the design of protective reactors will be briefly mentioned.

(a) ABILITY TO WITHSTAND HEATING CAUSED BY HEAVY OVERLOADS

A protective reactor is of service only in an emergency, namely, in case of a heavy overload or a short-circuit on the line in which it is placed. It must be able to carry currents of the order of 25 times rated current for, say, five seconds. During this interval the rate of development of heat in the reactor winding is approximately 625 times its usual value. It is obvious that instead of the closely wound turns and layers of the inductance standard used in the laboratory the protective reactor must have its turns and layers spaced apart to allow free passage of air either by convection or forced circulation.

(b) ABILITY TO WITHSTAND DESTRUCTIVE FORCES DURING SHORT-CIRCUITS

Like the heating effect, these forces increase as the square of the current, and require the use of strong constructions. The turns and layers may be spaced apart and held by strong cleats of heat-resisting insulating material, or they may have concrete supports cast around them.

(c) HIGH FLASH-OVER VOLTAGE

Although the voltages from turn to turn and layer to layer are relatively small during normal operation, they attain large values during short-circuits or transient disturbances of high frequency. The spacing between turns and layers serves not only to permit escape of heat, but provides the necessary separation to avoid flash over.

(d) LOW SKIN-EFFECT RESISTANCE RATIO

This requirement is important to minimize the copper loss in the reactor during normal operation. Stranding the conductor, and in some cases enameling[21] certain combinations of the cable strands, are used for this purpose. When several cables are used in parallel to form the reactor winding they are symmetrically spaced and wound so that the total current will be equally divided and circulating currents will be avoided.

2. DESIGN PROCEDURES IN USE

The inductance of current-limiting reactors is determined in some cases by means of standard formulas,[22] such as those of Lorenz, Nagaoka, Rosa, Stefan, and Grover, and in other cases by means of formulas which, while based on standard formulas, also involve the use of families of curves from which values may be found by inter-

[21] Robert B. George, The Application of Current-limiting Reactors, Electric J., **26**, pp. 29–38; January, 1929.

[22] Lorenz's formula is given as equation (74), p. 118; Nagaoka's formula, equation (75), p. 119; Stefan's formula, equation (90), p. 137; Rosa's correction formula, equation (91) p. 139; all of B. S. Sci. Paper No. 169 (part of vol. 8); Grover's formula No. 4 is given on p. 458 of B.S. Sci. Paper No. 455 (part of vol. 18). See also paper by Grover on Formulas and Tables for the Calculation and Design of Single-Layer Coils, Proc. Inst. Radio Engrs., **12**, pp. 193–208, April, 1924.

polation with an accuracy sufficient for engineering purposes.[23] The consideration of these methods is outside the scope of the present paper, in which it is desired to suggest the possible uses of small model coils made to scale. The standard formulas usually involve considerable calculation, and for some forms of coil do not converge rapidly enough; the sets of curves may not cover the particular proportions of length and diameter of coil and spacing of conductors for a proposed new and different design; the mutual inductance between adjacent reactors is not easy to calculate and introduces an unbalancing of phase voltages,[24] and the internal short-circuit forces[25] and those between neighboring reactors are not readily calculated. In all of these matters it is felt that laboratory measurements on model reactors may be useful, not only in checking design values obtained by present methods, but also for determining quantities (such as skin-effect resistance ratio) which are not only difficult to compute in advance, but also difficult to measure in the actual reactors.

3. USEFULNESS OF MODELS TO DESIGNERS IN VARIOUS FIELDS [26]

Many problems of engineering design are too complicated for solution by ordinary mathematical methods and must be solved by experiment; but it often happens that the desired information can be obtained from inexpensive experiments on small models quite as well as from full-scale tests.

The classical example of this is the utilization by naval architects of the results of towing-tank experiments on models for predicting the resistance-speed curves of proposed ships; and in recent years the progress of airplane design has been largely dependent on information obtained from tests of models in the wind tunnel. Similar methods have also been used for studying the erosion of stream beds near dams or bridge piers, the formation of sand banks in tidal estuaries, etc.

Model experiments are particularly useful in hydraulics and aerodynamics because the mathematical treatment of the problems that arise nearly always presents insuperable difficulties; but the utility of the method is not confined to the field of fluid motion or of mechanics in general—it is also applicable to many problems in electrical and heat engineering, and it is believed that experiments on small models may be of service to the designer of large commercial reactors.

Whatever the shape or general design of an electrical apparatus may be, its mechanical and electromagnetic properties depend on its absolute size and will be affected in definite ways by a mere change of scale of the whole apparatus, in all its parts, without changing the materials of construction. For the planning and correct interpretation of model experiments the designer, therefore, needs a number of relations connecting the various characteristics in which he is interested with the size, when the shape, number of windings, etc., are fixed.

---

[23] See H. B. Dwight, Elec. J., **15**, pp. 166–168; 1918; Trans. Am. Inst. Elec. Engrs., **38**, pt. 2, pp. 1678–1696; 1919; Elec. J., **19**, pp. 268–270, 1922; S. L. Oesterreicher, Trans. Am. Inst. Elec. Engrs. **43**, pp. 892–901; 1924; A. Ytterberg, Elektrot. Zeit., **36**, pp. 309–311, 325–327; 1915; O. Gramisch, Elektrot. und Masch., **46**, pp. 105–110; 1928; J. Hak. Elektrot. Zeit., **50**, pp. 193–198; 1929; K. Faye-Hansen, Elektrot. Zeit., **51**, pp. 427–429; 1930.

[24] H. B. Dwight, Trans. A. I. E. E., **38**, pt. 2, pp. 1679–1681, 1919.

[25] W. M. Dann, The Mechanical Stresses in Reactance Coils, Elec. J., **11**, pp. 204–207; 1914; H. B. Dwight, Repulsion and Mutual Inductance of Reactors, Elec. World, **69**, pp. 1148–1150; 1917; and Trans. Am. Inst. Elec. Engrs., **38**, pt. 2, pp. 1681–1684; 1919.

[26] This section has been contributed by Dr. E. Buckingham, to whom the writer is indebted for valuable suggestions for the improvement of this paper.

4. SUGGESTED USE OF MODELS IN THE DESIGN OF CURRENT-LIMITING REACTORS

(a) USEFUL RELATIONS

Most of the relations needed in this part of the paper have been given in Part II (p. 296) as relations (*a*) to (*k*), inclusive, and in the following discussion of the uses of models they will be referred to by these letters. In applying these relations to the case of protective reactors, however, an important distinction between these reactors and the small standards of inductance previously discussed should be kept in mind, namely, that the latter (for the relatively low frequencies considered in this paper) are closely wound with insulated wire, so that the diameter of the wire over the insulation has a direct relation to the number of turns to fill a given channel. Protective reactors, on the contrary, usually have air spaces between adjacent turns and adjacent layers. The diameter of the wire over the insulation (if any) has, therefore, no direct relation to the inductance of the coil. However, relations (*b*), (*c*), (*e*), and (*h*) will still apply if for the "diameter over the insulation" one substitutes the square root of the product of the axial pitch by the radial pitch.[27] If we define the space factor of a reactor as the ratio of the net cross section of the conductor to the area of a rectangle of which the sides are, respectively, the axial pitch and the radial pitch, relations (*e*), (*f*), (*i*), (*j*), and (*k*) apply to coils in which open spaces separate turns and layers.

Another important distinction between the inductance standard and the current-limiting reactor must be noted. The diameter of the wire used in the former is usually so small (with respect to the frequency range to which this paper is limited) that the increase of resistance from skin effect is not serious. In current-limiting reactors, however, the wires or cables are often of relatively large cross section and the skin-effect resistance ratio may be of considerable importance even at the relatively low frequencies on which they are used, since the I^2R loss in the reactor during normal operation is proportional to it. The direct measurement of the I^2R loss is a somewhat difficult matter because of the large currents and the very low power factor. A special procedure, which will be described later, makes it possible to produce and measure, in the model reactor, a skin-effect resistance ratio equal to that in the full-size reactors.

Current-limiting reactors, in this country, are usually connected in circuits of frequency not exceeding 60 cycles per second, consequently the effect of distributed capacitance may be neglected, so far as effects of operating frequency are concerned.

(b) CHECKING THE SELF-INDUCTANCE OF FULL-SIZE REACTORS

To check the predetermined value of self-inductance of a proposed reactor, a model reactor is made in which all significant dimensions are $1/n$ times those of the proposed reactor. This factor applies to the copper conductor as well as to the axial length of coil, diameters of successive layers, etc. The conductor should be stranded in the same manner as the full-size conductor will be, in order that the same

[27] For coils in which the conductor is wound as a succession of layers the axial pitch is the distance from center to center of adjacent turns in a layer, measured in a direction parallel to the axis of the coil, and the radial pitch is, in general, the radial distance between adjacent imaginary cylinders which are coaxial with the coil, each cylinder bisecting the cross section of the conductors of a given layer. The terms axial pitch and radial pitch may be applied, with obvious modifications, to coils which are wound as a series of coaxial flat spirals or "pancakes."

model may be used to get the skin-effect resistance ratio also. The number of turns in the model should be the same as in the proposed reactor. Then by relation (*g*), page 296, the inductance of the full-size reactor will be n times that of the model. Neglecting skin effect, the d. c. resistance of the full-size reactor will be $1/n$ times that of the model. This resistance, however, can be so easily computed for the full-size reactor that there would be no object in making a model, so far as it is concerned.

(c) CHECKING THE SKIN-EFFECT RESISTANCE RATIO OF FULL-SIZE REACTORS

To determine the skin-effect resistance ratio for the full-size reactor, this ratio is determined for the model, using a frequency n^2 times the rated frequency of the full-size reactor.[28] The use of this value of frequency depends upon the fact that the skin-effect resistance ratio (that is, the ratio of a. c. resistance to d. c. resistance) for a conducting structure is a function of one parameter, $fd^2\mu/\rho$, where f denotes the frequency, d a given linear dimension, μ the permeability (equal to unity for air and for copper) and ρ the resistivity of the conductor material. While the form of the function depends on the shape of the structure, this form is the same for all geometrically similar structures of any size or material.

For example, if the proposed full-size reactor is to operate at 60 cycles, and the model is made with each linear dimension one-tenth that of the full-size reactor, the model should be tested for skin-effect resistance ratio at 6,000 cycles. It should be noted that in this case it is especially important that the model be wound with a conductor which has the same number of strands (or straps) as the conductor of the full-size reactor, each strand (or strap) having its dimensions $1/n$ times those of the conductor of the full-size reactor. The arrangement of the winding and the number of turns must be the same in the model as in the full-size reactor. If the individual components of the full-size conductor are insulated from each other, those of the conductor on the model should also be insulated, and the over-all dimensions of the conductor on the model should be $1/n$ of those of the full-size conductor. While these precautions involve some extra pains in construction, the result of the test gives a figure which would otherwise have to be found by the difficult procedure of measuring the very low power factor of the large current of the full-size reactor.

If it should not be convenient to make the test of the model reactor at n^2 times the working frequency, it may be made at a different frequency and corrected by using the fact that $\Delta r/r$, the relative increase of resistance caused by skin effect, varies for low frequencies almost exactly as the square of the frequency, and that $\Delta L/L$, the relative change of inductance with frequency, is usually very small compared with $\Delta r/r$.

It is worth noting, as pointed out by Dwight, that the preceding use of a model is applicable to other cases where the inductance and the skin-effect resistance ratio of large conducting structures, for example, busbars and furnace leads, are of importance and are not readily predetermined by calculation.

[28] This expedient was suggested by H. B. Dwight, Trans. Am. Inst. of Elec. Engrs., **37**, pt. 2, p. 1399; 1918. A more mathematical proof of the theorem was given by Joseph Slepian in the discussion of Dwight's paper, same volume, pp. 1401–1403.

(d) CHECKING THE MUTUAL INDUCTANCE BETWEEN FULL-SIZE REACTORS

If a small-scale model of two or more reactors is made with all the dimensions,[29] including the distances between the reactors, reduced to $1/n$ times their original values, the number of turns in each model reactor being the same as in the corresponding full-size reactor, the mutual inductance between any pair of reactors will be $1/n$ times the mutual inductance between the corresponding full-size reactors. The mutual inductance is so nearly independent of frequency[30] that its value may be determined with any convenient frequency.

The practical importance of a knowledge of the mutual inductance between protective reactors depends mainly on two effects which it produces. The first of these is an unbalancing of phase voltages for cases where the reactors A, B, and C, are unsymmetrically grouped; that is, where the three mutual inductances M_{AB}, M_{BC}, M_{AC} are unequal. As examples of usual unsymmetrical groupings may be mentioned, first, all three reactors having a common vertical axis; second, all three axes vertical and in a common vertical plane, and the centers of the coils in the same horizontal line.[31]

(e) CHECKING THE ELECTRODYNAMIC FORCES BETWEEN FULL-SIZE REACTORS

These forces constitute the second effect of practical importance resulting from the mutual inductance between the parts of the winding of a given reactor, or between adjacent reactors. Increasing as the product of the currents in the two reactors (times the cosine of the time phase angle between the currents), these forces may become relatively very high[32] during short circuit conditions. The use of model reactors for determining the translational forces between full-size reactors depends upon an ideally simple relation which applies to geometrically similar pairs of coils or other conducting structures, and which will now be developed.

The force F_x in any direction x between any two circuits traversed by currents I_1 and I_2 which are displaced in time phase by an angle θ is given by the well known formula

$$F_x = I_1 I_2 \cos\theta \frac{dM}{dx} \tag{12}$$

Referring to Figure 9, let the curve $MM'N$ represent the mutual inductance between two coils as a function of the distance (in the direction x) between their axes. The ordinate MX, corresponding to the axial distance OX, is the maximum possible value of mutual inductance, and is for the case of coils in contact. As the distance between the axes increases the mutual inductance decreases as shown by the curve $MM'N$, and for any given value of $I_1 I_2 \cos\theta$ the force in the direction x will be proportional to the slope of this curve.

---

[29] An exception is the diameter of the conductors; it is not necessary, in the determination of mutual inductance, to adhere at all closely to proportionality of conductor diameter, nor do the conductors need to be stranded or enameled as for the previous case where the skin-effect resistance ratio was an important item to be determined.

[30] This statement would not apply accurately to extreme cases where the two circuits are very closely coupled; for example, two coaxial disk or "pancake" coils separated by a relatively small axial distance. Such a case would hardly be even approximated, as far as the protective reactors under consideration are concerned.

[31] This second case is treated by H. B. Dwight, with a numerical example, in Trans. Am. Inst. Elec. Engrs., **38**, pt. 2, pp. 1675-1681; 1919.

[32] Kierstead and Stephens, Trans. Am. Inst. of Elec. Eng., **43**, p. 909; 1924; report having observed forces as high as 33,000 pounds. They state that in the case of average feeder reactors the force is not over 10,000 pounds.

Consider now a second pair of coils, geometrically similar to the first pair, similarly located with respect to each other, with the same number of turns in corresponding coils, but with all the dimensions reduced to $1/p$ times those of the first pair. By relation (n), page 297, the mutual inductance of this second pair of coils for any relative position will be $1/p$ times the mutual inductance of the larger pair for the corresponding position. The values of mutual inductance of the smaller pair, plotted to the same coordinates as the curve $MM'N$ (fig. 9), will give the curve $mm'n$, in which mx is the maximum possible ordinate, for coils in contact, and corresponds to the ordinate MX for the larger coils. Since the two curves have their corresponding abscissas differing only by the constant factor $1/p$, and their corresponding ordinates also differing only by this same factor, the

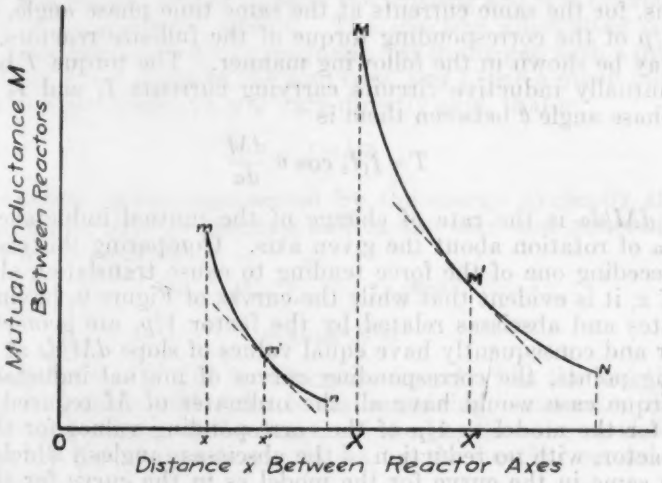

FIGURE 9.—*Manner of variation of the mutual inductance of two pairs of reactors as a function of the distance between their parallel axes*

The smaller curve mn refers to a pair of coils geometrically similar to a larger pair to which the curve MN applies. For geometrically similar configurations the value of dM/dx is the same for each pair, as indicated by the tangents drawn as dotted lines.

tangent to $mm'n$ at any point m' is equal to the tangent to the curve $MM'N$ at the corresponding point M'. But this tangent is equal to dM/dx, which (equation (12)) determines the force between a pair of coils for the given currents I_1 and I_2. This equality of forces is independent of the form of the coils and of the direction in which the force between them is resolved. Consequently, model reactors will develop the same force per ampere squared as the large reactors, for any given relative position, regardless of the scale to which the models are made.[33]

In general, even when immersed in oil the model reactors would not be able to carry currents equal to those which the full-size reactors must carry. On the assumption that the current density in the windings of the models is the same as in the full-size reactors, the models would carry $1/p^2$ times as much current as the latter, and for the

[33] Dwight, Formulas for Reactance Coils, Trans. A. I. E. E., 38, pt. 2, p. 1682; 1919.

same time-phase angle between the currents the force would be $1/p^4$ times that between the full-size reactors.

The force F_x given by equation (12) is the average force, on the assumption that both reactors are rigidly secured to nonyielding supports, so that the relation of the natural frequency of oscillation (which depends on mass and resilience) to the electrical frequency does not introduce additional forces.[34]

(f) ELECTRODYNAMIC TORQUE BETWEEN REACTORS

In the preceding discussion the mutual electrodynamic forces tending to cause translation have been considered. If two reactors are so located that a torque can result from the interaction of their fields, the corresponding torque between two model reactors geometrically similar to them, to a scale of $1/p$, with the same numbers of turns, for the same currents at the same time phase angle, will be only $1/p$ of the corresponding torque of the full-size reactors. This fact may be shown in the following manner. The torque T between two mutually inductive circuits carrying currents I_1 and I_2 with a time phase angle θ between them is

$$T = I_1 I_2 \cos\theta \frac{dM}{d\alpha} \tag{13}$$

where $dM/d\alpha$ is the rate of change of the mutual inductance with angle α of rotation about the given axis. Comparing this case with the preceding one of the force tending to cause translation along an axis of x, it is evident that while the curves of Figure 9, having both ordinates and abscissas related by the factor $1/p$, are geometrically similar and consequently have equal values of slope dM/dx at corresponding points, the corresponding curves of mutual inductance for the torque case would have all the ordinates of M reduced in the curve for the model to $1/p$ of the corresponding values for the full-size reactor, with no reduction of the abscissas (angles), which would be the same in the curve for the model as in the curve for the full-size reactor; consequently the slope $dM/d\alpha$ at each point on the curve for the model is $1/p$ of the slope at the corresponding point of the curve for the full-size reactor.

V. IRON-CORE AIR-GAP REACTORS

1. SCOPE OF THIS DISCUSSION

The following discussion is intended to apply to reactors for frequencies of the ordinary values used for light and power circuits. It is not intended to apply without qualification to reactors for audio- and radio-frequencies, nor to reactors having an initial polarization produced by a direct current.

2. REASON FOR THE USE OF AN AIR GAP

The inductance of an iron-core reactor is a maximum when there is no air gap in the magnetic circuit, and the question naturally arises, why is an air gap generally used? The first and more obvious reason is that with a closed iron core the inductance varies greatly with the

[34] See Short-Circuit Forces on Reactor Supports I, by Doherty and Kierstead, Trans. Am. Inst. Elec. Engrs., 42, pp. 552–561; 1923.

current because of the wide variation in the permeability of the core with change in flux density. Furthermore, the current will be relatively very small because of the very low reluctance; consequently a very small value of reactive volt amperes is obtained at the expense of the full amount of iron loss. Another important consideration in most cases is that the reactor should usually have the smallest possible ratio of total loss to reactive volt-amperes,[35] or what is nearly the same thing, the smallest possible power factor, for a given bulk or weight or cost of the reactor. The following reasoning will show that this requires the presence of an air gap in the magnetic circuit.

The inductance of an iron-core air-gap reactor is

$$L = 4\pi N^2/\mathfrak{R} \tag{14}$$

where N is the number of turns in the winding and $\mathfrak{R}$ is the reluctance of the entire magnetic circuit. The effective alternating current I required to produce a cyclic magnetic flux in the gap with a prescribed maximum flux density in the iron core, and hence a given power loss in the iron per kilogram, will vary directly as $\mathfrak{R}$, that is

$$I = k\mathfrak{R} \tag{15}$$

The reactive power represented by the energy cyclically stored in the magnetic field in the gap and in the core and restored to the circuit by this current is

$$P_r = L\omega I^2 = L\omega k^2 \mathfrak{R}^2 \tag{16}$$

$$= 4\pi\omega k^2 N^2 \mathfrak{R} \tag{17}$$

The reactive power will thus increase linearly [36] as the length of the gap is increased, with iron losses remaining constant. The permissible upper limit to the length of the gap (for the condition of a constant value of iron losses) is set by the heating caused by the copper loss.

3. CONDITION FOR THE DESIRABLE MINIMUM POWER FACTOR

The purpose of a reactor being to introduce reactance into a circuit, and the unavoidable copper loss and iron loss being usually undesirable, it is of interest to determine the condition for which the power factor of the reactor will have its desirable minimum value. In the following it is again assumed that the magnetic flux density and, therefore, the total iron loss P_i is kept constant as the total reluctance $\mathfrak{R}$ is increased by lengthening the gap. The current I to maintain the chosen value of total flux will increase in proportion to $\mathfrak{R}$. The resistance of the winding being r, the total loss is the sum of the constant iron loss P_i and the variable copper loss I^2r. The value of the reactive volt-amperes may be expressed by the relation

$$P_r = a\mathfrak{R} \tag{18}$$

[35] This is equivalent to stating that the time-constant should be as high as possible. Unlike air-core inductance standards, iron-core reactors of the kinds under discussion are ordinarily designed for operation on a definite frequency, which makes the above terminology more convenient.

[36] This assumes that the cross section of the path of the magnetic flux in air does not change as the gap in made longer. Actually, the cross section increases. As an approximation, it has been suggested by Reed (Essentials of Transformer Practice, 2d ed., pp. 236–237) that each of the dimensions of the cross section of the air-gap flux, in the case of a rectangular iron core, be taken as equal to the corresponding dimension of the core increased by the length o ithe gap.

where a is a constant. It is more convenient to deal with cot θ, the ratio of total loss to reactive volt-amperes, than with the power factor cos θ, and the condition which makes cot θ a minimum also makes cos θ a minimum. Replacing the current I by its equivalent $k\mathfrak{R}$ by equation (15),

$$\cot\theta=(P_i+k^2\mathfrak{R}^2r)/a\mathfrak{R} \tag{19}$$

By differentiating this expression for cot θ with respect to $\mathfrak{R}$ it may be shown that for a minimum value of cot θ

$$P_i=k^2\mathfrak{R}^2r=I^2r \tag{20}$$

That is, the ratio of total loss to reactive volt-amperes, and, therefore, the power factor, will be a minimum when the copper loss equals the total iron loss.[37]

4. SUGGESTED USE OF MODEL REACTORS AS A CHECK ON PRESENT METHODS OF DESIGN

The inductance and other properties of an iron-core air-gap reactor may be predetermined by more or less approximate design procedures,[38] for the details of which the reader is referred to textbooks and original articles. It is the purpose of this section to show how a proposed design for such a reactor may be checked by the use of a small model. This would be done, in general, only when the full-size reactor is relatively large and expensive, for obviously if the reactor to be designed is of relatively small size (such as might be used, for example, as part of a frequency meter) it would be preferable to construct one of the actual design dimensions and to modify the design on the basis of its performance.

The performance of a proposed full-size iron-core air-gap reactor may be predetermined by tests made on a geometrically similar model reactor having all its dimensions $1/n$ times the corresponding dimensions of the full-size reactor, including the diameter of the wire used in the winding. The number of turns in the coil of the model should be the same as the number proposed for the full-size reactor. However, in order that the iron loss per unit volume, at a given frequency and maximum induction, shall be the same in the model as in the full-size reactor, the steel sheets used in the model should be of the same material and the same thickness as those to be used in the full-size reactor. These conditions being complied with, and the model being tested with a current $1/n$ times the rated current to be carried by the winding of the full-size reactor, at the same frequency, the following relations will hold:

(o) The reactance of the full-size reactor will be n times that of the model.

(p) The reactive volt-amperes of the full-size reactor will be n^3 times the corresponding value for the model.

(q) The iron losses in the full-size reactor will be n^3 times those in the model.

---

[37] Compare this with the similar relations for transformers; Reed, Essentials of Transformer Practice, 2d ed., pp. 60, 113.

[38] Reed, Essentials of Transformer Practice, pp. 146–148; Pender's Handbook for Electrical Engineers, 2d ed., p. 1332; Standard Handbook for Electrical Engineers, 5th ed., p. 456; Edgcumbe, Industrial Electrical Measuring Instruments, 2d ed., p. 77; Drysdale and Jolley, Electrical Measuring Instruments, I, p. 62; Wiggins, Elec. Jour., 24, pp. 20–22, 1927; Emde, Elektrot. und Maschinenbau, 48, pp. 521–530; 1930.

(*r*) The copper loss in the full-size reactor, when rated current flows, will be n times the copper loss in the model.

It may be that the use on the model of a winding having the same number of turns as in the proposed full-size reactor will result in a value of reactance in the model which is inconveniently low for measurement. To take care of this difficulty, the model may be wound with p times the number of turns to be used in the full-size reactor. The resulting value of reactance of the model must in this case be multiplied by n/p^2 to get the reactance of the full-size reactor. Similarly, if the cross-sectional area of the wire used in winding the model is $1/pn^2$ times that of the wire to be used on the full-size reactor, the resistance of the winding of the model must be multiplied by $1/p^2n$ to get the resistance of the full-size winding.

The statement made above concerning the copper loss of the full-size winding neglects the greater skin-effect resistance ratio in this winding. It is obviously impracticable to test the model at a higher frequency to take care of this matter, as can be done for a coil having no iron core, because of the uncertainty as to the effect of this higher frequency on the iron losses.

The fact that the copper loss of the full-size reactor is only n times that of the model while the value of reactive volt-amperes is n^3 times as great means that the small size of the model makes it inefficient for the same reason that small transformers and small generators are inefficient. It implies also that to obtain the necessary data with the model it will be necessary to overload its winding considerably. This is evident from the fact that the wire used in winding the model, with only $1/n^2$ times the cross section of the wire to be used on the full-size reactor, must carry $1/n$ times the current of the latter. The resulting heating can be kept down, if necessary, by immersing the model in oil and by passing current through it only long enough to obtain readings. The container for the oil should be such as not to affect the performance of the model, either by altering the magnetic leakage flux or by providing a path for eddy currents.

It follows from relations (*o*) to (*r*), page 322, that the power factor of the full-size reactor will be lower than that of the model, and can be determined from these relations. After experiments have been made on the model with various lengths of gap, values of reactance and of power factor of the full-size reactor for the various corresponding gap lengths can be computed and plotted as a function of gap length in order to find what gap length gives the required reactance, and what the corresponding value of power factor will be. These curves will have the general form shown in Figure 10. In this figure it will be noted that instead of power factor the ratio of watts loss (iron plus copper) to reactive volt-amperes has been used. The latter ratio is found by a simple division, while the power factor requires squaring these two quantities, extracting the square root of their sum, and dividing the watts loss by the result. Much labor will be saved by using cot θ, the ratio of watts to reactive volt-amperes, during the design process. It approximates more and more closely to the power factor cos θ as the latter approaches zero, as may be seen from the following table, in which values of the ratio are rounded to the nearest unit in the third decimal place.

TABLE 3

Power factor, cos θ	Ratio of watts loss to reactive volt-amperes, cot θ	Power factor, cos θ	Ratio of watts loss to reactive volt-amperes, cot θ
0.000	0.000	0.120	0.121
.010	.010	.140	.141
.020	.020	.160	.162
.030	.030	.180	.183
.040	.040	.200	.204
.050	.050	.250	.258
.060	.060	.300	.314
.070	.070	.350	.374
.080	.080	.400	.436
.090	.090	.450	.504
.100	.101	.500	.577

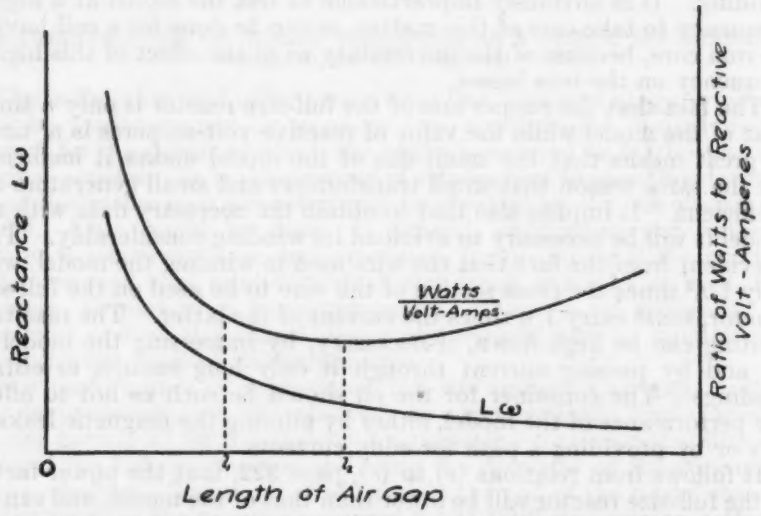

FIGURE 10.—*Performance of an iron-core air-gap reactor as a function of the length of the air gap, with constant frequency, and with the current varied to maintain a constant value of maximum magnetic flux density in the core*

From the curve $L\omega$ of Figure 10 the gap length which will give the required reactance can be ascertained, and also the corresponding value of the ratio of watts to reactive volt-amperes, which may be translated into power factor with the aid of Table 3. Referring to Figure 10, if the required value of reactance corresponds to the gap length Ol_1, the ratio of watts to reactive volt-amperes will be greater than the minimum value possible with a reactor of these core dimensions, which minimum value is had when the gap length is Ol_2. This latter gap length, however, corresponds to a value of reactance lower than the required value. Hence if the ratio of watts to reactive volt-amperes must be made lower the only remedy is to increase the dimensions of the proposed full-size reactor. A new set of curves is to be plotted from the data already observed on the model, using a somewhat larger dimension ratio n_2 in place of n. On the assumption that the rated current and the cross section of the conductor of the

full-size reactor are to remain as originally planned, it is evident that the proposed larger full-size reactor will have a coil cross section greater than that originally proposed by the factor $(n_2/n)^2$, and that the number of turns will, therefore, be greater by this factor. The values of reactance of the proposed larger reactor, for any given relative gap lengths, will be n_2^5/n^4 times the corresponding values already observed for the model.[39] Similarly, the reactive volt-amperes for the proposed larger reactor, with $(n_2/n)^2$ times the originally proposed number of turns, will be n_2^5/n^2 times the reactive volt-amperes of the model, for corresponding relative gap lengths; the iron loss will be n_2^3 times that in the model, and the copper loss will be n_2^3/n^2 times that in the model, for corresponding relative gap lengths. These ratios may be derived from relations (*o*) to (*r*), inclusive. P. 322.

The new curves will resemble the set relating to the first proposed full-size reactor, but the required value of reactance (if n_2 has not been chosen too much greater than n) will be associated with a value of the ratio of watts to reactive volt-amperes lower than in the case of the first proposed reactor. If n_2 has been chosen too large, the required value of reactance may correspond to an unduly large relative length of air gap. This means a waste of material, at least, and possibly with it a needlessly large value of the ratio of watts to reactive volt-amperes. A smaller trial value of dimension ratio, intermediate between n and n_2, should be tried, and the process repeated until a design is found in which the desired value of reactance occurs near the minimum value of the above ratio.

For very short relative lengths of gap the performance of the model reactor may approximate too closely (for some purposes) to that of an iron-core reactor without an air gap, in that the reactance will vary too much with the current. For such purposes, only those values of relative gap length should be considered for adoption for which the reactance of the model is sufficiently independent of the value of the current to satisfy the requirements of the particular application.

5. SUGGESTED USE OF MODEL REACTORS AS AN INDEPENDENT BASIS OF DESIGN

(a) UNCERTAINTY AS TO GAP RELUCTANCE, STRAY FLUX, ETC.

The uncertain elements in the methods of design now in use arise from the fact that the magnetic flux flows in part through leakage paths in a manner difficult to predetermine, and the flux across the air gap fringes out so that the cross section of the air-gap flux is greater than that of the iron core. When the gap is very short in comparison with the dimensions of the core perpendicular to the flux path, the reluctance of the gap will not differ greatly from that computed on the assumption of no leakage and no fringing of flux at the gap. As the relative length of the gap increases, the effects of leakage and fringing increase and it becomes increasingly difficult to predetermine the reluctance accurately. The use of models (or of a single model, the length of its gap being varied by steps) has

[39] If the number of turns on the larger proposed reactor had been left the same as the number originally planned, its reactance would have been simply n_2 times the corresponding value for the model. Increasing the number of turns by the factor $(n_2/n)^2$ increases the reactance by the further factor $(n_2/n)^4$, that is, to n_2^5/n^4 times that of the model.

the advantage that the manner of leaking of the flux and fringing at the gap will be the same in the model as in any larger reactor which is geometrically similar in all dimensions,[40] including gap length, provided the steel is worked at the same frequency and the same maximum value of induction. It is therefore suggested that the designer may begin by experiments on a model of suitable form, tested at a suitable value of maximum induction, and from the results compute the dimensions of a full-size reactor to have the desired electrical properties. The following general procedure is suggested:

(b) CHOICE OF FORM OF CORE AND LOCATION OF GAP

Various forms of core and locations of gap are used, and few general rules can be given. For economy of manufacture form-wound coils should be used if possible. From the standpoint of reducing leakage it is best to have the gap near the axial center of the coil, but this is not so convenient in some respects as are other arrangements where the gap is visible and accessible for measurement. The reader is referred to text books[41] in which typical forms are shown and their advantages and disadvantages discussed.

(c) CHOICE OF CORE MATERIAL AND MAXIMUM FLUX DENSITY

As previously stated, the material for the core is ordinarily silicon steel sheets of the grade and thickness used in power and lighting transformers (about 0.35 mm = 0.014 inch), and the maximum value of induction is properly chosen at about the same value as used in such transformers for the given frequency.

(d) EXPERIMENTS TO BE MADE WITH THE MODEL

Two windings should be used—one of relatively fine wire which does not surround the air gap and the regular winding which may or may not do so. The fine-wire winding is intended for use as a test coil to indicate when the flux in the iron has its desired value. The voltage E in volts induced in it when current flows in the regular winding is to be measured[42] and from it and the number of turns N in the test coil, the frequency f and the net cross-sectional area A_{cm} of the iron core in cm^2, the maximum magnetic induction in the core, B_{max}, in maxwells per cm^2, should be found by using the ordinary transformer equation

$$E=4.44\ Nf\ B_{max}A_{cm}\times10^{-8} \tag{21}$$

from which

$$B_{max}=\frac{10^8E}{4.44NfA_{cm}} \tag{22}$$

Some American designers, while expressing B_{max} in maxwells per cm^2, prefer to express the net cross-sectional area of the core in square

[40] Except the thickness of the sheet steel, which, as previously suggested, should be the same in the model and in the full-size reactor.

[41] Drysdale and Jolley, Electrical Measuring Instruments, Pt. I, p. 65; Keinath, Die Technik der elektrischen Messgeräte, 3d ed., 1, pp. 467–470.

[42] If an a. c. potentiometer is available to measure this voltage, no correction for the resistance of the test coil is necessary. If it is necessary to use an a. c. voltmeter to measure the voltage induced in the test coil, the voltmeter should preferably have a relatively high resistance. If R_v is the resistance of the voltmeter and R_c that of the test coil, the voltmeter reading should be multiplied by $(R_v+R_c)/R_v$ to obtain the induced voltage.

inches, for which case the expression for maximum induction takes the form

$$B_{max}=\frac{3.49\times10^8E}{NfA_{in}} \tag{23}$$

The current I in the main winding of the model during this test consists of two components; the one with which the designer is concerned, which sends the flux through the magnetic circuit, and another which by transformation supplies the current to operate the voltmeter. If the model core is of relatively small dimensions, or if the voltmeter is of relatively low resistance, it is necessary to eliminate the component of I which by transformation operates the voltmeter. This can be done as follows: Note the increase ΔI of the main current when a second voltmeter of the same type and practically equal resistance is put in parallel with the first voltmeter; then reduce the original reading I by an amount ΔI to get an approximate value of the current in the main winding which will excite the model core to the desired magnetic flux density.

The above procedure is to be repeated with the length of the air gap increased by successive steps of relatively moderate amount. Each time the current I is to be adjusted to give the desired magnetic flux density in the core, as shown by the voltmeter reading, and the net current $I-\Delta I$ is to be determined.

(c) WORKING UP THE RESULTS OF EXPERIMENTS WITH THE MODEL

The next step is to assume some value of n, and on this basis to compute the performance of a larger, geometrically similar reactor. The results having been plotted as in Figure 10, the designer can judge whether the assumed full-size reactor will have the desired properties, and, if not, whether the next value of n to be tried should be larger or smaller than the first one.

6. CONDITION FOR MINIMUM POWER FACTOR IN EACH OF A SERIES OF GEOMETRICALLY SIMILAR REACTORS

In a paper[43] on the calculation of iron-core reactors of high time-constant, Emde gives computed data for six reactors which form an ascending series with all the dimensions (except the length of the air gap) in the ratios 1:2:4:8:16:32. The equivalent air-gap lengths,[44] however, are in the ratios 1:4:16:64:256:1024; in other words, the reactor which is larger in all its other dimensions by the factor n has an equivalent air-gap length which is greater by the factor n^2. This one deviation from geometrical similarity is necessary to obtain the desirable minimum power factor for every reactor in the series, with the same frequency and the same flux density in the iron. To demonstrate this fact, assume that a reactor is available in which the equivalent air-gap length has the value which makes copper loss equal to iron loss for a given flux density and given frequency, and that a larger reactor is to be made of the same materials with all its dimensions n times as great. For simplicity, assume a single conducting turn

[43] F. Emde, Elektrotechnik und Maschinenbau, **48**, pp. 521–530; 1930. This paper covers the subject in a very thorough manner, including calculation of dimensions, minimum total cost of materials, cooling surface, etc.

[44] The equivalent length of air gap may be defined as the length of an air gap having the same cross section as the actual air gap and a reluctance equal to the total reluctance of the given magnetic circuit.

around the core in each reactor. With the same density of current in the copper and the same magnetic flux density in the core the copper losses and the iron losses of the second reactor will each be n^3 times the corresponding quantities for the first reactor. As shown above (p. 322), equality of these two losses is necessary to obtain the minimum power factor; therefore, the current in the second reactor is definitely fixed as n^2 times that in the first reactor. It remains to determine what length of air gap in the second reactor is compatible with this required current.

The cross section of the magnetic circuit in the larger reactor is n^2 times that of the smaller reactor, and the condition of equal flux density implies that the total flux in the second reactor is n^2 times that in the first. The setting up of n^2 times the flux by n^2 times the current means that the total reluctance is the same in both reactors, and this in turn means that the larger reactor with n^2 times the area of flux path must have an equivalent air-gap length n^2 times that of the smaller reactor.

The relatively greater equivalent length of gap in the larger reactor, with the same value of magnetic energy density, makes the ratio of total magnetic energy to total losses n times as great in the larger reactor. This is equivalent to saying that cot θ for the second reactor (which is very nearly the same as the power factor cos θ) is $1/n$ times the value of cot θ for the smaller reactor. Emde's table of data for his computed series of reactors includes values of time-constant and of cot θ. The ratio of mean length of flux path in iron to the equivalent air-gap length for the series decreases as $1/n$ from the value 546 in the smallest reactor to 17 in the largest. Emde points out that one would usually have to discard as useless the two reactors at the lower end of his series because the air gaps are so short in comparison with the length of the flux path in iron that the curvature of the magnetization line is too great. For small values of time constant it may therefore be advantageous to use an air-core reactor.

VI. ACKNOWLEDGMENT

The writer is greatly indebted to Dr. Frederick W. Grover for his careful reading of the manuscript, for many constructive suggestions for its improvement, for checking the correctness of the similitude relations concerning reactors (pp. 296, 297, 322, and 323), and for the computation of the data given in Table 1.

WASHINGTON, May 12, 1931.

RP343

THE HEAT OF FORMATION OF WATER AND THE HEATS OF COMBUSTION OF METHANE AND CARBON MONOXIDE. A CORRECTION

By Frederick D. Rossini

The data on the heat of formation of water and the heats of combustion of methane and carbon monoxide, which were obtained in this laboratory last year,[1] were reduced to a constant pressure of 1 atmosphere by means of the formula used by Schuller and Wartha[2] for this purpose. This procedure is incorrect. No reduction of the present data, or of the data of Schuller and Wartha, to 1 atmosphere is necessary because the pressure coefficient of the heat of these reactions is negligibly small.

For gaseous reactions occurring at constant pressure, the change of the heat of reaction with pressure is zero when the reactants and the products are "ideal" gases. For real gases at pressures near 1 atmosphere, the change in the heat content with pressure is entirely negligible (of the order of 0.001 calorie per mole per mm Hg) in comparison with the heat of reaction. For a liquid or a solid, the change in heat content with pressure is also negligible.

Although the error which results from the procedure used is significant for some of the individual experiments, the final "best" values for the heat of formation of water and for the heats of combustion of methane and carbon monoxide are affected to a neglibible extent. Therefore, the final "best" values for the heat of these reactions are not changed, but the statements made in the original papers with regard to the change with pressure of the heat of these reactions should be deleted.

In the papers under consideration,[3] the following parts of the text are incorrect and should be omitted:

Page 23. The second paragraph.

Page 38. The paragraph beginning near the bottom of the page.

Page 49. The words in the last sentence of each of the first two paragraphs which give the pressure coefficient.

In Table 2, page 24, Table 4, page 26, Table 7, page 29, Table 4, page 43, and Table 8, page 47, the corrections shown in the column headed "presssure correction to 1 atmosphere" should not be made.

[1] Rossini, B. S. Jour. Research, **6**, pp. 1, 36; 1931.
[2] Schuller and Wartha, Ann. Physik, **2**, p. 378; 1877.
[3] See footnote 1.

The correct mean values of the various series of experiments, with their average deviations, are:

	Former mean	Corrected mean
Water, Set I, Table 2, page 24	285, 749±53	285, 756±43
Water, Set II, Table 4, page 26	285, 781±28	285, 788±23
Water (Schuller and Wartha), Table 7, page 29	285, 890±38	285, 850±50
Methane, Table 4, page 43	889, 700±218	889, 720±230
Carbon monoxide, Table 8, page 47	282, 925±109	282, 938±110

WASHINGTON, June 8, 1931.

RP344

ELASTIC PROBLEM OF A WIRE-WOUND CYLINDER

By Chester Snow

ABSTRACT

The elastic problem here treated is that of an infinitely long circular cylinder around which is wrapped an endless set of equal wires, equally spaced, with given tension. The deformation in cylinder and wires is found after determining the pressure distribution and the shape and size of the contact surface between a wire and the cylinder. The latter are found by a method which is a natural extension of Hertz's theory of contact. The contact surface is a ring of finite length instead of an infinitesimal ellipse as in Hertz's method so that the integral equation determining the pressure function and its range is in this case a logarithmic potential instead of a Newtonian one. Numerical application is made to measurements on a precision standard of inductance, which is a single layer coil on a porcelain cylinder. It is concluded that errors due to deformation of wire and cylinder will be negligible in the computation of the inductance provided that the over-all diameter is measured after winding.

CONTENTS

		Page
I.	Introduction	331
II.	Fundamental equations	332
III.	Formal solution for the wire	336
	1. Particular solution for a single turn of wire	336
	2. The stress function χ for the wire	338
IV.	Formal solution for the cylinder	346
V.	Determination of the pressure distribution and the contact surface	350
VI.	Summary	355

I. INTRODUCTION

A very long circular cylinder of known unstressed radius a is uniformly wound with circular turns of wire of spacing $2\pi p$. The unstressed radius of the wires ρ_0 and their tension T being given, the deformation in wires and cylinder is desired. This problem arises in connection with absolute electrical measurements which are based upon the computed inductance of a single-layer solenoid. The solution here presented gives the elastic displacement and stresses to the first order inclusive in the small ratio $\frac{\rho_0}{a}$. Formal solutions of the equations of elastic equilibrium in wires and cylinder being obtained, the satisfaction of the boundary conditions and the expression of contact lead to an integral equation (of the logarithmic potential type) for the determination of the pressure distribution between wire and cylinder and the shape and size of the contact dent.

II. FUNDAMENTAL EQUATIONS

If σ and E denote Poisson's ratio and Young's modulus, respectively, the cylindrical components u_r u_θ and u_z of the elastic displacement must satisfy the three equations of equilibrium

$$\left.\begin{aligned} \frac{\partial \Delta}{\partial r}+(1-2\sigma)\left\{\nabla^2 u_r-\frac{u_r}{r^2}-\frac{2}{r^2}\frac{\partial u_\theta}{\partial \theta}\right\}=0 \\ \frac{1}{r}\frac{\partial \Delta}{\partial \theta}+(1-2\sigma)\left\{\nabla^2 u_\theta-\frac{u_\theta}{r^2}+\frac{2}{r^2}\frac{\partial u_r}{\partial \theta}\right\}=0 \\ \frac{\partial \Delta}{\partial z}+(1-2\sigma)\Delta^2 u_z=0 \end{aligned}\right\} \quad (1)$$

where the dilatation Δ is

$$\Delta=\frac{\partial u_r}{\partial r}+\frac{u_r}{r}+\frac{1}{r}\frac{\partial u\theta}{\partial \theta}+\frac{\partial u_z}{\partial z} \quad (2)$$

The stress components are derived from the displacement by the formulas

$$\left.\begin{aligned} \widehat{rr}=\frac{E}{1+\sigma}\left\{\frac{\sigma}{1-2\sigma}\Delta+\frac{\partial u_r}{\partial r}\right\} \text{--------} \widehat{rz}=\frac{E}{2(1+\sigma)}\left\{\frac{\partial u_z}{\partial r}+\frac{\partial u_r}{\partial z}\right\} \\ \widehat{zz}=\frac{E}{1+\sigma}\left\{\frac{\sigma}{1-2\sigma}\Delta+\frac{\partial u_z}{\partial z}\right\} \text{--------} \widehat{r\theta}=\frac{E}{2(1+\sigma)}\left\{\frac{\partial u_\theta}{\partial r}-\frac{u_\theta}{r}+\frac{1}{r}\frac{\partial u_r}{\partial \theta}\right\} \\ \widehat{\theta\theta}=\frac{E}{1+\sigma}\left\{\frac{\sigma}{1-2\sigma}\Delta+\frac{u_r}{r}+\frac{1}{r}\frac{\partial u_\theta}{\partial \theta}\right\} \text{--} \widehat{z\theta}=\frac{E}{2(1+\sigma)}\left\{\frac{\partial u_\theta}{\partial z}+\frac{1}{r}\frac{\partial u_z}{\partial \theta}\right\} \end{aligned}\right\} \quad (3)$$

In the case where $u_\theta=0$ while u_r and u_z are independent of θ, a displacement satisfying the equations of equilibrium may be derived from a stress function χ which satisfies

$$\nabla^4 x \equiv \nabla^2\nabla^2\chi=0 \text{ (where } \chi \text{ is independent of } \theta) \quad (4)$$

by the formulas

$$\left.\begin{aligned} \frac{E}{1+\sigma}u_r=-\frac{\partial^2 \chi}{\partial r \partial z} \\ \frac{E}{1+\sigma}u_z=2(1-\sigma)\ \nabla^2\chi-\frac{\partial^2 \chi}{\partial z^2} \end{aligned}\right\} \quad (5)$$

In this case the dilatation is given by

$$\frac{E}{1+\sigma}\cdot\frac{\sigma}{1-2\sigma}\Delta=\sigma\frac{\partial}{\partial z}\nabla^2\chi \quad (6)$$

and the stress components are

$$\left.\begin{aligned} \widehat{rr} &= \frac{\partial}{\partial z}\left[\sigma\nabla^2\chi - \frac{\partial^2\chi}{\partial r^2}\right] \text{---------} \widehat{rz} = \frac{\partial}{\partial r}\left[(1-\sigma)\nabla^2\chi - \frac{\partial^2\chi}{\partial z^2}\right] \\ \widehat{zz} &= \frac{\partial}{\partial z}\left[(2-\sigma)\nabla^2\chi - \frac{\partial^2\chi}{\partial z^2}\right] \text{-----} \widehat{r\theta} = 0 \\ \widehat{\theta\theta} &= \frac{\partial}{\partial z}\left[\sigma\nabla^2\chi - \frac{1}{r}\frac{\partial\chi}{\partial r}\right] \text{---------} \widehat{z\theta} = 0 \end{aligned}\right\} \quad (7)$$

The foregoing equations are appropriate in considering the stress and strain in the cylinder.

In considering the elastic equilibrium of a torus or single turn of circular wire which is wrapped tightly around an elastic circular cylinder whose unstressed radius is a, we have to find a displacement satisfying the equations of equilibrium and such that the stresses derived from it reduce to a normal pressure at the boundary of the wire. It is convenient to use in this case the coordinates ρ, β, and θ instead of the cylindrical coordinates r, z, and θ where ρ, β are plane polar coordinates of any section of the wire made by a plane through the z-axis. The single turn of wire when unstressed is the torus generated by rotating about the z-axis the circle whose equation in the r, z plane (or any plane θ-const) is $(r-a_0)^2+z^2=\rho_0^2$ where ρ_0 is the radius of the wire and a_0 is the initial r-coordinate of the center of its section and less than $a+\rho_0$. The origin for the plane polar coordinates is the point $r=a_0$, $z=0$, so that the equation of the wire section when unstressed is $\rho=\rho_0$. The angle β will be taken as zero at the point of the section nearest the z-axis and will range from $-\pi$ to π. (See fig. 1.) We may imagine the very long elastic circular cylinder of unstressed radius a which is greater than $a_0-\rho_0$, subjected to a uniform hydrostatic pressure on its convex surface, which is sufficient to compress its radius from a to $a_0-\rho_0$ so that it will just slip into the ring of wire. When this is done and the two ends of the cylinder are a great distance from the wire, the hydrostatic pressure may be imagined to be removed from the cylinder, which, by expansion, puts the wire under tension whose average value $\overline{T}=\frac{1}{\pi\rho_0^2}\int\int T\,d\,S$ taken over the wire section will be considered as known and this will ultimately determine a_0.

Any particle of the wire whose coordinates were ρ, β, θ, moves to a point whose coordinates are $\rho+u_\rho(\rho,\beta)$, $\beta+\frac{1}{\rho}u_\beta\ (\rho,\beta)$, $\theta+\frac{1}{r}u_\theta(\rho,\beta,\theta)$, where the plane polar coordinates ρ, β, are referred to the original center of the wire section as origin, which is the point $r=a_0$, $z=0$. The passage from the coordinates ρ, β, to the cylindrical coordinates r, z is made by

$$r=a_0-\rho\cos\beta \text{ and } z=\rho\sin\beta \quad (8)$$

and the displacement is transformed by the formulas

$$\left.\begin{aligned} u_\rho &= -u_r\cos\beta+u_z\sin\beta \\ u_\beta &= u_r\sin\beta+u_z\cos\beta \end{aligned}\right\} \text{or} \left\{\begin{aligned} u_r &= -u_\rho\cos\beta+u_\beta\sin\beta \\ u_z &= u_z\sin\beta+u_\beta\cos\beta \end{aligned}\right. \quad (9)$$

The boundary conditions to be satisfied are that at the surface of the wire where $\rho = \rho_0$, the stresses become

$$\widehat{\rho\rho} = -P(\beta) = -\tfrac{1}{2}P_0 - \sum_{n=1}^{\infty} P_n \cos n\beta \qquad (10)$$
$$\widehat{\rho\beta} = 0$$
$$\widehat{\rho\theta} = 0$$

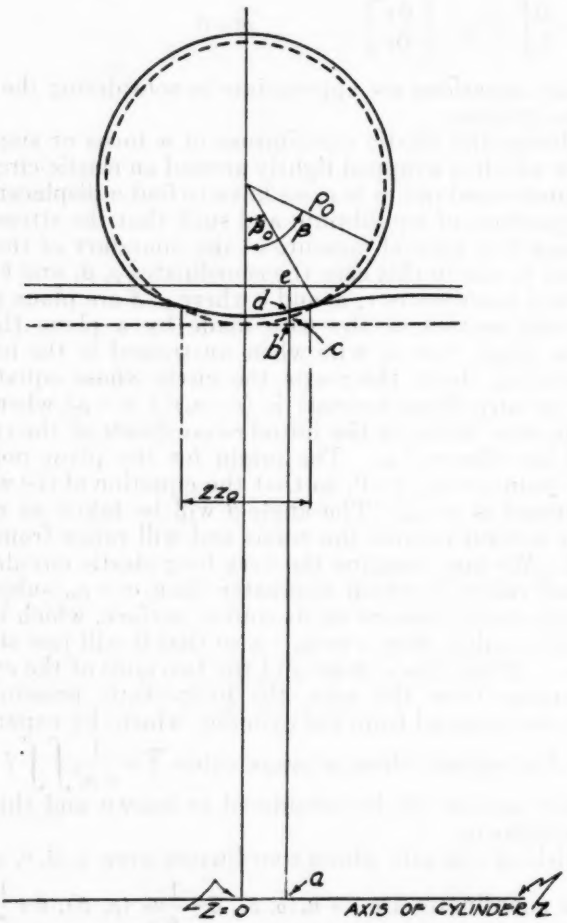

FIGURE 1.—*Section of one wire and cylinder by a plane through the cylindrical axis*

Heavy lines=section when stressed. Dotted circle=section of unstressed wire. Dotted straight line=section of cylinder when uniformly compressed. $\overline{ab} = a_0 - \rho_0$ = radius of cylinder when compressed to just slip in the ring of wire. $ae = a$ = radius of cylinder before compression. $\overline{ad} = r(z)$ = radius of the contact surface at point z.

where $P(\beta)$ is the unknown normal pressure exerted by the cylinder upon the wire. It is evidently an even function of and may be written

$$P(\beta) = \tfrac{1}{2}P_0 + \sum_{n=1}^{\infty} P_n \cos n\beta \text{------} -\pi \leqq \beta \leqq \pi \qquad (11)$$

where

$$P_n=\frac{1}{\pi}\int_{-\pi}^{\pi}P(\beta)\cos n\beta d\beta=\frac{1}{\pi}\int_{\beta_0}^{\beta_0}P(\beta)\cos n\beta d\beta \tag{12}$$

The last integral expresses the fact that the contact ring has the range $-\beta_0<\beta<\beta_0$, since outside this range of β there is nothing touching the surface of the wire. This angle β_0 is also unknown and must be determined by the solution of the problem of elastic equilibrium of the two bodies in contact. Since β_0 is obviously a small fraction of π, it is evident that the coefficients P_n will not differ appreciably for small values of n. These preliminaries are in no way altered if we have an infinite number of equally spaced wires wrapped around an infinitely long cylinder. The stress and strain in each wire will be a duplicate of that in the one we shall consider whose center remains in the plane $z=0$.

The stress components are derived from the displacement by the general formulas

$$\widehat{\rho\rho}=\frac{E}{1+\sigma}\left[\frac{\sigma\Delta}{1-2\sigma}+\frac{\partial u_\rho}{\partial\rho}\right]\text{----}\widehat{\rho\beta}=\frac{E}{2(1+\sigma)}\left[\rho\frac{\partial}{\partial\rho}\left(\frac{u_\beta}{\rho}\right)+\frac{\partial}{\partial\beta}\left(\frac{u_\rho}{\rho}\right)\right]$$

$$\beta\beta=\frac{E}{1+\sigma}\left[\frac{\sigma\Delta}{1-2\sigma}+\frac{1}{\rho}\left(u_\rho+\frac{\partial u_\beta}{\partial\beta}\right)\right]$$

$$\widehat{\rho\theta}=\frac{E}{2(1+\sigma)}\left[r\frac{\partial}{\partial\rho}\left(\frac{u_\theta}{r}\right)+\frac{\partial}{\partial\theta}\left(\frac{u_\rho}{r}\right)\right]\text{---}\theta\theta=\frac{E}{1+\sigma}\left[\frac{\sigma\Delta}{1-2\sigma}\right. \tag{13}$$

$$\left.+\frac{1}{r}\left(u_r+\frac{u_\theta}{\partial\theta}\right)\right]\text{---}\beta\theta=\frac{E}{2(1+\sigma)}\left[\frac{1}{r}\frac{\partial u_\beta}{\partial\theta}-\frac{u_\theta\sin\beta}{r}+\frac{1}{\rho}\frac{\partial u_\theta}{\partial\beta}\right]$$

where the dilatation is

$$\Delta=\frac{\partial u_\rho}{\partial\rho}+\frac{u\rho}{\rho}+\frac{1}{\rho}\frac{\partial u_\beta}{\partial\beta}+\frac{u_r}{r}+\frac{1}{r}\frac{\partial u_\theta}{\partial\theta} \tag{14}$$

According to equation (9), the formulas for transforming directional derivatives are

$$\left.\begin{aligned}\frac{\partial}{\partial\rho}&=-\cos\beta\frac{\partial}{\partial r}+\sin\beta\frac{\partial}{\partial z}\\ \frac{1}{\rho}\frac{\partial}{\partial\beta}&=\sin\beta\frac{\partial}{\partial r}+\cos\beta\frac{\partial}{\partial z}\end{aligned}\right\}\text{ or }\left\{\begin{aligned}\frac{\partial}{\partial r}&=-\cos\beta\frac{\partial}{\partial\rho}+\frac{\sin\beta}{\rho}\frac{\partial}{\partial\beta}\\ \frac{\partial}{\partial z}&=\sin\beta\frac{\partial}{\partial\rho}+\frac{\cos\beta}{\rho}\frac{\partial}{\partial\beta}\end{aligned}\right. \tag{15}$$

When $u_\theta=0$ and u_r and u_z are functions of r and z only (that is, of ρ and β), then the stress function χ is a function of ρ and β, and the ρ and β components of the displacement are found by use of (15) in the equations (5). These give

$$\begin{aligned}\frac{E}{1+\sigma}u_\rho&=2(1-\sigma)\sin\beta\nabla^2\chi-\frac{\partial}{\partial\rho}\left(\frac{\partial\chi}{\partial z}\right)\\ \frac{E}{1+\sigma}u_\beta&=2(1-\sigma)\cos\beta\nabla^2\chi-\frac{1}{\rho}\frac{\partial}{\partial\beta}\left(\frac{\partial\chi}{\partial z}\right)\end{aligned} \tag{16}$$

where $\frac{\partial \chi}{\partial z}$ is merely the abbreviation for $\sin \beta \frac{\partial \chi}{\partial \rho} + \frac{\cos \beta}{\rho} \frac{\partial \chi}{\partial \beta}$ as in (15). Similarly we find in this way from (13) the following formulas for the stress components

$$\begin{aligned}
\rho\theta &= \beta\theta \equiv 0 \\
\rho\rho &= \sigma \frac{\partial}{\partial z} \Delta^2 \chi + \frac{E}{1+\sigma} \frac{\partial u_\rho}{\partial \rho} \\
\rho\beta &= (1-\sigma)\left[\cos \beta \frac{\partial}{\partial \rho} + \frac{\sin \beta}{\rho} \frac{\partial}{\partial \beta}\right] \nabla^2 \chi - \frac{\partial}{\partial \rho}\left[\frac{1}{\rho} \frac{\partial}{\partial \beta} \cdot \frac{\partial \chi}{\partial z}\right] \\
\theta\theta &= \sigma \frac{\partial}{\partial z} \nabla^2 \chi + \frac{E}{1+\sigma} \frac{u_r}{r} \qquad (17) \\
\beta\beta &= \sigma \frac{\partial}{\partial z} \nabla^2 \chi + \frac{E}{1+\sigma} \cdot \frac{1}{\rho}\left(u_\rho + \frac{\partial u_\beta}{\partial \beta}\right)
\end{aligned}$$

We have in mind applications to the case where the ratio $\frac{\rho_0}{a}$ is small (0.002) and shall have to consider displacements which are the sum of terms of the three relative orders of magnitude $\frac{a^2}{\rho_0^2}$, $\frac{a}{\rho_0}$, and 1, although all three will be small due to a common factor E^{-1} which is of the order of 10^{-12}.

III. FORMAL SOLUTION FOR THE WIRE

In this section a formal solution will be constructed for points in a wire, which satisfy the elastic equations and boundary conditions, but which contain in their expression certain undetermined constants and the unknown pressure function and its range. In the next section the same is done for points in the cylinder, and in Section V the two solutions are brought together in the statement of contact, by which all the unknown constants and pressure distribution will be determined.

As a matter of convenience, a particular solution will be presented and then a more general type of solution which is derivable from a stress function χ. The particular solution is not a special case of the latter, but their sum gives a solution with a sufficient number of constants to satisfy the boundary conditions.

1. PARTICULAR SOLUTION FOR A SINGLE TURN OF WIRE

It is found that whatever the constants $A \ldots\ldots A_4$, the following displacement represents a particular solution of the equations of elastic equilibrium (1).

$$\begin{aligned}
\frac{E}{1+\sigma} u'_\theta &= Ar\theta \\
\frac{E}{1+\sigma} u'_r &= (A+A_1)\, r + \frac{a^2_0 A_2 + A_4 z^2}{r} \qquad (18) \\
\frac{E}{1+\sigma} u'_z &= 2\,(1-2\sigma)\,(A-A_4)\, z \log r + A_3 z
\end{aligned}$$

If we take

$$\epsilon \equiv \frac{\rho_0}{4a_0}$$

$$A_1 = \frac{1-5\sigma-2\sigma^2}{2\sigma\ (1+\sigma)}\,A$$

$$A_2 = -A_4 = \frac{1-2\sigma}{2\sigma}\,A \tag{19}$$

$$A_3 = \left[\frac{1-\sigma}{1+\sigma} + \frac{1-2\sigma}{\sigma}\log a_0\right]A$$

$$A = \frac{\sigma}{1-\sigma}\cdot\frac{C}{4\epsilon}$$

then expanding to the second order in ϵ we find the stresses $\widehat{\rho\theta}' \equiv 0$

$$\widehat{\rho\rho}' = -\epsilon C\frac{9-14\sigma}{4(1-\sigma)}\left(\frac{\rho}{\rho_0}\right)^2 - C\frac{\rho}{\rho_0}\cos\beta - \epsilon C\frac{1-2\sigma}{2(1-\sigma)}\left(\frac{\rho}{\rho_0}\right)^2\cos 2\beta - \epsilon C\frac{3(1-2\sigma)}{4(1-\sigma)}\left(\frac{\rho}{\rho_0}\right)^2\cos 4\beta \tag{20}$$

$$\widehat{\rho\beta}' = \epsilon C\frac{1-2\sigma}{2(1-\sigma)}\left(\frac{\rho}{\rho_0}\right)^2\sin 2\beta + \epsilon C\frac{3(1-2\sigma)}{4(1-\sigma)}\left(\frac{\rho}{\rho_0}\right)^2\sin 4\beta \tag{21}$$

$$\widehat{\theta\theta} = \frac{C}{4\epsilon} + \epsilon C\frac{2-5\sigma}{1-\sigma}\left(\frac{\rho}{\rho_0}\right)^2 + C\frac{1-3\sigma}{1-\sigma}\frac{\rho}{\rho_0}\cos\beta + \epsilon C\frac{4-9\sigma}{1-\sigma}\left(\frac{\rho}{\rho_0}\right)^2\cos 2\beta \tag{22}$$

The displacement is then given by

$$\left.\begin{aligned}
\frac{E}{1+\sigma}\frac{u_\theta'}{a_0} &= \theta\frac{\sigma}{1-\sigma}\left[\frac{C}{4\epsilon} - C\frac{\rho}{\rho_0}\cos\beta\right] \\
\frac{E}{1+\sigma}\frac{u_r'}{a_0} &= \frac{1-2\sigma-\sigma^2}{1-\sigma^2}\cdot\frac{C}{4\epsilon} + \frac{\sigma C}{1+\sigma}\frac{\rho}{\rho_0}\cos\beta + 2\epsilon C\frac{1-2\sigma}{1-\sigma}\left(\frac{\rho}{\rho_0}\right)^2\cos 2\beta \\
\frac{E}{1+\sigma}\frac{u_z'}{a_0} &= -\frac{\sigma C}{1+\sigma}\frac{\rho}{\rho_0}\sin\beta - 2\epsilon C\frac{1-2\sigma}{1-\sigma}\left(\frac{\rho}{\rho_0}\right)^2\sin 2\beta
\end{aligned}\right\} \tag{23}$$

The ρ and β components of u' are given by

$$\left.\begin{aligned}
\frac{E}{1+\sigma}\frac{u_\rho'}{a_0} &= -\frac{\sigma C}{1+\sigma}\cdot\frac{\rho}{\rho_0} - \left[\frac{1-2\sigma-\sigma^2}{1-\sigma^2}\cdot\frac{C}{4\epsilon} + 2\epsilon C\frac{1-2\sigma}{1-\sigma}\left(\frac{\rho}{\rho_0}\right)^2\right]\cos\beta \\
\frac{E}{1+\sigma}\frac{u_\beta}{a_0} &= \left[\frac{1-2\sigma-\sigma^2}{1-\sigma^2}\cdot\frac{C}{4\epsilon} - 2\epsilon C\frac{1-2\sigma}{1-\sigma}\left(\frac{\rho}{\rho_0}\right)^2\right]\sin\beta
\end{aligned}\right\} \tag{24}$$

The solution is being considered for the single turn of wire whose center remains in the plane $z=0$. The stress and strain in all other wires are repetitions of this.

2. THE STRESS FUNCTION χ FOR THE WIRE

Using ρ, β instead of the cylindrical coordinates r, z, it is readily found that a solution of the equation (4) to the first order inclusive in ϵ is

$$\chi=\rho_0^3\sum_{n=1}^{\infty}\left\{D_n\left(\frac{\rho}{\rho_0}\right)^n+B_n\left(\frac{\rho}{\rho_0}\right)^{n+2}+\epsilon B_{n\mathrm{H}}\left(\frac{\rho}{\rho_0}\right)^{n+4}\right\}\sin n\,\beta \quad (25)$$

To avoid duplicating certain terms included in the particular solution, we shall here take $D_1=D_2=0$. The constants D_n and B_n are assumed to be of the same order of magnitude as the pressure applied to the wire. The corresponding value of $\nabla^2\chi$ is to the first order.

$$\begin{aligned}\nabla^2\chi=4\rho_0\sum_{n=1}^{\infty}\Bigg\{&\left(\frac{\rho}{\rho_0}\right)^n[(n+1)(B_n-\epsilon D_{n+1})-\epsilon B_{n-1}]\\&+(n+2)\epsilon B_{n+1}\left(\frac{\rho}{\rho_0}\right)^{n+2}\Bigg\}\sin n\,\beta\end{aligned} \quad (26)$$

The displacement is then found by use of formulas (16)

$$\begin{aligned}\frac{\mathrm{E}}{1+\sigma}\cdot\frac{u_\rho}{\rho_0}=&-\epsilon\left\{6B_1\left(\frac{\rho}{\rho_0}\right)^2+4(1-\sigma)\left[D_1-2B_1\left(\frac{\rho}{\rho_0}\right)^2\right]\right\}\cos\beta\\&-\sum_{n=0}^{\infty}\cos n\,\beta\Bigg\{\left(\frac{\rho}{\rho_0}\right)^{n-1}[n(n+1)D_{n+1}+(3-4\sigma)nB_{n-1}\\&-4\epsilon(1-\sigma)\ (nD_n+B_{n-2})]+\left(\frac{\rho}{\rho_0}\right)^{n+1}(n+2)\ [(n-2\\&+4\sigma)B_{n+1}+2\epsilon\ ((1-2\sigma)B_n+2(1-\sigma)D_{n+2})]\\&+\left(\frac{\rho}{\rho_0}\right)^{n+3}(n+3)\ (n+4\sigma)\epsilon B_{n+2}\Bigg\}\end{aligned} \quad (27)$$

$$\begin{aligned}\frac{E}{1+\sigma}\frac{u_\beta}{\rho_0}=&\epsilon\left\{2B_1\left(\frac{\rho}{\rho_0}\right)^2+4(1-\sigma)\left[D_1-2B_1\left(\frac{\rho}{\rho_0}\right)^2\right]\right\}\sin\beta\\&+\sum_{n=1}^{\infty}\sin n\beta\Bigg\{\left(\frac{\rho}{\rho_0}\right)^{n-1}[n(n+1)D_{n+1}+(3-4\sigma)nB_{n-1}\\&-4(1-\sigma)\epsilon(nD_n+B_{n-2})]+\left(\frac{\rho}{\rho_0}\right)^{n+1}[(n+2)(n+4-4\sigma)B_{n+1}\\&+2\epsilon((1-2\sigma)_nB_n-2(1-\sigma)(n+2)\,D_{n+2})]+\left(\frac{\rho}{\rho_0}\right)^{n+3}\\&(n+3)(n+4-4\sigma)\epsilon B_{n+2}\Bigg\}\end{aligned} \quad (28)$$

(where it is understood that $D_n \equiv 0$ if $n<3$ and $B_n = 0$ if $n<1$). These expressions enable one by formulas (17) to compute the stresses. It is found that

$$\widehat{\rho\beta} = \left[6B_2\frac{\rho}{\rho_0} + 16(2-\sigma)\epsilon B_3\left(\frac{\rho}{\rho_0}\right)^3\right]\sin\beta + \sum_{n=2}^{\infty}\sin n\beta\Big\{(n-1)[n\ (n+1)$$
$$D_{n+1} + (3-4\sigma)nB_{n-1} - 4(1-\sigma)\,\epsilon\,(nD_n + B_{n-2})]\left(\frac{\rho}{\rho_0}\right)^{n-2} \qquad (29)$$
$$+ n(n+1)[(n+2)B_{n+1} + 2(1-2\sigma)\,\epsilon\,B_n]\left(\frac{\rho}{\rho_0}\right)^n + (n+3)$$
$$[(n+1)(n+2) + 2(1-2\sigma)]\,\epsilon\,B_{n+2}\left(\frac{\rho}{\rho_0}\right)^{n+2}\Big\}$$

and

$$\widehat{\rho\rho} = 4B_1 - 12\sigma\epsilon B_2\left(\frac{\rho}{\rho_0}\right)^2 + \Big\{[6B_2 - 24\epsilon D_3 - 8\epsilon B_1]\frac{\rho}{\rho_0}$$
$$- 16(1+\sigma)\epsilon B_3\left(\frac{\rho}{\rho_0}\right)^3\Big\}\cos\beta - \sum_{n=2}^{\infty}\cos n\beta\Big\{(n-1)[n(n+1)D_{n+1}$$
$$+ (3-4\sigma)nB_{n-1} - 4(1-\sigma)\epsilon(nD_n + B_{n-2})]\left(\frac{\rho}{\rho_0}\right)^{n-2} \qquad (30)$$
$$+ (n+1)[(n+2)(n+2)B_{n+1} + \epsilon(4(n+2)D_{n+2} + 2(2 + (1$$
$$- 2\sigma)n)B_n)]\left(\frac{\rho}{\rho_0}\right) + (n+3)[(n+1)(n+2)$$
$$- 2(1-2\sigma)]\epsilon B_{n+2}\left(\frac{\rho}{\rho_0}\right)^{n+2}\Big\}$$

(Also $\widehat{\rho\theta} \equiv 0$)

These give the stress components to the first order inclusive in ϵ.

The boundary conditions (10) may be satisfied by the sum of the particular solution of the preceding section and the solution here obtained. We, therefore, add to the $\widehat{\rho\beta}$ component given by (29) the component $\widehat{\rho\beta}'$ given by (21), and after placing $\rho = \rho_0$, equate the sum to zero. This gives

$$B_2 = -\frac{8}{3}(2-\sigma)\epsilon B_3 \qquad (31)^1$$

and for $n>2$ (remembering that $D_1 \equiv D_2 \equiv 0$)

$$D_n = -(3-4\sigma)\frac{B_{n-2}}{n} - \frac{n+1}{n-2}B_n + \epsilon\Big\{4(1-\sigma)\Big(\frac{D_{n-1}}{n} + \frac{B_{n-3}}{(n-1)n}\Big)$$
$$- \frac{2(1-2\sigma)}{n-2}B_{n-1} - \frac{(n+2)[n(n+1)+2(1-2\sigma)]B_{n+1}}{(n-2)(n-1)n} \qquad (31)^n$$
$$- \frac{1-2\sigma}{4(1-\sigma)}Ct_n\Big\}$$

where

$$t_n = \frac{1}{3} \text{ if } n=3$$

$$= \frac{1}{20} \text{ if } n=5$$

$$= 0 \text{ otherwise}$$

The remaining boundary condition is satisfied by adding to the expression (30) for $\rho\rho$ the corresponding expression (20) for $\rho\rho'$ and equating their sum when $\rho = \rho_0$ to $-P(\beta)$. Doing this and making use of the corresponding equations (31)^1 and (31)^n gives, on equating coefficients of cos $n\beta$,

$$4B_1 - 4\epsilon\left[3\sigma B_2 + \frac{9-14\sigma}{16(1-\sigma)}C\right] = -\frac{1}{2}P_0 \qquad (32)^0$$

$$-C - 8\epsilon\,[B_1 + 3D_3 + 6B_3] = -P_1 \qquad (32)_1$$

and for $n>2$

$$B_n = -\frac{1}{2}\frac{P_{n-1}}{n(n+1)} + 2\epsilon\left[D_{n+1} + \frac{B_{n-1}}{n+1} - \frac{(1-2\sigma)(n+2)B_{n+1}}{n(n+1)}\right] \qquad (32)^n$$

Since the two sets of equation (31) and (32) are valid to the first order in ϵ inclusive, we solve them by placing

$$\left.\begin{aligned} B_n &= B_n^0 + \epsilon B_n' \text{ for } n=1, 2, 3, \cdots \\ D_n &= D_n^0 + \epsilon D_n' \text{ for } n=3, 4, 5, \cdots \\ C &= C^0 + \epsilon C' + \epsilon^2 C'' \end{aligned}\right\} \qquad (33)$$

where B_n^0, B_n', etc., are assumed to be of the same order as the P_n. Each equation of the two sets then gives two relations, by equating finite parts and by equating first-order parts. The constant C'' will appear only in (32)^1 and can not be determined by these equations, since the left side of (32)^1 neglects second-order terms in ϵ so that the retention of $\epsilon^2 C''$ there would not be justifiable.

We find by equating finite terms in equation (31)^1, (32)^0, and (32)^n that

$$\left.\begin{aligned} B_1^0 &= -\frac{1}{8}P_0 \\ B_2^0 &= 0 \\ B_n^0 &= -\frac{1}{2}\frac{P_{n-1}}{n(n+1)} \text{ if } n>2 \end{aligned}\right\} \qquad (34)$$

The finite terms in (32)^1 give

$$C^0 = P_1 \qquad (35)$$

Using these values the finite parts of $(31)^n$ then give (since $D_1 \equiv D_2 \equiv 0$)

$$\left.\begin{aligned} D_3^0 &= \frac{3-4\sigma}{2}\frac{1}{1\cdot 2\cdot 3}\cdot\frac{P_0}{2}+\frac{1}{2}\left(\frac{P_2}{1\cdot 3}\right) \\ D_4^0 &= \qquad\qquad +\frac{1}{2}\left(\frac{P_3}{2\cdot 4}\right) \\ D_n^0 &= \frac{3-4\sigma}{2}\frac{P_{n-3}}{(n-2)(n-1)n}+\frac{1}{2}\frac{P_{n-1}}{(n-2)n} \text{ if } n>4 \end{aligned}\right\} \tag{36}$$

Using these values and next equating first order terms in $(32)^0$ and $(32)^1$ gives

$$\left.\begin{aligned} \epsilon C' &= -2\epsilon[(1-2\sigma)P_0+P_2] \\ \epsilon B_1' &= \frac{9-14\sigma}{16(1-\sigma)}\epsilon P_1 \end{aligned}\right\} \tag{37}$$

The remaining constants $\epsilon D'_n$ and $\epsilon B'_n$ may now be found by equating first-order terms in all the equations of the two sets, but their evaluation would be useless unless C were known with even greater precision than is represented by the retention of the terms $\epsilon^2 C''$. In fact, if this term $\epsilon^2 C''$ could not be found, the values of B_n^0 and D_n^0 here obtained would be useless for it, like them, contributes first-order terms to the displacement, but, unlike them, it contributes only second-order terms to the $\widehat{\rho\rho}-$ and $\widehat{\rho\beta}-$components of stress. We consider, however, that the average tension $\overline{T}$ in the wire is given. It is defined by

$$\overline{T}=\frac{1}{\pi\rho_0^2}\int_0^{\rho_0}\rho d\rho\int_{-\pi}^{\pi}\widehat{\theta\theta}\,d\beta \tag{38}$$

To compute $\overline{T}$ we note that the $\widehat{\theta\theta}$-component of stress, which is derivable from the stress function χ is

$$\sigma\frac{\partial}{\partial z}\nabla^2\chi+\frac{E}{1+\sigma}\frac{u_r}{r}$$

so that by the expressions (26), (27), and (28) we find that χ contributes to the tension the amount

$$\overline{T}_\chi=8\sigma B_1+12(1+\sigma)\epsilon B_2=-\sigma P_0+\frac{\sigma(18-28\sigma)}{4(1-\sigma)}\epsilon P_1 \tag{39}$$

Also from (22) the particular solution contributes

$$\overline{T'}=\frac{C}{4\epsilon}+\frac{\epsilon C(4-10\sigma)}{4(1-\sigma)}=\frac{P_1}{4\epsilon}-\frac{P_0+P_2}{2}+\sigma P_0+\frac{\epsilon}{4}\left[C''+\frac{4-10\sigma}{1-\sigma}P_1\right] \tag{40}$$

Hence we find

$$\begin{aligned}\overline{T}&=\frac{P_1}{4\epsilon}-\frac{P_0+P_2}{2}+\frac{\epsilon}{4}\left[C''+\frac{4(1+2\sigma-7\sigma^2)}{1-\sigma}P_1\right] \\ &=\frac{C}{4\epsilon}-\sigma P_0+\frac{1+2\sigma-7\sigma^2}{1-\sigma}\epsilon P_1\end{aligned} \tag{41}$$

Since $\overline{T}$ is absolutely given, this equation determines C'' in terms of $\overline{T}$, P_0, P_1, and P_2. This term C'' only enters the expression for the displacement in the factor $\frac{C}{4\epsilon}$ so it is more convenient to avoid the explicit use of $\epsilon^2 C''$ and use the formula

$$\frac{C}{4\epsilon}=\overline{T}+\sigma P_0-\frac{1+2\sigma-7\sigma^2}{1-\sigma}\epsilon P_1 \tag{42}$$

If we now use the values given above of B_n^0 and D_n^0, we find for that part of the displacement in the wire which is derivable from the stress-function χ; that is, the finite terms of (27) and (28).

$$u_\rho(\rho,\ \beta)=-\frac{\rho_0(1+\sigma)}{2E}\left\{(1-2\sigma)\frac{\rho}{\rho_0}P_0+\sum_{n=2}^{\infty}P_n\left[\frac{n}{n-1}\left(\frac{\rho}{\rho_0}\right)^{n-1}-\frac{n+1-3+4\sigma}{n+1}\left(\frac{\rho}{\rho_0}\right)^{n+1}\right]\cos n\beta\right\} \tag{43}$$

$$u_\beta(\rho,\ \beta)=\frac{\rho_0(1+\sigma)}{2E}\sum_{n=2}^{\infty}P_n\left[\frac{n}{n-1}\left(\frac{\rho}{\rho_0}\right)^{n-1}-\frac{n+1+3-4\sigma}{n+1}\left(\frac{\rho}{\rho_0}\right)^{n+1}\right]\sin n\beta \tag{44}$$

If we introduce the integral (12) for the Fourier coefficient P_n and sum the series, these expressions are transformed into integrals, and we find for that part of the displacement in the wire derivable from χ

$$u_\rho(\rho,\ \beta)=\frac{1+\sigma}{E}\left\{(1-\sigma)\rho P_0+\left[\frac{3-4\sigma}{4}\left(\frac{\rho}{\rho_0}\right)^2-2(1-\sigma)\log\rho_0\right]\rho_0 P_1\cos\beta\right.$$
$$-\frac{\rho}{\rho_0}\left(1-\frac{\rho^2}{\rho_2^0}\right)\frac{\rho_0^2}{2\pi}\int_{-\beta_0}^{\beta_0}P(\beta^1)\left(1-\frac{2\rho_0}{\rho}\sin\psi\right)\frac{\cos\psi}{R}\,d\beta' \tag{45}$$
$$-\frac{(1-2\sigma)}{\pi}\rho_0\int_{-\beta_0}^{\beta_0}P(\beta')\,\psi\sin(\beta-\beta')\,d\beta'$$
$$\left.+\frac{2(1-\sigma)\rho_0}{\pi}\int_{-\beta_0}^{\beta_0}P(\beta')\cos(\beta-\beta')\log R\,d\beta'\right\}$$

$$u_\beta(\rho,\beta)=\frac{1+\sigma}{E}\left\{\left[\frac{3-4\sigma}{4}\left(\frac{\rho}{\rho_0}\right)^2+2(1-\sigma)\log\rho_0\right]\rho_0 P_1\sin\beta\right.$$
$$-\frac{\rho}{\rho_0}\left(1-\frac{\rho^2}{\rho_0^2}\right)\frac{\rho_0^2}{2\pi}\int_{-\beta_0}^{\beta_0}P\beta'\left(1-2\frac{\rho}{\rho_0}\cos(\beta-\beta')\right)\frac{\sin\psi}{R}d\beta' \tag{46}$$
$$-\frac{(1-2\sigma)\rho_0}{\pi}\int_{-\beta_0}^{\beta_0}P(\beta')\psi\cos(\beta-\beta')d\beta'$$
$$\left.-\frac{2(1-\sigma)\rho_0}{\pi}\int_{-\beta_0}^{\beta_0}P(\beta')\sin(\beta-\beta')\log R d\beta'\right\}$$

where R is the distance from the point of integration ρ_0, β' upon the arc of the section of wire, to the point ρ, β within, and ψ is the angle between R and the interior normal, so that

$$R^2=\rho^2-2\rho\rho_0\cos(\beta-\beta')+\rho_0^2 \text{ and } \begin{cases} R\cos\psi=\rho_0-\rho\cos(\beta-\beta') \\ R\sin\psi=\rho\sin(\beta-\beta') \end{cases} \tag{47}$$

When the point ρ, β approaches as a limit any point ρ_0, β on the circular boundary of the wire section, then

$$R=2\rho_0\left|\sin\frac{\beta-\beta'}{2}\right|$$

$$\psi=-\frac{1}{2}(\beta-\beta')+\frac{\pi}{2} \text{ if } \beta-\beta'>0 \tag{48}$$

$$=-\frac{1}{2}(\beta-\beta')-\frac{\pi}{2} \text{ if } \beta-\beta'<0$$

Resolving the displacement in the direction of increasing r, we find from (43) and (44) the following expression for the u_r which is due to the stress function

$$u_r(\rho,\beta)\equiv-\frac{1+\sigma}{E}\left\{\frac{2(1-\rho)P_0}{\pi}\int_{-\beta_0}^{\beta_0}P(\beta')\cos\beta'\log R d\beta'\right.$$

$$+\frac{(1-2\sigma)p_0}{\pi}\int_{-\beta_0}^{\beta_0}P(\beta')\sin\beta'\,\psi d\beta' \tag{49}$$

$$+\frac{\rho}{\rho_0}\left(1-\frac{\rho^2}{\rho_0^2}\right)\frac{\rho_0^2}{2\pi}\int_{\beta_0-}^{\beta_0}\frac{P(\beta')}{R}\Big[\cos(\beta+\psi)+2\frac{\rho}{\rho_0}\sin\psi\,(\sin(\beta-\beta')\sin\beta$$

$$-\cos\beta\,\text{us}\,\psi)\Big]d\beta'-2(1-\sigma)\log\rho_0\cdot\rho_0P_1+(1-\sigma)\rho P_0\cos\beta+\frac{3-4\sigma}{4}\left(\frac{\rho}{\rho_0}\right)^2$$

$$\left.\rho_0P_1\cos\beta\right\}$$

When the point ρ, β, is on the contact ring, β^2 like β'^2 becomes negligible and (49) reduces to

$$u_r(\rho_0,\beta)=-\frac{1+\sigma}{E}\left\{\frac{2(1-\sigma)\rho_0}{\pi}\int_{-\beta_0}^{\beta_0}P_{(\beta')}\log R d\beta'+(1-\sigma)\rho_0P_0\right.$$

$$\left.+\left[\frac{3-4\sigma}{4}+2(1-\sigma)\log\rho_0\right]\rho_0P_1\right\} \tag{50}$$

Since this represents only the contribution of the function χ, we must add to it the corresponding component given by equation (23) for the particular solution. Using the value of C we have found, this is

$$u_r(\rho_0,\beta)=\frac{a_0}{E(1-\sigma)}\left\{(1-2\sigma-\sigma^2)(\overline{T}+\sigma P_0)+\sigma(1-\sigma)P_1\right\}$$

$$+\frac{\rho_0}{4E}\left\{-2\sigma\left[(1-2\sigma)P_0+P_2\right]\right. \tag{51}$$

$$\left.+\frac{2(1-\sigma^2)\,(1-2\sigma)-(1-2\sigma-\sigma^2)\,(1+2\sigma-7\sigma^2)}{(1-\sigma)^2}P_1\right\}$$

The total u_r component on the contact surface is the sum of (50) and (51).

Since ρ_0 is a very small angle, we may write $z_0=\rho_0\beta_0$ and $z=\rho_0\beta$ so that the definitions (12) for P_n may be written

$$P_n=\frac{1}{\pi}\int_{-\beta_0}^{\beta_0}P(\beta')\cos n\,\beta'\,d\beta'=\frac{1}{\pi\rho_0}\int_{-z_0}^{z_0}P(z')\cos\frac{nz'}{\rho_0}\,d\,z'$$

Since the width $2z_0$ of the contact strip is obviously very small compared with the radius ρ_0 of the wire, we may here write $\cos\frac{nz'}{\rho_0}=1-\frac{1}{2}\left(\frac{nz'}{\rho_0}\right)^2$ and for small values of n, such as $n=1$ or 2, this is equal to 1 to the first order, inclusive. That is, the approximations already made do not justify us in distinguishing between P_0, P_1, and P_2, and require that we place

$$P_0=P_1=P_2 \tag{52}$$

If we denote by λ_1, λ_2, and λ_3 the three positive elastic constants which depend only upon the dimensionless σ

$$\lambda_1\equiv\frac{1-2\sigma-\sigma^2}{(1+\sigma)\,(1-\sigma)^2},\quad\lambda_2\equiv\frac{\sigma\,(2-3\sigma-\sigma^2)}{(1+\sigma)\,(1-\sigma)^2}$$
$$\lambda_3\equiv\frac{6-7\sigma-21\sigma^2+35\sigma^3-5\sigma^4}{4\,(1+\sigma)\,(1-\sigma)^3} \tag{53}$$

we then find by addition of (50) and (51) for the r component of the total displacement of those particles of the wire which are on the contact surface, where $\rho=\rho_0$ and $-z_0<z=\rho_0\,\beta<z_0$

$$u_r=c\{a_0[\lambda_1\overline{T}+\lambda_2P_0]-\rho_0P_0[\lambda_3-2\log\rho_0]$$
$$-\frac{2}{\pi}\int_{-z_0}^{z_0}P(z')\log|z-z'|dz'\} \tag{54}$$

where

$$c\equiv\frac{1-\sigma^2}{E}$$

when

$$\sigma=\tfrac{1}{3},\ \lambda,=\tfrac{3}{8},\ \lambda_2=\tfrac{1}{2}\text{ and }\lambda_3=1\tfrac{5}{8} \tag{55}$$

so that these three positive constants are of ordinary magnitude. All of the terms in the second member of (54) are small, due to the factor c which is of the order of 10^{-12} absolute cgs. units. Since a_0 is very nearly $a-\rho_0$ it is evident that the terms in ρ_0P_0 and the integral are small compared to the first term, and the tension $\overline{T}$ contributes the greater part of this term.

It is important to recall what is our hypothesis as to the initial or unstressed shape of the wire in order to properly interpret the dis-

placement (54). The initial r coordinate of any point z on the surface of the wire which later comes into contact with the cylinder was

$$a_0-\rho_0+\rho_0(1-\cos\beta)=a_0-\rho_0+\frac{\rho_0\beta^2}{2}=a_0-\rho_0+\frac{z^2}{2\rho_0}$$

Therefore, when equilibrium is attained, its r coordinate is

$$r(z)=a_0-\rho_0+\frac{z^2}{2\rho_0}+u_r \tag{56}$$

Or using (54)

$$r(z)=a_0-\rho_0+\frac{z^2}{2\rho_0}+c\left\{a_0[\lambda_1\overline{T}+\lambda_2P_0]-\rho_0P_0[\lambda_3-2\log\rho_0]\right.$$
$$\left.-\frac{2}{\pi}\int_{-z_0}^{z_0}P(z')\log|z-z'|\,dz'\right\} \tag{57}$$

The small quantity $\left(\frac{z_0}{\rho_0}\right)^2$ like $\left(\frac{z}{\rho_0}\right)^2$ is by no means negligible here, but its neglect in those terms of (57) which contain the factor c was justified since c is of the order of 10^{-12}. The unknowns in the second member of (57) are a_0, P_0, z_0 and the pressure distribution $P(z)$. When the second member of this equation is known, it becomes the equation of the curve which is a section of the surface of contact, by a plane through the z axis. We may obtain another independent integral relation between $\overline{T}$, $r(z)$ and $P(z)$ by considering the equilibrium of a segment of the wire included between two planes through the z axis corresponding to $\theta=\theta_1$ and $\theta=-\theta_1$. At each circular section the total tension T acts on the part of the wire considered and the two amount to a force $2\,T\sin\theta_1=2\pi\,\rho_0^2\,\overline{T}\sin\theta_1$, directed toward the z axis. This force is counter balanced by the component in the opposite direction of the pressure exerted by the cylinder upon the segment of the wire which is

$$\int_{-\theta_1}^{\theta_1}\cos\theta d\theta\int_{-z_0}^{z_0}P(z)\;r\;(z)\;d\;z=2\;\sin\;\theta_1\int_{-z_0}^{z_0}P(z)\;r\;(z)\;d\;z$$

whence

$$2\;T\;\sin\;\theta_1=2\;\sin\;\theta_1\pi\rho_0^2\overline{T}=2\;\sin\;\theta_0\int_{-z_0}^{z_0}P\;(z)\;r\;(z)\;d\;z$$

so that

$$\frac{1}{\pi\rho_0^2}\int_{-z_0}^{z_0}r\;(z)\;P\;(z)\;d\;z=\overline{T} \tag{58}$$

This relation will be used after we know more about the form of the function $r(z)$.

IV. FORMAL SOLUTION FOR THE CYLINDER

In this section a formal solution of the elastic equations and boundary conditions will be constructed for points in the cylinder. Like that obtained above for the wire, its expression will involve the unknown pressure distribution and its range.

In this case the boundary conditions to be satisfied by the stresses at $r=a$ are

$$\widehat{rz}=0$$

$$\widehat{r\theta}=0$$

$$\widehat{rr}=-P(z)=-\left\{\frac{1}{2}f_0+\sum_{n=1}^{\infty}f_n\cos\frac{nz}{p}\right\} \text{ for } -\infty<z<+\infty \tag{59}$$

where

$$f_n=\frac{1}{\pi p}\int_{-\pi p}^{\pi p}P(z)\cos\frac{nz}{p}\,dz=\frac{1}{\pi p}\int_{-z_0}^{z_0}P(z)\cos\frac{nz}{p}\,dz \tag{60}$$

Since $2\pi p$ is the distance between centers of the endless set of wires, the pressure $P(z)$ must be a periodic function of z with period $2\pi p$. The Fourier's Series in (59) for $P(z)$ has a different range from the corresponding development (11) and hence the coefficients P_n and f_n are different. For the coefficients P_n defined by (12) may be written $\left(\text{letting } \beta=\frac{z}{\rho_0}\right)$

$$P_n=\frac{1}{n\rho_0}\int_{-z_0}^{z_0}P(z)\cos\frac{nz}{\rho_0}\,dz$$

which shows by comparison with (60) in the particular case, $n=0$, the relation

$$pf_0=\rho_0 P_0=\frac{1}{\pi}\int_{-z_0}^{z_0}P(z)dz \tag{61}$$

We shall be able to satisfy the boundary condition (59) by a displacement which at all points in the cylinder is derivable from a stress function x satisfying the equation (4). A stress function which is a particularly simple solution of (4)

$$\chi_0=\frac{f_0}{4(1+\sigma)}\left[(1-\sigma)r^2z-\frac{2}{3}(2-\sigma)z^3\right] \tag{62}$$

gives rise to the displacement by (7)

$$u_r^0=-\frac{1-\sigma}{2E}f_0r$$

$$u_\theta^0=0 \tag{63}$$

$$u_z^0=\frac{\sigma}{E}f_0z$$

with the stress components

$$\widehat{rr}=\widehat{\theta\theta}=-\frac{1}{2}f_0=\text{constant} \tag{64}$$

All other stress components are identically zero, and, in particular, the cylinder is not under longitudinal tension, $\widehat{zz}\equiv 0$. If J_0 and J_1 denote Bessel's function, we begin with a solution of equation (4) of the form

$$\chi=\chi_0+\sum_{n=1}^{\infty}\left\{A_nJ_0\left(\frac{inr}{p}\right)+B_n\frac{inr}{p}J_1\left(\frac{inr}{p}\right)\right\}\sin\frac{nz}{p} \tag{65}$$

which gives

$$\nabla^2\chi=-\frac{f_0z}{1+\sigma}-2\sum_{n=1}^{\infty}\frac{n^2}{p^2}B_nJ_0\left(\frac{inr}{p}\right)\sin\frac{nz}{p} \tag{66}$$

This gives by the formula (6) the dilatation

$$\frac{E}{1+\sigma}\cdot\frac{\sigma}{1-2\sigma}\Delta=\sigma\frac{\partial}{\partial z}\nabla^2x=-\sigma\left\{\frac{f_0}{1+\sigma}+2\sum_{n=1}^{\infty}\frac{n^3}{p^3}B_nJ_0\left(\frac{inr}{p}\right)\cos\frac{nz}{p}\right\} \tag{67}$$

Hence, the formulas (7) give the stress components

$$\widehat{r\theta}=0$$

$$\widehat{rz}=i\sum_{n=1}^{\infty}\frac{n^3}{p^3}\sin\frac{nz}{p}\left\{A_nJ_1\left(\frac{inr}{p}\right)-B_n\left[\frac{inr}{p}J_0\left(\frac{inr}{p}\right)+2(1-\sigma)J_1\left(\frac{inr}{p}\right)\right]\right\}$$

$$\widehat{rr}=-\frac{1}{2}f_0-\sum_{n=1}^{\infty}\frac{n^3}{p^3}\cos\frac{nz}{p}\left\{A_n\left[J_0\left(\frac{inr}{p}\right)-\frac{J_1\left(\frac{inr}{p}\right)}{inr/p}\right]\right. \tag{68}$$

$$\left.-B_n\left[(1-2\sigma)J_0\left(\frac{inr}{p}\right)-\frac{inr}{p}J_1\left(\frac{inr}{p}\right)\right]\right\}$$

If we let

$$\alpha=\frac{na}{p} \tag{69}$$

the vanishing of $\widehat{rz}$ at the boundary is assured by taking

$$A_n=\frac{i\alpha J_0(i\alpha)+2(1-\sigma)J_1(i\alpha)}{J_1(i\alpha)}B_n \tag{70}$$

Using this relation and satisfying the remaining boundary condition of (59) we find

$$\begin{aligned}A_n&=a\frac{p^2}{n^2(i\alpha)^2(J_0^2(i\alpha)+J_1^2(i\alpha))-2(1-\sigma)J_1^2(i\alpha)}\cdot f_n\\ B_n&=a\frac{p^2}{n^2(i\alpha)^2(J_0^2(i\alpha)+J_1^2(i\alpha))-2(1-\sigma)J_1^2(i\alpha)}f_n\end{aligned} \tag{71}$$

All the stress and strain components in the cylinder may now be found. In particular we find by (5) for the boundary value of u_r

$$u_r(a, z) = -ac'\left\{\frac{f_0}{2(1+\sigma')} + 2\sum_{n=1}^{\infty}\frac{f_n \cos\frac{nz}{p}}{(ia)^2\left[\left(\frac{J_0(ia)}{J_1(ia)}\right)^2+1\right]-2(1-\sigma')}\right\} \quad (72)$$

where

$$c' \equiv \frac{1-\sigma^2}{E'} \text{ and } \sigma',\ E' \quad (73)$$

are now used for σ, E to distinguish between the constants of the wire and the cylinder.

When $\frac{p}{a}$ is less than 5, reference to tables of Bessel's functions show that there will be an error of less than 1 part in 10,000 made by using the asymptotic expression for these functions, which enables us to write since $\alpha = \frac{na}{p}$

$$(ia)^2\left[\left(\frac{J_0(ia)}{J_1(ia)}\right)^2+1\right] = \frac{na}{p}+1 \quad (74)$$

neglecting terms of order of $\frac{p}{a}$ which is 0.001 when $2\pi p = 0.1$ and $a = 15$. Hence, we replace the exact expression (72) by

$$u_r(a, z) = -ac'\left\{\frac{f_0}{2(1+\sigma')} + \frac{2p}{a}\sum_{n=1}^{\infty}\frac{f_n \cos\frac{nz}{p}}{n-(1-2\sigma')\frac{p}{a}}\right\}$$

or since we neglect $\frac{p^2}{a^2}$ in comparison with 1

$$u_r(a, z) = -ac'\left\{\frac{f_0}{2(1+\sigma')} + \frac{2p}{a}\sum_{n=1}^{\infty}\frac{f_n \cos\frac{nz}{p}}{n}\right\} \quad (75)$$

If we now place

$$f_0 = \frac{\rho_0 P_0}{p} \text{ by (61) and } f_n = \frac{1}{\pi p}\int_{z_0} P(z') \cos\frac{nz'}{p}\, dz'$$

this becomes

$$u_r(a,z) = -c'\left\{\frac{a\rho_0 P_0}{2p(1+\sigma')} + \frac{1}{\pi}\int_{-z}^{z_0} P(z')dz' \sum_{n=1}^{\infty}\frac{2\cos\frac{nz}{p}\cos\frac{nz'}{p}}{n}\right\}$$

$$= -c'\left\{\frac{a\rho_0 P_0}{2p(1+\sigma')} + \frac{1}{\pi}\int_{-z_0}^{z_0} P(z')dz' \sum_{n=1}^{\infty}\frac{\cos\frac{n}{p}(z+z') + \cos\frac{n}{p}(z-z')}{n}\right\} \quad (76)$$

$$= -c'\left\{\frac{a\rho_0 P_0}{2p(1+\sigma')} + \frac{2}{\pi}\int_{-z_0}^{z_0} P(z')dz' \sum_{n=1}^{\infty}\left[\frac{1}{n}\cos\frac{n}{p}(z-z')\right.\right.$$

since $P(z')$ is an even function of z'. Now if $-x-$ denotes the absolute value of x

$$\sum_{n=1}^{\infty} \frac{1}{n} \cos \frac{n}{p}(z-z') = -\log \left| 2 \sin \frac{z-z'}{2p} \right|$$

Hence (76) becomes

$$u_r(a,z) = -c' \left\{ \left[\frac{a}{2p(1+\sigma')} + 2 \log p \right] \rho_0 P_0 - \frac{2}{\pi} \int_{-z_0}^{z_0} P(z') \log \left| 2p \sin \frac{z-z'}{2p} \right| dz' \right\} \quad (77)$$

The negative of the second member gives the shrinkage in radius of the cylinder at any point z. The constant term represents a uniform shrinkage of radius, the variable part is a periodic function of z which is small compared to the constant term.

When the point (a, z) is inside the contact ring both $\frac{z}{p}$ and $\frac{z'}{p}$ are of order of magnitude of $\frac{z_0}{p}$ and their squares are negligible so that (77) becomes for $-z_0 < z < z_0$

$$u_r(a, z) = -c' \left\{ \left[\frac{a}{2p(1+\sigma')} + 2 \log p \right] \rho_0 P_0 - \frac{2}{\pi} \int_{-z_0}^{z_0} P(z') \log \left| z-z' \right| dz' \right\} \quad (78)$$

Since the particle z to which this refers, had the coordinate $r = a$ when the cylinder was unstressed, the distance of this particle from the z axis when equilibrium is attained is $r(z) = a + u_r(a, z)$. Using (77) this gives for the deformed shape to the cylinder the equation

$$r(z) = a - c' \left\{ \left[\frac{a}{2p(1+\sigma')} + 2 \log p \right] \rho_0 P_0 - \frac{2}{\pi} \int_{-z_0}^{z_0} P(z') \log \left| 2\, p \sin \frac{z-z'}{2p} \right| dz' \right\} \quad (79)$$

which holds for all values of z and is a periodic function of z with period $2\pi p$ which is the distance between centers of the endless series of wires, all alike and uniformly spaced, which are wrapped tightly around the cylinder, whose unstressed radius was a. The z coordinates of the wire centers are $z = 0 \pm 2\pi pk$ where k is an integer.

When the point z on the surface of the cylinder is on the contact area, of say that wire whose center is at $z = 0$ the deformation of the cylinder is then given by

$$r(z) = a - c' \left\{ \left[\frac{a}{2p(1+\sigma')} + 2 \log p \right] \rho_0 P_0 - \frac{2}{\pi} \int_{-z_0}^{z_0} P(z') \log \left| z-z' \right| dz' \right\} \quad (80)$$

V. DETERMINATION OF THE PRESSURE DISTRIBUTION AND THE CONTACT RANGE

The Sections III and IV have been concerned with the construction of formal solutions giving the stress and strain in the wires and cylinder which satisfy the boundary conditions, but which contain in their expression the unknown pressure distribution $P(z)$, the range of contact $2z_0$, the constant P_0, and the constant a_0, the latter being the distance of the center of a circular turn of wire from the z axis before the (compressed) cylinder was inserted. In this section we take over these results, and since the ideas here involved are different we number the equations anew in order to concentrate upon the present argument.

The equation of the contact surface, or dent in the cylinder, Section IV, equation (80), we rewrite as

$$r(z)=a-c'\left[\frac{a}{2p\,(1+\sigma')}+2\log p\right]\rho_0P_0+\frac{2c'}{\pi}\int_{-z_0}^{z_0}P(z')\log|z-z'|\,dz' \quad (1)$$

The equation of the dent in the wire, Section III, equation (57) is

$$r(z)=a_0-\rho_0+\frac{z^2}{2\rho_0}+c\left[a_0\,(\lambda_1\overline{T}+\lambda_2P_0)-(\lambda_3-2\log\rho_0)\,\rho_0P_0\right]$$
$$-\frac{2c}{\pi}\int_{-z_0}^{z_0}P(z')\log|z-z'|\,dz' \quad (2)$$

where by Section IV, equation (61)

$$\rho_0P_0=\frac{1}{\pi}\int_{-z_0}^{z_0}P(z')\,dz' \quad (3)$$

and by Section III, equation (58)

$$T=\pi\rho_0{}^2\overline{T}=\int_{-z_0}^{z_0}r(z)\,P(z)\,dz \quad (4)$$

The fact of contact is implied by $r(z)$ being the same in equations (1) and (2). Eliminating it gives the integral equation to determine the pressure distribution $P(z)$ and its contact range $2z_0$

$$-2\int_{-z_0}^{z_0}\frac{2\,(c+c')\,\rho_0}{z_0}P(z')\log|z-z'|\,dz'=A-\pi\frac{z^2}{z_0} \quad (5)$$

where the constant A (independent of z) is

$$A=\frac{2\pi\rho_0}{z_0}\left\{a+\rho_0-a_0\,(1+\lambda_1c\overline{T})-\left[c\left(\frac{a_0\lambda_2}{\rho_0}-\lambda_3+2\log\rho_0\right)\right.\right.$$
$$\left.\left.+c'\left(\frac{a}{2p\,(1+\sigma')}+2\log p\right)\right]\rho_0P_0\right\} \quad (6)$$

To solve (5) we recall that the logarithmic potential at any point z on a thin cylindrical strip of width $2z_0$ upon which there is a surface density of electricity of amount $\sqrt{1-\left(\frac{z}{z_0}\right)^2}$ is

$$-2\int_{-z_0}^{z_0}\sqrt{1-\left(\frac{z'}{z_0}\right)^2}\log|z-z'|\,dz'=\pi z_0\left(\frac{1}{2}+\log\frac{2}{z_0}\right)-\frac{\pi z^2}{z_0} \qquad (7)$$

Comparing this with (5) shows that the solution of that equation is obtained by imposing the two conditions

$$P(z)=\frac{\sqrt{z_0^2-z^2}}{2(c+c')\rho_0} \text{ for } -z_0<z<z_0 \qquad (8)$$

and

$$A=\pi z_0\left(\frac{1}{2}+\log\frac{2}{z_0}\right) \qquad (9)$$

If A were known (9) would determine z_0 and (8) then give $P(z)$. However, A is a function of the unknown z_0, a_0, and P_0 as shown by (6) so that (6) and (9), together by elimination of A give one relation between these three unknown constants from which a_0 may be later found. The equations (1) and (2) will thus be rendered compatible by (6), (8), and (9). The next equation (3) becomes by the use of (8)

$$\rho_0 P_0=\frac{1}{2\pi\rho_0(c+c')}\int_{-z_0}^{z_0}\sqrt{z_0^2-z^2}\,dz=\frac{z_0^2}{4\rho_0(c+c')}$$

which may be written

$$\frac{z_0}{\rho_0}=\sqrt{4(c+c')P_0} \qquad (10)$$

To satisfy the remaining condition (4) we first replace the integral in (1) by its value from (5). This gives by use of (10)

$$r(z)=a(1-bc'P_0)+\frac{c'z^2}{2(c+c')\rho_0}=a\left\{1-c'P_0\left[b-\frac{2\rho_0}{a}\left(\frac{z}{z_0}\right)^2\right]\right\} \qquad (11)$$

where

$$b=\frac{\rho_0}{2p(1+\sigma')}+\frac{\rho_0}{a}\left(1+\log\frac{\rho^2}{(c+c')\rho_0^2P_0}\right) \qquad (12)$$

The equation (4), therefore, becomes

$$\pi\rho_0^2\bar{T}=\frac{1}{2(c+c')\rho_0}\int_{-z_0}^{z_0}\left[a(1-bc'P_0)+\frac{c'}{2(c+c')\rho_0}z^2\right]\sqrt{z_0^2-z^2}\,dz$$

which gives

$$\rho_0\bar{T}=a(1-bc'P_0)\frac{(z_0/\rho_0)^2}{4(c+c')}+\frac{c'\rho_0}{2}\left[\frac{(z_0/\rho_0)^2}{4(c+c')}\right]^2 \qquad (13)$$

Expressing z_0 in terms of P_0 by (10), this equation gives the following to determine the one unknown $\left(\frac{a P_0}{\rho_0 \overline{T}}\right)$

$$\frac{aP_0}{\rho_0 \overline{T}} = 1 + \frac{\rho_0 c' \overline{T}}{a}\left(b - \frac{\rho_0}{2a}\right)\left(\frac{aP_0}{\rho_0 \overline{T}}\right)^2 \tag{14}$$

According to the assumptions underlying this derivation $\frac{\rho_0}{a}$ is of the order of magnitude of, say, 10^{-3}, while c and c' are about 10^{-12}, while the average tension of the wire, $\overline{T}$, is say $(10)^9$ dyne cm^{-2} (corresponding to a total tension of 7 pounds). Consequently the term $\frac{\rho_0 c' \overline{T}}{a}$ is 10^{-6}, which shows (since b is of the order of magnitude of unity) that $\frac{aP_0}{\rho_0 \overline{T}} = 1$ (to 1 part in 1,000,000). We have, therefore, the final value of P_0.

$$P_0 = \frac{\rho_0 \overline{T}}{a} \tag{15}$$

whence the final value of the width $2\ z_0$ of the contact ring becomes

$$2z_0 = 4\rho_0 \sqrt{(c + c')\frac{\rho_0 \overline{T}}{a}} \tag{16}$$

The equation of the contact ring becomes

$$r(z) = a - \rho_0 c' \overline{T}\left[b - 2\frac{\rho_0}{a}\left(\frac{z}{z_0}\right)^2\right] \tag{17}$$

where the b is to be computed by the formula

$$b = \frac{\rho_0}{2p(1+\sigma')} + \frac{\rho_0}{a}\left[1 + \log \frac{a\rho^2}{\rho_0^3 (c + c')\overline{T}}\right] \tag{18}$$

The pressure distribution is given by equation (8). The remaining constant a_0 (the initial distance of wire center from z axis) is found by eliminating A between (6) and (9) to be [neglecting 1 part in 1,000,000; that is, $(c\overline{T})^2$ compared to 1]

$$a_0 = a + \rho_0 - a\lambda_1 c\overline{T} - \rho_0[bc'\overline{T} + (\lambda_1 + \lambda_2)c\overline{T}] \tag{19}$$

The shape of the cylinder at points outside a contact ring such as for $z_0 < z < 2\pi p - z_0$ may now be found by using the values of P_0 and $P(z)$ from (15) and (8) in the equation (79) of Section IV. This leads to

$$r(z) = a - \rho_0 c' \overline{T}\left\{\frac{\rho_0}{2p(1+\sigma')} + \frac{2\rho_0}{a}\left[\log p - \frac{2}{\pi z_0}\int_{-z_0}^{z_0} \sqrt{1 - \left(\frac{z'}{z_0}\right)^2} \log\left(2\rho \sin \frac{z - z'}{2\rho}\right)\right]\right\} \tag{20}$$

Now

$$\int_{-z_0}^{z_0}\sqrt{1-\left(\frac{z'}{z_0}\right)^2}\log\left(2p\sin\frac{z-z'}{2p}\right)=\frac{\pi z_0}{2}\log 2p$$
$$+\int_{-z_0}^{z_0}\sqrt{1-\left(\frac{z'}{z_0}\right)^2}\log\left(\sin\frac{z}{2p}\cos\frac{z'}{2p}-\cos\frac{z}{2p}\sin\frac{z'}{2p}\right)dz'$$

When the point z is near the halfway point between the two wires, $\sin\frac{z}{2p}$ is near unity and $\cos\frac{z}{2p}$ is small, while $\cos\frac{z'}{2p}$ is near unity and $\sin\frac{z'}{2p}$ is small. Hence (as before), by neglecting second-order terms of the order of $\left(\frac{z_0}{p}\right)^2$ we find

$$\int_{-z_0}^{z_0}\sqrt{1-\left(\frac{z'}{z_0}\right)^2}\log\sin\frac{z-z'}{2p}\,dz'=\frac{\pi z_0}{2}\log\sin\frac{z}{2p}$$

which is a good approximation if z is not very close to a contact surface. Hence, the shape of the cylinder at points not very close to a contact ring is found by equation (20) to be very approximately

$$r\ (z)=a-\rho_0 c'\ \overline{T}\left[\frac{\rho_0}{2\ p\ (1+\sigma')}-\frac{2\rho_0}{a}\log\ 2\ \sin\frac{z}{2p}\right] \tag{21}$$

This shows that at a point midway between two wires, where, say, $z=\pi p$

$$r(\pi p)=a-\rho_0 c'\ \overline{T}\left[\frac{\rho_0}{2\ p\ (1+\sigma')}-\frac{\rho_0}{a}\log 4\right] \tag{22}$$

This is the thickest part of the cylinder. Its thinnest part is at $z=0$, where $r=r(0)$. The difference between its greatest and least radius is found by (17) and (22) to be

$$r\ (\pi p)-r\ (o)=\rho_0 c'\overline{T}\,\frac{\rho_0}{a}\left[1+\log\frac{4\ ap^2}{{\rho_0}^3(c+c')\overline{T}}\right] \tag{23}$$

This is seen to be small compared to the compression at the mid-point which by (22) may be written

$$a-r(\pi p)=\rho_0 c'\overline{T}\left[\frac{\rho_0}{2\ p\ (1+\sigma')}-\frac{\rho_0}{a}\log 4\right. \tag{24}$$

Hence, the cylinder is almost uniformly compressed with relatively shallow depressions where the wires touch it.

To find the deformations of the wires, we must use the values here found $P_0=P_1=\frac{\rho\overline{T}}{a}$ in the equation (42) of Section III, which gives

$$\frac{C}{4\epsilon}=\overline{T}\left\{1+\frac{\rho_0}{a}\left[\sigma-\frac{\rho_0}{4a}\left(\frac{1+2\sigma-7\sigma^2}{1-\sigma}\right)\right]\right\} \tag{25}$$

If we neglect terms of the order of 1 part in 1,000,000 and consider $\frac{\rho_0}{a}$ and cT, as each of the order of 10^{-3}, then this becomes

$$\frac{C}{4\epsilon} = \overline{T}\left\{1 + \frac{\rho_0\sigma}{a}\right\} \tag{25'}$$

The components of the displacement in the wire corresponding to the stress function χ are, therefore, of the order of 10^{-12} and may be neglected, but the particular solution of Section III gives by equation (24)

$$u_\rho(\rho_0, \beta) = -\frac{\sigma a_0 \overline{T} \rho_0}{E\, a} - a_0 c \overline{T} \lambda_1 \left(1 + \frac{\rho_0\sigma}{a}\right) \cos \beta \tag{26}$$

$$u_\beta\ (\rho_0, \beta) = a_0 c \overline{T} \lambda_1 \left(1 + \frac{\rho_0\sigma}{a}\right) \sin \beta \tag{27}$$

The cylindrical components of this displacement of points initially on a circular section of the wire are

$$u_r\ (\rho_0, \beta) = a_0 c \overline{T} \lambda_1 \left(1 + \frac{\rho_0\sigma}{a}\right) + \frac{\sigma a_0 \overline{T} \rho_0}{E\, a} \cos \beta \tag{28}$$

$$u_z\ (\rho_0, \beta) = \frac{\sigma a_0 \overline{T} \rho_0}{E\, a} \sin \beta \tag{29}$$

In these four equations a_0 may be replaced in terms of given constants by means of (19).

The two equations (26) and (27) show that the points on the circular section of the wire suffer a uniform contraction of radius, together with a translation in the r direction, both of which leave its section circular. The amount of the contraction of radius of the wire is given by

$$\rho_0 - \rho = \frac{\sigma \overline{T} a_0 \rho_0}{E\, a} = \frac{\sigma \overline{T} \rho_0}{E} \tag{30}$$

The translation is much larger, being

$$u_r\left(\rho_0, \frac{\pi}{2}\right) = a_0 c \overline{T} \lambda_1 \left(1 + \frac{\rho_0\sigma}{a}\right) \tag{31}$$

The result reached in equation (30) is of interest in absolute measurements in which the inductance of a single-layer solenoid is computed from measurements of the diameter of the solenoid (over the windings), its length and the pitch of the windings, and from the radius ρ_0 of the wire measured before it was wound. The formula for the inductance requires a knowledge of the radius a' of a current sheet which passes through the centers of the wires. If D is the measured over-all diameter, this radius is $a' = \frac{D}{2} - \rho = \frac{D}{2} - \rho_0 + \sigma \frac{\overline{T}}{E} \rho_0$. For the solenoid $\frac{D}{2} = 14.5$ cm approximately; $\rho_0 = 0.03545$ cm; $\sigma = \frac{1}{3}$;

$E=1.2(10)^{12}$ and $\overline{T}=8(10)^8$ dyne cm^{-2}, since the wire was wound with a tension of 7 pounds. Hence, $\sigma\frac{\overline{T}}{E}\rho_0=8(10)^{-6}$ cm, so that the correction due to contraction of the wire alters the radius of the current sheet by 1 part in 2,000,000.

VI. SUMMARY

It has been found that in the case of a long circular cylinder of radius a, uniformly wound with equal, and equally spaced, wires of radius ρ_0, each with tension T, that the pressure distribution under any wire (such as the one whose center is in the plane $z=0$, the z axis being the axis of the cylinder) is

$$P(z)=\frac{\sqrt{z_0^2-z^2}}{2(c+c')\rho_0} \text{ for } -z_0<z<z_0$$

where the width of the contact ring $2z_0$ is given by

$$2z_0=4\rho_0\sqrt{(c+c')\rho_0\frac{\overline{T}}{a}}$$

where $\overline{T}=T/\pi\rho_0^2=$ average tension in the wire, and

$$c=\frac{1-\sigma^2}{E},\quad c'=\frac{1-\sigma'^2}{E'}$$

σ and E being Poisson's ratio and Young's modulus, respectively, for the wire material, while σ', E' refer to the material of the cylinder. If the constant b is defined by equation (18) of Section V, the shape of the dent in the cylinder in which a wire makes contact is

$$r(z)=a-\rho_0c'\overline{T}\left[b-\frac{2\rho_0}{a}\left(\frac{z}{z_0}\right)^2\right] \text{ for } -z_0<z<z_0$$

where $r(z)$ denotes the distance from the z axis to the surface of the cylinder. At points on the surface of the cylinder outside a contact ring, and distant from the edges of one by a quantity which is not small of the order of z_0, the shape of the cylinder is given by the periodic function of z

$$r(z)=a-\rho_0c'\overline{T}\left[\frac{\rho_0}{2p(1+\sigma')}-\frac{2\rho_0}{a}\log\left(2\sin\frac{z}{2p}\right)\right]$$

where $2\pi p$ is the distance between centers of adjacent turns of wire. The cylinder is almost uniformly compressed, with a relatively small bulge between the wires. The circular section of the wire undergoes a practically uniform contraction of radius, $\rho_0-\rho=\frac{\sigma\overline{T}}{E}\rho_0$, together with a translation in the r direction (away from the axis of the cylinder) of amount $a_0c\,\overline{T}\lambda_1\left(1+\frac{\rho_0\sigma}{a}\right)$ where $\lambda_1=\frac{1-2\sigma-\sigma^2}{(1+\sigma)\,(1-\sigma)^2}$ and where a_0 is the distance of the center of the wire section from the axis of the cylinder when the turn of wire is unstressed. It is given by equation (19) of Section V.

It is believed that this evaluation of the pressure distribution is new. It differs from that of H. Hertz[4] in two respects. In Hertz's problem the area of contact was the infinitesimal neighborhood of a point so that its boundary was found to be an infinitesimal ellipse, and the integral equation determining the pressure distribution a Newtonian potential of that distribution. In the present problem this area has one large dimension, since it is a ring of small width $2z_0$ upon the face of the cylinder and the integral equation determining the pressure distribution is its logarithmic potential, a difference which seems natural.

The other point of difference is that Hertz considered the pressure to be so local in its effect that the stress and strain produced by it were confined to its immediate neighborhood so that he considered the two bodies as separated by an infinite plane. This magnification of the region so simplified his problem that the pressure and the pressure ellipse could be evaluated without reference to the actual shapes of the two bodies. However, as all points in this infinite plane were in reality points very close to the contact ellipse, his results (stress and strain) were only applicable to points in the immediate neighborhood of the contact. The problem here solved is considerably more general for we first formulated the elastic displacement at all points in a wire in terms of an integral over the pressure area, involving the unknown pressure distribution, which satisfied the condition of no stress at all other parts of the boundary of the wire. Only when the point was on the contact area did this integral reduce to a (logarithmic) potential integral. Similarly the elastic displacement at any point in the cylinder was formulated in terms of an integral involving the pressures of all the wires, which displacement satisfied the condition of no stress at points on the cylindrical surface between contact areas. When the point on the cylinder approached a point on a contact surface, a potential integral again appeared. By expressing the fact of contact between wires and cylinder, an integral equation resulted which determined the pressure distribution and its range. This being found, we have determined the deformation and stress not only in the immediate neighborhood of the contact area, but at all points in wires and cylinder. It must be pointed out, however, that the results here obtained are by no means exact solutions of the elastic equations. They are approximations limited by the fact that the ratio $\frac{\rho_0}{a}$ of the radii of wire and cylinder are small, and three relative orders of small quantities $\frac{a}{\rho_0}$, 1, $\frac{\rho_0}{a}$ are retained. The problem has also been limited to the case where the pitch of the windings $2\pi p$, (that is, distance between wires) is of the same order as the radius of a wire, but the removal of this restriction is obviously very easy, as it would not involve any modification of the solution for points in a wire, but only for points in the cylinder, and for this part of the problem we obtained an exact solution.

WASHINGTON, March, 1930.

[4] H. Hertz, J. f. Math. (Crelle), Bd. 92; 1881.

THE RESTORATION OF SOLARIZED ULTRA-VIOLET [1] TRANSMITTING GLASSES BY HEAT TREATMENT

By A. Q. Tool and R. Stair

ABSTRACT

In this paper data are given which show the relation between the ultra-violet transmissions of two commercial glasses (vita and helio glass) before and after solarization by ultra-violet radiations at ordinary temperatures and also after various heat treatments in the range 200° to 600° C.

It is shown that the highest ultra-violet transmission found for these glasses was obtained after heat treatments at temperatures in the annealing range; that is, somewhat above 500° C. Treatments at higher temperatures caused deformations and some surface deterioration while those at lower temperatures were less effective in rejuvenating the glass, although treatments at temperatures as low as 300° C. often approximately restored the transmissivity to its initial value on receipt of the glass.

Visible colorations, which on artificial solarization accompany the decrease in transmission of the shorter visible rays, apparently disappeared completely upon relatively short heat treatments at temperatures no higher than 200° or 300° C. The visible thermoluminescence accompanying this disappearance of the coloration and apparently persisting only during the time required for the restoration of the transmission near the visible spectrum was found to grow more intense and to continue for correspondingly shorter intervals as the temperature of heat treatment was raised.

Even after the visible coloration and thermoluminescence had disappeared as a result of heating at these low temperatures, the complete restoration of the transmission for the shortest wave lengths transmitted by these glasses required additional heat treatments near 500° C.

CONTENTS

		Page
I.	Introduction	357
II.	Glasses tested	361
	1. Samples used for transmission tests	361
	2. Approximate annealing and softening ranges	361
III.	Experimental procedure	363
	1. Sequence of tests and treatments	363
	2. Transmission measurements	363
	3. Solarization treatments	364
	4. Heat treatments	365
IV.	Results	366
	1. Transmission	366
	2. Thermoluminescence	372
V.	Conclusions	374

I. INTRODUCTION

During the last 10 years considerable activity in the production of glasses which to some extent replace fused and crystalline quartz for the transmission of ultra-violet radiations has been evident. This

[1] A report on the preliminary results of this investigation was read at the meeting of the American Ceramic Society held at Atlantic City in February, 1928.

activity has been encouraged chiefly by the demand for relatively large quantities of window glasses in hospital solariums, greenhouses, etc., where the need of glasses transmitting the "biologically active" ultra-violet rays [2] whose frequencies are just above those transmitted by ordinary window glass has long been felt.[3]

Prior to 1910 various glasses [4] transmitting ultra-violet radiation of the relatively short wave lengths absorbed by ordinary glass were produced and were for certain laboratory purposes available for replacing both fused and crystalline quartz which are still quite generally used in most laboratory experiments involving ultra-violet radiation. Generally these substitute glasses were expensive and unsuited for quantity production. Moreover, if they were not actually unstable, they usually lacked the resistance to weathering, etc.,[5] required of window glasses. Since that time, and especially since 1920, numerous glasses have been developed and tested [6] which transmit a fair percentage of ultra-violet radiation in the range between 280 and 320 mμ (the approximate limits of the range containing the more effective rays from a therapeutic standpoint).[7] Moreover, some of these glasses can be produced in quantity at relatively reasonable prices.

Although most of these new glasses when first installed seemed suitable for their intended purpose and were, in general, as resistant to weathering as could be expected, it was soon found that in many cases their transmissivity for the required ultra-violet radiation decreased rapidly on exposure to the sun's rays [8] and even more rapidly when the source of light was relatively rich in ultra-violet. This decrease in transmissivity is usually accompanied by a coloration or darkening which extends throughout the whole sheet although it may be more apparent near the surface on which the light is first incident.

---

[2] The ultra-violet radiation found in sunlight, but not transmitted by ordinary window glass, is often referred to in this way. Such radiations are in many cases also termed "health rays." These and similar terms are rather indefinite and should, perhaps, be avoided, since radiations of any wave length affects living organisms in some manner and to some degree and may under certain conditions at least contribute to health, while any given wave length may at times be injurious. Moreover, the wave length or combination of wave lengths producing the maximum effect often varies considerably with the type of physiological reaction, or other effects, coming under consideration. However, the term "biologically active ultra-violet rays," although quite loose and indefinite, has been so convenient as a general designation for those invisible rays which are in and immediately below the short wave sunlight spectrum and which are mainly responsible for sunburn, etc., that it has been very generally employed.

[3] Considering that it was known or suspected well before the beginning of the present century (see S. English, Glass, **5**, p. 338; 1928) that ultra-violet radiation had a special significance in the medical, chemical, bactericidal, and other fields, it seems strange that the serious attempts to make sheet glasses that were transparent to this light were not made earlier. However, it does appear from certain remarks by E. Zschimmer (Zeitschrift f. Instrumentenkunde, **23**, p. 360; 1903; and Physikalische Zeitschrift, **8**, p. 611; 1907) that plans were being laid for developing such glasses at the approximate dates of these articles; furthermore, a statement by E. Berger (see G. Jaeckel, Glastechnische Berichte, **6**, 292–293; 1928) asserts that glass transmitting ultra-violet rays was both produced in considerable quantities and used in windows prior to 1914. (See also, E. Berger, Sprechsaal, **61**, p. 564; 1928.)

[4] Eder u. Valenta, Denkschrift d. Wien. Akad. Wiss. (Math.-Nat. Kl.), **61**, p. 285; 1894. E. Zschimmer, Zeitschrift f. Instrumentenkunde, **23**, p. 360, 1903; Physikalische Zeitschrift, **8**, p. 611; 1907. G. Fritsche, Physikalische Zeitschrift, **8**, p. 518; 1907.

[5] G. Rose, Sprechsaal, **62**, p. 315; 1929. E. Zschimmer. (See footnote 4.)

[6] Coblentz and Stair, Trans. Illum. Eng. Soc., **23**, p. 1121; 1928. A. Salmony, Chemiker Zeitung, **52**, p. 269; 1928. A. Rüttenauer, Sprechsaal, **61**, pp. 453–467; 1928. S. English, Glass, **5**, pp. 338–388–501; 1928. G. Jaeckel, Glastechnische Berichte, **6**, p. 281; 1928. G. Rose, Sprechsaal, **62**, p. 314; 1929.

[7] Hess, Pappenheimer, and Weinstock, Proc. Soc., Exp. Biol. and Med., **20**, p. 14; 1922. C. Dorno, Strahlentherapie, **14**, p. 25; 1922–23. E. A. Park, Physiol. Rev., **3**, p. 106; 1923. Steenbock and Nelson, J. Biol. Chem., **56**, p. 355; 1923; **62**, p. 209; 1924. Steenbock and Black, J. Biol. Chem., **61**, p. 405; 1924. R. Pohl, Die Naturwissenshaften, **15**, p. 433; 1927. Morton, Heilbron, and Kamm, J. Chem. Soc., Pt. II, p. 2000; 1927. Hausser u. Vahle, Strahlentherapie, **13**, p. 41; 1921–22. A. Salmony, Chemiker Zeitung, **52**, p. 955; 1928. K. W. Hausser, Strahlentherapie, **28**, p. 25; 1928. C. Sonne, Strahlentherapie, **28**, p. 45; 1928. Reiter u. Gabor, Strahlentherapie, **28**, p. 125; 1928. P. Keller, Strahlentherapie, **28**, p. 152; 1928. A. Ruttenauer. (See footnote 6.) G. Jaeckel. (See footnote 6.)

[8] Coblentz and Stair, B. S. Letter Circular No. 235, 2d rev.; Sept. 29, 1927; Trans. Illum. Eng. Soc., **23**, p. 1129; 1928; B. S. Tech. News Bull. No. 126; 1927; and No. 130; 1928. S. English, Glass, **5**, pp. 389–501; 1928. A. Rüttenauer, Sprechsaal, **61**, p. 467; 1928. G. Rose, Sprechsaal, **62**, p. 376; 1929.

Colorations [9] resulting from exposure to solar or artificial ultra-violet and to Röntgen or radium radiations had previously been observed in many glasses and other materials; and such colorations have been ascribed to various causes. Coloration produced in ordinary glass when exposed to the sun's rays has in some cases been associated with a content of manganese, selenium, etc.[10] In the ultra-violet transmitting glasses, however, the opinion of many investigators seems to be that the observed coloration on exposure to ultra-violet radiation is ordinarily due to a reoxidation of ferrous to ferric iron.[11] Investigations on the effect of these oxides on the transmission of glass and the fact that melting glasses in a reducing atmosphere or keeping the iron content to a minimum increases the ultra-violet transmissivity supports this opinion.[12]

It is possible, however, that other factors besides a change in the oxidation of the iron, and also that other elements besides iron may be operative in this reduction of ultra-violet transparency.

As an example of the variety of views which may be suggested by experience with similar effects in other materials, attention is drawn to one which has been advanced and which ascribes the reduction of the ultra-violet transmission to a gradual separation of finely divided sodium in the glass. Although this separation effect has been observed in some sodium compounds when they are subjected to certain radiations, its particular significance appears, however, to be very questionable [13] in the case of this aging effect in glass.

In this connection it may also be noted that samples of fully transparent crystalline quartz from certain sources appear to suffer, as a result of exposure either to ultra-violet or to cathode rays,[14] no coloration, and presumably, therefore, little, if any, diminution in their power of transmission for ultra-violet rays; while, on the other hand, fused quartz supposedly from crystals of the same kind has been found to show (at least in certain cases) both coloration and diminished transmission to some degree [15] after such exposures. It is also reported that the purple coloration of the latter material by cathode rays is formed in spots.[16] Such results would seem to indicate that the colorations are due to some impurity which is introduced or changed during the melting of the quartz and that this impurity, which may or may not be iron, is also the cause for the "solarization" occasionally observed in the resulting glass. They suggest, moreover, the possibility that the condition causing these spots is also involved in the formation of the thin filmy colorations sometimes observed in certain pieces of fused quartz which have

[9] W. Crookes, Phil. Trans. (II), p. 170; 1879. P. and M. Curie, Comp. Rend., **129**, p. 823; 1899. C. Doelter, Das Radium und die Farben (Steinkopf, Dresden); 1910. St. Meyer, Phys. Zeitschrift, **10**, p. 483; 1909. S. C. Lind, J. Phys. Chem., **24**, p. 437; 1920. Parmelee, Clark, and Badger, J. Soc. Glass Tech., **13**, p. 279; 1929.

[10] S. Avery, J. Am. Chem. Soc., **27**, p. 909; 1905. F. Fisher, Ber. d. Deut. Chem. Ges., **38**, p. 946; 1905. Meyer and Frzibram, Sitz. Ber. Akad. Wien (IIa), **121**, p. 1414; 1912. A. Dauvillier, Comp. Rend., **181**, p. 601; 1925. F. Eckert, Zeit. Tech. Physik., **7**, p. 300; 1926. Coblentz and Stair, B. S. Jour. Research, **3** (RP113), p. 629; 1929.

[11] Starkie and Turner, J. Soc. Glass Tech., **12**, p. 306; 1928.

[12] Corning Glass Works, Brit. Patent 263410; July 1, 1926. Starkie and Turner, J. Soc. Glass Tech., **12**, p. 27; 1928. A. Rüttenauer. (See footnote 8, p. 358.) G. Rose, Sprechsaal, **62**, p. 354; 1928.

[13] G. Rose, Sprechsaal, **62**, p. 375; 1929.

[14] Coolidge and Moore, J. Frank. Inst., **202**, p. 724; 1926.

[15] See footnote 14. Coblentz and Stair. (See footnote 10.)

[16] See footnote 14.

been heated [17] for some time at temperatures in the neighborhood of 1,000° C. Although there may be no definite relation between these two types of colorations the apparent similarity of the patterns formed certainly supports this view, since these patterns both seem to outline the shapes of the original crystal fragments. According to Coolidge and Moore, however, the cathode ray colorations disappear on strong heating; consequently the reactions causing the two effects must be different even if the basic conditions responsible for both are the same.

It is characteristic of the colorations caused in glass by various radiations that they will usually change, decrease, or completely disappear under the influence of heat; [18] and, in some cases, they change merely through exposure to radiation of a different character or frequency.[19] Generally this disappearance induced by heating is associated with a more or less brilliant thermoluminescence.[20] It has been reported by various investigators that both the brilliancy of this thermoluminescence and the rate of disappearance of the coloration increase rapidly as the temperature of the restoring heat treatment is increased.[21] In the case of ultra-violet transmitting glasses which have been solarized by exposure to radiation of the sun or quartz mercury lamps the transmissivity for the ultra-violet is, as might be expected from the disappearance of visible coloration, more or less restored by heat treatment [22] and the rate of this restoration also increases with temperature.

The results in the preliminary report of this investigation, which was undertaken early in 1927 for the purpose of gaining some notion of the relationship between solarization, coloration, thermoluminescence and the restoration of transmissivity by heat treatment for some of the glasses transmitting ultra-violet radiation, have already been reported.[23] The conclusions at the time of making the report were that the decoloration could be practically completed and visible thermoluminescence exhausted by heat treatments at temperatures near 300° C., but that a complete restoration of the transmissivity to the possible maximum required treatments at temperatures much nearer 500° C., which was in the annealing range [24] of the glasses tested.

In a sense this corresponds with the pervious experience of Lind [25] and others who found that the "discharge" of the brown color produced

---

[17] Tilton and Tool. B. S. Jour. Research, **3**, p. 616; 1929.
It has been suggested to the authors of the paper cited here that the markings caused by heat treatment may arise from some change in films of carbon and silica compounds which are formed (possibly) by the action of the carbon vapor atmosphere which is undoubtedly present during melting and which supposedly permeates all of the evacuated spaces between the individual fragments of the quartz charge. Presumably, reheating the resultant glass to temperatures near 1,000° C. might cause these films to darken so that they become visible, if finely divided silicon or carbon is deposited in the glass through some reducing action during prolonged heating at these temperatures. Furthermore, such films and impurities may ultimately induce devitrification causing the original pieces in the charge to be outlined by the light colored films sometimes observed after heating certain samples of the glass for a few hours at somewhat higher temperatures.

[18] Meyer and Przibram. (See footnote 10, p. 359.) S. C. Lind, J. Phys. Chem., **24**, p. 440; 1920. J. R Clarke, Phil. Mag., **45**, p. 735; 1923. F. Eckert, Zt. Tech. Physik, **7**, p. 300; 1926.

[19] F. Fisher. (See footnote 10, p. 359.) Meyer and Przibram, p. 415. (See footnote 10, p. 359.) P. L. Baley, Phys. Rev. (2), **24**, p. 495; 1924. Coblentz and Stair (B. S. Tech. News Bull., No. 160, p. 80; and No. 162, p. 97; 1930) report that in some cases at least the transmission of a solarized glass is increased when the glass is exposed to ultra-violet radiation of a longer wave length than that causing solarization.

[20] See reference under footnotes 18 and 21.

[21] Nyswander and Lind, J. Opt. Soc. Am., **13**, p. 660; 1926.

[22] Coblentz and Stair. (See footnote 10, p. 359.) H. P. Hood. (See footnote 24.)

[23] Tool and Stair, unpublished Progress Report read at the Annual Meeting Am. Ceram. Soc., Atlantic City, Feb. 5 to 11, 1928.

[24] This conclusion agrees with results obtained by Reinhardt and Schreiner, J. Phys. Chem., **32** (2), p. 1886; 1928. See also H. P. Hood (Corning Glass Works) Brit. Patent No. 298908, Oct. 15, 1927.

[25] S. C. Lind (See footnote 18.)

in a glass by radium radiation was accomplished by gentle heating and was accompanied by thermoluminescence, but that the discharge of the violet color caused by the same radiation did not take place until a tempreature of 500° C. was reached, which was near the softening point of the glass. Moreover, after the thermoluminescence was exhausted at 200° C. it did not appear again at higher temperatures between 200° and 500° C. On the other hand, in the year 1928 Shrum, Patten, and Smith [26] reported that the thermoluminescence could be not only exhausted at temperatures near 300° C., but further that the effect of solarization also disappears completely at the same time.

The transmission results given in the above-mentioned preliminary report are shown in Figure 5 (circles), and indicate the degree of restoration then attained by heat treating at different temperatures certain solarized samples of one of the ultra-violet transmitting window glasses (vita glass) on the market at that time. Since the conclusions reached in this report were based mainly on the results obtained by the use of only two wave lengths, namely 280 mμ and 313 mμ, and since it was apparent that results at other wave lengths might have additional interest, it was decided to repeat the work on a more elaborate scale using five wave lengths as follows: 280 mμ, 313 mμ, 334 mμ, 365 mμ, and 405 mμ. The method employed and the results obtained are discussed in the following paragraphs:

II. GLASSES TESTED

1. SAMPLES USED FOR TRANSMISSION TESTS

Two window glasses bearing the trade names vita and helio glass were used in this investigation. Strips were cut from panes of these glasses and divided into a number of samples from which 10 for each glass were chosen. The samples selected were those which apparently had the best surfaces and the fewest imperfections (such as striæ) although some effort was made at the same time to obtain for each glass a set of samples which would be representative of the whole length of a single strip. The dimensions were about 2 by 3 cm, while the thickness varied considerably. This variation was not so marked over any single sample but for the vita glass the thickest and thinnest samples measured 3.13 and 2.87 mm, respectively, and for the helio glass 2.39 and 2.05 mm.

2. APPROXIMATE ANNEALING AND SOFTENING RANGES

In order to gain some indication of the annealing and softening ranges of these glasses heating curves [27] were obtained. These curves are shown in Figure 1, and a description of the individual curves is given in the accompanying legend. Based on general experience with other glasses it appeared from these curves that the annealing ranges for ordinary purposes were in both cases near and somewhat above 500° C. and that considerable deformation might be expected if the glasses were heated for any extended time at 600° C.

[26] Shrum, Patten, and Smith, Trans. Roy. Soc. Canada, (3) **22**, p. 433; 1928.
[27] Tool and Valasek, B. S. Sci. Papers, **15**, p. 537; 1920. Tool and Eichlin, J. Opt. Soc. Am., **4**, p. 340; 1920.

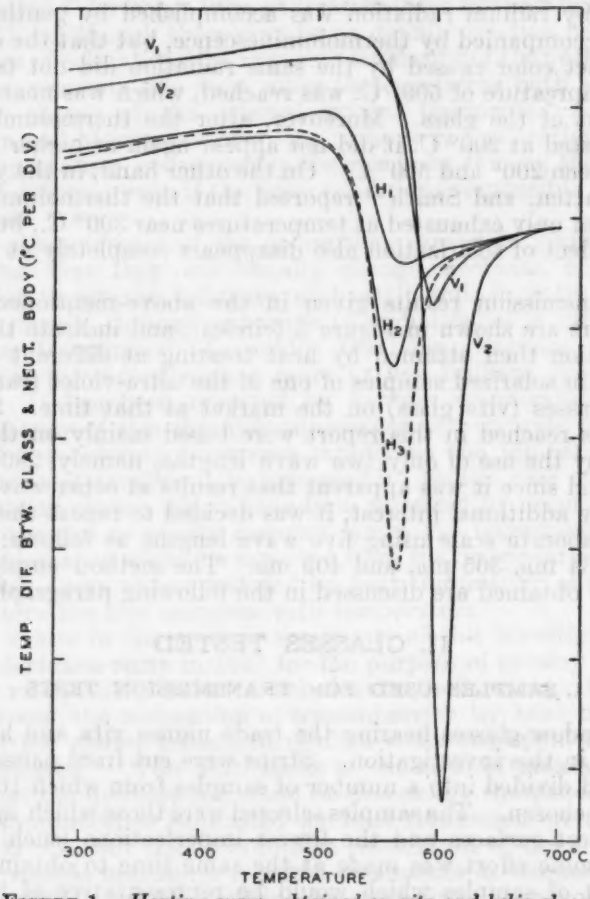

FIGURE 1.—*Heating curves obtained on vita and helio glasses*

Tests on the glasses in their original condition resulted in heating curves V_1 and H_1 for the vita and helio glass, respectively. The relatively pronounced drop of V_1, as compared to that of H_1, to a minimum below the final level of the curves indicates that the original vita glass was annealed to a somewhat greater degree than the original helio glass. This indication was supported to some extent by the character of the resistance of the panes to the glass cutter; that is, the helio glass pane appeared to have a thin surface layer which was still under a relatively high compression.

Curves V_2 and H_2 were obtained on samples of these glasses after they had been heat treated together. In this treatment the samples were heated to 530° C. and cooled according to a schedule which would approximate a steadily decreasing rate requiring 12 days to reach 490° C., the point at which they were removed from the furnace to cool rapidly to room temperature. This treatment increased the degree of annealing over that of the original in the case of both glasses, but was far more efficient for the vita than for the helio glass. These conclusions are reached in view of the increases in the heat absorption effects and the relatively large effect shown by curve V_2. This difference between the heat absorption effects of curves V_2 and H_2 is in part, at least, accounted for when it is noted that the heat absorption range, and consequently the annealing range, of the helio glass is not less than 30° below that of the vita glass.

To show more clearly that the discrepancy in the indicated degrees of annealing of the two glasses was probably due to the fact that 490° C. is not a comparable point in the annealing range of these glasses and to show also that it may be reduced by continuing the treatment of the helio glass to a lower temperature, this glass was reheated to 490° C. and cooled slowly to 470° C. before again taking it from the furnace. Curve H_3 was obtained after this treatment and the increase in the heat absorption effect indicates that the degree of annealing was increased. (See article entitled "Variations Caused in Heating Curves of Glass by Heat Treatment," by Tool and Eichlin, B. S. Jour. Research, **6**, p. 523; 1931.) It also shows that if the two glasses were annealed to a comparable degree; that is, if they were brought to equilibrium at temperatures which were about equally distant from the temperatures determined by the minima of their respective heating curves, the heat absorption effects as measured by the magnitude of the drop below the final level of the curves would probably not be greatly different for the two glasses.

(Legend continued on p. 363.)

III. EXPERIMENTAL PROCEDURE

1. SEQUENCE OF TESTS AND TREATMENTS

After the samples had been chosen the transmission of each was measured for the five wave lengths previously mentioned. All samples were then artificially solarized and the transmissions again determined. Following this the power to transmit ultra-violet radiation was more or less restored by heat treatments.

For these heat treatments five samples of each glass were put in lot A and the rest in lot B. The samples of each lot were always treated together. Those in lot A were first treated at 200° C., and then, as indicated in Tables 3 and 4, they were retreated successively at the higher temperatures until 575° C. was reached. Those in lot B were first treated at 575° C. and were later given treatments successively at the lower temperatures indicated. Finally all samples were treated at 600° C. This treatment was given last because it was known that some deformation and possibly some injury to the surfaces would result.

After each of these heat treatments at any temperature the transmissions were determined, and the samples were then solarized again before the next heat treatment. As a check on the uniformity of the degree of solarization caused by the ultra-violet treatments the transmissions of at least two samples from each glass in a lot were determined for 313 mμ after each solarization.

2. TRANSMISSION MEASUREMENTS

The transmission of the glass samples at the five wave lengths chosen were obtained radiometrically by using a quartz mercury lamp, a quartz spectrometer, and a vacuum [28] thermopile. An ironclad [29] galvanometer used in conjunction with the thermopile was adjusted to a sensitivity sufficient to obtain deflections of several centimeters for the weakest mercury emission lines used. A fluorescent screen (a coating of anthracene) on each side of the entrance slit of the thermopile furnished a visual method of calibration for the spectrometer.

Measurements at a given wave-length setting consisted in observing the galvanometer deflections with and without the sample inserted in the beam of light at the entrance slit of the spectrometer. Several readings were made for each wave length and each sample. The ratio of the readings (sample in to sample out) at any setting gave the transmission of the glass at that wave length.

[28] Coblentz, B. S. Sci. Paper No. 413, **17**, p. 187; 1921.
[29] Coblentz, B. S. Sci. Paper No. 282, **13**, p. 423; 1916.

FIGURE 1—Continued

It will be noted that the difference between the initial and final levels of these curves is in every case much greater for the vita than for the helio glass. The discrepancy between these differences indicates merely that, during the passage of the glasses through their heat absorption ranges, the change in the thermal properties of the vita glass is such that the temperature gradient from the containing walls into the sample must be increased on reaching points above the absorption range by a relatively large amount as compared to that required in the case of helio glass if the heating rate chosen as standard is to be maintained.

Although the heat absorption range, and presumably the annealing range also, of the helio glass is below that of the vita glass, it was found that on heating the former to temperatures above 650° C. it showed slightly less sintering between the particles used in the heating curve test than the latter glass under the same conditions. This indicates that the rate of softening is lower for the helio than for the vita glass and explains why the former withstood the rejuvenating treatment at 600° C. as well as the latter, although the relative thinness of the helio glass samples seemed to make deformation more probable.

In all cases the glasses were thoroughly washed with soap and water, carefully rinsed in clear water, and dried both before making transmission measurements and before placing them in the lamp box for solarization treatments.

3. SOLARIZATION TREATMENTS

Upon exposure to the radiation from a quartz mercury arc lamp all glasses that have been examined decrease in ultra-violet transmission, some decreasing more than others. Certain samples of fused quartz have also been found to decrease slightly in transmission in the shorter wave lengths (265 mμ and below).

For vita and helio glass, however, the greatest change in transmission from such an artificial solarization treatment occurs, as might be expected, in the range of wave lengths below 405 mμ since it is near this point that the region of high absorption of radiation by these glasses first becomes noticeable. In consequence, the transmission experiments of this investigation have been confined entirely to this region of rapidly increasing absorption with decreasing wave lengths and of greatest change in transmission from solarization.

The time of exposure used for these glasses was chosen after a study of the solarization results obtained by exposing samples for different periods of time. From such results it was found that, when the samples were exposed (at a distance of 15 cm) to a 110-volt quartz mercury arc lamp operated with 70 volts across the burner, most of the change occurred in the first 3 or 4 hours and that after 5 hours any further change was very slow. This indicated that the practically flat portion of the time-solarization curves had been reached; hence a period of five hours was chosen for all the exposures in these tests. In the beginning some tests were made to determine the effect of turning the samples over once during this time in order to expose both sides directly; and while this increased the effectiveness of the treatments somewhat the difference did not appear to be enough to warrant a continuance of the practice.

On each exposure throughout these experiments, therefore, the samples were placed upon a board 15 cm beneath the lamp and, excepting the few cases noted, the marked sides were always toward this source. The distance of 15 cm was sufficient to prevent any heating which might unduly counteract [30] the desired effect of this

[30] One of the first preliminary tests concerned this possibility. A sample while being held at temperatures somewhat above 400° C. suffered no solarization when exposed to the radiation concentrated on it from a small quartz mercury lamp by a quartz lens. In reality its transmissivity increased somewhat if there was any effect.

As a matter of fact the data available at present on these glasses indicate that the rates of restoration by heating and of solarization by ultra-violet radiation decrease, respectively, as the maximum restoration and solarization obtainable are approached and that both decrease with the temperature, the former decreasing more rapidly. At relatively high temperatures, it appears that the rate of rejuvenation from heating alone may be much greater than the rate of solarization caused by a given source while the glass is held at these temperatures. Consequently, the kinetic equilibrium established by a solarization treatment at any such temperatures (by simultaneous solarization and rejuvenation treatments) should result in an ultra-violet transmission relatively near the maximum obtainable by the heating alone; that is, the solarization of a sample previously rejuvenated in the absence of radiation will be small or negligible on being subjected to a solarization treatment at temperatures near 500° C. With a sample previously solarized at a lower temperature, however, a considerable increase in its transmission may be noted as the result of such a simultaneous treatment.

At somewhat lower temperatures the counteracting effect of the heating being relatively lower causes the resulting equilibrium conditions from a simultaneous solarization to yield lower transmissions; but even so the effect of temperature has considerable significance in the case of glass bulbs used in ultra-violet lamps since such bulbs are usually heated to no small degree and so continue to possess a satisfactory transparency to ultra-violet radiation.

At temperatures nearer that of the atmosphere, however, the rate of restoration by heat is apparently much less than that of the solarization received from a reasonably effective ultra-violet source by a sample which is in an intermediate condition as a result of previous treatments; consequently a solarization at

aging treatment; furthermore, since the samples were small, this distance was large enough so that their relative positions with respect to the lamp differed very little. These conditions, together with the fact that the time of exposure corresponded to a relatively flat portion of the time-solarization curve, aided in erasing and in preventing the building up of any possible differences of undue magnitude between the degrees of solarization of the different individual samples of either of the glasses.

These solarization treatments, as previously stated, always followed the transmission tests and preceded the heat treatments. The above-mentioned check transmission measurements on a few samples after each solarization treatment showed that within reasonable limits these various radiation treatments always reduced the transmissions for a given wave length to practically the same minimum value.

4. HEAT TREATMENTS

The glasses were heat treated in an electric furnace which could be maintained at a relatively constant temperature for several days. During these treatments the samples were packed quite closely together, although the surfaces were never in contact with each other or with other materials except near the edges where the platinum or aluminum foil spacers rested. To protect the surfaces from dust, the carefully cleaned and dried samples were inclosed in a small aluminum box.

Before the treatment began the furnace was raised to, and stabilized at, the desired temperature. After introducing the samples the temperature seldom fluctuated by as much as $\pm 5°$ C. and the average was always very close to the desired treating temperature. The possible errors in the temperature determinations by the platinum, platinum-rhodium thermocouple employed was considered to be of about the same order as the fluctuations. It is to be noted, however, that these errors in the indicated temperatures would in most cases be of the same sign; consequently the intervals between the average temperatures of the successive treatments are probably accurate to within 5° C.

The heat treatments of the two lots, A and B, were begun at opposite limits of the treating range because it was believed that the results at any point in the series of tests might depend somewhat on the temperature of the previous treatments. As indicated in Tables 3 and 4, the periods of treatment for lot A were longer than those for

these temperatures produces a marked reduction in transmission. Within this whole range of intermediate temperatures it appears that solarization (regardless of whether equilibrium is or is not reached) may always be carried well beyond the degree of reasonable constancy after the radiation is stopped. The return, accompanied by increasing transmission, to an approximately constant condition (such conditions may fall far short of the limits approached at such temperatures in the absence of radiation) probably causes much of the brilliant phosphorescence observed at these temperatures whenever the radiation of a sensitive glass by the ultra-violet source ceases.

At relatively low temperatures, however, where the rate of solarization becomes still lower it is probably impossible to reach an equilibrium condition by a solarization treatment of any practical length; and it may even be impossible to reach those degrees of solarization which are easily obtainable at higher temperatures (somewhat above that of the atmosphere, for example). If this be the case, it should be possible by a series of ultra-violet treatments for equal times from a given source to establish the temperatures yielding optima for solarization, phosphorescence, thermoluminescence, etc.

With regard to the effect of temperature on solarization near atmospheric temperatures, Coblentz and Stair (B. S. Jour. Research, **3**, p. 647; 1929) found that at a distance of 15 cm from the quartz mercury arc lamp the temperature was of the order of 70° C. and that at this temperature vita and helio glass solarized to a lower transmission value than when exposed at 15° C. to the same radiation. This probably indicates that, under the conditions of their experiments, the optimum temperature for solarizing to the lowest level was above 15° C., but below 200° C., since heating to the latter temperature rejuvenates these glasses appreciably.

B and in the cases of both A and B they were considerably longer at low temperatures. The object of these differences in the periods of treatment of the two lots was to determine whether the periods, particularly at low temperatures, were great enough to procure approximately the maximum effect at each treating temperature.

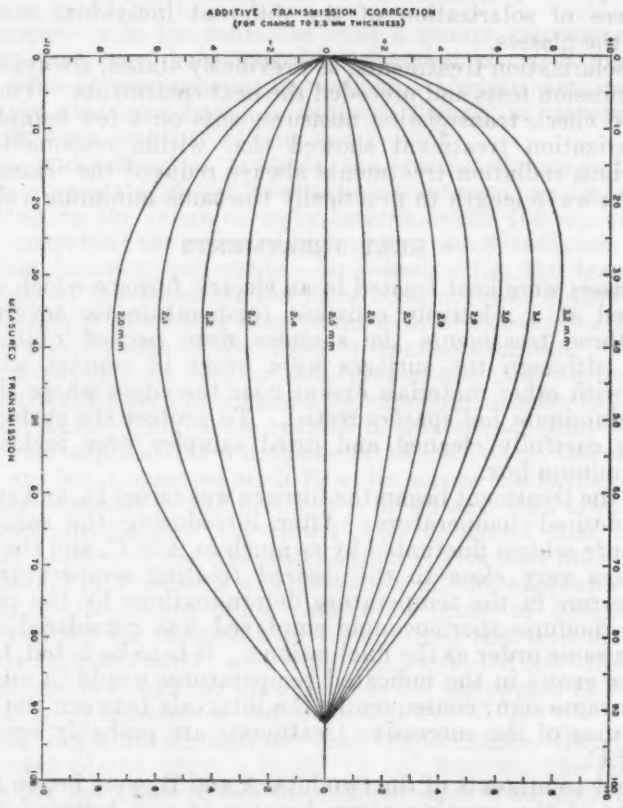

FIGURE 2.—*Curves giving transmission corrections required because of variations in sample thickness*

The equations necessary for computing the data used in the preparation of such curves may be obtained from the relations which show the variation of transmission with thickness and which are to be found in various texts and articles; for example, the article by Gibson and McNicolas in B. S. Tech. Paper, No. 119, p. 11; 1919. The above curves were prepared on the basis of a 4 per cent reflection at each surface of the specimen. At times it is necessary to allow for a larger percentage of reflection, especially near absorption regions. This may require the preparation of additional graphs, but usually sufficiently accurate adjustments can be made without this additional labor if the actual reflection percentage does not deviate too greatly from that assumed in the preparation of the curves. For a different type of correction chart see the revised edition of the Gibson and McNicolas paper cited above.

IV. RESULTS

1. TRANSMISSION

For the purpose of easier comparison the transmission values given in Tables 1 and 2 are adjusted to a thickness of 2.5 mm, which is about the mean thickness when all of the samples of the two glasses tested are considered. (For adjustment method employed see fig. 2.) These adjusted values for all 5 wave lengths and for all 20 samples,

both before and after their first solarization, are given here in order to indicate the degree to which the results were consistent. To show something of the magnitude of the corrections required in the adjustments, the observed transmissions and the corrections for the two extreme wave lengths employed are also included in the tables.

In making these adjustments it was found that the same results for the average adjusted transmissions could be obtained by using the average observed transmissions and thickness. Further tests in applying such corrections to the individual and average results both after heat treating and after resolarizing the samples showed that sufficiently accurate adjustments could be made if the average

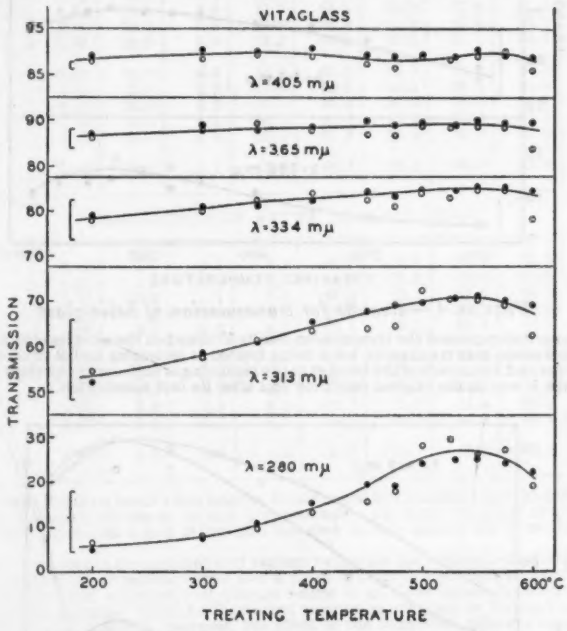

FIGURE 3.—*Results for transmission of vita glass*

The circles and large dots represent the transmission results obtained on the samples of lots A and B, respectively, after the various heat treatments, lot A being treated at increasing and B at decreasing temperatures. The upper and lower ends of the bracket at the beginning of each curve represent the transmissions of the glass when it was in the original condition and after its first solarization.

transmissions and thickness were used for each of the sets of five samples designated as lots A and B. Consequently this method of adjusting the averages was followed in obtaining the results (Tables 3 and 4) showing the effects of alternate solarization and heat treatment. These results are also graphically represented in Figures 3 and 4, while for the purpose of comparison Figure 5 reproduces on a different scale the probable curves found in Figures 3 and 4 for the wave lengths 280 mμ and 313 mμ. The circles in Figure 5 represent the preliminary transmission results on vita glass which were discussed in the progress report read at the American Ceramic Society meeting previously mentioned.

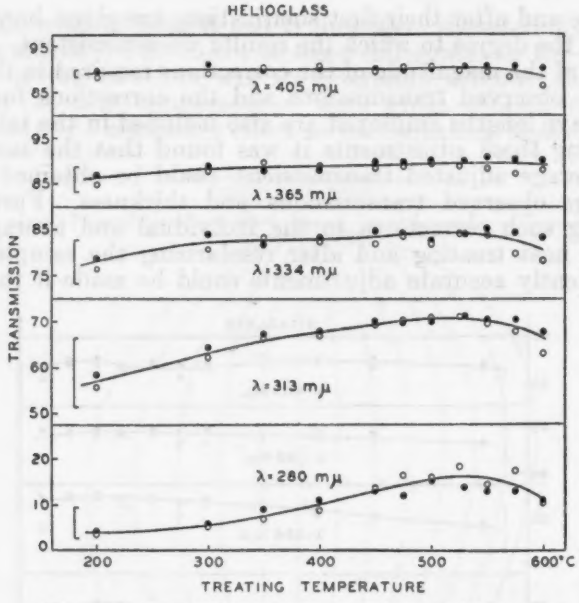

FIGURE 4.—*Results for transmission of helio glass*

The circles and large dots represent the transmission results obtained on the samples of lots A and B, respectively, after the various heat treatments, lot A being treated at increasing and B at decreasing temperatures. The upper and lower ends of the bracket at the beginning of each curve represent the transmission of the glass when it was in the original condition and after its first solarization.

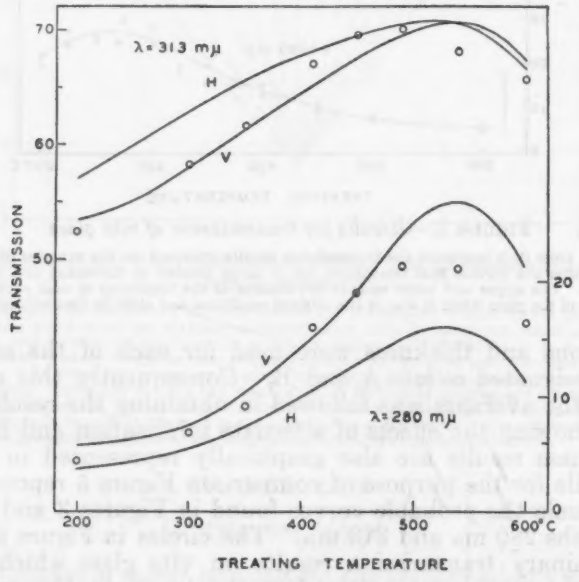

FIGURE 5.—*Comparison of results on transmission of vita and helio glasses*

Curves *V* and *H* reproduce on a different scale the trends of the curves for 280 mμ and 313 mμ shown in Figures 3 and 4, respectively. The circles represent some preliminary results for vita glass.

TABLE 1.—*Vita glass*

INITIAL TRANSMISSIONS [1]

Sample No.	Thickness	Wave lengths— 280 Observed	280 Correction	280 Adjusted	313 Adjusted	334 Adjusted	365 Adjusted	405 Observed	405 Correction	405 Adjusted
	mm									
2	3.10	12.1	5.8	17.9	65.6	81.8	87.1	84.4	1.4	85.8
3	3.12	12.1	6.0	18.1	67.0	80.6	89.2	87.1	1.0	88.1
4	3.12	11.8	5.9	17.7	65.3	82.2	87.8	85.8	1.2	87.0
5	3.16	12.3	5.9	18.2	65.3	82.2	87.6	86.5	1.1	87.6
6	3.08	12.2	5.8	18.0	66.2	82.8	87.1	88.3	.7	89.0
7	3.06	12.5	5.5	18.0	65.2	83.9	88.9	86.5	.9	87.4
8	3.02	12.6	5.2	17.8	64.8	82.3	88.3	88.0	.7	88.7
10	2.92	12.9	4.2	17.1	65.6	81.6	88.6	87.1	.7	87.8
11	2.89	14.0	4.1	18.1	66.6	82.7	87.9	87.5	.6	88.1
12	2.87	14.2	3.8	18.0	65.8	81.5	88.0	88.0	.5	88.5
Average	3.03	12.7	5.1	17.8	65.7	82.2	88.0	86.9	.8	87.7
TRANSMISSIONS AFTER SOLARIZATION										
2	3.10	2.0	2.2	4.2	46.3	72.4	80.6	84.0	1.5	85.5
3	3.12	2.2	2.4	4.6	45.9	72.9	83.6	85.6	1.2	86.8
4	3.12	2.6	2.7	5.3	48.2	73.2	83.0	85.8	1.2	87.0
5	3.16	2.5	2.6	5.1	48.5	73.5	84.5	84.5	1.4	85.9
6	3.08	2.3	2.3	4.6	48.5	73.7	83.8	85.3	1.2	86.5
7	3.06	2.2	2.1	4.3	46.8	72.6	84.6	85.6	1.1	86.7
8	3.02	2.5	2.2	4.7	47.1	72.4	84.1	84.5	1.2	86.7
10	2.92	2.8	1.9	4.7	46.9	73.7	84.5	84.9	1.0	85.9
11	2.89	3.2	1.8	5.0	48.5	73.7	84.9	85.0	.8	85.8
12	2.87	3.0	1.7	4.7	49.7	74.0	84.6	86.9	.6	87.5
Average	3.03	2.5	2.3	4.8	47.7	73.2	83.8	85.2	1.2	86.4

[1] Besides the adjusted values for all wave lengths, the observed transmissions and the corrections required in adjusting to a uniform thickness of 2.5 mm (approximately the mean thickness of all the samples for which data are given in Tables 1 and 2) are also included in the cases of the 2 extreme wave lengths employed.

The observed data on which the adjusted and average values are based are all effectively the averages of at least 5 determinations which seldom varied over a range as great as 3 per cent in terms of transmission. Consequently, the observed, adjusted, and average values in all these tables should show even smaller spreads. Between the adjusted values for the several samples represented in Tables 1 and 2, the spread (for a given wave length) includes, however, the effect of the somewhat different transmissions of the various samples.

TABLE 2.—*Helio glass*

INITIAL TRANSMISSIONS [1]

Sample No.	Thickness	Wave lengths— 280 Observed	280 Correction	280 Adjusted	313 Adjusted	334 Adjusted	365 Adjusted	405 Observed	405 Correction	405 Adjusted
	mm									
1	2.27	10.9	2.2	8.7	66.0	81.2	87.3	90.5	0.2	90.3
2	2.31	11.0	1.7	9.3	67.5	82.3	89.4	90.1	.2	89.9
3	2.30	11.3	1.9	9.4	63.2	82.6	89.1	89.5	.2	89.3
4	2.33	11.5	1.6	9.9	67.7	81.0	88.8	89.5	.2	89.3
5	2.38	11.0	1.1	9.9	66.0	82.2	88.2	89.8	.1	89.7
6	2.39	10.3	1.0	9.3	65.5	81.8	88.9	90.3	.1	90.2
7	2.25	12.1	2.4	9.7	66.1	86.1	89.7	90.3	.2	90.1
8	2.05	14.1	4.8	9.3	70.3	86.0	88.4	90.7	.3	90.4
9	2.26	12.1	2.4	9.7	66.1	82.7	90.5	91.0	.2	90.8
10	2.32	11.1	1.7	9.4	67.5	84.2	89.1	90.0	.1	90.9
Average	2.29	11.5	2.0	9.5	66.5	82.9	88.9	90.2	.2	90.0

[1] See note following Table 1.

TABLE 2.—*Helio glass*—Continued

TRANSMISSIONS AFTER SOLARIZATION

Sample No.	Thickness	Wave lengths—								
		280			313	334	365	405		
		Observed	Correction	Adjusted	Adjusted	Adjusted	Adjusted	Observed	Correction	Adjusted
	mm									
1	2.27	3.2	0.9	2.3	48.9	78.4	82.7	88.9	0.3	88.6
2	2.31	3.7	.8	2.9	49.3	73.0	84.5	88.5	.3	88.2
3	2.30	3.2	.8	2.4	49.3	72.9	82.3	87.4	.4	87.0
4	2.33	3.2	.9	2.3	49.7	72.3	84.0	87.5	.3	87.2
5	2.38	2.8	.5	2.3	50.0	72.6	83.6	88.4	.2	88.2
6	2.39	2.9	.4	2.5	51.2	73.6	84.7	87.0	.2	86.8
7	2.25	3.4	1.1	2.3	50.8	73.9	82.6	88.7	.4	88.3
8	2.05	4.3	2.1	2.2	50.5	72.4	80.8	90.3	.4	89.9
9	2.26	3.7	1.1	2.6	55.3	72.5	84.3	89.4	.3	89.1
10	2.32	3.6	.8	2.8	56.4	74.2	82.3	89.8	.2	89.6
Average	2.29	3.4	.9	2.5	51.2	73.1	83.2	88.6	.3	88.3

TABLE 3.—*Per cent transmission (adjusted to 2.5 mm)*

VITA GLASS, LOT B (AVERAGE THICKNESS 2.95 MM)

Treatment No.	Treatment	Treatment period	Wave lengths				
			280	313	334	365	405
	Temperature, ° C.	*Days*					
1	575	1	24.2	70.0	84.7	89.1	89.1
2	550	1	25.1	71.0	85.2	89.8	90.4
3	530	1	25.0	70.5	84.4	88.9	88.8
4	500	1	24.1	69.9	84.3	89.2	88.9
5	475	1	19.2	69.1	83.2	88.7	88.9
6	450	1	19.4	67.6	84.2	88.9	89.2
7	400	2	15.2	65.4	82.5	88.5	90.7
8	350	6	10.7	61.4	81.0	87.7	89.9
9	300	6	7.3	58.6	80.7	88.8	90.1
10	200	6	4.9	52.2	78.7	86.5	89.2
11	600	1	22.1	69.0	84.3	89.4	88.7
12	200	5	20.1	68.3	85.2	89.4	89.8
	515	1					

HELIO GLASS, LOT B (AVERAGE THICKNESS 2.25 MM)

1	575	1	12.8	70.2	84.3	90.3	90.5
2	550	1	12.7	70.2	85.1	90.8	90.6
3	530	1	13.7	71.1	83.9	90.0	90.6
4	500	1	15.4	69.8	82.4	89.8	90.0
5	475	1	11.6	69.7	84.0	89.6	89.7
6	450	1	13.1	69.9	94.6	89.8	89.9
7	400	2	10.8	67.8	83.3	88.3	90.1
8	350	6	8.9	67.1	81.7	87.9	89.7
9	300	6	5.5	64.2	83.9	88.6	91.0
10	200	6	4.0	58.4	78.7	86.9	89.7
11	600	1	10.8	67.6	83.2	90.1	90.1
12	200	5	12.8	69.3	84.1	89.5	90.0
	515	1					

TABLE 4.—*Per cent transmission (adjusted to 2.5 mm)*

VITA GLASS, LOT A (AVERAGE THICKNESS 3.11 MM)

Treatment No.	Treatment	Treatment period	Wave lengths				
			280	313	334	365	405
	Temperature, ° C.	*Days*					
1	200	14	6.5	54.4	77.7	86.2	87.8
2	300	14	8.1	57.8	80.4	87.6	88.4
3	350	13	9.6	61.4	82.4	89.2	89.3
4	400	14	13.2	63.7	83.9	88.8	88.8
5	450	14	15.6	63.9	82.3	86.8	87.1
6	475	14	17.9	64.4	80.7	86.7	86.3
7	500	14	28.2	72.5	84.1	89.2	89.2
8	525	7	29.8	70.3	82.7	88.4	88.3
9	550	7	25.3	70.3	84.5	88.6	88.9
10	575	7	27.0	69.1	84.7	89.3	89.0
11	600–610	7	19.1	62.2	78.0	83.5	85.8
12	515	7	22.2	63.8	77.8	83.4	84.2

HELIO GLASS, LOT A (AVERAGE THICKNESS 2.32 MM)

1	200	14	3.4	55.6	76.3	84.8	88.2
2	300	14	5.3	62.1	80.6	87.8	89.0
3	350	13	6.6	66.1	83.1	89.6	90.0
4	400	14	8.6	66.8	82.3	88.6	90.3
5	450	14	13.4	69.5	81.8	88.3	89.5
6	475	14	16.2	70.0	83.8	88.6	90.3
7	500	14	15.6	70.5	82.0	89.4	90.2
8	525	7	18.2	71.0	84.2	88.9	89.6
9	550	7	14.4	69.4	83.7	88.3	89.3
10	575	7	17.2	67.7	79.5	87.2	88.2
11	600–610	7	10.1	62.9	78.2	87.9	86.4
12	515	7	13.8	64.6	81.8	86.9	88.9

In Figures 3 and 4 the circles indicate the results obtained on lot A for which the succeeding treating temperatures were increased, while the large dots represent the results on lot B, for which the temperatures were decreased. These results give some indication that the treatments from 550° to 600° C. injure the surfaces somewhat, since the transmissions fall off noticeably from the maximum values as the treating temperatures near 600° C. Moreover, the transmissions of lot B for the shortest wave length after the treatments at temperatures from 575° to 500° C. are in general lower than those of lot A, although this discrepancy may, of course, be ascribed to the longer heat treatments received by the latter sets of samples. On the other hand, length of treatment is not always the controlling factor since, from 350° to 475° C., the results for lot A are in many cases lower than those of lot B. This, however, may very well be considered as an indication that the repeated solarization and partial restoration at temperatures below 500° C. caused a condition to develop in the glass that progressively and materially depressed the restoration possible at all temperatures well below this point without greatly affecting the minimum transmissions obtained after the various solarizations. If such a condition does build up as a result of repeated solarization and restoration at low temperatures it is apparently destroyed by heat treatments in the annealing range.

In all other respects (that is, outside of the variations which lead to the possibilities mentioned in the above paragraph) the results are usually as consistent as could be expected in view of the possible experimental errors which include the effect of the impossibility of always being certain that the light traversed exactly the same area of a sample in the various transmission measurements. This consistency indicates that, at the low temperatures especially, the shorter periods of treatment for lot B were sufficient to restore the glass approximately to the maximum possible degree for the various treating temperatures, since otherwise larger differences between the results for the two lots (with those of lot A more generally exceeding those of lot B) would have been observed.

It will be noted that the initial transmissions for the shorter wave lengths are intermediate between those obtained after solarization and those reached after restoration by heat treatments just above 500° C. That these values after approximately complete restoration at the higher temperatures were above those obtained on the untreated samples is not surprising because the glasses through exposure to light after their production and before being procured for these tests were undoubtedly solarized to some degree. On considering Tables 1 and 2, together with 3 and 4, it also seems that the treatments for reasonably long periods at temperatures very little if any higher than 400° C. were always adequate to restore the solarized glasses to their initial power of transmitting light of the shorter wave lengths, while treatments at temperatures as low even as 200° C. always erased a noticeable portion of the effect of solarization.

Solarization caused only a relatively small reduction in the transmission at the wave length 405 mμ, and it was consequently difficult to establish any marked difference in the effects due to heat treatment at different temperatures until those temperatures were reached which caused surface deterioration and deformation. It appears, however, that a much greater proportion of the effect of solarization is erased by heat treatments at 200° and 300° C. in the case of the long wave lengths than in that of the short, although the ratio of the maximum effect of either solarization or restoration to the initial transmission usually increases rapidly as the wave length decreases. It appears also that the treating temperature required to restore a solarized glass to its initial transmission for a given wave length decreases as this wave length increases and that this is more apparent in the case of vita glass than in that of helio glass which was found to give the weaker visible thermoluminescence.

2. THERMOLUMINESCENCE

Several tests were made on the thermoluminescence effects which, as is well known, are found after these glasses are solarized, but only those tests made on lots A and B will be mentioned specifically. The vita glass samples of lot A, after all the transmission tests had been made and after being again solarized, were heat treated for one week at 300° C. Relatively speaking, the thermoluminescence was very bright and lasted for about 20 minutes, the maximum being reached after about half that time. After this treatment the samples were removed from the furnace so that its temperature might be adjusted to 500° C. for the second part of the test. The samples on being reintroduced at this temperature gave no noticeable glow, which

seemed to indicate that the power to emit visible thermoluminescent radiation had been exhausted by the 300° C. treatment, since solarized glass of this kind when directly introduced into a furnace at 500° C. glows even more brightly than at lower temperatures, although for a shorter time.

The helio-glass samples of lot A when treated according to the same schedule glowed less than the vita glass and for a shorter time at 300° C. They also gave no detectable glow on reheating at 500° C. Since only visual tests were made it is quite possible, however, that both glasses at this temperature emitted radiations of wave lengths shorter than those of the visible spectrum.

The samples of lot B were tested in much the same manner except that the first treating temperature was 200° C. and the treating period was five days, while the second temperature was 515° C. In this test both glasses were treated together, so that the difference in the brilliance of their glows was more apparent. The more brilliant vita-glass glow reached its maximum after about 20 minutes at 200° C. and lasted at least 3 hours. As before, the period of glowing appeared somewhat shorter in the case of helio glass, but the difference in brilliancy may have been the reason for this. On receiving the added treatment at 515° C. the vita glass glowed very slightly, but this was no longer detectable after 20 minutes, while the helio glass did not seem to glow at all.

The visible radiation obtained in these tests when examined with a small spectroscope appeared to be continuous throughout its spectrum, which seemed not to reach the longest visible wave lengths, while the shorter wave-length regions were relatively bright. As a matter of fact, however, the glows were too weak for definite conclusions on these points unless much more refined methods of observation had been used, and such refinements seemed unnecessary for the purpose of this investigation.

From these tests it is clearly evident that treatments at relatively low temperatures practically exhaust the power of solarized glasses to glow visibly, while from the transmission measurements, it would seem that they are at the same time relatively more effective in restoring the loss in power of the glasses to transmit radiation at the longer wave lengths than they are in doing the same thing at the shorter ones. Moreover, it was noted from cursory inspections that all the treatments at low temperatures seemed to decolorize the glasses as completely as those at the higher temperatures. This may be an indication that the visible thermoluminescence accompanies the reversal of those processes which during solarization are relatively more effective in decreasing the transmission in the range of the visible and longer ultra-violet wave lengths; and if it should be shown ultimately that an invisible radiation of shorter wave lengths is emitted more intensely by the glass at the higher temperatures it might well be that such radiation accompanies the reversal of other solarization processes which are relatively more potent in decreasing the transmission for the ultra-violet wave lengths near the lower end of the transmission range. In other words, the disappearance of the coloration and the coincident visible thermoluminescence appear to be more closely associated with transmissivity restorations at the longer

ultra-violet wave lengths than they appear to be to similar restorations at the wave lengths included in the therapeutic range.

V. CONCLUSIONS

In a series of tests made for the purpose of determining the effect of heat treatments at different temperatures on artificially solarized samples of commercial glasses having fairly high transmissivities for ultra-violet radiation, the following conclusions were reached.

1. Heat treatments at temperatures in the annealing range of such glasses are the most effective ones in gaining the highest degree of transmission for ultra-violet radiation; and in the cases of the glasses tested, such temperatures are somewhat above 500° C.

2. Heating a solarized sample of these ultra-violet transmitting glasses for a few hours at temperatures near or somewhat above 300° C. will often approximately restore the transmissivity to its initial value, since this value is ordinarily considerably less than that which may be reached by treatments at higher temperatures, especially if the glass is one that is easily solarized.

3. Regardless of their length, heat treatments at temperatures below 300° C. are apparently inadequate for restoring the solarized glasses to their original transmission except possibly for relatively long wave lengths.

4. The visible coloration which appears coincident with solarization of these glasses disappears almost completely with treatments of reasonable length even at temperatures below 300° C.

5. The power to emit thermoluminescence and the coloration seem to disappear simultaneously; and, after these have disappeared, the transmissivity for wave lengths near the visible spectrum appears to be practically restored although that for those shorter wave lengths which are nearer the limit of the transmission range has by no means undergone a full restoration.

6. As other investigators have shown, the thermoluminescence and coloration disappear more and more rapidly as the temperature is increased; consequently the intensity of the luminescence is greatly increased while the period of its visibility is correspondingly decreased as the treating temperature approaches the annealing range.

7. Likewise, the restoration of the power of transmission is also achieved much more rapidly, as well as more completely, by increasing the temperature of treatment.

WASHINGTON, March 1, 1931.

THE DETERMINATION OF OXYGEN AND NITROGEN IN IRONS AND STEELS BY THE VACUUM FUSION METHOD

By H. C. Vacher and Louis Jordan

ABSTRACT

Results of an extended study of the vacuum-fusion method for the determination of gases in steels are presented. The apparatus consists of a vacuum furnace and an analytical train for determining carbon monoxide, hydrogen, and nitrogen at low pressures. Simplification of the analytical procedure, the use of a mercury diffusion pump, and the adoption of a sample loading device have improved the method. The method (in the absence of interferences) gives values reproducible to within 0.002 per cent for both oxygen and nitrogen. The accuracy of the oxygen determination is affected by the presence of certain oxides which are decomposed with difficulty, and by the presence of certain reactive metallic vapors during the evolution of carbon monoxide. The accuracy of the nitrogen determination is not affected by these factors.

CONTENTS

	Page
I. Introduction	375
II. Apparatus and procedure	377
1. Improvements in the gas analysis train	377
(*a*) General description of train	378
(*b*) Elimination of first 2 tubes from earlier apparatus	378
(*c*) Construction and operation of analytical train	379
2. Improvements in furnace conditions and technique	382
(*a*) Design and construction of furnace	383
(*b*) Operation of furnace	385
III. Accuracy of the vacuum fusion analysis	386
1. Sampling	386
2. Interference by vaporized metals	389
3. Reduction of certain oxides	393
4. Probable accuracy of the oxygen determination	395
5. Accuracy of the nitrogen determination	399
IV. Summary and conclusions	400
V. Acknowledgments	401

I. INTRODUCTION

The history of the development and summaries of methods for the determination of oxygen and other gases in iron and steel have been published by Meyer,[1] by Hessenbruch,[2] and by Meissner [3] within the past few years. The experimental work described in this paper is a continuation of work initiated by Jordan and Eckman [4 5] in developing methods for the determination of oxygen, hydrogen, and nitrogen in iron and steel. Since the publication of their work, papers have appeared describing certain improvements in procedure and giving data to show the precision and accuracy to be expected from these methods.

[1] O. Meyer, Über den heutigen Stand der Bestimmung von Sauerstoff in Stahl und Eisen, Z. Angew. Chem., 41, pp. 1273–1275, 1295–1298; 1928.
[2] W. Hessenbruch, Die Unterschung der Gase in den Metallen, Z. Metallkunde, 21, pp. 46–55; 1929.
[3] F. Meissner, Beitrag zur Bestimmung der Oxyde in Eisen und Stahl, Mitt. Forschungs-Inst. Ver. Stahlwerke Aktienges., Dortmund, 1, pp. 223–79; 1930.
[4] Louis Jordan and J. R. Eckman, Gases in Metals. II. The Determination of Oxygen and Hydrogen in Metals by Fusion in Vacuum, B. S. Sci. Paper No. 514; 1925.
[5] Louis Jordan and J. R. Eckman, Gases in Metals. III. The Determination of Nitrogen in Metals by Fusion in Vacuum, B. S. Sci. Paper No. 563; 1927.

Walker and Patrick [6] showed that oxygen contained in iron probably could be recovered as carbon monoxide by a vacuum fusion in graphite, although the furnace conditions and technique employed by them made it difficult to obtain precise results. However, the promising possibility of complete conversion of oxides to a readily determinable form, together with the possibility of using carbon as a material for crucibles, made this method very attractive. Jordan and Eckman, after a survey of existing vacuum fusion methods, undertook to improve the furnace condition and technique of the Walker and Patrick method. By using a high-frequency induction furnace they showed that precise results could be obtained and that the oxygen of oxides usually encountered in steel could be recovered when contained in relatively pure iron, such as ingot iron. The method, as described by Jordan and Eckman has been modified by Hessenbruch and Oberhoffer,[7] by adding (*a*) a sample loading device, whereby the crucible at the temperature of the analysis may be loaded with one or more samples of steel without opening the furnace to the atmosphere and (*b*) the use of a mercury diffusion pump in order to extract the gases more rapidly from the furnace. Von Seth [8] further modified the apparatus by water cooling the walls of the evacuated furnace tube and by keeping all refractory oxides outside of the high temperature zone. Diergarten [9] constructed a resistance type of furnace as a substitute for the high-frequency furnace. His results, obtained with this resistance furnace, were in good agreement with results obtained with a high-frequency furnace.

Hessenbruch and Oberhoffer pointed out the interference of manganese in analyses made according to the procedure used in the early part of their work, but their final conclusion was that such interference was not serious in their recommended procedure, namely, melting under lower pressures attained by means of a mercury diffusion pump. Von Seth concluded from his work, that methods for determining oxygen in metals by a vacuum fusion in graphite did not yield accurate results on account of gas reactions with condensed metals or metal vapors in the colder parts of the furnace.

Thanheiser and Müller,[10] using essentially the improved method of Oberhoffer and Hessenbruch, concluded that, of the oxides possibly present in steel, only iron oxide and manganese oxide were completely reduced. The oxygen which was present in combination with silicon or aluminum was only partially recovered at a temperature of 1,500° C. If higher temperatures were used in order to reduce the oxides of aluminum and silicon more completely, the blank corrections became excessively large and the increased vaporization of manganese made the results inaccurate. Thanheiser and Müller also found that very considerable losses of oxygen often resulted when the fusion was made in a crucible containing residues from previous analyses.

---

[6] W. M. Walker and W. A. Patrick, Determination of Oxygen in Iron and Steel by Reduction in an Electric Vacuum Furnace, Eighth Int. Cong. App. Chem., **21**, pp. 139–148; 1912.

[7] W. Hessenbruch and P. Oberhoffer, Ein verbessertes Schnellverfahren zur Bestimmung der Gase in Metallen, insbesondere des Sauerstoffs im Stahl, Archiv Eisenhüttenwesen, **1**, pp. 583–600; 1928.

[8] R. Von Seth, Jernk. Ann., **112**, pp. 113–150; 1928; Stahl u. Eisen, **48**, pp. 1374–1375; 1928.

[9] Hans Diergarten, Zur Bestimmung der Gase in Metallen, usw., Archiv Eisenhüttenwesen, **2**, pp. 813–828; 1929.

[10] G. Thanheiser and C. A. Müller, Beitrag zur Bestimmung des Sauerstoffs im Stahl nach dem Heissextraktionsverfahren, Mitt. Kaiser Wilhelm Inst. Eisenforsch., II, pp. 87–94; 1929.

Recently Diergarten [11] has fully confirmed the earlier results of Walker and Patrick and of Jordan and Eckman to the effect that silica is completely reduced in the vacuum-fusion method and that recoveries of over 90 per cent of oxygen combined as alumina can be made. He also calls attention to errors caused by reactions between the vapors of manganese, or aluminum, and carbon monoxide. The analysis, in his opinion, becomes inaccurate when material in the crucible at the start of an analysis contains manganese or aluminum in excess of 0.7 and 0.3 per cent, respectively.

II. APPARATUS AND PROCEDURE

The apparatus for the vacuum-fusion method at present in use in the laboratories of the National Bureau of Standards differs in several respects from the earlier apparatus described by Jordan and Eckman. The analytical train has been simplified by eliminating two of the four absorption tubes. Provision has been made for the determination of nitrogen with oxygen and hydrogen, and the complete analysis (oxygen, hydrogen, and nitrogen) is carried out in a closed analytical train. The furnace is of new design and is provided with a sample loading device similar to that used by Hessenbruch and Oberhoffer. A mercury diffusion pump is used to allow melting the sample under lower pressures than in the earlier apparatus, and the same pump serves to circulate the gases in the closed analytical train.

1. IMPROVEMENTS IN THE GAS ANALYSIS TRAIN

Gravimetric methods for the determination of oxygen and hydrogen are employed in the improved apparatus. This method of analysis of gases at low pressure has the distinct advantage of eliminating a collecting pump (necessary if a volumetric method at atmospheric pressure is to be used) and of being easily adaptable to either large or small quantities of gas, as compared with the difficulties involved if a volumetric method of analysis at low pressures is to be used.

In the earlier apparatus a mechanical vacuum pump drew the gases, evolved in the vacuum furnace, through an evacuated absorbent train. Water, carbon dioxide, hydrogen, and carbon monoxide were determined by the increase in weight of four tubes filled with solid absorbents, 2 with phosphorus pentoxide and 2 with ascarite.

Jordan and Eckman [12] showed that nitrogen also could be recovered from iron and steel by a vacuum-fusion method. In their method the sample was fused in vacuo in a graphite crucible, and the gases evolved from the sample were absorbed in calcium vapor. The nitrogen of the calcium nitride thus formed, was determined by the ordinary acid solution and distillation method. The analysis of a ferrous material for oxygen, hydrogen, and nitrogen required two samples and two complete operations.

In the improved apparatus, where the gases are retained in a closed system, the residual gas, after the absorption of water and carbon dioxide, consists of nitrogen. The determination of the volume of this residual gas, therefore, permits the determination of oxygen,

[11] H. Diergarten, Zur Bestimmung der Gase in Metallen, usv., Archiv Eisenhüttenwesen, **3**, pp. 577–586; 1930.

[12] See footnote 5, p. 375.

hydrogen, and nitrogen on one sample and in one operation. This determination is possible in the improved train.

(a) GENERAL DESCRIPTION OF TRAIN

A drawing of the improved train is shown in Figure 1. The complete train, furnace, and absorbent tubes may be evacuated by a mechanical vacuum pump which is connected at *M* or they can be filled independently with dry, carbon dioxide-free air through *H*. The gases evolved from the metal sample are removed from the furnace (*A*) by means of a 2-stage mercury diffusion vacuum pump (*B*) which delivers the gases to the reservoirs (R_1 and R_2). Subsequently, the gases are circulated over hot copper oxide (*C*) and through absorbent tubes containing phosphorus pentoxide (T_1) and ascarite (T_2).

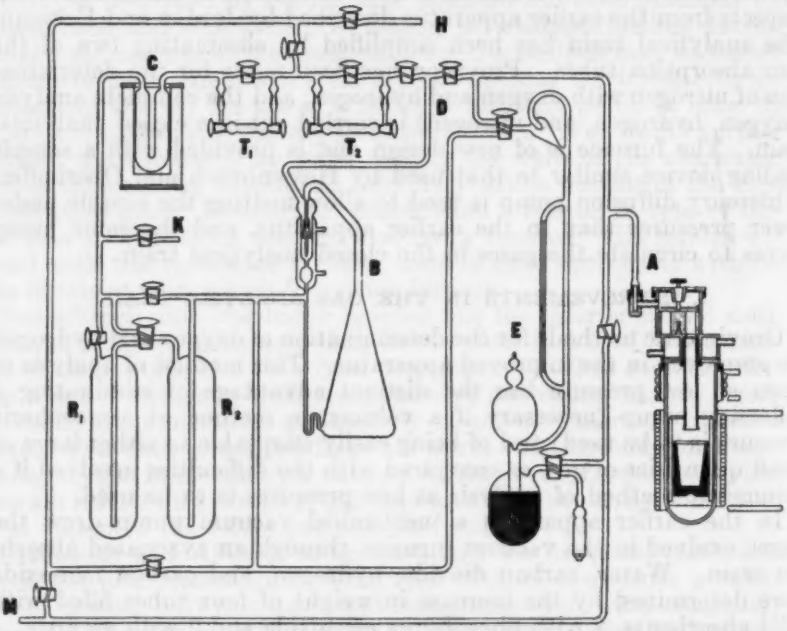

FIGURE 1.—*Diagram of apparatus for the determination of gases in metals by the vacuum-fusion method*

Any unoxidized or unabsorbed gas is returned to the low-pressure side of the diffusion pump (*D*). The pressure at the furnace inlet (*A*) and the pressure in the reservoirs can be measured by means of the McLeod gage (*E*). In order to reoxidize the copper oxide, air is drawn into the train at *H* and removed by the laboratory vacuum at *K*.

(b) ELIMINATION OF FIRST TWO TUBES FROM EARLIER APPARATUS

In the 4-tube train the first two tubes absorbed water vapor and carbon dioxide, respectively, if these gases were present in the gases evolved in the furnace. After passing through the first two tubes the gases were passed over hot copper oxide, to oxidize hydrogen and carbon monoxide to water vapor and carbon dioxide, respectively.

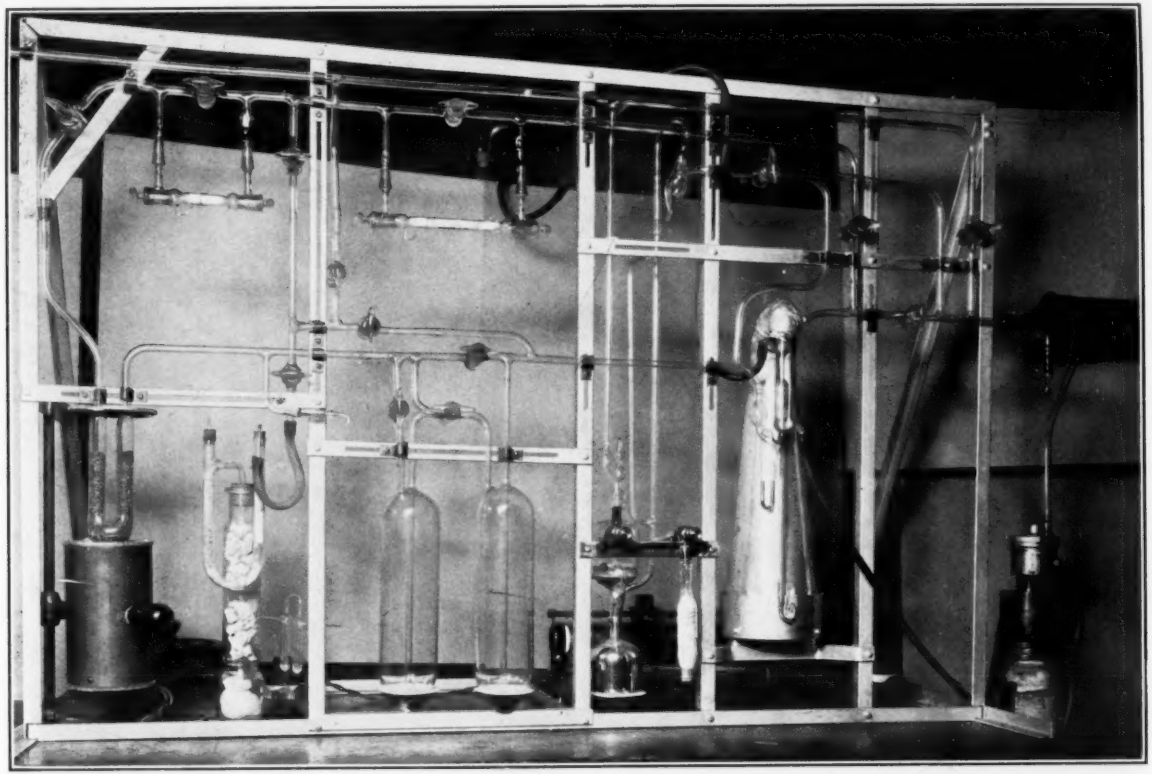

FIGURE 2.—*Assembled apparatus*

This water vapor and carbon dioxide were recovered in a second pair of absorption tubes. A review of the data obtained showed that the increase in weight of the first two tubes during a run seldom exceeded the blank correction. In other words, the amounts of water vapor and of carbon dioxide evolved from the sample were negligible, and consequently the first two absorption tubes might just as well be eliminated. The data in Table 1 show that the amounts of oxygen recovered in a 4-tube train, corrected for the blank determination, and the amount of oxygen recovered in a 2-tube train, corrected for the blank determination, are identical within the limits of experimental error. Similar data are available for the determination of hydrogen, which is present only in minute amounts in ordinary ferrous materials. The absence of appreciable amounts of carbon dioxide and of water vapor in the furnace gases, therefore, is established and the simplification of the train by the elimination of two absorption tubes is justified.

TABLE 1.—*Comparison of analyses made with four tubes and with two tubes in the absorption trains*

4-tube train oxygen	2-tube train oxygen
Per cent	*Per cent*
0.020	0.021
.008	.007
.012	.011
.013	.013
.003	.002
.003	.002
.133	.132
.143	.143

(c) CONSTRUCTION AND OPERATION OF ANALYTICAL TRAIN

The train is mounted on a 31 by 45 inch frame made from ¾-inch angle iron. (Fig. 2.) The uprights and cross pieces within the frame are slotted so that the clamps holding the glass tubes of the train are movable. This facilitates the construction of the train and also repairs and changes in design.

The mercury diffusion pump is a 2-stage Stimson [13] pump, modified so that one condenser will serve both stages. This type of pump is capable of working against a fore pressure of 15 to 20 mm of mercury. The same pump is used to extract gases from the furnace, to collect them in one or two 600 to 700 ml reservoirs, and to circulate the gases through the copper oxide furnace and the absorbent tubes. It has been found advisable to use only one reservoir when making analyses of samples of 20 g of iron or steel. If the volume of the train is increased the time for clean-up of oxidized gases is correspondingly increased.

The vacuum gage is of the McLeod type with multiple compression volumes to allow use over a range of pressures from 20 to 0.001 mm of mercury. This gage is connected to the train to permit reading pressures on both the high pressure and low pressure sides of the diffusion pump.

[13] H. F. Stimson, A Two-stage Diffusion and Jet Pump, J. Washington Acad. Sci., **7**, p. 477; 1917.

The extracted gases are passed over copper oxide in order to oxidize any hydrogen or carbon monoxide present. The copper oxide is contained in a U tube of 1.8 cm diameter Pyrex glass tubing, and fills each side of the U to a height of 15 cm. The tube is heated in a vertically adjustable resistance furnace. It is advisable to reduce the commercial copper oxide "wire" with hydrogen or with carbon monoxide at a low temperature (150° to 200° C.) and then to reoxidize at 300° C. This treatment increases the rate of oxidation of gases in the analytical procedure. The copper oxide is kept at approximately 300° C. during the analyses.

The construction of the weighed absorption tubes (T_1 and T_2, fig. 1) is shown in detail in Figure 3. These tubes are connected to

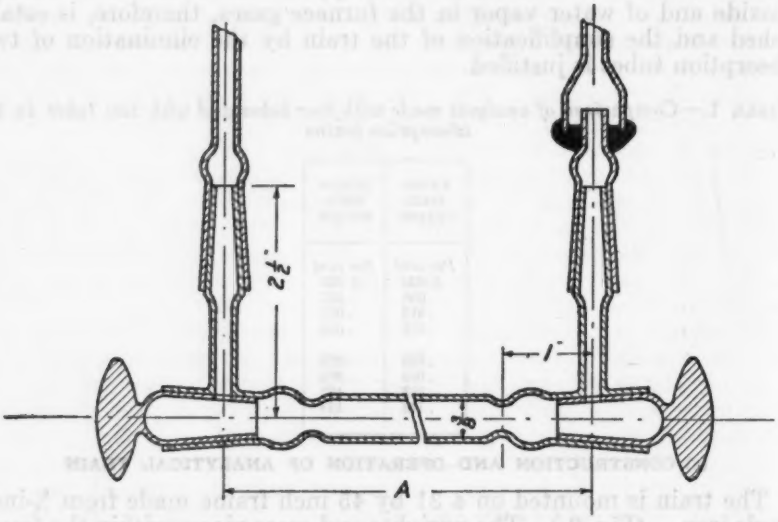

FIGURE 3.—*Details of construction of absorption tube*

the train by lubricated ground glass joints. The lubricant used in these joints and in the stopcocks throughout the train is the high vacuum lubricant described by Shepard and Ledig.[14] The ground joints of the absorption tubes are made interchangeable, and one of the connections to the train for each tube is made through a wax seal as shown in Figure 3. This provides for greater ease in adjusting the train to receive tubes of slightly different lengths or tubes whose connecting arms may not be exactly parallel.

Two sizes of tubes are used. The phosphorus pentoxide tube (T_1) is 4 inches long (dimension A, fig. 3) and the ascarite tube (T_2) is 6 inches long. These tubes are filled with the absorbents by clamping the tube vertically in a ring stand and packing a small plug of glass wool against the end of a fixed rod entering the tubes from the lower end. A short piece of rubber tubing, about three-eighths inch long is fitted over a funnel stem in such a position that the rubber will fit tightly in the barrel of the stopcock at the opening of the side arm of the tube and thus prevent fine particles of the absorbents from

[14] G. M. Shepard and P. G. Ledig, Rubber Stopcock Lubricants for High Vacuum and Other Uses, Ind. Eng. Chem., **19**, p. 1059; 1927.

collecting in this arm. The absorbent is then poured in through the short-stem glass funnel and the tube is gently tapped to distribute the absorbent evenly. Another small plug of glass wool is then gently pressed on top of the absorbent material. Tight packing of absorbents is to be avoided as it retards the circulation of gases through the analytical train. In filling the ascarite tube, phosphorus pentoxide is placed on both sides of the ascarite to guard against the escape from the tube of the water liberated when the tubes are evacuated. The ascarite, which is about 8 mesh as received, is crushed to about 20 mesh just before loading in the tube. A 2-inch column of ascarite thus prepared will absorb at least 0.2 g carbon dioxide (100 ml at N. T. P.). The arms of the tubes are carefully wiped with ether, to remove the lubricant from the ground glass joints before weighing. The weighings are made against a similar tube used as a counterpoise.

After the oxidized gases have been absorbed, the residual gas is pumped from the copper oxide tube and absorbent tubes and collected in the reservoirs. The pressure of the residual gas is read on the McLeod gage and this pressure reading is converted to grams of nitrogen by means of a previously determined factor.

This train has been discussed as a gravimetric train, but it is equally adaptable to volumetric analysis, if desired. In the volumetric procedure the gases to be analyzed are collected in the reservoir system and the pressure recorded. The gases are then circulated through the copper oxide furnace and the phosphorus pentoxide tube until there is no further decrease in pressure in five minutes while the gases are still circulating. The gases are again collected in the reservoir system and the pressure recorded, the remaining gases are again circulated through the copper oxide, and this time through the ascarite tube (T_2) until there is again no decrease in pressure in five minutes. The residual gas is again collected and the pressure recorded. Since there is no change in volume when hydrogen and carbon monoxide are oxidized, the differences in the pressure readings before and after each of the two periods of circulation are the respective partial pressures of the hydrogen and carbon monoxide. These changes in pressures are then converted to grams hydrogen, oxygen, and nitrogen by means of factors previously determined.

The calculation of these volumetric factors may be illustrated as follows:

	mm
In the determination of carbon dioxide in a gas mixture, the pressure in the reservoir system, before absorption of CO_2	= 8
The pressure after absorption of CO_2	= 2
The change in pressure, due to removal of CO_2 by absorption	= 6
	g
The weight of this volume of CO_2 absorbed in an ascarite tube	= 0.006

Therefore, for this reservoir system at room temperature, a change in pressure of 6 mm is equivalent to 0.006 g of CO_2, or 1 mm pressure is equivalent to 0.001 g of CO_2.

From this relation the weight of any other gas, equivalent to a change in pressure of 1 mm, in this reservoir system can be computed from the respective molecular weights of the gas in question and of the carbon dioxide. For instance, the equivalent weight of hydrogen would be 2/44 that of carbon dioxide, and the equivalent weight of

nitrogen would be 28/44 that of carbon dioxide. The factor for carbon monoxide would be the same as for nitrogen, 28/44. Therefore, in this reservoir system, a change in pressure of 1 mm is equivalent to 0.001 g CO_2; or to 0.000045 g H_2; or to 0.00064 g N_2; or to 0.00064 g CO.

In the gravimetric procedure the gases to be analyzed usually are allowed to accumulate in the reservoirs and absorption train until the gas evolution in the furnace is complete; that is, until the gas pressure in the furnace drops to the pressure shown before the sample was dropped into the crucible. After the evolution of gas is complete, the furnace is cut off from the analytical train and the gases which have been accumulated in the reservoir are circulated through the complete analytical train until there is no further decrease in pressure as shown by the McLeod gage. The residual gas is then collected in the reservoir system and its pressure determined. This pressure is converted to weight of nitrogen by means of a factor, as previously described in the volumetric procedure. The hydrogen and oxygen are determined from the increase in weight of absorption tubes T_1 and T_2, which contain, respectively, water and carbon dioxide formed by oxidation of the original hydrogen and carbon monoxide of the gas mixture.

In cases where the gas evolution is unusually large, it has been found advisable to vary the above procedure slightly. If the pressure in the train exceeds 10 to 15 mm of mercury, the gases are circulated through the absorbents for short intervals of time without waiting to complete the extraction of the gases from the furnace. This absorption of gas reduces the pressure in the system and is advisable as the diffusion pump ceases to function efficiently when the fore pressure becomes too great.

The volumetric and gravimetric procedures yield the same results and require about the same time for an analysis. The gravimetric procedure has been used in the National Bureau of Standards laboratories, mainly because it requires less time when only oxygen is desired. Results obtained by these two procedures in analyses of a series of samples of the same steels are given in Table 2.

TABLE 2.—*Comparison of results obtained by gravimetric and volumetric procedures of gas analyses*

	Gravimetric			Volumetric		
	O_2	H_2	N_2	O_2	H_2	N_2
	Per cent	*Per cent*	*Per cent*	*Per cent*	*Per cent*	*Per cent*
Open-hearth iron No. 3	----------	0.0002	0.002	----------	0.0001	0.002
	----------	.0002	.001	----------	.0001	.002
	----------	.0001	.001	----------	.0001	.002
	----------	----------	----------	----------	.0003	.001
Welding rod	0.044	----------	.003	0.043	.0000	.004
Open-hearth iron No. 2D	.065	----------	.002	.060	----------	.002
	.064	----------	.002	.062	----------	.003
	----------	----------	----------	.064	----------	.003

2. IMPROVEMENTS IN FURNACE CONDITIONS AND TECHNIQUE

The furnace procedure for the earlier apparatus in the vacuum-fusion method called for a preliminary outgassing of the crucible and

furnace at 1,600° C., usually for a period of from one-half to one hour. The furnace was then allowed to cool to room temperature, opened, and the crucible removed, charged with the sample, and returned to the furnace as soon as possible. The furnace cap was then replaced, sealed, the furnace tube evacuated, and the apparatus was then ready for heating, melting of the sample, and analysis of the evolved gases. The three latter operations required a total of about one hour. A similar analysis, without a sample, determined the gases evolved from the furnace and crucible and the values so obtained for oxygen and hydrogen were used as a blank correction. Hessenbruch and Oberhoffer have improved this procedure as already indicated, by adopting a sample loading device, similar to that used by Oberhoffer and Shenck,[15] to introduce the sample into the crucible. A similar sample loading device has been adopted for the present furnace.

The present furnace procedure consists essentially in outgassing at a high temperature, 1,700° to 1,750° C., then cooling to the analysis temperature, usually about 1,600° C., dropping the sample at once from the sample loading device into the crucible, and analyzing the gases evolved. The amount of gases coming from the furnace and crucible—that is, the "blank" correction—is determined by analyzing the gases pumped from the furnace for approximately the same length of time as that used in making a sample analysis.

(a) DESIGN AND CONSTRUCTION OF FURNACE

A drawing of the assembled furnace is shown in Figure 4. It consists of three major units—a sample loading device and water-cooled furnace cap (*A*), a furnace tube and water-cooled collar (*B*), a crucible, radiation screen, and crucible rest (*C*). The sample chamber of the sample loading device and the water-cooled furnace cap are constructed as a single unit. The furnace cap is sealed to the water-cooled collar and furnace tube with a picein wax. The cover of the sample chamber contains a window to permit observation of the melt and temperature measurements. This cover is sealed to the sample loading device with picein wax in a small channel provided for the purpose. A tapered metal plug for turning the revolving cylinder which contains the samples projects through the cover. The plug is lubricated with high vacuum lubricant. The whole cap unit is made of brass, the entire outer wall of the combined unit being machined from a single piece of wrought brass. This avoids all soldered joints except for attaching the brass disk forming the bottom of the water chamber of the cap.

A five-eighths-inch diameter fused silica tube which acts as a guide for the falling metal samples is suspended from two brass hooks which are soldered to the underside of the furnace cap. A small brass collar, carrying two pins (shown in detail at *D*, fig. 4) is clamped tightly about this silica tube to provide means for its support from the water-cooled cap. The lower end of the silica tube projects through a quartz disk, which serves as a screen against upward radiation from the crucible. The disk rests on the walls of the radiation screen. The lower end of the tube is flanged to facilitate removal of the disk from the furnace. If spattering of metal from the crucible is troublesome, it has been

[15] P. Oberhoffer and H. Shenck, Theoretische und experimentelle Untersuchungen über die Desoxydation des Eisens mit Mangan, Stahl, u. Eisen, 47, pp. 1526–1536; 1927.

found advantageous to use a silica guide tube with a straight lower end. A thin walled graphite tube is slipped over the end of the silica tube and extends downward to the level of the top of the graphite crucible. The lower end of this graphite sleeve is split to prevent excessive heating by high-frequency induction. A graphite disk is

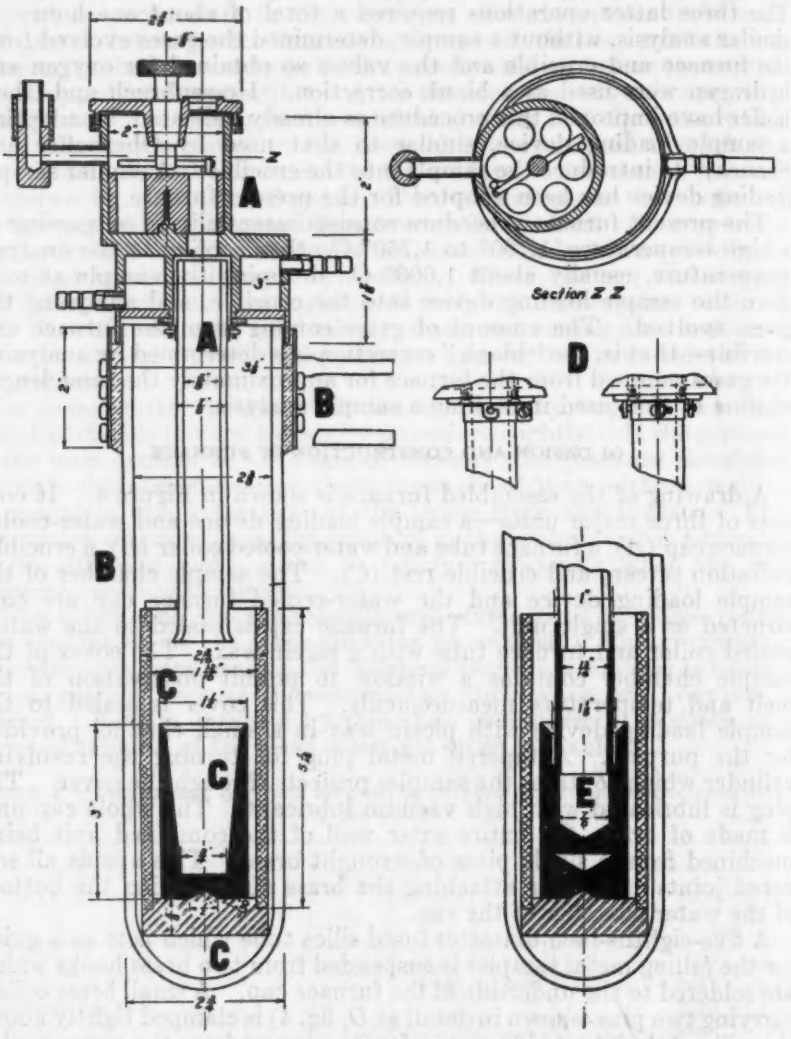

FIGURE 4.—*Details of vacuum furnace and sample loading device*

fitted over the end of the graphite extension tube and rests on the top of the graphite crucible. For analysis where it is desired to use a new crucible for each determination, the graphite extension tube and silica tube rest on a small graphite crucible which is contained within a graphite shell as shown in Figure 4, *E*. The fused silica furnace tube has a drawn-down closure at its lower end and a water-cooled

collar at its top. This water-cooled collar is fastened to the silica tube with a zinc powder-sodium silicate cement [16] in such a way that there is provided a channel for retaining in place the wax which makes the vacuum tight seal to the furnace cap. The furnace cap should rest upon the open end of the silica tube rather than on the wax or zinc cement.

The crucibles in which the metal samples are melted are machined from Acheson graphite. The base of each crucible is recessed to fit over a small cone in the center of the magnesia block upon which both the crucible and the cylindrical radiation screen rest. This construction serves to keep the crucible and radiation screen properly centered. The radiation screen may be made from sintered magnesia or more conveniently of mullite or sillimanite porcelain.

The magnesia block for supporting the crucible and radiation screen is made by tamping electrically sintered and ground magnesia, moistened with a 2 per cent magnesium chloride solution, into a machined graphite form, drying and calcining at about 1,700° C. It is important that this magnesia support should rest in the bottom of the silica furnace tube as shown in Figure 4; that is, fitting loosely with only approximately line contact with the silica, or, that it be supported on a short section of a small silica tube (⅝ or 1 inch bore) so that it never becomes tightly wedged in the larger silica tube. If the magnesia block fits the larger tube too tightly thermal expansion during heating of the graphite crucible may break the silica tube.

The assembled furnace is connected to the analytical train by a picein wax seal as shown in Figure 1.

(b) OPERATION OF FURNACE

In preparing the furnace for an analysis, the crucible is maintained at 1,700° to 1,750° C., with the diffusion pump in operation, until the pressure in the furnace drops to about 0.1 mm. Hg. Experience has shown that, if the preheating is carried to this point, subsequent gas evolution during an actual analysis at about 1,600° C. will not cause an excessively large blank. The above-mentioned pressure is arbitrary and depends upon the assembly of the furnace and the capacity of the diffusion pump. It represents a pressure that decreases but slightly during three or four hours' heating. After the preliminary heating at 1,700° to 1,750° C., the temperature is maintained at about 1,600° C. while the blank run and actual determinations are made. The pressure of the gases within the furnace during a blank analysis will be referred to as the base pressure. For a given apparatus this base pressure should be closely approximated for all blanks and at the beginning and end of all sample analyses. The precision of the blank analyses to a large extent determines the over-all precision of a sample analysis.

The data in Table 3 demonstrate the uniformity of the blank corrections for oxygen, hydrogen, and nitrogen when the same temperature and base pressure are used. In the absence of conditions which would obviously cause errors, oxygen determinations on commercial

[16] The zinc powder-sodium silicate cement is made by mixing 2 volumes of 20-mesh zinc powder and 1 volume of zinc dust. This mixture is moistened with sufficient dilute sodium silicate to form a plastic cement. Technical sodium silicate is diluted with an equal volume of water. When the cement has been packed in place it is first air dried and then further dried and hardened by heating in the flame of a hand torch.

steels are reproducible to within 0.002 per cent. If larger amounts of oxygen are present, to the extent of 0.03 to 0.06 per cent, the agreement between individual determinations usually is within 0.004 per cent.

TABLE 3.—*Magnitude of blank corrections*

	O_2	H_2	N_2
	Per cent	*Per cent*	*Per cent*
Blank No. 1	0.0031	0.00028	0.0011
Blank No. 2	.0034	.00000	.0010
Blank No. 3	.0024	.00005	.0015
Blank No. 4	.0022	.00005	.0015

NOTE.—These blanks represent the gases evolved during a 30-minute heating following the preliminary heating of the furnace. Temperature 1,550° to 1,600° C.; base pressure 0.04 to 0.03 mm. Weights of gases evolved are calculated to equivalent per cent by weight of a 20 g. metal sample.

The preceding discussion of the amount of the blank correction assumes a furnace temperature of about 1,600° C. Experience has shown that this is the optimum temperature of operation for this apparatus. Higher temperatures invariably result in larger and more irregular blanks. These factors are of greater importance than the possibility of more complete recovery of oxygen from difficultly reducible oxides at a higher temperature.

III. ACCURACY OF THE VACUUM FUSION ANALYSIS

It is common practice in determining the accuracy of analytical methods to prepare synthetic samples containing known amounts of the constituents to be determined. This was done by Jordan and Eckman [17] and the conclusion reached was that the oxygen and nitrogen of the oxides and nitrides usually encountered in commercial ferrous materials can be determined by the vacuum-fusion method. A condition was made, however, that manganese if present in sufficient quantity might affect the recovery of oxygen. In the analysis of many samples of ferrous materials, irregularities were encountered which indicated clearly that, when manganese and carbon monoxide were evolved simultaneously from the fused sample, variable amounts of oxygen would remain in the furnace. Such a condition made it impossible to assume that synthetic samples of known oxygen and manganese contents would indicate correctly the loss of oyxgen to be expected for commercial steels of the same manganese content. A close study of these analyses, considering inaccuracies caused by segregation, the conditions under which the oxides were decomposed, the manganese content of the material, and the probable composition of the oxides as indicated by residue analyses, has made it possible to define more clearly the limitations of the vacuum-fusion method.

1. SAMPLING

Iron or steel when crushed or cut to small pieces in contact with atmospheric oxygen may absorb or react with variable amounts of oxygen often sufficient to make oxygen analyses inaccurate. This

[17] See footnotes 4 and 5, p. 375.

has been previously discussed by numerous investigators [18 19 20 21] who have encountered this error in studying methods for determining oxygen in various kinds of ferrous materials. In order to avoid this difficulty, a procedure for securing and preserving samples milled under oil has been described by Cain and Pettijohn.[22] Such procedures are not commonly used with the vacuum fusion method as it is much simpler to select a few relatively large pieces, preferably only one, from the material to be analyzed and clean the samples by grinding off the surface.

The uneven distribution of oxygen in the ingot and, consequently, in finished steel has made sampling a difficult matter and the difficulty is greatly increased if the samples consist of only one or two pieces. It has been shown by Diergarten [23] that as the center of an ingot is approached from the sides, the material becomes richer in oxygen. This is also true for a short distance from the bottom of the ingot. Under these conditions the selection of one or two small pieces to represent the entire specimen, is a difficult matter. Much better agreement in results is obtained between duplicate samples taken from the same longitudinal plane than is obtained from duplicate samples in the same horizontal plane. The magnitude of these transverse segregations of oxygen will depend on the size of the original ingot and the conditions under which it was cast. As an illustration of the segregation which may be encountered, Grossman [24] cites an ingot of rimming steel which contained 0.02 per cent oxygen in the outer portions and 0.07 per cent oxygen in the core.

TABLE 4.—*Oxygen values from different portions of a commercial ingot iron plate*

Plate No.	Location of samples	
	Center portion, *a, b, c, d,* oxygen	Outer portion, *e, f, g, h,* oxygen
	Per cent	*Per cent*
812404	0.070	0.062
80496T	.081	.057
812406	.067	.059

[18] J. R. Cain and E. Pettijohn, A Critical Study of the Ledebur Method for Determining Oxygen in Iron and Steel, B. S. Tech. Paper No. 118; 1919.
[19] J. R. Eckman, Louis Jordan, and W. E. Jominy, The Oxygen Content of Coke and Charcoal Cast Irons, Trans. Am. Foundrymen's Assoc., **33**, p. 431; 1926.
[20] P. Oberhoffer and E. Piwowarsky, Ueber den Sauerstoff im Roh und Gusseisen, Stahl u. Eisen, **47**, pp. 521–533; 1927.
[21] Bengt Kjerrman and Louis Jordan, A Study of the Hydrogen, Antimony, Tin Method for the Determination of Oxygen in Cast Irons, B. S. Jour. Research, **1**, pp. 701–721; 1928.
[22] See footnote 18.
[23] See footnote 11, p. 377.
[24] M. A. Grossmen, Oxygen in Steel, Trans. Am. Soc. Steel Treat., **18**, pp. 601–631; 1930.

TABLE 5.—*Variation of oxygen values with type of sample and with location in original ingot*

Sample No.	Type of sampling	
	I, oxygen	II, oxygen
	Per cent	*Per cent*
17M	0.011 .012	0.013
17B		.018
19M	.009 .010	.017
19B		.017
21M	.007 .007	.009
21B		.009

Table 4 presents the results obtained from a series of analyses of three pieces of commercial ingot iron. Each piece was one-half of a

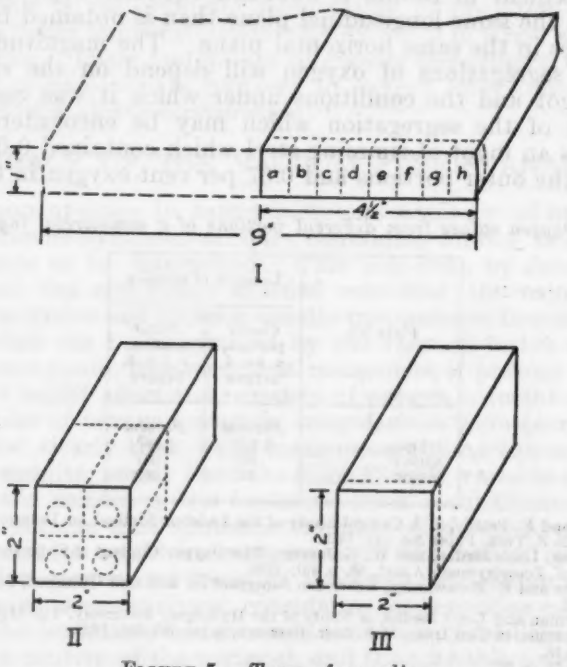

FIGURE 5.—*Types of sampling*

section cut transversely from a 1-inch thick by 9-inch wide plate of ingot iron. The pieces were sampled as indicated in Figure 5, *I*. Two groups of four pieces, *a*, *b*, *c*, *d* and *e*, *f*, *g*, *h*, were each analyzed as one sample. The analyses of the center portion of the plate, *a*, *b*, *c*, *d*, representing the center portion of the ingot, gave higher values for the oxygen content than did the outer portions of the plate. The importance of the location of check samples in the material to be analyzed is again emphasized by the results given in Table 5. Pieces were cut for sampling from 2-inch square bars of carburizing steel. Each of the

bars represented material which was initially the middle or bottom portions of the original ingot. Two types of samples were used for the oxygen determinations: First, one-half inch cylinders were machined from quarter sections of the bar (fig. 5, *II*); second, thin slices, one-eighth to three-sixteenths inch thick were cut from the bars (fig. 5, *III*). It was possible to obtain good agreement between check samples when the same type of sample was used, but it was not always possible to obtain good agreement between the two types of samples. The analyses of bars 17M from middle of ingot 17 and 17B from bottom of ingot 17 show that differences in oxygen content from bars taken from the same ingot may be encountered.

It is evident, therefore, that commercial steel which has been worked from ingots may vary considerably in oxygen content and that care should be taken in the selection of samples for an oxygen determination. As a rule, adjacent samples taken transversely to the original ingot have been found to vary considerably in oxygen content, but if taken longitudinally, the variations are usually small enough to be within the limits of the method. There does not seem to be any general rule to follow in sampling pig irons or steel castings.

2. INTERFERENCE BY VAPORIZED METALS

In the earlier work on the vacuum fusion method, it was observed that, in the case of certain materials, duplicate samples would not yield duplicate results for oxygen, no matter how carefully the samples were selected. The variation in results was greater than could be ascribed to segregation in the material, and it was observed that in any such series of samples the first analysis invariably produced much higher results for oxygen than did subsequent samples of the same material. Analyses No. 1, 2, 3, and 4 in Table 6 illustrate the results obtained on a typical series of samples. This difficulty occurred chiefly with materials which were relatively high in manganese and it was observed that after a series of runs on such material, a ring of metallic condensate had been formed on the inner wall of the heat insulator and on the silica tube just above the graphite crucible. Analysis of this condensate showed that it was chiefly manganese. The samples were all of the same composition and, therefore, should evolve the same amounts of gas when melted under the same conditions. The higher recovery of oxygen from the first sample must be due not to incomplete evolution of gas from the succeeding samples, but rather to incomplete recovery of the gases evolved. It was shown that the presence of the metallic condensate on the walls of the furnace above and near the crucible was the source of the trouble. Presumably a secondary reaction occurred, between some of the carbon monoxide evolved from a fresh sample and the condensed manganese evolved from previous samples, perhaps, according to the reaction:

$$CO + Mn = MnO + C$$

This manganese oxide is retained in the metallic condensate on the furnace walls and the amount of carbon monoxide recovered in the analytical train is correspondingly lowered.

It was found that, if the furnace was carefully cleaned after each run and all traces of metallic condensate were removed, the difficulty

disappeared and all samples of a series yielded comparable results. It was also found that if lower pressures were maintained in the apparatus throughout an analysis, comparable results could be obtained from successive samples even though the manganese condensate was present. Analyses 5, 6, 7, and 8 in Table 6 illustrate a series of results obtained at a lower pressure. It is believed that at these lower operating pressures the carbon monoxide evolved from the sample is removed from the furnace so rapidly that no appreciable reaction can occur between the carbon monoxide and the manganese condensate.

It was evident, therefore, that if manganese condensate was allowed to accumulate in the furnace, and if the carbon monoxide evolved from the samples was allowed to remain in contact with this condensate for appreciable lengths of time, low results for oxygen were obtained. This difficulty is avoided by carefully cleaning the apparatus before each determination or by operating at very low pressures.

The above discussion applies to the older procedure [25] in which a new crucible was employed for each determination. In the newer apparatus a sample loading device allowed the analysis of a number of consecutive samples without opening the furnace between runs. In this procedure the second and successive samples are melted in a crucible which contains the molten residues from the preceding determinations.

TABLE 6.—*Oxygen determinations, by the vacuum-fusion method*

Analyses No.	Type of sample	Condensed manganese	Content of crucible before addition of sample	Oxygen
				Per cent
1	Cast-iron "E," 1.29 per cent Mn.	Absent	Empty	0.040
2		Present	do	.032
3		do	do	.016
4		do	do	.003
5	do	do	do	.038
6		do	do	.036
7		do	do	.039
8		do	do	.042
9	do	Absent	Mn free residue of Ni	.045
10		Present	Mn free residue + residue No. 9	.012
11		do	Mn free residue + residue No. 9 and 10	.010
12		do	Mn free residue + residue No. 9, 10, 11	.016
13	Ingot iron, 0.059 per cent O_2	do	Residue from run 12	.033
14		do	Residue from runs 12 and 13	.037
15		do	Empty	.058
16	Cast steel "270," 0.74 per cent Mn.	do	do	.006
17		do	1 residue of 0.74 per cent Mn	.001
18	Cast steel "5922," 0.74 per cent Mn.	do	Empty	.005
19		do	2 residues of 0.74 per cent Mn	.000
20	Cast steel "5923," 0.74 per cent Mn.	do	Empty	.006
21		do	3 residues of 0.74 per cent Mn	−.001
22	Ball-bearing steel, 0.40 per cent Mn.	do	Empty	.006
23		do	do	.006
24		do	1 residue of 0.40 per cent Mn	.004
25		do	do	.005
26	Si Steel No. 1, 0.09 per cent Mn., 4.0 per cent Si.	do	Empty	.080
27		do	1 residue of 0.09 per cent Mn., 4.0 per cent Si.	.077
28	Si steel No. 2, 0.06 per cent Mn, 4.24 per cent Si.	do	Empty	.076
29		do	1 residue of 0.06 per cent Mn, 4.24 per cent Si.	.074

[25] See footnote 4, p. 375.

It was found that, under these new conditions, the troubles due to manganese reappeared even though the furnace was operated at very low pressures. If the material contained appreciable amounts of manganese the first sample of a series invariably yielded higher results for oxygen than could be obtained from the second or subsequent samples. It was concluded that, in the case of the first sample of a series, carbon monoxide is evolved from the molten sample and is carried to the absorption train, before appreciable amounts of manganese are volatilized. The second and subsequent samples, however, are melted in the residues from the preceding runs and these residues are constantly evolving manganese vapor. The carbon monoxide evolved from the second, or subsequent samples, therefore, must pass through an atmosphere relatively rich in manganese vapor before it can escape from the furnace and reach the absorption train. Carbon monoxide and freshly evolved manganese vapor might be expected to react in the same way as did carbon monoxide and condensed manganese in the earlier work. That the reaction between carbon monoxide and manganese vapor does occur, and produces low results for oxygen in the second and latter determinations of a series, is illustrated by analyses 9 to 15 in Table 6. The comparison of analyses 16 to 25, in Table 6, further shows that whenever manganese is present in appreciable amounts in the residual matter in a crucible, subsequent analyses made in that crucible will be low in oxygen but that if the crucible is empty or contains only manganese-free material, the manganese present in the sample itself does not appear to cause trouble.

TABLE 7.—*Oxygen values obtained by the vacuum-fusion method from commercial steels*

Steel No.	Chemical analyses			Vacuum-fusion analyses		
	Manganese	Silicon	Carbon	Empty crucible, oxygen	Crucible containing Mn free iron, oxgyen	Crucible containing residues of same steel, oxygen
	Per cent	*Per cent*	*Per cent*	*Per cent*	*Per cent*	*Per cent*
C-1	0.37	0.013	0.07	0.041 .041 .043	0.045 .043 .042	0.032 .029 .029
C-2	.72	.02	.13	.020	.019 .020	.013 .007 .005
C-4	.80	.15	.34	.010	.009 .010	.004 .001 < .001
C-6	.50	.24	.41	.003	.003	[1]
C-5	.65	.17	.63	.007	.008	
C-3	.24	.12	1.29	.003	.003 .004	.001 .003 .001

[1] Less than blank.

The use of the sample loading device, melting successive samples in the residues from previous determinations, presents such a saving in time and convenience, in the determination of a number of samples, that further information was desired as to the maximum amount of manganese which could be present in the residues without affecting

the results. Diergarten [26] concluded that more than 0.7 per cent manganese would cause trouble. The data in Table 6 show that manganese contents from 1.29 per cent to 0.4 per cent produce noticeable effects. In a further study of this phenomenon several steels, of different manganese contents, were each run in three different ways: (1) In an empty crucible, (2) in a crucible which contained a residue of iron quite low in manganese (about 0.05 per cent Mn), and (3) in a crucible which contained a residue with approximately the same manganese content as the sample. The results of these experiments, presented in Table 7, show that as little as 0.24 per cent manganese in the residue may produce a definite effect on the oxygen determination, and that the residue in the crucible must be essentially free from manganese if oxygen results comparable to those obtained in an empty crucible are desired. A study of these data further shows that for a given manganese content the amount of the error varies with the amount of oxygen present. It is evident, therefore, that complete recovery of oxygen can be anticipated only when an empty crucible or one containing only a manganese-free residue is used. It has been shown that as little as 0.24 per cent manganese in the residue is dangerous. It is believed that in the general run of ferrous materials the manganese present in the sample does not affect the oxygen determination, since the carbon monoxide usually is completely evolved before appreciable amounts of manganese are volatilized. Exceptional cases in which the carbon monoxide is evolved slowly, so that evolution is not complete before volatilization of manganese occurs, will be discussed in subsequent sections of this paper.

In view of this observed effect of the presence of manganese in the crucible residue, the question arose whether other metallic vapors would act in a similar manner. Analyses 26 to 29 in Table 6 indicate that the presence of about 4 per cent silicon in the residues has only a slight effect, if any, on the oxygen recovery, and certainly has no effect comparable to that of manganese.

It might be expected that aluminum, if present in appreciable amounts in the residue, would vaporize and that the aluminum vapor would interfere with the oxygen recovery as did manganese. Diergarten [27] has reported that the presence of more than 0.3 per cent aluminum caused difficulties. Metallic aluminum, at least in appreciable amounts, is not a common constituent of ferrous materials but its presence should be considered in connection with oxygen determinations.

To summarize this interference by metallic vapors in the determination of oxygen; manganese, as low as 0.24 per cent, if allowed to accumulate in the crucible will cause low results to be obtained for oxygen. This is due presumably to a secondary reaction, between evolved carbon monoxide and manganese vapor, through which some of the oxygen of the carbon monoxide is retained in the upper portions of the furnace, probably in the form of nonvolatile manganese oxide. It is evident that if 0.24 per cent manganese, or more, is present in the samples, accurate results for oxygen can be obtained only if the sample is melted in an empty crucible or in one which contains a residue free from manganese. In other words, if manganese is present in the samples the successive analysis of consecutive sam-

[26] See footnote 11, p. 377. [27] See footnote 11, p. 377.

ples in the same crucible will yield low results for oxygen. The presence of manganese in a single sample is not believed to affect the results of that determination appreciably, for the usual run of ferrous materials; that is, for samples from which the gases are evolved rapidly. The effect of condensed manganese on the upper walls of the heating chamber, from previous runs, can be largely avoided by rapid withdrawal of the evolved gases, through the use of low pressures in the furnace. A clean furnace obviously is desirable.

Some experimental evidence indicates that metallic silicon in the residues does not interfere appreciably with the determination of oxygen.

It is believed that metallic aluminum, if present in appreciable amounts, would generate vapors which would interfere with the oxygen determination in a manner similar to the interference by manganese vapor. However, metallic aluminum in appreciable amounts is not a common constituent of ordinary ferrous materials.

3. REDUCTION OF CERTAIN OXIDES

Oxygen may be present in ferrous materials in a variety of forms, such as oxides of iron, manganese, silicon, and aluminum, or in more complex combinations, such as silicates of different compositions. Furthermore, these compounds may be present in solution in the metal or as separate particles, commonly referred to as oxide inclusions. The number and size of these oxide inclusions will depend upon the steel-making practice employed, but in clean steel the total amount of inclusions and the average size are relatively small. Occasional large inclusions, if present, should be avoided in the selection of samples.

The different oxide compounds will vary in ease of reduction and for a given compound the rate of reduction will vary inversely with the size of the particles. Obviously, complete reduction of the oxide compounds is essential. It is also important that this reduction be completed within a reasonable time, since the blank correction becomes unreliable and too large if the determination is unduly prolonged. Oxides of silicon and aluminum and complex silicates obviously will be more difficult to reduce than the oxides of manganese or iron. It is believed that these latter oxides are quickly and completely reduced under the conditions of a vacuum-fusion analysis, namely, saturation of the melted sample with carbon in a graphite crucible maintained at about 1,600° C., and the maintenance of a low pressure (about 2 mm. of mercury) over the fused sample during reduction.

Jordan and Eckman [28] investigated the reduction of silica and silicates in a number of synthetic samples. In the preparation of these samples electrolytic iron was freed from oxygen by vacuum fusion in a graphite crucible. The resulting iron-carbon alloy, oxygen free, was divided into portions of about 20 g. each, and a small hole was drilled in each piece. A weighed amount of silica was placed in the hole and the sample of iron-carbon alloy plus silica, in a graphite crucible was subjected to a vacuum fusion determination for oxygen. The high recoveries of oxygen obtained from this relatively coarse silica led to the belief that satisfactory recovery could be expected for

[28] See footnote 4, p. 375.

the oxygen present as silica or silicates in steel, in the finely divided form normally encountered. Diergarten [29] confirmed this belief but Thanheiser and Müller [30] reported that oxygen combined as silica was only partially recovered by the vacuum-fusion method. Their conclusions were based on the observation that only 70 per cent of the oxygen in a low-carbon steel was recovered when the sample was melted in a crucible which already contained a high-silicon residue. This experiment was repeated in the present investigation. Approximately 12 g. of ingot iron which contained 0.06 per cent oxygen was dropped into a residue which contained 4 per cent silicon. After one hour of heating at 1,500° to 1,550° C., twice the time required for decomposition of a normal sample, the pressure within the furnace was still above the base pressure, indicating that reduction of oxides was not yet complete. During this hour about 70 per cent of the oxygen present in the sample was recovered in the analytical train. Visual observations during the run indicated the presence of relatively large particles floating on the surface of the melt. From these observations and from the fact that the pressure in the furnace remained higher than usual, it was concluded that the oxygen present in the ingot iron had reacted with silicon of the residue, to form relatively large agglomerates of silica which were decomposed only slowly. It is believed that this agglomeration of silica into relatively large particles, which are only slowly decomposed, is a phenomenon peculiar to the conditions of this and Thanheiser and Müller's experiment; that is, the addition of a sample rich in iron oxide to a residue rich in silicon. The presence of a high-silicon residue in the crucible did not produce a definite effect on the recovery of oxygen in analyses 26 to 29 cited in Table 6. Many samples of steel known to contain silicon and silica or silicates have been analyzed by the vacuum-fusion method and in the great majority of cases decomposition has proceeded rapidly to completion, as indicated by the observations of pressure within the furnace. Comparison of results for oxygen by the vacuum-fusion method and by the HCl residue analysis method, discussed in subsequent sections of this paper, indicates that complete recovery of oxygen from silica and silicates is obtained by the vacuum-fusion method.

It is believed, therefore, that oxygen is satisfactorily recovered, by the vacuum-fusion method, from the silica or silicates ordinarily present in steel, but that the presence of unusually large silica or silicate particles may require an abnormal length of time for complete reduction. If manganese is present in the sample it has been shown that satisfactory results for oxygen can be obtained only when the gas evolution is rapid as well as complete. Since manganese is present in practically all ferrous materials, large silicate inclusions or any other compounds which extend the time required for complete reduction are undesirable. It is believed, however, that in a normal determination the rapid return of the pressure in the furnace to the initial pressure indicates the complete reduction of silica or silicates present. If difficulty develops it will be indicated by abnormal pressures in the furnace.

Alumina is another difficultly reducible oxide which must be considered. Jordan and Eckman [31] and Diergarten [32] concluded that

[29] See footnote 11, p. 377. [30] See footnote 10, p. 376. [31] See footnote 4, p. 375. [32] See footnote 11, p. 377.

alumina could be decomposed in a vacuum-fusion analysis. This conclusion is believed to be correct for the amount of alumina (a very few thousandths of 1 per cent) ordinarily encountered in commercial ferrous materials. However, experiments have shown that if unusual amounts of alumina are present, decomposition is not always complete within the time limit imposed by the presence of manganese. This statement is based on the identification of unreduced alumina in the residues from vacuum fusion determinations on certain steels known to contain relatively large amounts of alumina.

The data presented in Table 8, discussed in subsequent paragraphs, show that when the alumina in steel is not more than the few thousandths of 1 per cent ordinarily encountered, the amount of oxygen recovered by a vacuum fusion determination is at least as great as, and usually greater than, the oxygen recovered by residue methods of analysis. The results for sample C–6 in Table 8 particularly show that as much as 0.003 per cent alumina is completely recoverable within reasonable limits of error by a vacuum fusion determination. This is about the maximum amount of alumina present in most commercial steels. However, the data in Table 8 also show that if larger amounts of alumina, one or two hundredths of 1 per cent, should be present as in the TA samples, the oxygen recovered by a vacuum fusion is definitely less than that recovered by residue methods of analysis. Attention is called to the fact that in these TA samples the greater part of all the oxygen present is present as alumina due to unusually large additions of aluminum to the ladles. It is evident that these amounts of alumina are not completely reduced rapidly enough to avoid the interference of secondary reactions such as that with manganese vapor.

It is concluded that the vacuum-fusion method of an analysis is applicable to steels which contain only the customary few thousandths of 1 per cent of alumina, but that if unusual amounts of alumina are present in the sample, low recoveries of oxygen will be obtained.

4. PROBABLE ACCURACY OF THE OXYGEN DETERMINATION

It is obvious that the successful application of the vacuum-fusion method for oxygen depends upon the complete decomposition of the oxides present in the sample. Earlier investigators concluded that all of the oxides normally present in ferrous materials could be decomposed in a vacuum-fusion analysis. This conclusion was based on analysis of synthetic samples. More recently, it has been recognized that this decomposition in many cases must be rapid as well as complete, to avoid interference by the vapors of volatile metals, such as manganese, which are present in many ferrous materials. The determination of the accuracy of the method for oxygen is made difficult by the lack of reliable, independent methods of analysis, to confirm or disprove the results obtained by the vacuum-fusion method.

TABLE 8.—*Analyses of steels*

Steel No.	Analyses of HCl residue [1]			Vacuum-fusion oxygen	Chemical analyses		
	Silica oxygen	Alumina oxygen	Total oxygen		Silicon	Manganese	Carbon
	Per cent	*Per cent*	*Per cent*	*Per cent*	*Per cent*	*Per cent*	*Per cent*
98T	0.004	0.002	0.006	0.013	0.40	0.72	0.22
98TA	.003	.013	.016	.012			
99T	.009	.001	.010	.015	.30	.67	.21
99TA	.001	.016	.017	.011			
04T	.012	.001	.013	.019	.37	.69	.25
04TA	.004	.009	.013	.008			
05T	.014	.002	.016	.025	.35	.73	.19
05TA	.001	.020	.021	.016			
C–1	.002	.002	.004	.043	.013	.37	.07
C–2	.002	.001	.003	.020	.02	.72	.13
C–4	.003	.001	.004	.010	.15	.80	.34
C–5	.001	.001	.002	.007	.17	.65	.63
C–6	.001	.003	.004	.003	.24	.50	.41

[1] These values were obtained from an analysis of the hydrochloric acid residue; the details of procedure are briefly described in B. S. Jour. Research, 5, p. 1141; 1930.

The data in Table 8 illustrates results obtained for certain samples of steel. Each pair of T and TA samples represent material from the same ladle of finished steel, the T sample containing no ladle addition and the TA sample representing the T metal after a ladle addition of 1 pound of aluminum per ton of steel. The C samples were selected from stock material. The results for the T series (0.70 Mn) show that when appreciable amounts of silica, but only small amounts of alumina are present, more oxygen is recovered by the vacuum-fusion method than by the residue methods. The difference between the oxygen values by the vacuum-fusion method and by the HCl-residue method averages 0.006 per cent in favor of the vacuum-fusion oxygen. Herty [33] has calculated that iron prepared under steel-making conditions to contain 0.2 per cent carbon, will probably contain about 0.03 per cent dissolved oxygen, whereas if 0.2 or 0.3 per cent silicon is present the steel will contain approximately 0.006 per cent of dissolved oxygen. If this amount of dissolved oxygen is added to the total from the residue analysis of each of the T samples, the agreement with the corresponding vacuum-fusion results is almost perfect. This indicates that the vacuum-fusion results for oxygen correctly represent the total oxygen present in the case of samples which contain appreciable amounts of silica and small amounts of alumina, even in the presence of about 0.70 per cent manganese.

In the C series, samples 1 and 2 contain less of both carbon and silicon than do the T series. The dissolved oxygen, therefore, would be greater and, hence, the vacuum-fusion results are higher than the sum of the residue analyses. Samples 4 and 5 approach the previous composition and for these two samples the assumption of 0.006 per cent dissolved oxygen brings excellent agreement between the vacuum fusion and residue determinations. In sample 6 evidently more heavily deoxidized with aluminum than were the other C samples, it appears that little or no dissolved oxygen is present. In this case the vacuum fusion and residue oxygens agree directly without correction. It appears, therefore, from consideration of these C samples, that

[33] C. H. Herty, Jr., and coworkers, The Physical Chemistry of Steel Making, Min. and Met. Investig. Bull., 34, and Bull. 36, Carnegie Inst. of Tech., Pittsburgh, Pa.

complete recoveries of oxygen can be obtained when small amounts of silica and alumina are present, even in the presence of appreciable amounts of manganese.

In the case of the TA samples different conditions are encountered. Deoxidation of the steel in the ladle, through the addition of unusually large amounts of aluminum, resulted in the presence of unusually large amounts of alumina in the samples. The fact that the silica content of each TA sample is lower than that of the corresponding T sample indicates that the dissolved oxygen has been eliminated from the TA samples, since the reaction between aluminum and dissolved oxygen presumably would precede any reaction between aluminum and silica. In view of this absence of dissolved oxygen, and the previous discussion of the slow decomposition of alumina, it is not surprising that in these TA samples the oxygen recovered by the vacuum-fusion method is less than the sum recovered by residue methods of analysis. Attention is directed to the fact that the T and TA samples were identical except for the addition of aluminum in the ladle in the case of the TA samples. The total oxygen of the T and corresponding TA samples, therefore, should be the same although the oxygen is present in different states of combination. In the TA series the sum of the oxygen combined as alumina and silica, determined by residue analyses, is in good agreement with the vacuum-fusion oxygen for the corresponding samples of the T series. This is further evidence of the correct determination of total oxygen by the vacuum-fusion method for samples such as the T series, where manganese and only small amounts of alumina are present. If larger amounts of alumina are present, and if all the oxygen present is combined as silica and alumina, as in the TA series, the vacuum-fusion results for total oxygen will be low, but for such material the HCl-residue method of analysis will indicate the correct result. The vacuum-fusion method, therefore, is preferable when dissolved oxygen is present, and residue methods of analysis are preferable when a large part of the oxygen is combined in difficultly reducible forms.

The oxygen, presumably present as ferrous oxide, in ingot iron or in other forms of relatively pure iron, is readily determined by the vacuum-fusion method. The only exception to this statement so far encountered, was in the case of a high oxygen ingot iron melted in the presence of a high-silicon residue. Under these conditions silica was formed and for some unknown reason the silica agglomerated to form a few unusually large masses which decomposed very slowly. Oxygen recovery in this case was low, but the circumstances were unusual and the results are not at all representative of results for this type of material.

The cooperative analysis in Table 9, previously published elsewhere,[34 35] illustrate the results which may be obtained on material such as ingot iron. Samples prepared at the National Bureau of Standards were submitted to Prof. C. H. Desch, at the University of Sheffield, Sheffield, England, and to the late Prof. P. Oberhoffer, at the Institute für Eisenhüttenkunde, Aachen, Germany. After the death of Professor Oberhoffer the analyses at Aachen were completed by Doctor Hessenbruch. At Sheffield the hydrogen reduction method

[34] B. S. Tech. News Bull. No. 128, December, 1927.
[35] W. Hessenbruch, Procédé rapide amélioré pour la determination dez gaz dans les métaux, en particulier de l'oxygène dans l'acier, Rev. Met., **26**, pp. 93–114; 1929.

was employed, with the addition of antimony-tin alloy. At Aachen the samples were decomposed by vacuum fusion in graphite and the gases were determined by volumetric methods. At the National Bureau of Standards the samples were decompoesd by vacuum fusion and the gases were determined by a gravimetric method. These results for the hydrogen reduction and vacuum-fusion methods, show that the oxides in this type of material are completely decomposed by the vacuum-fusion procedure. The data also illustrate the agreement which can be obtained between different operators using the vacuum-fusion method. Similar agreement has been obtained in other cooperative analyses.

TABLE 9.—*Cooperative analyses of ingot iron*

(0.04 C, 0.03 Mn, 0.02 S, 0.006 Si.)

Sheffield hydrogen reduction (oxygen)	Aachen vacuum fusion, volumetric (oxygen)	National Bureau of Standards vacuum fusion, gravimetric (oxygen)
Per cent	*Per cent*	*Per cent*
0.056	0.055	0.057
.057	.059	.059
.049	.062	.058
.048	----------	.058
.049	----------	----------
.051	----------	----------
Ave. 0.051	0.059	0.058

It is believed, therefore, that the total oxygen in many ferrous materials is correctly indicated by a vacuum-fusion determination when the oxygen is present in the sample in the form of ferrous oxide, manganese oxide, and finely divided silica or silicates. Large particles of silica or silicates require too much time for complete decomposition, but the presence of such large particles in a sample indicates either poor material or faulty sampling. If alumina is present in ordinary amounts, not more than 0.003 per cent, satisfactory results are obtained by the vacuum-fusion method for oxygen. If unusual amounts of alumina are present (more than 0 01 per cent) low recovery of oxygen will result because of the slow decomposition of alumina. The presence of manganese in a sample does not interfere with the vacuum-fusion determination of oxygen unless the evolution of carbon monoxide from the sample is unduly prolonged on account of the presence of refractory oxides, particularly alumina. However, the successive determination of a series of samples, using the sample loading device to drop each fresh sample into the crucible which contains the residues from previous samples, is not feasible if the samples contain manganese. Any manganese present in the crucible, in residues from previous fusions, evolves manganese vapor which will result in low recoveries of oxygen from subsequent samples melted in that crucible.

The foregoing considerations and data are interpreted to indicate that the total oxygen in ingot iron, in other forms of relatively pure iron, and in plain carbon steels, is correctly indicated by the results of a vacuum-fusion analysis. The principal difficulty encountered

has been due to the presence of unusually large amounts of alumina and this difficulty is increased by the presence of manganese in the sample. It is difficult to determine the effect of metallic alloying elements on the recovery of oxygen by a vacuum fusion, but so far none of the common alloying elements, except manganese, has been shown to be dangerous. It is believed that the method is adaptable to many alloy steels as well as to the plain carbon steels. The presence of refractory oxides, such as alumina, causes low recovery of oxygen by the vacuum fusion method. With such samples, better recoveries of oxygen are obtained by residue methods.

5. ACCURACY OF THE NITROGEN DETERMINATION

Analyses of synthetic nitrides by solution methods and by the vacuum-fusion method [36] showed that the nitrides, which might be present in ordinary steels, are decomposed as completely, sometimes more completely, by the vacuum-fusion method than by the solution methods. In these experiments the nitrogen evolved in the vacuum fusion was absorbed in calcium vapor and was subsequently determined by a solution-distillation method. This required the use of separate samples for the nitrogen and for the oxygen determinations. In the procedure described in this paper, the residual gas in the analytical train, after the absorption of carbon dioxide and water vapor, is assumed to be nitrogen. The amount of this gas is determined by a volumetric method, thus permitting the determination of hydrogen, oxygen, and nitrogen on the same sample. Comparison with results obtained by a solution method, illustrated by the data in Table 10, indicates that this vacuum-fusion method yields correct values for nitrogen. The data in Table 10 also show that the presence of manganese does not affect the determination of nitrogen. In fact, no interferences of any kind have been observed in the determination of nitrogen by the vacuum-fusion method.

It is believed, therefore, that the present vacuum-fusion procedure for nitrogen in ferrous materials yields correct results and is not subject to interference.

No attempt has been made to establish the accuracy of the vacuum-fusion method for hydrogen, since hydrogen is present only in insignificant amounts in most ferrous materials.

[36] L. Jordan and F. E. Swindells, Gases in Metals: I. The Determination of Combined Nitrogen in Iron and Steel and the Change in Form of Nitrogen by Heat Treatment, B. S. Sci. Paper No. 457; 1922.

TABLE 10.—*Nitrogen values obtained from commercial steels by vacuum fusion and solution methods*

Steel No.	Nitrogen by vacuum-fusion method			Nitrogen by solution method, nitrogen	Manganese
	Empty crucible, nitrogen	Crucible containing Mn free iron, nitrogen	Crucible containing residues of same steel, nitrogen		
	Per cent	*Per cent*	*Per cent*	*Per cent*	*Per cent*
C-1	0.009 .008 .010	0.008 .007 .007	0.008 .009 .008	0.007	0.37
C-2		.014 .013	.013 .012 .010	.014	.72
C-4	.004	.004 .005	.004 .004 .003	.006	.80
C-6	.004	.004	.003	.005	.50
C-5	.004	.004	.002 .002	.005	.65
C-3	.007	.006 .008	.006 .007 .007	.006	.24

IV. SUMMARY AND CONCLUSIONS

Apparatus and procedure for the determination of hydrogen, oxygen, and nitrogen in ferrous materials by the vacuum-fusion method are described in detail.

The results of a number of analyses of ferrous materials are discussed. The data indicate that the method, (in the absence of interferences) gives values reproducible to within 0.002 per cent for either oxygen or nitrogen. The data also indicate that the accuracy of the oxygen determination is affected only when the steel contains a relatively large amount of alumina and manganese or when the fusion is made in a crucible which already contains a residue in which manganese is present. No similar influences have been encountered, which would affect the accuracy of the nitrogen determination.

The oxides commonly encountered in ferrous materials, with the exception of alumina, are probably completely decomposed shortly after the sample has melted. The time of decomposition, when the sample does not contain relatively large amounts of alumina, is approximately five minutes. If the decomposition should require a longer time, the harmful effect of manganese is increasingly evident.

Manganese affects an oxygen determination when it is simultaneously present as vapor with carbon monoxide immediately above the crucible. Such a condition results in the formation of a nonvolatile compound, presumably manganese oxide, which deposits in the cooler parts of the furnace and, consequently, is not determinable with the present apparatus. The effect of manganese vapor has been detected from residues containing as little as 0.2 per cent manganese. Therefore, it is recommended that analyses be made in crucibles

free from manganese. A relatively slow decomposition of oxides in the presence of manganese vapor is considered to be the most serious source of error so far identified in the oxygen determination.

V. ACKNOWLEDGMENTS

The authors acknowledge their indebtedness to R. J. Kranauer and L. H. Phelps, former members of the staff of the National Bureau of Standards, for assistance in the experimental work; to J. S. Acken for analyses by the residue and solution methods; and to H. A. Bright for advice in the development of the project.

WASHINGTON, May 21, 1931.

SOME ELECTRICAL PROPERTIES OF FOREIGN AND DOMESTIC MICAS AND THE EFFECT OF ELEVATED TEMPERATURES ON MICAS

By A. B. Lewis, E. L. Hall, and F. R. Caldwell

ABSTRACT

A number of samples of mica, fairly representative of the major sources of the world's supply of mica, have been tested for dielectric constant, power factor, dielectric strength, and ability to withstand elevated temperatures. The results of these tests are as follows:

For clear ruby muscovite, in the frequency range from 100 to 1,000 kc., a dielectric constant of 7.2 and a power factor of 0.02 per cent may be expected on the average. Individual samples may be expected to vary on the average from these values by ± 0.3 in dielectric constant and ± 0.01 per cent in power factor. The presence of stains or inclusions so seriously affects the power factor as to render such stained micas unsuited for radio purposes. The power factor of phlogopite is found to be so high as to render it unsuited for radio purposes.

The dielectric strength of mica is found to be relatively unaffected by the presence of air bubbles, and but slightly affected by the presence of moderate amounts of stains in the form of metallic oxides. Curves showing the average dielectric strength of various classes of mica as a function of the thickness of the specimen are given.

With but two exceptions all the micas investigated were unaffected by an exposure to a temperature of 600° C. for 30 minutes. Above that temperature the phlogopites withstood heating better than did the muscovites.

In none of these tests was it possible to make any distinction between the various micas based solely on the geographical origin of the samples.

CONTENTS

	Page
I. Introduction	403
II. Experimental procedure	404
1. Classification of specimens	404
2. Dielectric constant and power factor measurements	404
3. Dielectric strength measurements	406
4. Effects of elevated temperatures	408
III. Results	409
1. Dielectric constant and power factor	409
2. Dielectric strength	410
(*a*) Preliminary investigations	410
(*b*) Final measurements	412
3. Effects of elevated temperatures	416
IV. Discussion and conclusions	417

I. INTRODUCTION

Much work has been done at various times and by various workers on those properties of mica which are of importance to the electrical industry. Little attempt seems to have been made, however, to make a comprehensive comparison of the properties of micas obtained from widely separated localities. Such information should be of

interest and value to users of mica as well as to those who are called upon to set up specifications for its purchase. Such a comparison should indicate the average values of power factor or dielectric strength, for example, to be expected from the various grades of mica as well as the normal variations from those averages which must be expected in commercial lots of mica. It should indicate also whether or not there is any correlation between the properties of mica and its geographical origin. Such data would form a more satisfactory basis for the choice and specification of mica than has heretofore been available.

It was the purpose of the present investigation to compare the average dielectric constant, power factor, dielectric strength, and ability to withstand heat of micas of different qualities as well as the average differences in these properties to be expected between samples taken from the same locality, and between samples of like quality taken from widely different localities. It is recognized that this list of properties is far from complete. Many important properties, such as resistance to abrasion, ability to split into thin perfect sheets, ability to withstand rolling into small tubes, etc., have not been considered. The uses of mica are so manifold and specialized that an exhaustive investigation was not considered practicable at this time. It is believed, nevertheless, that the data presented here should be useful to both the producer and the buyer of mica.

This investigation was undertaken at the suggestion of the United States Bureau of Mines. The writers are indebted to F. W. Horton, of the Bureau of Mines, for supplying and identifying the large number of samples of mica used in these tests.

II. EXPERIMENTAL PROCEDURE

1. CLASSIFICATION OF SPECIMENS

There were available for the purposes of these tests 57 separate lots of mica. Of these, 19 lots were from foreign sources and 38 from domestic. The domestic micas consisted of ruby and green muscovite and one specimen of biotite. The foreign micas consisted of ruby muscovite from Africa, Argentine, Brazil, and India; green muscovite from Guatemala; brown mica from Africa; and amber mica or phlogopite, from Madagascar and Canada.

These micas were roughly classified when received as being clear, slightly stained, or heavily stained. For the purposes of the dielectric strength measurements the stained micas were further subdivided into two groups according to whether the staining was caused by the presence of air bubbles or of characteristic black or red inclusions. Concerning these latter stains it may be said in general that they are metallic oxides, generally iron oxides in the form of magnetite or hematite.

2. DIELECTRIC-CONSTANT AND POWER-FACTOR MEASUREMENTS

The power loss of a specimen is derived from the measured equivalent resistance of a circuit containing a condenser prepared from an individual sheet of the insulating material under investigation. The resistance of the circuit is again measured after replacing the sample condenser by a standard condenser whose losses are either negligible or known. The difference between the two measured values gives

the resistance of the sample condenser. The power factor in per cent is then calculated from the equation:

$$\text{Power factor (in per cent)} = 6.283 \times RCf \times 10^{-7}$$

where

R = resistance of the sample in ohms.
C = capacitance of the sample in micromicrofarads.
f = frequency in kilocycles per second at which the measurement was made.

The dielectric constant is calculated from the observed data by the following equation:

$$K = \frac{11.3\ C\ t}{S}$$

where

K = the dielectric constant.
C = capacitance of the sample in micromicrofarads.
t = thickness of the sample in centimeters.
S = area of sample in square centimeters.

Further details of the method of measurement may be found in Bureau of Standards Scientific Paper No. 471, Methods of Measurement of Properties of Electrical Insulating Materials. Similar specifications for such radio-frequency measurements may be found in the American Society for Testing Materials specifications Tentative Methods of Testing Electrical Insulating Materials for Power Factor and Dielectric Constant at Frequencies of 100 to 1,500 Kilocycles, A. S. T. M. designation: D150–27T.

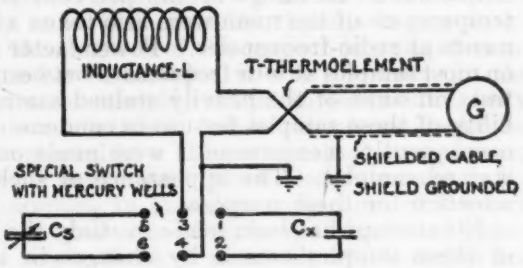

FIGURE 1

A schematic diagram of the circuits used is shown in figure 1.

The question of the best method of preparing the test condensers is one for which no perfectly satisfactory solution has yet been found. The usual method of floating the test specimen on mercury with an upper mercury electrode is impracticable here because of the thinness and flexibility of the samples. On the other hand, the method of inserting the sheet of material between the plates of a parallel plate condenser of known dimensions, as well as that of using mercury electrodes contained between rubber dams,[1] each seems open to serious objections. Test condensers were, therefore, made up in the following manner from the samples of mica submitted. A sheet of mica was covered on one side with a sheet of tin foil, linseed oil being first applied to the mica and then removed by wiping with a clean, dry cloth. After this process, sufficient oil remained to cause the tin foil to adhere to the mica. One or two pieces of tin foil 3 by 4 cm. were then attached to the opposite side of the mica in the same manner.

[1] D. W. Dye and L. Hartshorn, The Dielectric Properties of Mica, Proc. Roy. Soc., 37, pp. 42–57; 1924.

Care was taken to apply these small tin foil plates on sections of mica free from air pockets or other appearances of nonuniformity. It is well known that the presence of air pockets seriously affects the dielectric properties of mica.[2] The use of two pieces of tin foil gave two test condensers for a given mica sample, but measurements were not made on all the condensers thus prepared. This method of preparing the sample is itself open to the objection that it introduces two films of oil of unknown thickness into the test condenser. It was found experimentally that clear muscovite specimens prepared in this manner showed a power factor of 0.01 to 0.03 per cent. (See Table 1.) This is a quantity of the order of magnitude of the sensitivity of the apparatus and of the losses present in the air condenser used as a standard. These data are taken to indicate that the effect of the oil films on the power factor is certainly not more than 0.01 per cent. The effect of the oil films on the dielectric constant is more difficult to estimate. Fortunately, however, an exact knowledge of the dielectric constant is of much less importance commercially than a knowledge of the power factor.

The capacitance of the test condenser was first measured on a direct reading microfaradmeter at 500 cycles per second. This measurement was of value in starting the measurements at radio-frequencies. Readings of the per cent relative humidity and the temperature of the room were also taken at the time of the measurements at radio-frequencies. Power-factor measurements were made on most samples at four frequencies between 100 and 1,000 kc. A few tests on some of the heavily stained samples indicated the unsuitability of these samples for use in condensers for radio purposes, and, consequently, measurements were made on only a few of the heavily stained samples. The appearance of such samples is against their selection for these purposes.

No attempt has been made to study the effect on the power factor of these samples caused by changes in temperature or humidity. Both of these factors are known to alter the power factor.

3. DIELECTRIC STRENGTH MEASUREMENTS

Several factors must be considered in specifying the experimental conditions under which the dielectric strength of a material is determined. It is of primary importance that the arrangement of the electrodes and the nature of the surrounding medium be such as to subject the specimen under test to a known, reproducible, and preferably uniform, electric stress. Some observers have obtained this result by using flat electrodes with well rounded edges, immersed in a medium having the same dielectric constant as the material under test.[3] In this case a uniform electric stress is produced in the specimen. Other observers have used spherical electrodes, or one spherical electrode against a plane electrode.[4] In case the surrounding medium has the same dielectric constant as the medium under test a nonuniform, but known, electric field is produced. In case the surrounding medium has a dielectric constant different from that of the material under test a nonuniform field is produced which

[2] J. R. Weeks, The Dielectric Constant of Mica, Phys. Rev., **19**, pp. 319-322, 1922.
[3] F. Grünwald, The Breakdown of Solid Laminated Insulating Materials Under Various Experimental Conditions, Archiv. f. Elektrot., **12**, p. 79; 1923.
[4] L. Inge and A. Walther, The Breakdown of Glass in Homogeneous and Nonhomogeneous Electric Fields, Archiv. f. Elektrot., **19**, p. 257; 1927. Breakdown of Solid Insulators, Archiv. f. Elektrot., **22**, p. 410; 1929.

is not as yet capable of computation. The American Society for Testing Materials specifications for testing sheet materials [5] call for 2-inch flat electrodes immersed in oil to prevent corona and flash over. Other observers have used mercury electrodes[6] and other devices suitable for use with materials which can be worked or molded.

Within the range of ordinary power frequencies it is probable that the effect upon the breakdown voltage of a change in the frequency of the applied alternating voltage is slight. Such an effect exists, however, and it has been shown that the dielectric strength of mica at frequencies of the order of 200,000 cycles per second is appreciably lower than at 50 cycles per second.[7] How much of this difference is real and how much is due to the inherent difficulties in measuring such high-frequency voltages is not certain. In the light of the theories of breakdown as caused by the formation of hot spots or hot filaments it is also important to specify the time interval during which the specimen was subjected to the electric field before breakdown occurred, as well as the temperature of the specimen.

It is assumed that such self-evident factors as the elimination of corona and flash over at the surface of the specimen and the choice of a suitable power supply need not be discussed here.

It is to be expected that the results in work of this kind will scatter widely. Where large numbers of samples are to be tested the number of observations necessary to obtain consistent results begins to be considerable. As it was the purpose of the present investigation to test a relatively large number of samples, it was necessary, in the choice of apparatus, to give considerable weight to ease and rapidity of operation. For these reasons it was decided to use as electrodes 1-inch metallic spheres immersed in a light mineral oil (transformer oil) to prevent corona and flash over. Such electrodes are easily constructed and are self-aligning in operation. Because of the fact that the spheres test only a small area of surface, a number of punctures can be made on a single sheet of material, which makes for rapidity in testing. This fact, however, will also tend to produce an increased scattering among the individual observations and to indicate a higher average dielectric strength than would be the case if flat electrodes were used. The fact that the electric field in a sheet of dielectric material placed between two spheres is not readily capable of computation is a disadvantage when comparing the results presented here with the results of other observers, but is of no great importance in the relative comparisons made in this paper.

In making the tests one of the spherical electrodes was connected to one high-voltage terminal of a step-up transformer giving a maximum of 25,000 volts and rated at 3 kilovolt amperes. The other side of the transformer as well as the other sphere was grounded. This transformer was supplied with 60-cycle alternating voltage of practically sine wave form. The high voltage was measured by means of a step-down transformer of the same ratio and rating as the supply transformer. The high-voltage coils of this step-down transformer were placed in parallel with the sphere gap and with the high-voltage coils of the step-up transformer, and the resulting secondary voltage was read from a voltmeter across the secondary terminals of the step-down transformer. These voltage readings could be made with

[5] Am. Soc. Testing Materials Specification D 149-30*T*.
[6] P. H. Moon and A. S. Norcross, Three Regions of Dielectric Breakdown, J. Am. Inst. Elec. Eng., 49 p. 125; 1930.
[7] See footnote 3, p. 406

an accuracy of about 1 per cent. These voltage readings multiplied by the ratio of transformation of the step-down transformer, which was accurately known, gave the total voltage across the specimen under test. The thickness measurements were made on a dial micrometer on which 0.1 mil [8] could be read by estimation.

A schematic diagram of the circuit used is shown in Figure 2.

In making the tests three representative samples were taken from each lot of mica and split to thicknesses of approximately 1, 5, and 9 mils, respectively. With careful splitting it was possible to obtain specimens of sufficient size on which the thickness was constant to within 0.1 or 0.2 mil over the entire surface of the specimen. In the case of the amber micas (phlogopites), their uneven surface made this measurement uncertain to about 0.5 mil on the thicker pieces. The specimen was then inserted between the spheres and an initial low, 60-cycle, voltage applied. The voltage was then raised continuously at the rate of approximately 800 volts per second until breakdown occurred. During this process the voltage across the secondary terminals of the step-down transformer was continuously observed

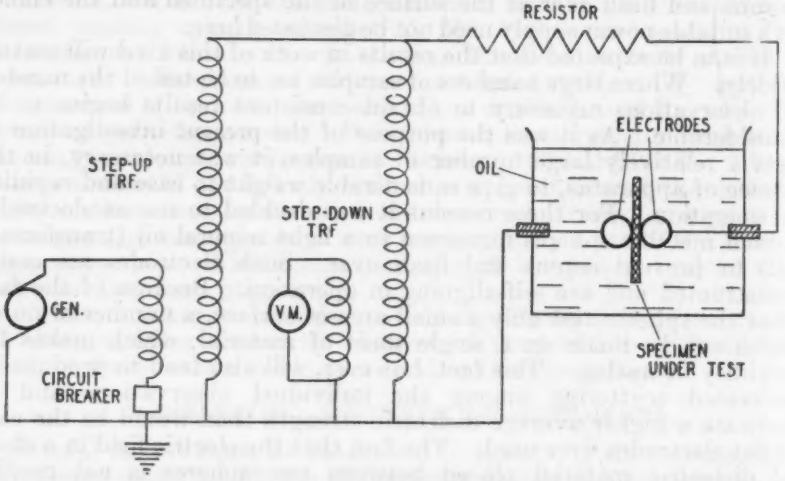

FIGURE 2.—*Schematic diagram of dielectric-strength apparatus*

by means of a voltmeter connected across its secondary terminals. The maximum reading of this voltmeter, taken at the instant breakdown occurred, when multiplied by the known ratio of transformation of the transformer, was taken to be the voltage across the specimen at the instant of breakdown. Excessive surges in the line at the instant of breakdown were prevented by a resistor of approximately 20,000 ohms in series with the test specimen, as is shown in Figure 2.

4. EFFECTS OF ELEVATED TEMPERATURES

The samples used in investigating the effects of elevated temperatures were 1 by 2.5 cm, cut from the best pieces of each kind of mica available. Eight samples of each kind were used in these tests, all samples from the same lot being originally of the same thickness. One sample from each lot was not heated. The other seven samples were heated on an alumina plate in a furnace of sensibly uniform temperature to temperatures of 600°, 700°, 800°, 900°, 1,000°, 1,100°,

[8] 1 mil is 0.001 inch.

and 1,200° C., respectively, and held at these temperatures for one-half hour. The rate of heating was rapid, the time required to reach the test temperature ranging from 35 minutes in the tests at 600° C. to about one and one-half hours in the tests at 1,200° C. No external force was applied to the specimens during these tests. The deformations and other changes observed are thus due solely to the temperatures to which the specimens were subjected.

After the samples had been heated they, together with the unheated samples, were mounted and examined to determine the effects of the heating. The various properties of the samples were graded according to the following scheme: (*a*) Color, (*b*) condition of surface, (*c*) opacity of the sample, (*d*) separation of laminae, (*e*) texture, (*f*) form and size as given by the dimensions of the sample before and after heating.

III. RESULTS

1. DIELECTRIC CONSTANT AND POWER FACTOR

A few measurements on stained micas served to confirm the well-known conclusions of other observers that stained micas are unsuited for radio purposes. Slightly stained samples showed power factors of the order of 0.10 per cent, while heavily stained samples showed power factors of 8.0 per cent or higher. The phlogopite specimens also showed power factors of from 0.4 to 7.0 per cent. In both of these cases the power factor was a function of frequency, increasing with decreasing frequency. There was no definite evidence that the dielectric constant was a similar function of frequency, or that there was any close relation between the dielectric constant and the amount of stain present.

In the case of the clear micas, both dielectric constant and power factors were, within the accuracy of the measurements, independent of the frequency. In Table 1 are given the average values of dielectric constant and power factor obtained in the present investigation. In the same table are included, for comparison, some of the values reported in the recent literature on mica.

TABLE 1.—*Dielectric-constant and power-factor measurements on mica*

Number of samples	Origin	Kind	Observers	Temperature	Frequency	Dielectric constant		Power factor	
						Average	Spread	Average	Spread
				° *C.*				*Per cent*	*Per cent*
16	United States and India.	Clear muscovite.	(1)	25	100–1,000 kilocycles.	7.20	8.69–6.57	0.02	0.04–0.01
12	United States	do	(1)	25	do	7.16	8.69–6.57	.02	.04–.01
4	India	do	(1)	25	do	7.32	7.90–7.07	.02	.02–.01
4	United States exclusive of North Carolina.	do	(1)	25	do	7.02	7.36–6.62	.02	.03–.01
8	North Carolina.	do	(1)	25	do	7.22	8.69–6.57	.02	.04–.01
4	Haywood County, N.C.	do	(1)	25	do	7.31	8.69–6.57	.02	.04–.01
17	United States and India.	Stained muscovite.	(1)	25	do		9.64–5.83		8.36–.06
2	Madagascar	Phlogopite	(1)	25	do		6.07–5.41		7.12–.38
		Clear muscovite.	(2)		800 cycles	7.0		.03 or less.	
6		do	(3)	20	do	7.1		.024	
2		Phlogopite	(3)	20	do	6.0		.68	

[1] Lewis, Hall, and Caldwell.
[2] D. W. Dye and L. Hartshorn, The Dielectric Properties of Mica, Proc. Roy. Soc., **37**, pp. 42–57; 1924.
[3] C. Darmath and L. E. Goodall, The Permittivity and Power Factor of Micas, J. Inst. Elec. Eng. (London), **69**, pp. 490–497; 1931.

2. DIELECTRIC STRENGTH

(a) PRELIMINARY INVESTIGATIONS

Before describing the results of the dielectric strength measurements it will be well to mention briefly the results of some preliminary experiments. These experiments were undertaken for the purpose of determining the effects of certain variables upon the breakdown voltages obtained. Since the dielectric constant of mica is approximately 7 and that of the transformer oil approximately 2, it is apparent that we have here the case of the nonuniform field between two spheres, and that we are unable to compute the maximum voltage gradient. We can form an approximate idea of the maximum voltage gradient, which is at the surface of the spheres, by noticing the case of two spheres immersed in a homogeneous dielectric. The

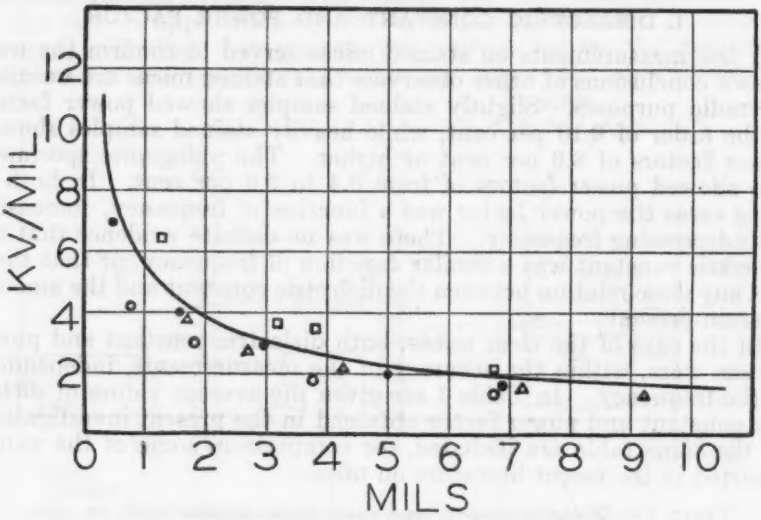

FIGURE 3.—*Effect of electrode shape, clear muscovite*

—— Average of a large number of observations using 1-inch spheres. Average deviation from the mean, 6 per cent.
● Observations using 0.5-inch spheres. Average deviation from the mean, 6 per cent.
○ Observations using 0.5-inch sphere against a small plane. Average deviation from the mean, 4 per cent.
△ Observations at 100° C., using 1-inch spheres.
□ Observations at 148° C., using 1-inch spheres.

equations for the electric field in this case are well known.[9] The maximum voltage gradient is given by the expression

$$G=\frac{V}{t}\left(1+\frac{t}{3\rho}\right)$$

Where

G = maximum voltage gradient.
V = total voltage between electrodes.
t = thickness of specimen.
ρ = radius of curvature of the electrodes, ρ being much greater than t.

[9] A. Schuster, The Disruptive Discharge Through Gases, Phil. Mag., **29**, p. 182; 1890.

In the present case where ρ is 500 mils and t is 10 mils or less, the correction term $\frac{1t}{3\rho}$ is of the order of 1 per cent or less, vanishing with t.

For a like sphere against a plane the correction factor is to be multiplied by 2. Because of the normal scattering of breakdown observations we can not expect to detect with certainty differences of this order of magnitude. In Figure 3 are plotted the results obtained on a clean ruby mica from Maine, using as electrodes 1-inch spheres, 0.5-inch spheres, and a 0.5-inch sphere against a plane. Each point is the average of five individual punctures. The average amount, in per cent, by which each individual puncture differs from the mean of its group has been noted. The solid line represents the average of a large number of observations taken with 1-inch spheres. (See fig. 6.)

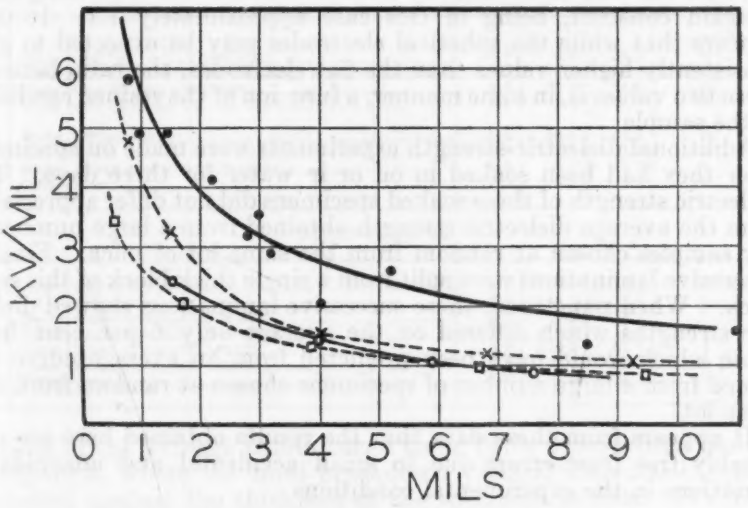

FIGURE 4.—*Effect of electrode shape*

● Clear domestic ruby, 1-inch spheres under oil.
○ Clear domestic ruby, A. S. T. M. electrodes under oil.
× Heavily stained (oxides) domestic ruby, 1-inch spheres under oil.
□ Heavily stained (oxides) domestic ruby, A. S. T. M. electrodes under oil.
Each point represents the average of five individual observations.

It is seen that the results for the 1-inch spheres and the 0.5-inch spheres do not differ from each other by an amount greater than that to be expected from the normal scattering of the individual observations. The results for the 0.5-inch sphere against a plane are definitely lower than would have been predicted on the basis of the equation given above, but no further investigation of these unusually low values has been attempted. These data were taken at a temperature of about 20° C. In the same figure are plotted the results obtained with 1-inch spherical electrodes at two elevated temperatures, 100° and 148° C. Here again no definite effect was observed. This observation is in agreement with those of others who have reported that within this range of temperature the dielectric strength of mica is independent of temperature.[10]

[10] See footnote 6, p. 407.

In Figure 4 are shown comparisons of the results obtained on two separate samples of mica using 1-inch spherical electrodes and flat electrodes in accordance with the specifications of the American Society for Testing Materials. The solid curves represent the values obtained on a clear ruby muscovite from Maine. The dotted curves represent the values obtained on a heavily stained sample of muscovite from North Carolina. The staining material in this sample was identified as magnetite. Each of the points on these curves represents the average of five individual punctures. Within the range from 4 to 9 mils the ratio between the breakdown voltages obtained with the two kinds of electrodes is approximately constant. In the case of the clear mica from Maine this ratio $\frac{KV\ (\text{Spheres})}{KV\ (\text{ASTM})}$ is approximately 2.0. In the case of the heavily stained mica the corresponding ratio is again constant, being in this case approximately 1.1. It thus appears that while the spherical electrodes may be expected to give consistently higher values than the flat electrodes, the ratio between these two values is, in some manner, a function of the stained condition of the sample.

Additional dielectric-strength experiments were made on specimens after they had been soaked in oil or in water for three days. The dielectric strength of these soaked specimens did not differ appreciably from the average dielectric strength obtained from a large number of dry samples chosen at random from the same lot of mica. Finally, successive laminations were split from a single thick block of this same mica. When punctured, these successive laminations showed dielectric strengths which differed on the average only 6 per cent from those which would have been predicted from an average curve obtained from a large number of specimens chosen at random from this same lot.

It appears from these data that the results obtained here are reasonably free from errors due to small accidental and unavoidable variations in the experimental conditions.

(b) FINAL MEASUREMENTS

As stated previously, three specimens were selected at random from each lot of mica and split to thicknesses of approximately 1, 5, and 9 mils, respectively. Five observations of breakdown voltage were made on each thickness, and the average of these five observations was taken to be the breakdown voltage at that thickness. The average deviation of each individual observation from the mean of its group was computed and expressed as a percentage. The average of the three nnmbers thus obtained for each lot of mica was then taken. This "average deviation" gives a rough idea of the reproducibility of the data and the uniformity of the material. The three values of breakdown voltage obtained for each lot of mica were plotted against thickness and a smooth curve drawn through the three points. From this curve was read the breakdown voltage (effective volts) at exactly 1, 5, and 9 mils.

These data have been summarized in Table 2 according to the origin of the mica samples and the classification of the samples. In column A have been given the average amounts, in percentage, by which the individual observations differ from the averages of the corresponding groups of observations. These numbers, therefore, represent the scat-

tering which must be expected between observations made on a single lot of mica. In column B have been listed the average amounts by which the average breakdown voltages for an individual lot of mica differ from the corresponding average breakdown voltages for that class of mica listed in Table 2. These numbers therefore represent the average scattering which must be expected between observations made on different lots of mica.

TABLE 2.—*Average values of breakdown voltage in kilovolts (effective)*

DOMESTIC MICA

Number of lots	Classification	Kilovolts (effective)			*a*, Average deviation within lots	*b*, Average deviation between lots
		1 mil	5 mils	9 mils		
					Per cent	*Per cent*
19	Clear ruby (all of United States)	5.7	9.9	13.2	6	11
6	Clear ruby (United States excluding North Carolina)	5.7	9.6	12.6	5	11
13	Clear ruby (North Carolina)	5.7	10.0	13.3	6	10
7	Clear ruby (Yancey Co., N. C.)	5.6	9.5	12.7	6	8
9	Ruby, air bubbles	5.4	10.4	14.2	6	16
4	Ruby, slight metallic oxide stain	5.3	9.6	12.6	6	9
2	Ruby, heavy metallic oxide stain	4.1	9.7	12.0	7	13
5	Clear green	5.5	9.7	12.4	6	6

FOREIGN MICA

3	Clear ruby (all from India)	4.2	9.1	11.8	6	-------
4	Ruby, air bubbles	5.4	10.5	13.5	5	10
1	Ruby, slight metallic oxide stain	5.3	8.6	13.1	7	-------
5	Ruby, heavy metallic oxide stain	5.4	9.2	11.3	8	18
1	Clear brown (2 complete runs)	5.0	10.9	15.6	5	-------
1	Clear green (2 complete runs)	5.0	12.8	16.3	10	-------
4	Phlogopite	5.0	11.0	13.2	6	10

Some of the average values taken from Table 2 have been plotted in Figure 5, where the total breakdown voltage, kilovolts effective, is plotted against the thickness of the specimen in mils. It should be remarked that since the curves of Figure 5 were obtained as the averages of a number of individual curves, it is not to be expected that any one of the average curves of Figure 5 will necessarily be similar to any one of the individual curves from which it was derived.

In Figures 6 and 7, respectively, have been plotted the results, expressed as kilovolts per mil, obtained from a large number of observations on a clear, ruby mica from Maine and a clear, green mica from Guatemala. It appears that these results can be expressed with a reasonable degree of accuracy by the empirical formula ;

$$KV/\text{mil} = \frac{A}{\sqrt{t}} + B$$

where

t = thickness in mils.

A and B = constants.

The constants of the equations shown in Figures 6 and 7 were determined from the experimental data by the method of least squares.

Curve	Classification	Number of lots
1	Domestic, clear ruby	18
2	Domestic, stained ruby (air bubbles)	9
3	Domestic, slightly stained ruby (metallic oxides)	4
4	Domestic, badly stained ruby (metallic oxides)	2
5	India, clear ruby	3
6	India, stained ruby (air bubbles)	4
7	India, badly stained ruby (metallic oxides)	5

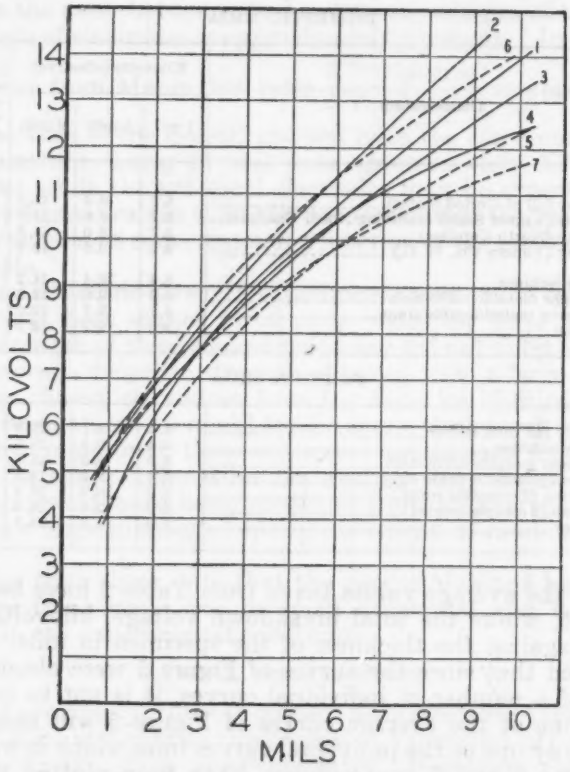

FIGURE 5.—*Total breakdown voltage average values*

In many of these tests it was observed that the actual puncture rarely took place at exactly the point of contact between the spheres and the specimen, but slightly to one side. This effect has been reported by other observers.[11] In the case of the micas which were badly stained with metallic oxides and the phlogopites, "preliminary" sparks were often noticed playing about the electrodes at voltages considerably lower than that at which the actual breakdown took place. After failure of the specimen the actual puncture was observed to be surrounded by a series of charred pits.

[11] E. H. Rayner, High Voltage Tests and Energy Losses in Insulating Materials, J. Inst. Elec. Eng. (London), **49**, pp. 3-71, 1912.

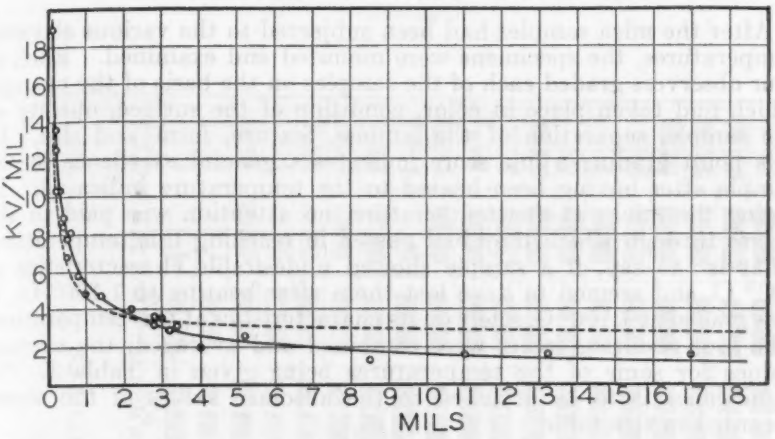

FIGURE 6.—*Breakdown voltage in kilovolts per mil. Clear ruby muscovite from Maine*

○ Observed points, each point the average of 5 individual observations.

— Plotted from the equation $\frac{KV}{\text{mil}} = \frac{5.75}{\sqrt{t}} - 0.16$.

– – – Plotted from the equation $\frac{KV}{\text{mil}} = \frac{1.84}{t} + 2.32$.

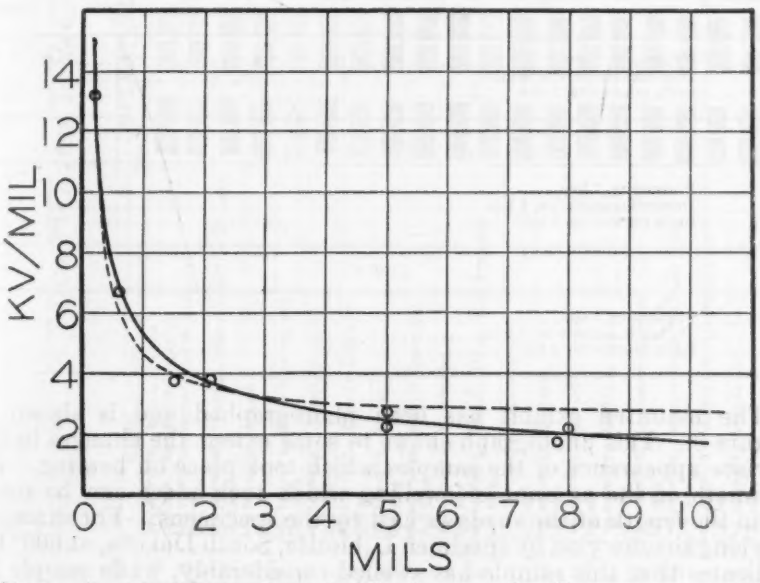

FIGURE 7.—*Breakdown voltage in kilovolts per mil. Clear green muscovite from Guatemala*

○ Observed points each point being the average of 5 individual observations.

— Plotted from the formula $\frac{KV}{\text{mil}} = \frac{5.88}{\sqrt{t}} - 0.35$.

– – – – Plotted from the formula $\frac{KV}{\text{mil}} = \frac{2.16}{t} + 2.52$.

3. EFFECTS OF ELEVATED TEMPERATURES

After the mica samples had been subjected to the various elevated temperatures, the specimens were mounted and examined. Each of four observers graded each of the samples on the basis of the changes which had taken place in color, condition of the surface, opacity of the sample, separation of the laminæ, texture, form and size. In this point grading a low score indicates a general excellence in the sample after having been heated to the temperature indicated. In listing the micas at one temperature, no attention was paid to the stages through which they had passed in reaching this temperature. That is to say, if a sample showed undesirable characteristics at 700° C. and seemed to have lost them after heating to 1,100° C., it was graded at 1,100° C. solely on its characteristics at this temperature. The four resulting tables were combined and averaged, the average values for some of the temperatures being given in Table 3. No significance is to be attached to the absolute values of the scores recorded in this table.

TABLE 3.—*Classes of mica in the order of their ability to withstand elevated temperatures*

[A small score indicates relative excellence in the samples after having been heated to the temperature indicated]

Rating	Class and origin	Average points scored
	700° C.	
1	Phlogopite, 7 lots	30
2	Domestic muscovite, 6 lots	39
3	India muscovite, 3 lots	50
	900° C.	
1	Phlogopite, 7 lots	25
2	Domestic muscovite, 6 lots	47
3	India muscovite, 3 lots	47
	1,100° C.	
1	Phlogopite, 7 lots	33
2	Domestic muscovite, 6 lots	36
3	India muscovite, 3 lots	36

The mounted exhibit has been photographed and is shown in Figure 8. This photograph shows to some extent the changes in the surface appearance of the samples which took place on heating. An estimate of the amount of swelling which took place can be made from the length of the shadows cast by the specimens. For example, the long shadow cast by specimen L, biotite, South Dakota, at 600° C., indicates that this sample has swelled considerably, while sample K, muscovite, Brazil, has been relatively unaffected by this temperature. It seems hardly necessary to emphasize the essentially qualitative nature of these particular observations.

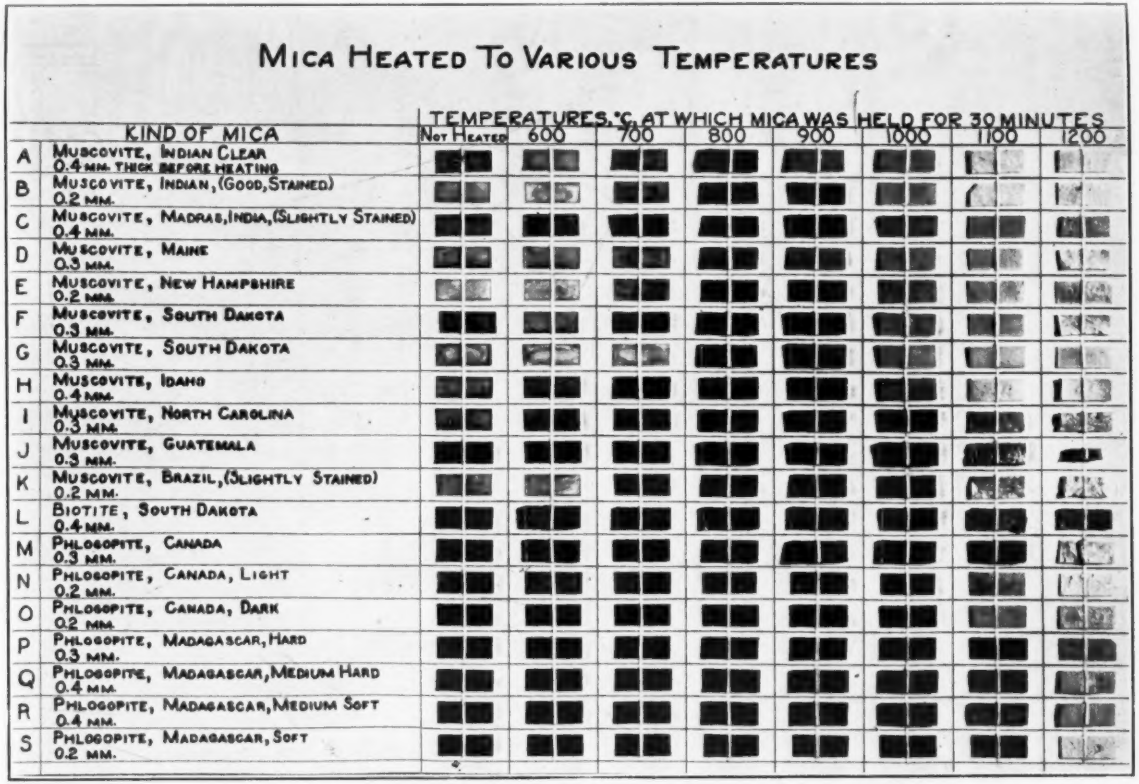
MICA HEATED TO VARIOUS TEMPERATURES
KIND OF MICA
TEMPERATURES, °C, AT WHICH MICA WAS HELD FOR 30 MINUTES
NOT HEATED
600
700
800
900
1000
1100
1200
A MUSCOVITE, INDIAN CLEAR 0.4 MM. THICK BEFORE HEATING
B MUSCOVITE, INDIAN, (GOOD, STAINED) 0.2 MM.
C MUSCOVITE, MADRAS, INDIA, (SLIGHTLY STAINED) 0.4 MM.
D MUSCOVITE, MAINE 0.3 MM.
E MUSCOVITE, NEW HAMPSHIRE 0.2 MM.
F MUSCOVITE, SOUTH DAKOTA 0.3 MM.
G MUSCOVITE, SOUTH DAKOTA 0.3 MM.
H MUSCOVITE, IDAHO 0.4 MM.
I MUSCOVITE, NORTH CAROLINA 0.3 MM.
J MUSCOVITE, GUATEMALA 0.3 MM.
K MUSCOVITE, BRAZIL, (SLIGHTLY STAINED) 0.2 MM.
L BIOTITE, SOUTH DAKOTA 0.4 MM.
M PHLOGOPITE, CANADA 0.3 MM.
N PHLOGOPITE, CANADA, LIGHT 0.2 MM.
O PHLOGOPITE, CANADA, DARK 0.2 MM.
P PHLOGOPITE, MADAGASCAR, HARD 0.3 MM.
Q PHLOGOPITE, MADAGASCAR, MEDIUM HARD 0.4 MM.
R PHLOGOPITE, MADAGASCAR, MEDIUM SOFT 0.4 MM.
S PHLOGOPITE, MADAGASCAR, SOFT 0.2 MM.

FIGURE 8.—*Micas after having been heated to various temperatures*

IV. DISCUSSION AND CONCLUSIONS

From the data of Table 1 it is apparent that stained muscovite micas and phlogopite show power factors entirely too high to permit their use in applications calling for materials having low power loss. For perfectly clear muscovite mica one may predict, from these data, a power factor of 0.02 per cent with deviations from this value of ± 0.01 per cent on the average. The average dielectric constant of these micas is found to be 7.2 with a deviation from this value of ± 0.3 on the average.

These figures are shown (see Table 1) to be in good agreement with those reported by other observers.

From the curves of Figure 5 it is apparent that the differences between the breakdown voltages of clear ruby mica, ruby mica stained with air bubbles, and ruby mica slightly stained with metallic oxides, does not exceed that which might be expected from the normal scattering of the individual observations. (See columns A and B of Table 2.) The dielectric strength of mica is thus less sensitive to the presence of inclusions than is the power factor which, as is shown by the preceding section, is seriously affected by the slightest trace of air bubbles or metallic oxides. The curves for the domestic ruby micas, heavily stained with metallic oxides, show a small but definite decrease of dielectric strength due to the stains, with a correspondingly increased average scattering of the individual points, see columns A and B, Table 2. This increased scattering is particularly noticeable at the smaller thicknesses. The decrease in dielectric strength is not, however, as large as would have been expected from the appearance of the samples, which were so heavily stained as to be practically opaque in 10-mil thicknesses.

To emphasize this last point attention should be called to the curve in Figure 5 giving the breakdown voltage of clear ruby mica from India. This curve indicates that the foreign clear ruby specimens have a dielectric strength considerably less than the foreign slightly stained specimens, lower even than the heavily stained specimens in thicknesses less than 5 mils. No explanation is offered for this apparent anomaly except to point out that the curve for the clear India ruby mica is the average of a relatively small number of lots of mica. This curve should, therefore, perhaps be considered as being more characteristic of the individual lots used than of the corresponding class of mica in general.

Low as these values for clear India mica seem in comparison with the data on other micas, they are nevertheless in excellent agreement with values reported by Rayner.[12] Rayner used as electrodes 2-inch steel spheres immersed in oil to prevent corona and flash over. His experimental conditions were, therefore, almost identical with those of the present investigation. Although the origin of his mica samples is not specifically given, it is very probable that they came from India.

The presence of numerous thin layers of conducting material in the badly stained micas will tend to seriously distort the electric field within the crystal. This is probably the explanation both for the increased scattering of the results obtained on these badly stained samples, and for the preliminary sparking which took place at the electrodes.

---

[12] See footnote 11, p. 414.

It is not possible on the basis of the data recorded in Table 4 to make any distinction between micas of like quality obtained from different geographical locations. We see from these data that not only are the average values of breakdown voltage practically indistinguishable, but that the scattering of results obtained on micas taken from widely separated localities is no greater than the scattering of results obtained on micas taken from the same State, or even from the same county.

Other observers working on the dielectric strength of thin films have arrived at the conclusion that the dielectric strength, expressed as volts per mil, should vary inversely as the thickness of the specimen. Joffé [13] arrived at this conclusion from theoretical considerations and confirmed it by experiments on thin glass films. Moon and Norcross [14] have reached the same conclusion as a result of experiments on thin mica films. All of these observations were taken on thicknesses below 2 mils. In Figure 7 are shown the curves obtained by fitting, by least squares, the two laws

$$KV/\text{mil} = \frac{A}{t} + B$$

and

$$KV/\text{mil} = \frac{A}{\sqrt{t}} + B$$

to the same set of data. Here t is the thickness in mils, A and B are constants. It is seen that below about 3 mils the two laws are practically identical and, with such data as is here presented, it would be impossible to distinguish between them. For thicker specimens, however, the observed values of KV/mil fall off more rapidly than $\frac{1}{t}$, and over the range from 0.1 mil to 17 mils (see figs. 6 and 7) the data seems to be most adequately represented by the equation

$$KV/\text{mil} = \frac{A}{\sqrt{t}} + B$$

From an observation of the mounted exhibit (see fig. 8) it is apparent that, with one or two exceptions, all of the samples remained practically unchanged after exposure to 600° C. Above this temperature (see Table 3) the phlogopites retained their initial properties to a greater extent than the muscovites or the biotite. None of the micas investigated withstands 1,200° C. well, and except for possible exceptional uses, they may be said to have undergone such great changes as to be rendered unsuitable for use.

Finally it was not found possible on the basis of the data presented in Tables 1, 2, and 3 to make any essential distinction between micas of like commercial grades based solely on the geographical origin of the samples.

WASHINGTON, May 22, 1931.

[13] A. Joffé, The Mechanism of Dielectric Breakdown, J. Math. and Physics, M. I. T., 6, p. 133, 1926.
[14] See footnote 6, p. 407.